PLEASE TYPE

UNIVERSITY OF NEW SOUTH WALES

Thesis/Project Report Sheet

Surname or Family name: WATERS

First name: Michael Other name/s: Thomas

Abbreviation for degree as given in the University calendar: PhD

School: Civil & Environmental Engineering / Faculty: Engineering

Title: EFFECTS OF VEGETATION ON THE HYDRODYNAMICS OF FRESHWATER WETLANDS

Abstract 350 words maximum: (PLEASE TYPE)

This thesis examines the effects of vegetation on hydrodynamics in wetlands. These effects were examined primarily by the collection and analysis of data obtained at two field sites adjacent to Manly Reservoir, complemented by literature review and scaling analysis as appropriate.

Intensive investigations were undertaken at a field site dominated by *Typha orientalis* for one week. Profiles of temperature and velocity fluctuations in the water column were made within the vegetated and unvegetated parts of the wetlands. Velocity and solar radiation profiles were taken above the water surface in the plant canopy and meteorological parameters were measured above the plant canopy.

Within the water column, temperature stratification in the vertical was observed to occur; however, due to the shallow nature of the wetland, stratification was found to be transient, developing quickly due to solar radiation and decaying rapidly due surface cooling.

Analysis of fluctuating velocity data indicated that wind driven surface waves generated in the reservoir decreased with distance from the reservoir; however, turbulence initially increased and then decreased with distance from the reservoir. It appears that surface waves were dissipated by vortex shedding on the vegetation within the water column, giving rise to turbulence.

Significant temperature differences were found between the water in the reservoir and the water in the wetland. Shading of the water column from solar radiation by the plant canopy by day kept temperatures here lower than in the reservoir, causing buoyancy driven convection between the warmer reservoir water and the cooler water in the wetland.

Long term investigations were undertaken at the two sites by recording temperatures within the water column and meteorological parameters.

Long term monitoring indicated that during summer, temperature differences between the open water and vegetated areas persisted for many days, potentially causing convection between the vegetated and open water areas. In winter these buoyancy differences were only diurnal, so convections would also be diurnal.

From this study, a number of implications for water quality management in wetlands are apparent. Most significantly, the transport of constituents, will depend mainly on wind effects and buoyancy driven convection between open water and vegetated areas.

EFFECTS OF VEGETATION ON THE HYDRODYNAMICS OF FRESHWATER WETLANDS

MICHAEL THOMAS WATERS

BE Civil (Hons), BSc, UNSW

A thesis submitted in fulfilment of the requirements
for the degree of Doctor of Philosophy

Water Research Laboratory,
School of Civil and Environmental Engineering,
University of New South Wales

23 January, 1998

DECLARATION

I hereby declare that this submission is my own work and that to the best of my knowledge and belief, it contains no material previously published or written by another person nor material which to a substantial extent has been accepted for the award of any other degree or diploma of a university or institute of higher learning, except where due acknowledgement is made in the text.

Michael Waters

ABSTRACT

This thesis examines the effects of vegetation on hydrodynamics in wetlands. These effects were examined primarily by the collection and analysis of data obtained at two field sites adjacent to Manly Reservoir, complemented by literature review and scaling analysis as appropriate.

Intensive investigations were undertaken at a field site dominated by *Typha orientalis* for one week. Profiles of temperature and velocity fluctuations in the water column were made within the vegetated and unvegetated parts of the wetlands. Velocity and solar radiation profiles were taken above the water surface in the plant canopy and meteorological parameters were measured above the plant canopy.

Within the water column, temperature stratification in the vertical was observed to occur; however, due to the shallow nature of the wetland, stratification was found to be transient, developing quickly due to solar radiation and decaying rapidly due surface cooling.

Analysis of fluctuating velocity data indicated that wind driven surface waves generated in the reservoir decreased with distance from the reservoir; however, turbulence initially increased and then decreased with distance from the reservoir. It appears that surface waves were dissipated by drag on the vegetation within the water column, giving rise to turbulence.

Significant temperature differences were found between the water in the reservoir and the water in the wetland. Shading of the water column from solar radiation by the plant canopy by day kept temperatures here lower than in the reservoir, causing buoyancy driven convection between the warmer reservoir water and the cooler water in the wetland.

Long term investigations were undertaken at the two sites by recording temperatures within the water column and meteorological parameters.

Long term monitoring indicated that during summer, temperature differences between the open water and vegetated areas persisted for many days, potentially causing convection between the vegetated and open water areas. In winter these buoyancy differences were only diurnal, so convections would also be diurnal.

From this study, a number of implications for water quality management in wetlands are apparent. Most significantly, the transport of constituents, will depend mainly on wind effects and buoyancy driven convection between open water and vegetated areas.

ACKNOWLEDGEMENTS

Thanks first and foremost are due to Dr David Luketina my supervisor for his support, advice, guidance, his thoroughness in reviewing drafts of this thesis, for his assistance during the fieldwork and for the use of his Fourier transform program.

Mr John Hart and Mr Mark Groskops are thanked for their work in constructing much of the equipment. Mr Ian Matthews helped with equipment installation, surveying and vegetation analysis. Mr David Ferguson, Mr Peter Horton and all of those previously mentioned gave generously of their time during the intensive monitoring, their help was greatly appreciated. Mr John Baird's assembly of electronic equipment was much appreciated. Thanks to other staff and students at the UNSW Water Research Laboratory for their support, especially the Director, Professor Ron Cox and Dr James Ball.

Thanks to staff and students of the Centre for Wastewater Treatment (CWT) for their encouragement, particularly Mr Terry Schulz, Mr Peter Maslen, both formerly of CWT and Professor James Moore of Oregon State University, a former visiting fellow at CWT.

The author is grateful to Dr Ian Webster and Dr Brad Sherman of the CSIRO Centre for Environmental Mechanics for their advice and for the loan of the Li-Cor quantum sensor, the fp07 microprofiler and the Vaisala relative humidity probe.

Warringah Shire Council and particularly Mr Chris Buckley are thanked for allowing access to the wetland and the use of their boat. Manly Hydraulics Laboratory are acknowledged for providing the dam water level data. Macquarie University School of Earth Sciences are acknowledged for allowing the use of data from their weather station.

Thanks to Ms Stephanie Wallace of WRL for proof-reading the final draft, to my father Noel for proof-reading two drafts and helping with the vegetation analysis, to the rest of my family, Helen, Peter, Elizabeth and Vanessa and to my friends for their encouragement.

Financial support for this project was provided by the Cooperative Research Centre for Waste Management and Pollution Control Limited (CRC), the author is most grateful to them, particularly to Professor John Bavor of University of Western Sydney from the CRC wetlands project and Professor Nicholas Ashbolt, formerly the CRC educational advisor.

TABLE OF CONTENTS

LIST OF TABLES

LIST OF FIGURES

LIST OF APPENDICES

LIST OF SYMBOLS

In Order of Appearance

Tn	Period of lake seiching
l or L	Horizontal length scale
H	Depth of water
g	Acceleration due to gravity
H_l	Average depth of the lake or reservoir
n	Harmonic number or number of samples in a data set
U_a	Air velocity
y	Height above the plant canopy
T	Temperature (of water unless otherwise noted)
t	Time
ρ or ρ_w	Density (of water unless otherwise noted)
C_p or c_p	Thermal capacity of water at a constant pressure
ϕ	Heat flux (shortwave radiation unless otherwise noted)
l_l	Distance light has penetrated into the water column
ϕ_s	Shortwave radiation heat flux at the water surface
η	Exponential decay constant for radiation, within water (Beer's constant)
θ_t	Angle to the vertical of light transmitted through the water column
τ	Ratio of transmitted to incident radiation
n_s	Snells coefficient
θ_i	Angle to the vertical of light incident on the water column
ϕ_{lw}	Nett longwave radiation heat flux at the air-water interface
σ	Stefan-Boltzmann constant
T_w	Water temperature
T_a or T_{air}	Air temperature
H_s	Sensible heat transfer
C_s	Dimensionless transfer coefficient for sensible heat
ρ_{air} or ρ_a	Density of air

H_l	Latent heat transfer
C_l	Dimensionless transfer coefficient for latent heat
L_w	Latent heat of evaporation of water
Q	Specific humidity
Q_o	Saturation specific humidity
R_H	Relative humidity
p_a	Air pressure
α and β	Empirical constants
H_c	Height of the plant canopy above the water surface
u_a*	Air-water interface shear (friction) velocity in air
u_w* or u_*	Air-water interface shear (friction) velocity in water
k	Von Karman's constant
z	Vertical distance above the water surface
z_o	Roughness length of the water surface
τ_r	Reynolds stress
u'	Difference between the instantaneous and average horizontal velocities
w'	Difference between the instantaneous and average vertical velocity
u_{rms}	Root mean square of the fluctuating velocity component
C_D	Drag coefficient
τ_s	Wind stress at the water surface
C_w	Drag coefficient at the water surface
C_t	Drag coefficient for flow in the atmosphere at the top of the canopy
η_p	Number of plant stems per unit area
d	Plant stem diameter
$f(i)$	Factor for Blackman window
i	Integer number
H	Depth of water
f_l	Lowest frequency of turbulent phenomena
f_k	Highest frequency of turbulent motion (Kolmogorov frequency)
ε	Rate of dissipation of Turbulent Kinetic Energy (TKE)

ν	Kinematic viscosity
f_b	Buoyancy (Brunt Vaisala) frequency
f_w	Frequency of wind driven surface waves
F	Length of fetch for development of wind waves
u_f	Fall rate of fluid due to penetrative convection
α_T	Coefficient of thermal volumetric expansion of water
$\overline{H}$	Surface cooling rate
P	Rate of production of TKE
G	Rate of change of Potential Energy due to mixed layer deepening via penetrative convection
C_t^f	Coefficient of entrainment of hypolimnion waters by penetrative convection thermals
Φ	Rate of dissipation of TKE divided by the average fluid density
u	Velocity (in the horizontal unless otherwise noted)
C	Constituent concentration
D	Molecular diffusivity
D_T	Thermal diffusivity
p	Pressures in water
δ_{i3}	Kronecker delta for j = 3
ρ_o	reference density
ρ'	local variance from the reference density
H'	local variance from the reference water surface elevation
T'	local variance from the reference Temperature
T_x	Temperature gradient in the direction of the flow
S	Water surface slope
K_M	Kinematic eddy viscosity
K_c	Turbulent diffusivity of constituent c
R_e	Reynolds number
U	Velocity scale in the horizontal
R_i	Richardson number

G_r	Grashof number
R_a	Rayleigh number
A_L	Aspect ratio
P_r	Prandtl number
D_T	Thermal diffusivity
f_D	Drag force per unit volume
F_D	Total drag force
C_D	Drag coefficient
A	Area contributing to drag of a body
S_f	Shading factor in the drag equation
b	Width of the wetland
K	Empirical drag factor
W	Velocity scale in the vertical
t_s	Time scale

1. INTRODUCTION

1. INTRODUCTION

1.1. BACKGROUND

Wetlands may be defined as areas that are transitory between terrestrial and aquatic systems (Cowardin *et al*, 1979). Important distinctions exist between different types of wetlands that are permanently flooded or ephemerally flooded, free surface flow and subsurface flow wetlands. Aquatic macrophyte plants are common in wetlands and may be a characterising feature of them, as they are life forms that do not occur in either purely terrestrial or purely aquatic environments.

From Wetzel, (1983), aquatic macrophytes may be classified based on whether they are rooted in the soil or not, and on the location of their leaves relative to the water surface. Features of macrophytes classified into these groups are presented below.

- *Emergent macrophytes,* which are rooted in the bed of the wetland and have leaves that extend through the water column and into the atmosphere. These macrophytes can tolerate water levels from 0.5 m below the soil surface to 2.0 m above the soil surface and may grow in permanently or ephemerally flooded wetlands with free water surface or subsurface flow (Sainty and Jacobs, 1988).

- *Submergent macrophytes,* which are rooted in the bed of the wetland and have leaves that only extend part of the way through the water column. These macrophytes can tolerate water levels from 0.1 to 10m above the soil surface. They generally only grow in permanently flooded free water surface wetlands.

- *Floating leaved macrophytes*, which are rooted in the bed of the wetland and have leaves that float freely on the surface that are attached to the root system by flexible stems or petioles that extend through the water surface. These macrophytes can tolerate water levels from 0.1 m to 3.0 m above the soil surface. They generally only grow in permanently flooded free water surface wetlands.

- *Free floating macrophytes*, which are not attached in any way to the bed of the wetland. These macrophytes can grow in virtually any situation where the water level is above the soil surface. They generally only grow in permanently flooded free water surface wetlands.

Typical features of each of plants in each these categories are shown in Figure 1.1. Within each of these categories, a broad range of species may be found in Australia (Sainty and Jacobs, 1988) and internationally (Wetzel, 1983).

Figure 1.1. Classification of Aquatic Macrophytes

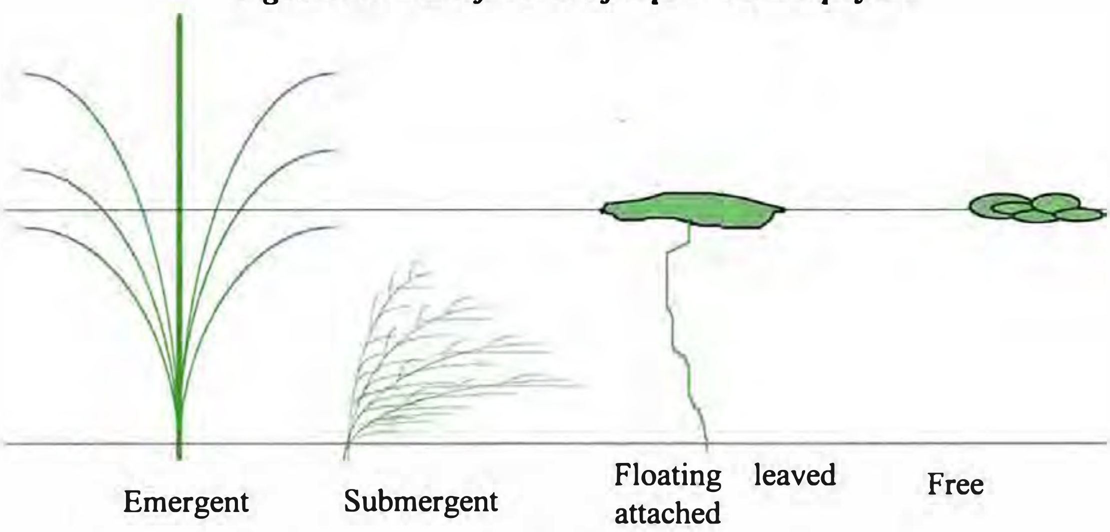

The chemical, biological and geomorphic processes that occur in wetlands, although still only poorly understood, have received wide attention in recent years with the realisation that they play an important role in regulating the quality of inland waters (Wetzel, 1983). Hydrodynamic processes in a wetland will play an important role in determining the nature of chemical, biological and geomorphic processes that operate in wetlands, yet they have received only limited attention to date (Roig, 1994).

The potential for hydrodynamics to effect water quality is demonstrated by Hatano *et al*

(1992), who found that populations of bacteria, actinomycetes and fungi vary widely both in number and in the rates at which they decompose organic material within an individual wetland. These variations were found to occur both laterally and vertically within the water column of the wetland.

The hydrodynamic processes that transport water quality constituents between sites in a system where varying microbial activity occur would play an important role in determining the effectiveness of the biological transformations at these sites in two ways:

1. Mixing in the vertical and the inhibition of such mixing by density stratification will determine the extent to which incoming constituents, initially in the water column, may be brought into contact with the soil, where microbial activity is highest and where dissolved oxygen levels are lowest (Hatano *et al*, 1992).

2. Horizontal convection will determine how constituents are transported laterally across the wetland.

1.2. PREVIOUS STUDIES OF WETLAND HYDRODYNAMICS

Previous studies of wetland hydrodynamics have described with some success the physical effects of vegetation on flows within the wetland. However, such studies have all considered wetlands where the mean flow rates into and out of the wetland dominated the motion within the wetland. Important recent studies that demonstrate the limits of knowledge in the literature are summarised below. Findings from these and other studies are examined in more detail in relevant chapters.

Kadlec (1990) reviewed previous literature in the field of flow through submergent and emergent vegetation and examined flow through several wetlands subject to mean flow rates large enough to give rise to measurable head losses between inlet and outlet. The review found that in previous studies, head loss due to vegetation had been accounted for by using drag theory, Mannings equation or the Darcy-Weisbach equation. The study recognised that for any given wetland, only three variables can be altered: the depth; the the slope of the water surface (under uniform, steady flow conditions); and the flow rate per unit width. When considered this way, any of the approaches listed above can be shown to give rise to a power law relationship between flow rate per unit width, depth and slope.

Kadlec (1990) showed that the results of all previous studies gave rise to a narrow range of constants when expressed in the manner of a power law relationship with flow rate per unit width as a function of depth and slope (see Chapter 5 for more details). Unfortunately however, this power law relationship leads to awkward units for the calibration coefficients so care is required in its use.

A different approach was taken by Lewandowski *et al* (1993) who examined flows into and out of the San Elijo Lagoon in California. This is a tidal wetland containing emergent vegetation. This wetland is 2.1 km^2 in area and consists of large shallow vegetated areas interspersed with narrow, deeper unvegetated slough channels.

Lewandowski *et al* (1993) recognised that to accurately measure flows into and out of the San Elijo Lagoon, it would be necessary to consider separately the effects of the vegetated areas and the slough channels; that is, they realised that non-uniform patterns of vegetation in a wetland must be accounted for to determine flows within a wetland. They constructed a quasi two dimensional numerical model of the wetland, making no attempt to simulate the flows within the vegetated areas which were modelled as acting purely as storage cells that fill and empty to the water levels at their boundaries along the slough channels. A disappointing aspect of the Lewandowski *et al* (1993) study was that no calibration data was presented. For this reason the accuracy of their model is uncertain and will not receive detailed consideration here.

Roig (1994) also addressed the issue of head loss due to emergent and submergent vegetation. This study measured flow resistance in a flume due to an array of dowels arranged to simulate vegetation. Dimensional analysis was used to formulate a relationship between the resistance force per unit bed area and the mean velocity, plant diameter, plant spacing, depth of water and length of submerged stem. Calibration coefficients were determined and a two dimensional depth averaged numerical model, was then used to successfully model flows due to tidal forcings in Hayward Marsh, an estuarine wetland in the San Francisco Bay area. Unfortunately, it seems Roig (1994) was unaware of the earlier work of Kadlec (1990) reported above, a comparison of their findings is reported in Chapter 5.

A number of other studies such as Kadlec and Hey (1992), Kadlec (1993) and Eberdorfer (1994) report the results of tracer studies in wetlands containing emergent and submergent vegetation. All such studies found quite complex flow patterns develop in the wetlands examined. Causes of these complex flow patterns were density stratification and non-uniform distribution of vegetation.

Kadlec (1993) reported success in reproducing tracer breakthrough curves for a wetland containing emergent vegetation in Carville Louisiana by modelling the wetland as a network of plug flow and continually mixed units. However such a model is entirely empirical and therefore site specific. To construct such a model, it would be necessary to perform a tracer experiment, then to perform trial and error fitting with different arrangements of plug flow and continually mixed units until an arrangement that produces suitable results were obtained.

Coates and Ferris (1995) studied buoyancy driven convection due to differential heating in laboratory experiments on a cavity consisting of an area containing free floating macrophytes (*Lemna* sp. L. and *Azolla* sp. Lam.) and an area where no plants were present. They found that strong thermal gradients developed between the area containing macrophytes and the area without macrophytes due to shading of the water surface by the macrophyte leaves. This temperature difference caused buoyancy driven convection to develop between the area containing macrophytes and the area without macrophytes. The warm intrusion that entered the vegetated area from the open water just below the water surface was displaced downwards by the presence of the floating vegetation; however, the frontal velocity was not affected by the vegetation.

Apart from the laboratory study by Coates and Ferris (1995), no other previous studies have directly examined interchanges between open water and vegetated sections of a wetland in the field, nor have there been studies that have examined mixing processes within the water column in open water and vegetated sections of a wetland in the field. Both of these phenomena would be expected to play a major role in determining the nature of water and constituent movement in wetlands and may have important consequences for wetlands ecology, as mentioned above and discussed in detail in Chapter 7.

1.3. AIMS AND OBJECTIVES

For this dissertation , investigations of hydrodynamic processes in the water column of a wetland, their causes and their nature were performed. As outlined above, these processes will have important consequences for chemical and biological processes; when the water column is stratified this may lead to the formation of anaerobic conditions at the bed of the wetland, whilst when the water is unstratified, aerobic conditions should persist throughout.

Preliminary estimates (Waters, Luketina & Ball, 1994) found that wind mixing, temperature stratification due to solar radiation and overturning of the water column due to night-time cooling at the surface (penetrative convection) are the main considerations in mixing in open water sections of wetlands.

The rationale behind the present study is discussed fully in Chapter 2. The aims of the study were to determine the forcings that dominate motion in wetlands, the resulting water movement through wetlands and particularly, to determine the effects of one of the four types of vegetation common in wetlands on these forcings and the resulting motions.

Specific objectives were:

- To quantify the forcings that are significant in producing:

  stratification,
  mixing and
  convective motion

  in a wetland containing a monoculture or near monoculture of one of the four types of macrophytes described earlier;
- To quantify the stratifications, convections and mixing arising due to these forcings;
- To determine the variability of behaviour with site location and season; and
- To consider the impacts of the above on water quality within wetlands and make suggestions for the design of constructed wetlands.

As the only previous research that relates to this area are those studies mentioned above, it was considered appropriate to perform this research primarily by the means of field studies, and to limit the study to defining and describing the dominant processes operating in a single wetland, rather than attempting to comprehensively cover all processes.

1.4. THESIS STRUCTURE

To address the objectives listed above, this thesis has been arranged into separate chapters covering each of the processes studied. Literature review, scaling arguments, experimental techniques and findings for each process are discussed within each chapter.

Chapters examining the processes studied all follow the same format, firstly comment is made on the literature relevant to the process being considered, and the effects of vegetation on that process. Following that, any necessary scaling analysis is performed, field results of relevant investigations are reported and their implications are discussed.

Prior to considering these processes, **Chapter Two** presents the methodology of the study generally, and of the field investigations in particular.

Chapter Three considers heat fluxes into and out of the water column and temperature induced density stratification of the water column.

Chapter Four considers mixing processes due to momentum driven by wind and wave motion and comments on penetrative convection due to heat loss at the water surface.

Chapter Five considers convection processes, concentrating primarily on buoyancy driven exchanges between open water and vegetated zones; brief comments are also made on convection due to wind motion.

Chapter Six considers differences in behaviour between the two sites studied, and seasonal variability in behaviour.

Chapter Seven examines the implications of the findings of the research on water quality issues within wetlands and **Chapter Eight** concludes the study by summarising the findings of the previous chapters and makes recommendations for future research.

1.5. CONTRIBUTIONS MADE BY THE AUTHOR

In these investigations, the author was primarily responsible for:

- determining the overall thrust of the project;
- choosing the processes to be studied;
- reviewing literature;
- scaling analyses performed;
- all aspects of the field studies including defining study objectives, site selection and evaluation, choice of appropriate objectives, techniques and equipment to be used, development of an experimental programme to meet these objectives, design of the physical set-up used, equipment installation, equipment maintenance, data gathering and the calibration and verification of all probes used, unless otherwise noted in the text; and
- Data analysis and interpretation.

2. EXPERIMENTAL METHODOLOGY

2. EXPERIMENTAL METHODOLOGY

2.1. INTRODUCTION

From a number of authoritative reviews of limnology and physical limnology, such as Imberger and Patterson (1990), Fischer *et al* (1979) and Wetzel (1983), and from the few studies that have considered wetland hydrodynamics, such as Eberdorfer, (1996), Coates and Ferris (1995) and Kadlec and Hey (1992), it can be seen that some of the processes that are important in lake hydrodynamics may also be important in wetland hydrodynamics. Such processes could include heat fluxes at the air-water interface, stratification within the water column, wind driven mixing, penetrative convection, convection due to differential heating and cooling and the effects of season on these factors. The effects of wetland vegetation on these processes would be expected to be significant, yet has received only limited attention in the literature. One of the few such studies was performed by Coates and Ferris (1995). As described in Chapter 1, Coates and Ferris (1995) studied temperature driven buoyancy driven convection between an open water area and an area containing free floating macrophytes through laboratory experiments. No evidence was given in the paper that observation of such behaviour had been made in the field.

Due to the limited number of previous studies performed, it was considered that the most appropriate approach for this study would be to undertake field investigations to allow the processes that dominate water movements in a wetland containing emergent aquatic macrophytes to be examined. Performing the study in this way had the advantages listed below.

- It would allow the laboratory results of Coates and Ferris (1995), to be confirmed or denied through observations in the field: that buoyancy driven flows are expected to occur in wetlands.
- The study would be performed in a sufficiently different type of wetland from that studied by Coates and Ferris (1995) to be significant in its own right.

- By performing the study in the field, the combined effects of a variety of different processes could be observed and it would be possible to determine which are the processes that dominate the hydrodynamics of the wetland, ensuring that the study would result in relevant findings.

- Data collected for the study would be able to be used in further research beyond this study. For example, through further research by numerical modelling to simulate the behaviour of the wetland.

As the field sites considered in this study were dominated by emergent macrophytes, the remainder of this thesis will be restricted mainly to effects that such types of plants would have on hydrodynamics of waterbodies in which they occur.

In accordance with the overall objectives of the study, the objectives of the field studies and techniques used to meet them are presented in Table 2.1. This chapter gives details of the techniques used to meet these objectives.

First a description is given of the factors considered in determining the most suitable site to study. Second, a full description of the sites selected is given. Details of the long term experiments are then provided, including specifications of the equipment deployed, installation procedures and monitoring techniques. Finally details of the intensive experiments are provided, following the same format as for the long term monitoring.

2.2. TECHNIQUES EMPLOYED TO MEET OBJECTIVES

The objectives of the study were stated in Chapter 1. The techniques used to meet particular objectives are given in Table 2.1.

Table 2.1. Study Objectives and Techniques used to meet these objectives

Objectives (see Section 1.2 for full details)	**Techniques used to meet objectives**
To quantify forcings	Measurement of meteorologic parameters during intensive investigations and calculations
To quantify stratifications	Measurement of temperature profiles during intensive investigations
To quantify mixing processes	Measurement of temperature and velocity profiles during intensive investigations
To quantify convections	Measurement of temperature and velocity profiles during intensive investigations
To determine the variability of behaviour with site location and season	Measurement of meteorologic parameters and temperature profiles during long term investigations
To determine the likely impacts of the hydrodynamics on water quality within wetlands	Compare and contrast the results of these hydrodynamic investigations with the results of previous studies that have related hydrodynamic processes to water quality processes in similar flows

2.3. SITE SELECTION AND EVALUATION

Before embarking on site investigations it was necessary to evaluate a suitable field site from the many wetlands available for study. The photograph shown in Figure 2.1 was taken during site evaluation in Manly Dam War Memorial Reserve. Site evaluation was performed by setting up a database of potential field sites and evaluating the merits of performing the study at these sites based on the criteria listed below.

- Access to the site and permission from the landowner or manager to perform the study on the site.
- Security at the site and the need to safeguard monitoring equipment against theft or vandalism.

Figure 2.1. Preliminary Field Site Evaluation at Manly dam wetlands

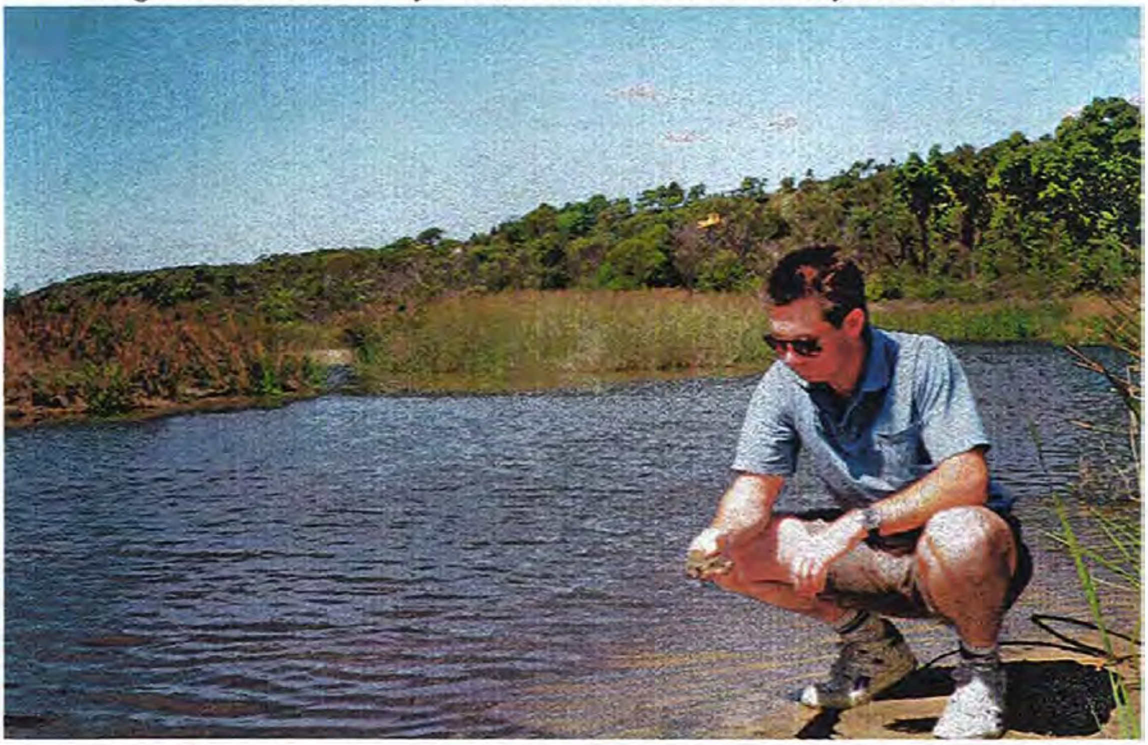

- Distance from the Water Research Laboratory, where the study was based. This was an important factor for a variety of reasons, such as: to allow quick access to the site for installation and maintenance of equipment; to facilitate data downloads; and in the event that an injury or other accident occurred while working on site.
- Hydrologic stability. It was desirable to have a site at which large or rapid fluctuations in water level or flow rate did not occur.
- Representability of conditions prevalent in other wetlands. A number of constructed wetlands sites were available for the study; however, at these sites plants were at most five years old, so that litter accumulation and build up of a humic layer were occurring at a more rapid rate than at other sites. These sites were therefore considered unsuitable as they would be unrepresentative of both natural wetlands and constructed wetlands in a fully mature state.
- Topography surrounding the site. Steep slopes around the site would be unsuitable as wind conditions at the water surface would be low and difficult to interpret.
- The presence of potential hazards at the site such as bush fire, vandalism and

contaminants in the water.

- Ongoing research being performed at the site by other researchers, leading to possibilities of maximising the research advantage through collaboration.
- The presence of a relatively homogenous monoculture of macrophytes so that results could be easily interpreted.

Potential sites that were evaluated, the methods used to evaluate them, features of the sites and literature relevant to the sites are presented in Table 2.2.

All sites had their particular advantages and disadvantages. The proximity of the wetlands in Manly Dam reserve was eventually the deciding factor as these wetlands could be accessed within fifteen minutes by car and foot, or by 30 minutes by car and boat.

Further advantages of the Manly Dam site were that the wetlands were in a quite mature state, homogenous monocultures of *Typha orientalis* and *Schoenoplectus validus* were present at one site, Site A, while the other site, Site B, had a single homogenous monoculture of *Typha orientalis*. Some water quality information was available for the dam (Cheng, 1993), and the rangers had in place a program of weekly water quality monitoring for water in the dam.

The Manly Dam site was also considered fairly safe from vandalism, and full access to the wetland was assured by the Park Manager for the Reserve, Mr Chris Buckley of Warringah Shire Council. It was known that the water level in the dam could fluctuate markedly over a 12 month period, but there was little concern that the water level would fluctuate rapidly from day to day as water levels in the dam were monitored and regulated as necessary by Sydney Water.

Minor disadvantages were that the surrounding topography was steep, the site could only be accessed by four wheel drive, boat or foot and there was little other ongoing research at the site.

Table 2.2. Evaluation of Field Sites

Site	Evaluation Techniques	Comments	References
Byron Shire wetlands (North Coast, NSW)	Site visits and interviews with onsite researchers and others familiar with the site	Full scale constructed wetland polishing tertiary treated municipal wastewater. **Advantages**: Ongoing active research at the site investigating performance of the wetland for nutrient removal, low risk of vandalism. **Disadvantages**: large distance from WRL (9 hour drive), immature wetland.	Bavor *et al* (1992)
Carcoar wetlands (Western Plains, NSW)	Interviews with onsite researchers and others familiar with the site	Full scale constructed wetland for removal of nutrients from rural runoff. **Advantages**: some research into nutrient removal at the site. **Disadvantages**: five hour drive from WRL, immature wetland, unknown vandalism risk.	White *et al* (1992)
Curl-curl lagoon (Northern Beaches, Sydney, NSW)	Site visits and interviews with onsite researchers and others familiar with the site	Littoral zone vegetation around Curl-curl lagoon. **Advantages**: 15 minute drive from WRL, water quality monitoring programme, mature wetland. **Disadvantages**: No known active research programme, very high risk of vandalism.	
Lett St wetlands (Katoomba, NSW)	Site visits and interviews with site operators and others familiar with the site	Pilot scale constructed wetland for treatment of urban runoff. **Advantages**: monitoring of nutrient and heavy metals removal. **Disadvantages**: two hour drive from WRL, high risk of vandalism, immature wetland	Swanson (1995)
Manly Dam reserve wetlands (Northern Beaches, Sydney NSW)	Site visits and interviews with the Park Manager and others familiar with the site	Littoral zone vegetation at two sites in side arms of Manly Dam **Advantages**: mature wetland, regular water quality monitoring of the dam water, 15 minutes from WRL, minor risk of vandalism **Disadvantages**: no current research program is active, access only by 4WD, boat or foot.	Cheng (1993)

Minmi wetlands (Hunter Valley, NSW)	Site visits and interviews with persons familiar with the site	Full scale constructed wetland polishing secondary treated municipal wastewater. **Advantages**: Ongoing research at the site for performance of the wetland for nutrient removal, mature wetland, low risk of vandalism **Disadvantages**: 2 hour drive from WRL	
Narrabeen lagoon (Northern Beaches NSW)	Site visits and interviews with persons familiar with the site	Littoral zone vegetation surrounding Narrabeen lagoon. **Advantages**: 20 minute driven from WRL, mature wetland. **Disadvantages**: no known active research program, estuarine wetland, high risk of vandalism.	
Raymond Terrace wetlands (North Coast, NSW)	Site visits and interviews with onsite researchers and others familiar with the site	Pilot scale wetlands for treatment of woodmill wastewater. **Advantages**: some research into removal of complex hydrocarbons from wastewaters by wetlands, low vandalism risk. **Disadvantages**: two hour drive from WRL, immature wetland.	
Richmond wetlands (Western Sydney, NSW)	Site visits, interviews with onsite researchers and others familiar with the site	Pilot scale constructed wetland. **Advantages**: established for research into nutrient removal from secondary treated municipal wastewater, low risk of vandalism. **Disadvantages**: 90 minute drive from WRL, very immature wetland	Maslen and Schulz (1995)

The Site A wetland, was monitored for six months from July 1994 to December 1994, when drought conditions caused the water level in the dam to drop, thereby draining the wetland. Fortunately, Site B was situated at a lower elevation and thus had not been affected by the drought.

2.4. SITE DESCRIPTIONS

This section contains descriptions of Manly dam, the water body with which the wetlands studied are associated, the Manly dam catchment and the two wetlands that were investigated.

2.4.1. MANLY DAM

Manly dam is a small freshwater reservoir used for recreational activities and as a water supply to two hydraulics laboratories and a golf course. Figure 2.2 presents a plan of the catchment and Figure 2.3 shows the dam and surrounding areas from the upper part of the catchment looking South East.

The dam has a maximum operating depth of approximately 20 m, and a design operating depth of about 18.1 m at the wall. Its maximum surface area is 32 ha and maximum volume is 2 Gl (Cheng, 1993). Cheng (1993) also reports that the lake is approaching an eutrophic condition due to the loadings of phosphates and nitrates entering the lake from the surrounding land areas. Secchi depths recorded in 1991 showed values between 0.86 m and 1.60 m, with an average value of 1.16 m and standard deviation of 0.3.

Land uses in the dam's catchment include a golf course, a nature reserve and low density residential areas.

To combat outbreaks of blue green algae, one of which was particularly severe in 1988, a 3.2 kW flygt propeller mixer was installed to destratify the reservoir at the beginning of 1991. The propeller is 2.1 m in diameter, rotates at 33 rpm and is in operation for 8 hours per day in summer, 6 hours in autumn and spring and 4 hours in winter (Chris Buckley, personal communications, 1995). Mechanisms by which stratification is related to algal growth are discussed in Cheng (1993). This destratification has so far been quite successful, with no outbreaks noted since its introduction.

Figure 2.2. Plan of Manly Dam

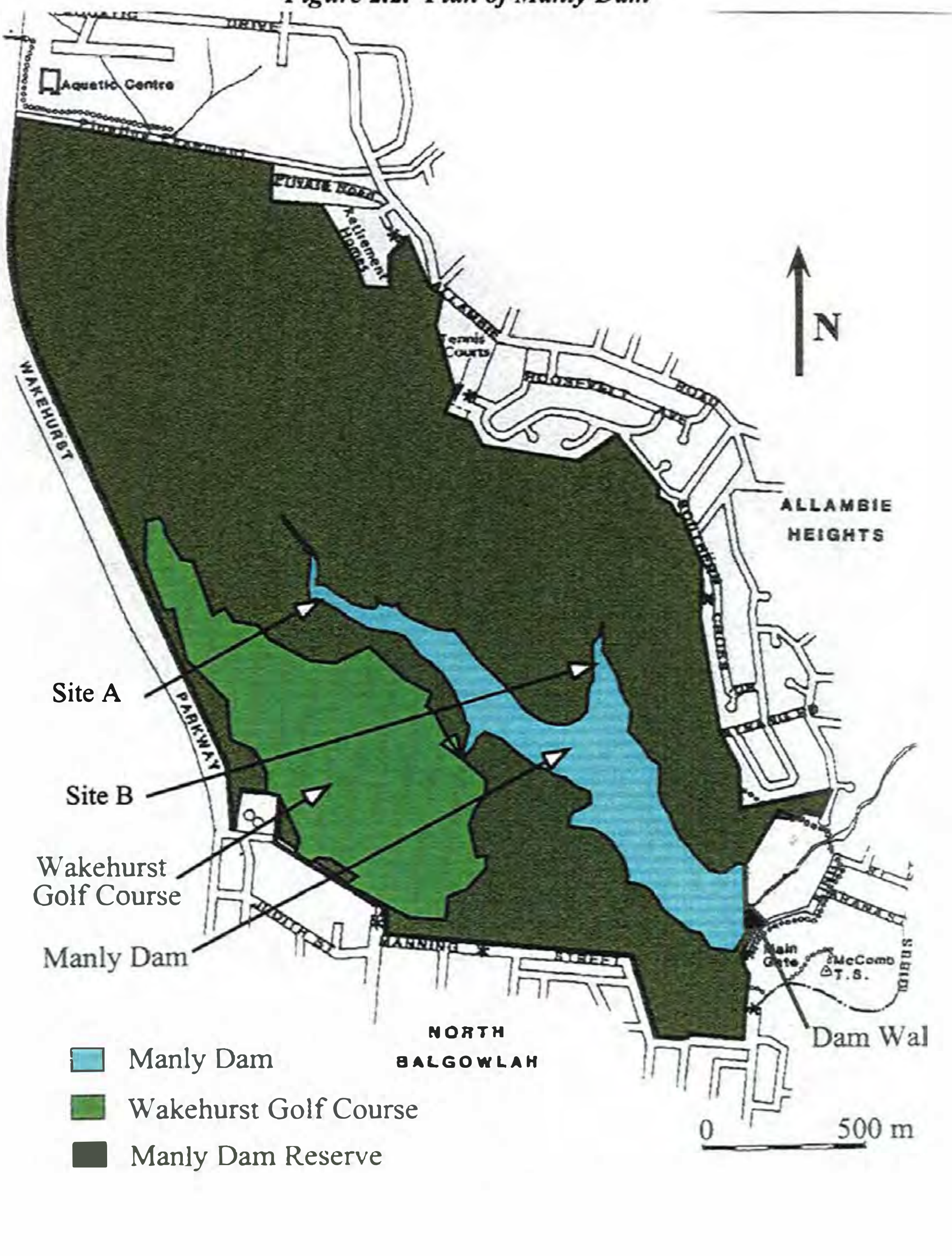

The thermocline in the dam occurs through summer, typically at depths of 4 to 5 m (Cheng, 1993), by comparison, the average depth of water in both wetlands is only 0.5 to 1 m. The impeller is expected to have minimal effect on the wetland the aim of the destratification, as its function is to break down the thermocline that would normally be present in the reservoir, rather than to disturb mixing and stratification development immediately below the water surface.

SEICHING IN MANLY DAM

Seiching is the periodic change in water level in a lake due to harmonic oscillation. From Hutchinson (1957), the seiching period is given by:

$$T_n = \frac{2l}{n\sqrt{gH_l}} \qquad 2.1$$

where l is the lake length, n is the harmonic number of the disturbance, g is gravity and H is the average lake depth. For the wetland in Manly dam, two lengths need to be considered, the overall length of the lake, and the length from the dam wall to the wetland, as the wetland is in its own embayment.

Figure 2.3. View looking to the South East over the Manly Dam Catchment

From Figure 2.2, the total lake length can be seen to be approximately 2000 m, while the distance from the dam wall to the wetland is around 1000 m; so oscillations between the dam wall and the wetland will occur close to the even harmonics of the oscillations in the main lake.

From Cheng (1993), the average lake depth is approximately 7.5 m, thus the first harmonic of the lake is approximately 460 seconds or 8 minutes. Any effects that are observed to occur on a time scale of approximately 8 minutes or multiples thereof should therefore be treated with caution.

2.4.2. SITE A

The site originally studied was a small wetland, approximately 500 m^2 in area within Manly Dam Reserve. Investigations were performed here between June and December 1994. Figure 2.4 is a schematic diagram of the site and Figure 2.5 shows the site looking towards the North West. When the dam is at its design water level, the average depth of water in the wetland is 0.5 m.

The site can be considered to consist of three separate regions:

- a large open water region in the middle of the site;
- a region dominated by the emergent macrophyte *Typha orientalis* along the southern bank; and
- a region dominated by another emergent macrophyte *Schoenoplectus validus* on the northern bank of the site.

At the commencement of the study, the *Typha* was in senescence; however there was still significant vegetative matter both in and above the water column. As the study proceeded, new shoots appeared in the *Typha* as spring advanced. Note that the *Typha* was present as a large single patch, at the bank of the wetland, however, the *Schoenoplectus* was present in sporadic clumps surrounded by open water.

Figure 2.4. Plan of Site A

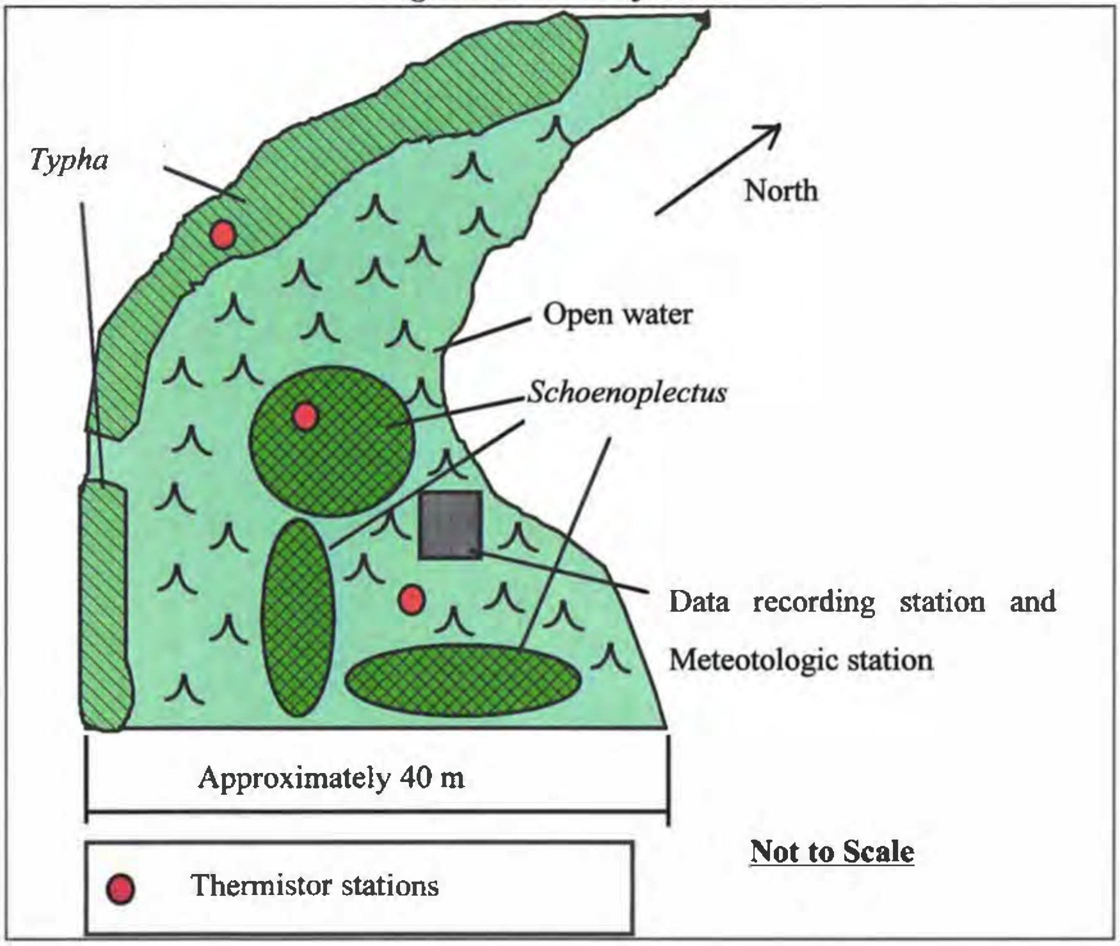

2.4.3. SITE B

As described above, due to drought conditions applying over the spring of 1994 and summer of 1994 to 1995, it was necessary to relocate long term monitoring equipment to another site, as the water level in the dam fell by approximately 800 mm, leaving the bed of Site A above the water line.

The second site, Site B, was located in a drowned creek bed, that drains into Manly dam from the North. Figure 2.6 is a plan of the site and Figure 2.7 is a photograph of the site taken from the South East along the Northern side arm of the dam.

Figure 2.5. View of Site A from the South East,
This Photograph was taken prior to the installation of monitoring equipment.
The Schoenoplectus stand studied is on the right, surrounded by open water.
The Typha stand studied is in the background on the left

Investigations at Site B took place between February 1995 and June 1996. At the commencement of the investigations at Site B, the wetland had a mean depth of approximately 400 mm. Following water level rise after intense, sustained rainfall which returned the water levels in the dam to their normal operating height in early March, the mean depth was approximately 1100 mm.

The wetland at Site B is approximately 250 m^2 in area. When the dam is at its design water level, the average depth of water in the wetland is 1.0 m.

The site is directly connected to the lake and consists of two distinct regions: a large region dominated by the emergent macrophyte *Typha orientalis*, and a small open water region that is separated from the lake by the *Typha*, as shown in Figure 2.6.

Figure 2.6. Plan of Site B

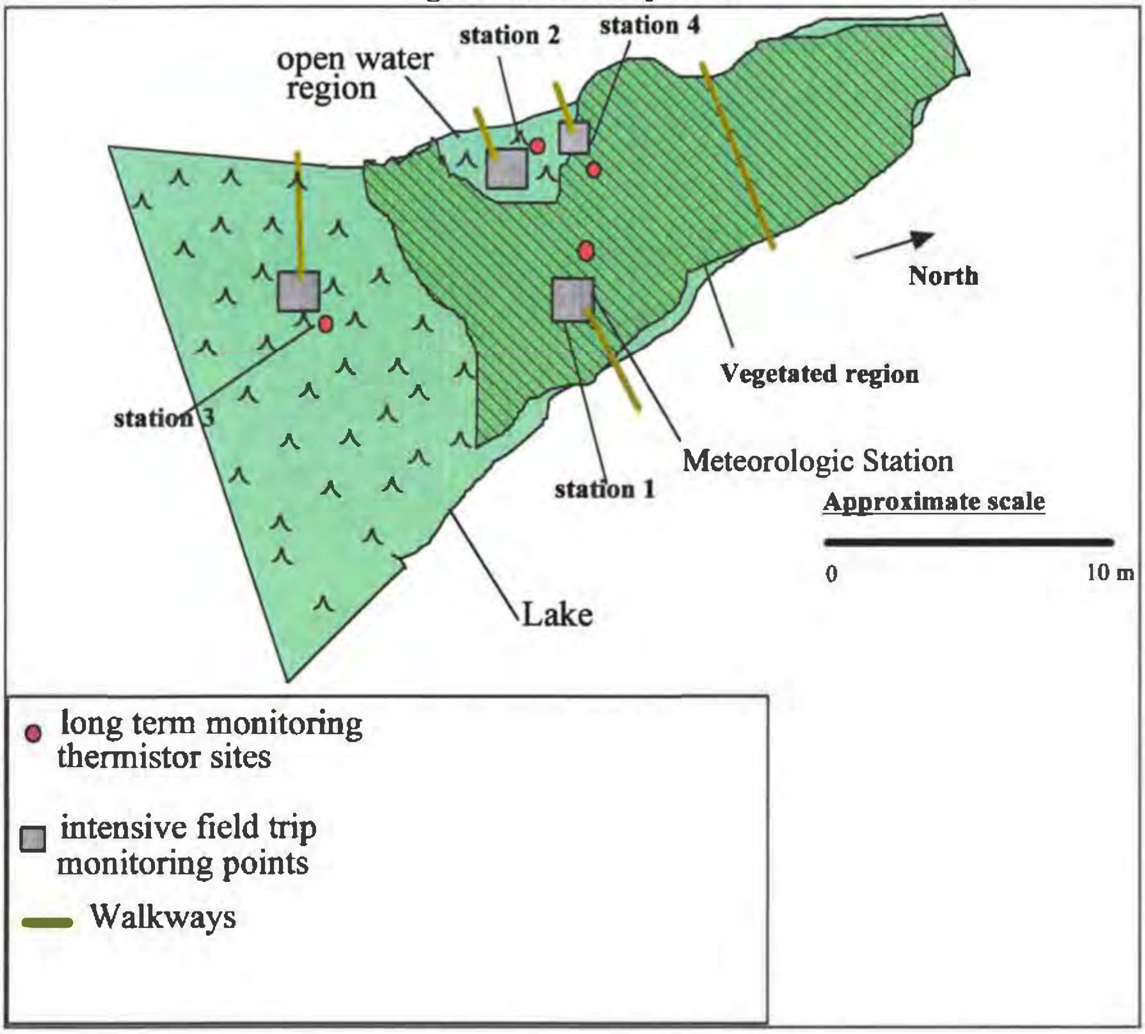

2.4.4 TERMINOLOGY

To avoid confusion, the following terminology has been adopted through the rest of this document. The water contained behind Manly dam is referred as "the lake" or "the reservoir but does not include the Site A or Site B wetlands. The phrase "open water" means any unvegetated areas close enough to macrophyte vegetation that the hydrodynamics there are significantly affected by the presence of the vegetation. The term "wetland" refers to a water body that contains sufficient macrophyte vegetation that these macrophytes play a significant role in determining the hydrodynamics of the water body. As such a wetland may be completely vegetated or may consist of both vegetated and open water areas, as long as the hydrodynamics of the open water areas are significantly affected by the presence of the vegetation.

2.5. EXPERIMENTAL TECHNIQUES

As described in Section 2.1, experiments were conducted in two phases, long term monitoring, and intensive monitoring. The techniques used for these two phases of monitoring are described separately below.

Figure 2.7. View of Site B from the South East
with the Northern Side arm of Manly Dam in the Foreground

2.5.1. LONG TERM EXPERIMENTS

Monitoring equipment used at the two sites consisted of:

- A meteorologic station recording rainfall, wind speed and direction, air temperature, relative humidity and solar radiation. This equipment was used to determine the general meteorologic conditions, thereby helping describe the conditions to which the wetland was subject during the investigations, and specifically, allowing wind speeds to be measured and heat fluxes to be calculated, as described in Chapter 3.
- 16 thermistors for recording temperatures within the water and in air below the plant canopy. Recording water temperatures allowed assessments to be made of the seasonality of stratifications in the open water and vegetated zones and buoyancy fluxes between the vegetated and open water areas. Temperature stratification is considered in detail in Chapter 3 and buoyancy driven convection is described in Chapter 5. Seasonality is considered in Chapter 6. Note that detailed investigations into stratification and buoyancy fluxes required the more sophisticated equipment used during the intensive monitoring, see Section 2.2.3.
- A data logger to record data from the thermistors.
- Water levels at the wetland were recorded using a pressure transducer; however, readings from the transducer were unreliable, therefore water level data was obtained from a recorder at the dam wall operated by the NSW Department of Public Works and Services Manly Hydraulics Laboratory (MHL).

It was also planned to use three wave probes to determine the impacts of surface water waves on water motion in the wetland and the damping effect of the wetland vegetation on surface waves; and a pressure transducer to determine water levels at the site itself. However the wave probes were not constructed in time for deployment and their use would have required a major reconfiguration of the data logger.

Specifications of all equipment used, and details regarding their calibration, are given in Appendix A.1. Throughout the long term monitoring, readings were generally taken from all instruments on an hourly basis; however during the intensive monitoring investigations readings from the meteorologic station were made every 6 minutes. From 1524, 11.7.95 to 1644, 12.7.95 thermistor readings were taken every minute to confirm that readings on an hourly basis were sufficiently representative of the state of the water column. The meteorologic station has an internal electronic data logger that records all meteorologic parameters. Readings from the thermistors were recorded by a 20 channel data logger.

Figure 2.8 is a photograph of the long term monitoring equipment as deployed at Site A.

2.5.3. LONG TERM EQUIPMENT INSTALLATIONS

METEOROLOGIC EQUIPMENT

At Site A the meteorologic equipment was installed in the open water section, at the location shown in Figure 2.4. A scaffold tower was erected, to which a pole was attached, as shown in Figure 2.8. The wind vane, anemometer and solar radiation sensor were set on top of the pole 3.3 m above the water level, approximately 1 m above the plant canopy. The instruments were placed at this height to minimise the risk of vandalism. Instruments could not be placed at the standard height of 10 m as the instrument tower would have been unstable due to the underlying loose sand, which made poor foundation material. The site was not accessible enough to bring in equipment to build a more robust structure.

To calculate sensible and latent heats, it was necessary to apply a correction factor to the wind velocity readings that were taken 1.0 m above the plant canopy, to make them equivalent to readings at the standard height of 10m above the water surface. Wind velocities above surfaces follow a logarithmic distribution (Schlichting, 1951); which is given by:

$$U_a = u_* \ln\left(\frac{y}{y_0}\right) \qquad 2.2$$

Where: U_a is the air velocity at height y above the surface;

u_* is the friction velocity at the surface; and

y_0 is the roughness height, a coefficient determined by the surface roughness of the boundary (here the plant canopy).

To use the logarithmic velocity profile to predict the velocity at the 10m height from that at 1.0m would require the estimation of a roughness height for the surface, that is, the plant canopy. However, the roughness height is difficult to specify for non solid surfaces such as plant canopies. Furthermore, it may be argued that the use of the conventional logarithmic velocity distribution is not valid above a plant canopy (Webster, 1997) as the surface is not solid.

Figure 2.8. Meteorologic Equipment and Data Recording Equipment
Photograph taken looking East with Open Water Thermistors on the left, Meteorologic Station and Data Logger Housing on the Scaffolding

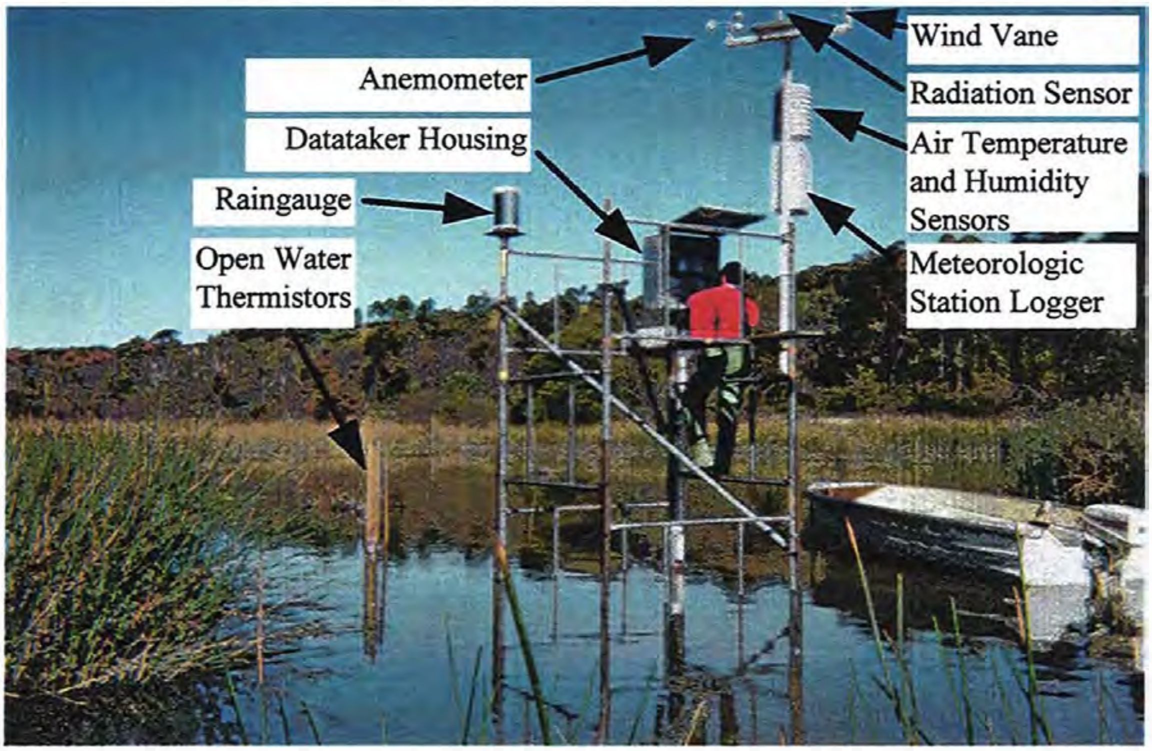

To overcome these problems, the $^1/_7$ power law was assumed to apply from the ground level to 10 m. The advantage of the $^1/_7$ power law is that no assumption of a roughness height is necessary. The $^1/_7$ power law can be expressed as:

$$U_a \propto y^{\frac{1}{7}} \qquad 2.3$$

Using this proportionality, the relationship between the velocity at 10 m and at 1.0 m above the plant canopy is:

$$\frac{U_{a10}}{U_{a1}} \propto \left(\frac{10}{1.0}\right)^{\frac{1}{7}} \qquad 2.4$$

Where U_{a10} is the air velocity 10 m above the canopy and U_{a1} is the velocity 1.0 m above the canopy. Unfortunately, as for the logarithmic law, the $^1/_7$ power law can be criticised on the basis that it may not hold above a plant canopy. Without more detailed knowledge of the air velocity profile, a more detailed correction could not be applied, furthermore an examination of the exact form of the velocity profile above plant canopies was not one of the objectives of the thesis. Considering these two factors, the $^1/_7$ law was adopted to correct the air velocity readings to give estimated air velocities at 10 m above the water surface.

The rain gauge was installed at the top of a 3 m pole, 1.5 m from the other meteorologic sensors. It can be seen on the corner of the scaffolding opposite the meteorologic station in Figure 2.8.

Installation of meteorologic equipment at Site B was performed in the same manner as at Site A, except in this case the equipment was installed within the plant stand as shown in Figure 2.6. The plant canopy was 3 m above the water level, so the wind vane, anemometer and radiation sensor were raised to 4 m above the water level to minimise boundary layer effects.

THERMISTOR DEPLOYMENT, SITE A

At Site A, thermistors were deployed in three assemblies, one each in the open water, *Schoenoplectus* and *Typha* regions as shown in Figure 2.9. The open water assembly can be seen in Figure 2.8 to the left of the tower.

The *Schoenoplectus* region was concentrated on as it was the area least likely to be vandalised. Seven thermistors were deployed here as follows.

- Three thermistors were suspended from a float, at depths below the water surface of 50, 100 and 150 mm.
- Three thermistors were placed at fixed depths of 50, 100 and 150 mm above the bed.
- One thermistor was placed on top of the float to monitor temperature in the air immediately above the water column, but below the canopy of the plants.

This pattern of deployment with depth was adopted for the following reasons:

- To ensure that readings from would be obtained from all thermistors with changing water level.
- To give good resolution of temperature gradients near the top of the water column, where radiation fluxes could be important.
- To give good resolution of temperature gradients near the bottom of the water column, where fluxes through the bed could be important.

There was concern that aligning the probes vertically as shown in Figure 2.9 would lead to false readings should stratification be present, as the 100 mm long metal body of the probe might conduct heat towards or away from the thermistor. To minimise such effects the probes were shielded in PVC to increase their thermal inertia. Checks made during calibration confirmed that with the PVC shielding, temperature gradients along the body of the thermistor had negligible effect on the temperatures recorded at the tip.

Figure 2.9. Thermistor Deployment, Site A

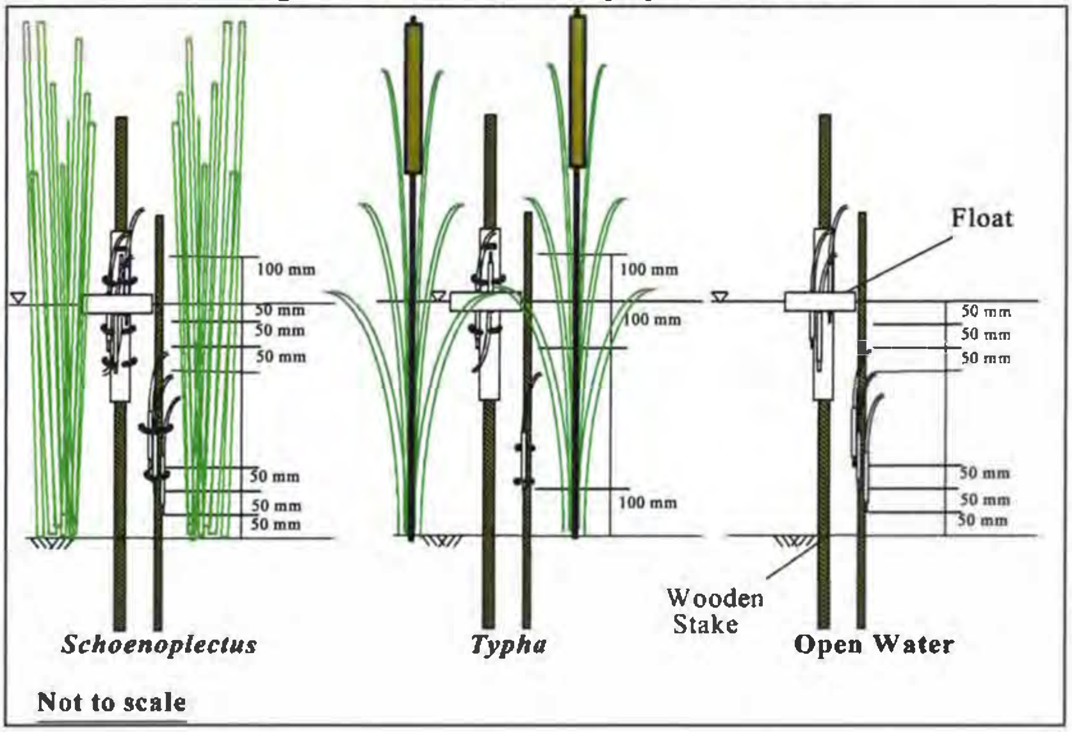

In the open water zone, six thermistors were deployed in the water column. These were in the same arrangement as in the *Schoenoplectus* stand; however, a thermistor was not deployed on top of the float in the air, as air temperature outside the canopy was being monitored at the meteorologic station.

In the *Typha* stand, three thermistors were used, one located 100 mm above the bed, one floating 100 mm below the water surface and one in air below the plant canopy.

Floats for the thermistors were made from PVC pipe of 45 mm diameter and 200 mm length, attached to a disc-shaped solid foam float, 100 mm in diameter and 60 mm long, as shown in Figure 2.9. Holes were drilled through the float, through which the thermistors were inserted and secured to the PVC pipe.

Thermistors at the base of the wetland were attached to a piece of marine ply, which was then secured to a wooden stake 80 mm from the stake the float was installed on.

Placing the fixed thermistors adjacent to, rather than directly under the floating thermistors ensured the floats had the maximum possible range of movement, in the event of low water levels.

Non metallic components were used wherever possible so that heat fluxes through the experimental set up were negligible, ensuring that observations were representative of the normal state of the wetland.

Each thermistor was calibrated seperately (see Appendix B). To ensure that thermistors were easily identified, they were labelled from A to Q. Thermistor locations are shown in Table 2.3 and Figure 2.6.

THERMISTOR DEPLOYMENT, SITE B

At Site B the thermistors were deployed in four assemblies, as shown in Figure 2.10. Two assemblies were deployed in the *Typha*, these were designated as Stations 1 and 4. One assembly was deployed in the sheltered open water section, designated as Station 2 and the remaining assembly was deployed in the shallows of the lake side arm, approximately 4 m from the vegetation, designated as Station 3. Locations of thermistors at Site B are given in Table 2.3.

The greatest concentration of thermistors was at Station 1. Thermistors were arranged in the same manner as at Site A, except that no thermistor was deployed 150 mm above the bed so that an additional station at Site B could be monitored. At Station 2, the probes were deployed in the same way as at Station 1, however no probe was used to measure air temperature. At Stations 3 and 4, probes were located 100 mm below the water surface and 100 mm above the bed. An extra probe was also used for air temperature monitoring at Station 4.

Figure 2.10. Thermistor Deployment, Site B

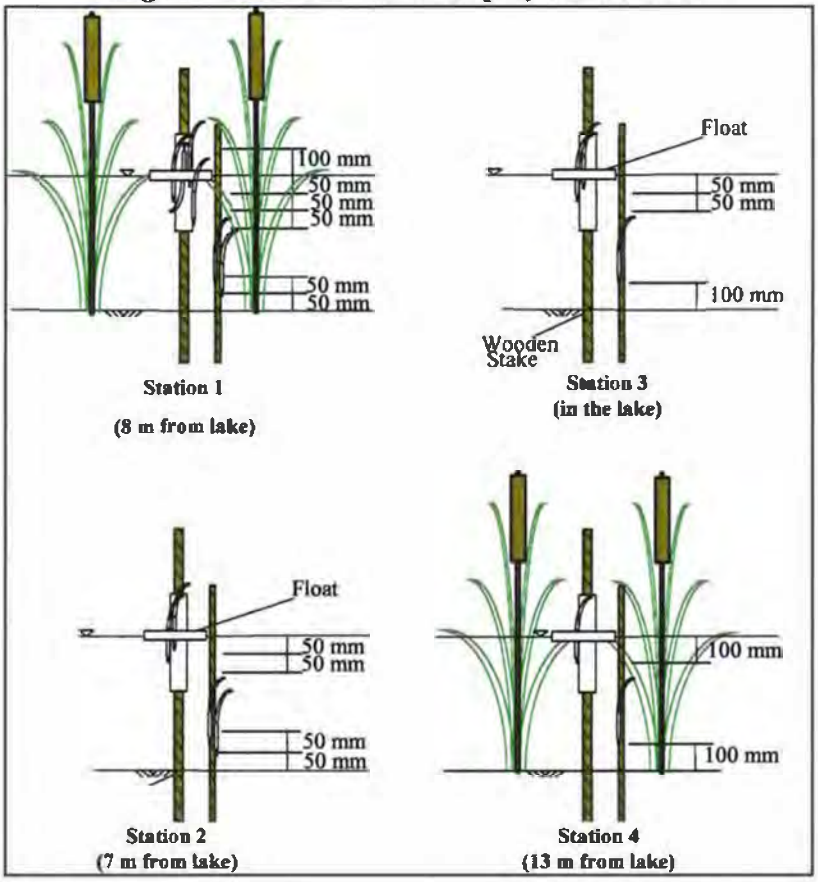

This pattern of deployment was chosen to:

- determine the influence of the lake dynamics on stratification and mixing in the wetland;
- Investigate differences between stratification and mixing in the vegetated and unvegetated areas;
- Assess the variability of stratification and mixing within a monocultural stand of plants.

DATA LOGGER

At both Site A and Site B the DT505 (Datataker) logger was installed inside a solid plastic enclosure wired to D9 connectors at the box to allow the leads from the thermistors to be connected to the logger. A connector was also installed on the box to allow RS232 communications. These connections made installations and data downloads at the field site much easier, ensured that there was no possibility of connecting probes to the wrong channels and allowed the logger or any of the probes to be easily detached in the event of breakdowns. This whole assembly was then installed in a large galvanised steel electrical meter box. The meter box ensured good protection from environmental conditions and vandalism. The meter box was mounted on the scaffolding adjacent to the meteorologic station, as shown in Figure 2.8. The box was located 3 m above the water level ensuring minimal risk of vandalism, flooding or bushfire damage.

Table 2.3. Thermistor Deployment, Sites A and B

	Site A		**Site B**	
Thermistor	**Location**	**Depth**	**Location**	**Depth**
A	*Schoenoplectus*	100 mm above surface	Station 1, *Typha*	100 mm above surface
B	*Typha*	100 mm above surface	Station 1, *Typha*	50 mm below surface
C	*Schoenoplectus*	50 mm below surface	Station 1, *Typha*	100 mm below surface
D	*Schoenoplectus*	100 mm below surface	Station 1, *Typha*	150 mm below surface
E	*Schoenoplectus*	150 mm below surface	Station 1, *Typha*	100 mm above bed
F	*Schoenoplectus*	150 mm above bed	Station 1, *Typha*	50 mm above bed
G	*Schoenoplectus*	100 mm above bed	Station 4, *Typha*	100 mm below surface
H	*Schoenoplectus*	50 mm above bed	Station 4, *Typha*	100 mm above bed
I	*Typha*	100 mm below surface	Station 2, *Open*	50 mm below surface
J	*Typha*	100 mm above bed	Station 4, *Typha*	100 mm above surface
K	*Open water*	50 mm below surface	Station 2, *Open*	100 mm below surface
L	*Open water*	100 mm below surface	Station 2, *Open*	150 mm below surface
M	*Open water*	150 mm below surface	Station 2, *Open*	100 mm above bed
N	*Open water*	150 mm above bed	Station 2, *Open*	50 mm above bed
O	*Open water*	100 mm above bed	Station 3, *Open*	100 mm below surface
P	*Open water*	50 mm above bed	Station 3, *Open*	100 mm above bed

2.5.4. LONG TERM MONITORING TECHNIQUES

For the long term monitoring, the DT505 and meteorologic station data logger were set to log the thermistors and meteorologic parameters hourly. It had been hoped to perform such logging continuously over a 12 month period; however, drought conditions over the second half of 1994 meant that the water level at Site A dropped until the entire wetland dried up forcing a change of sites. Furthermore, equipment failures at various times led to gaps in the data, so the final data set was composed of series of hourly readings of temperature at the two sites. There were significant gaps in both sets of data. Details of the data collected and problems encountered are discussed in Chapter 6.

The data loggers for the meteorologic station and the thermistors were generally downloaded weekly. Both had the capacity to log for much longer periods of time, but weekly downloading ensured that the risk of loss of large quantities of data was limited. Longer time intervals between downloads were experimented with in the early stages of the monitoring period, which occasionally resulted in large gaps in the data, when downloads were unsuccessful due to equipment malfunction.

2.5.5. INTENSIVE INVESTIGATIONS

A one week period of intensive monitoring was carried out at Site B in February 1995. The purpose of the intensive monitoring was to determine temperature and velocity profiles over the full depth of the water column and the changes that would occur in profiles with diurnal changes in meteorologic parameters. Specific features it was desired to investigate were stratification, wind mixing, penetrative convection, buoyancy driven convection and wind driven convection.

A series of experiments investigating solar radiation and wind velocities within the plant canopy were also carried out.

To allow investigations to be conducted with minimal disturbance to water column, four sets of scaffolds were constructed at Site B, each adjacent to one of the thermistor stations. These scaffold locations are shown in Figure 2.6 as the intensive field trip monitoring points. Planks were laid above the water surface from the bank to the monitoring points to allow access for equipment to be placed in position without disturbing the water column.

Adjacent to each of the monitoring points, sets of rails were installed to allow instruments to be lowered into the water column and in the same location quickly and smoothly. The layout of the scaffolds and rails are shown in Figure 2.11.

Specifications of all probes used in the intensive investigations are given below, followed by descriptions of the deployment and monitoring techniques used for the profiling equipment. Canopy experiments were sufficiently straightforward that it is not necessary to give separate descriptions of their deployment and monitoring techniques.

Figure 2.11. Profiling Equipment Set up

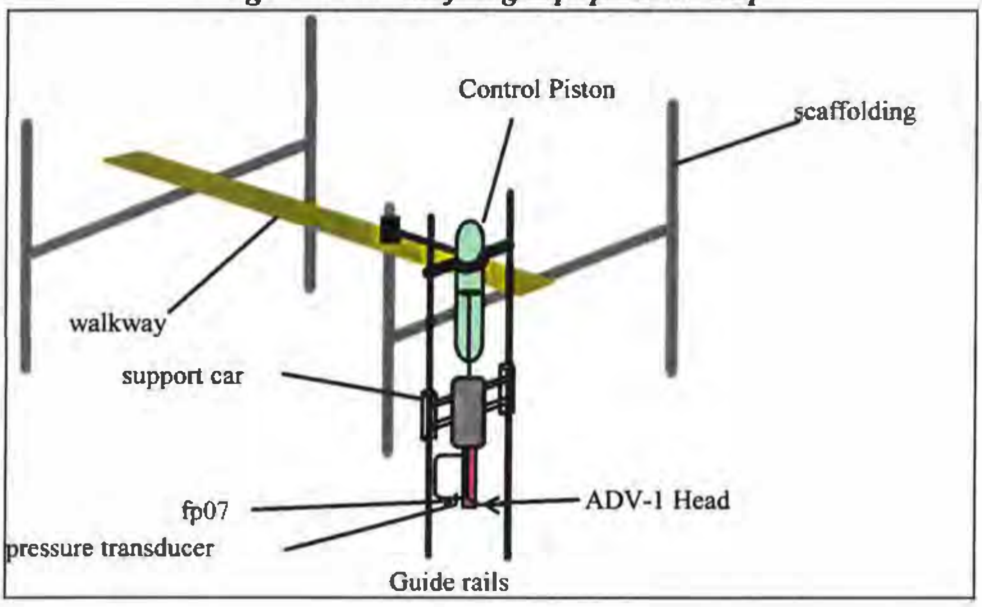

2.5.6. INTENSIVE INVESTIGATIONS, EQUIPMENT SPECIFICATIONS

Equipment used for intensive monitoring consisted of:

- A temperature profiler which measured temperature and depth. A thermometrics FP07 fast tip response thermistor was used for temperature measurements. The FP07 has a nominal resistance of 100 kΩ at 25 °C, thermal time constant of 0.007 s on water plunge and a dissipation constant of 0.25 mW/°C in still water. They are described in detail in the Thermometrics thermistor catalogue (1986). Depth was measured using a Keller PAA-10 pressure transducer, which uses a piezoresistive active 4 arm bridge to record absolute pressure. Full details are provided in Carter *et al* (1985). Depth and temperature readings from the microprofiler were sampled at 43 Hz. Signals from the PAA-10 and FP07 were routed through an analog-digital converter, then to the serial port of a laptop PC.

- An ADV-1 Acoustic Doppler Velocity probe was used to measure water velocities. The probe transmits an acoustic signal at 10 MHz from a single transducer. Three receiver transducers at 120° azimuth angles are oriented to receive the transmitted signal when it is backscattered from particles or bubbles within a sampling volume of 250 mm^3 located 50 mm from the transmitting transducer. Signal processing to measure doppler shifts in the acoustic signal received back from the sample volume is performed by a processing module which attaches to the serial port of a laptop PC. Having three transducers on different alignments allows a three dimensional velocity field to be described. The probe was operated with a velocity range of 0 to 30 mm/s, to an accuracy of 0.5 mm/s. The x, y and z velocity components from the ADV-1 were obtained at 25 Hz.

- Meteorologic parameters were recorded on a six minute interval using the meteorologic station, which is described in the long term monitoring specifications section.

- A TSI 1640 Omnisensor hot bulb anemometer was used to measure air velocities. Velocity profiles were taken by raising the TS50 sensor through the canopy on a bracket attached to a 4 m long stainless steel pole as shown in Figure 2.12. The pole was driven into the ground below the wetland until it was quite stable and air velocity readings were taken at 0.2 m, 0.5 m, 1.0 m and then at 0.5 m intervals until the top of the pole was reached. Readings were taken by observation of the readout on the face of the instrument.

- A Li-Cor LI-192SA quantum sensor was used to take solar radiation profiles in the plant canopy. Profiles were taken by attaching the probe to the bracket with the TSI1640, as shown in Figure 2.12. Readings were recorded as a voltage signal from the probe by a DT50 data logger.

Readings were taken by setting the probe at a fixed height for 5 minutes and recording the minimum velocities under "still" conditions, the maximum velocities under "still" conditions, and maximum velocities under "gust" conditions. After these readings had been taken, the anemometer was moved up to the next height. Performing the readings in this manner meant it was not possible to relate the readings from the meteorological station anemometer to readings in the canopy as the meteorologic station anemometer was set to record hourly average velocities only.

2.5.7. INTENSIVE INVESTIGATIONS, EQUIPMENT DEPLOYMENT

Water column profiling was performed using a free falling carriage system. The ADV-1 and microprofiler were attached to a carriage which was mounted on a set of rails, as shown in Figure 2.11, allowing the probes to be moved up and down through the water column. It was only necessary to move the carriage, with ADV-1 and microprofiler mounted, between sites as a set of rails was installed at each station. Figure 2.13 is a schematic diagram showing the features of the carriage system.

Figure 2.12. Canopy Air Velocity and Radiation Measurement Equipment

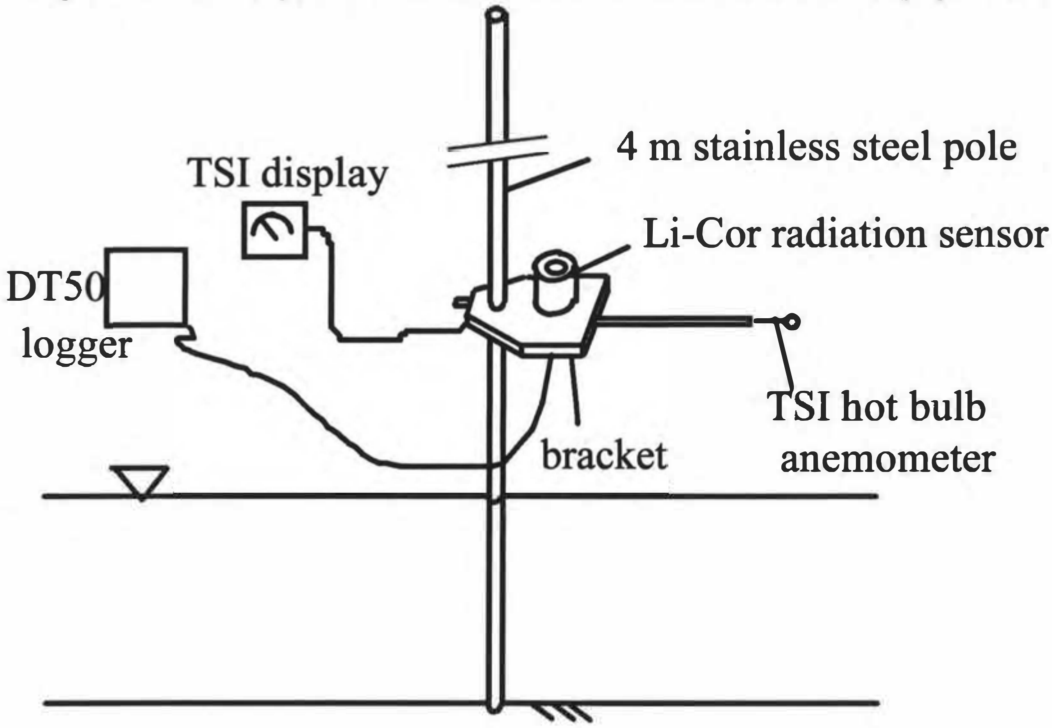

Teflon bushes between the rails and the carriage ensured the carriage fell as smoothly as possible, as it was intended to sample velocity profiles through the water column using the ADV. The carriage fell under its own weight, moderated by a braking piston which slowed the fall rate to a fairly constant rate of about 100 mm/s. The braking piston is shown in Figure 2.13, it had a maximum fall range of 1.0 m; this was quite adequate as depths at each site were between 480 mm and 800 mm.

The ADV-1 was powered by two 12 V, 25 Ah lead acid batteries connected in parallel to give a 24 V supply. The profiler was powered by a single 12 V, 25 Ah lead acid battery. The two PCs used for logging signals from the ADV-1 and microprofiler were powered by a 12 V, 40 Ah lead acid battery, via a DC-AC inverter.

All equipment was made to be easily setup and dismantled to minimise delays in moving from one site to the next. This deployment worked well and a team of two could take two free fall profiles at each of the four stations within an hour.

Figure 2.13. Schematic of the Profiling Equipment

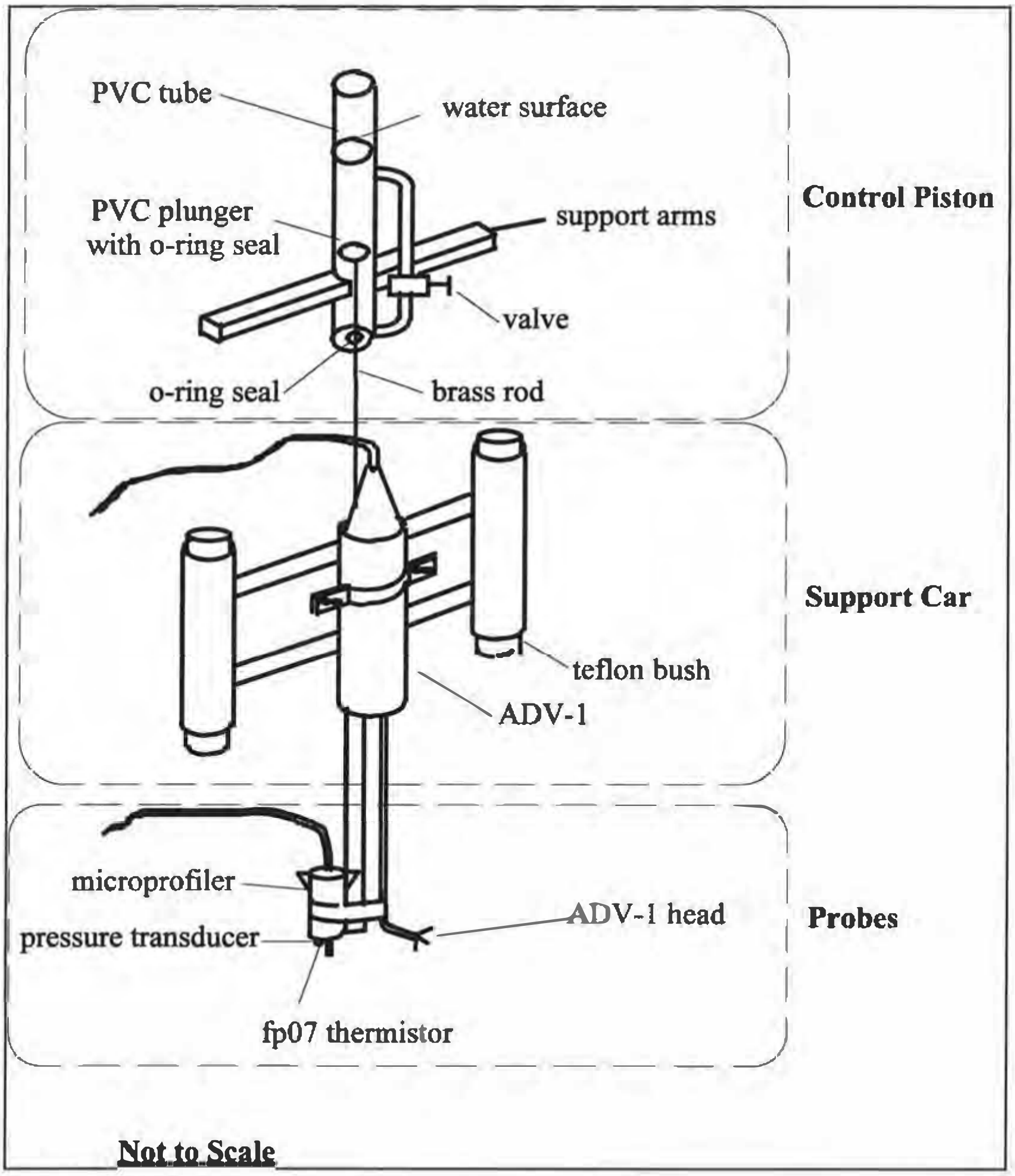

2.5.8. INTENSIVE INVESTIGATIONS, MONITORING TECHNIQUES

Data from the profiler and ADV-1 were obtained in two ways, firstly sets of two free fall temperature profiles were taken five minutes apart at each site (as later explained in Chapter 4, the ADV-1 was not able to sample accurately under this profiling scheme).

This allowed the maximum number of profiles to be collected at the site in a fixed period of time.

Secondly, a free fall temperature profile was taken, then five minutes later three fixed depth velocity time series were taken, as explained below. This allowed information on both temperature and velocity throughout the water column to be collected, however this was a much slower sampling scheme than the first one, involving only profiling.

FREE FALL SAMPLING

Free fall sampling was performed by holding the carriage with the ADV-1 and the microprofiler just out of the water, then releasing the carriage. The carriage fell to the bottom causing both probes to descend through the water column. The fall time of the carriage in 0.5 m of water was approximately 4 seconds. Considering the sampling rate of the microprofiler was 43 Hz, approximately 170 temperature readings were obtained over the depth of the profile, giving samples approximately 3 mm apart. Given the sampling rate of the ADV-1 as 25 Hz, samples were about 5 mm apart.

When free fall sampling alone was conducted, following the first free fall sample being made, the carriage was raised from the water, a period of five minutes was allowed for the effects of the movement of the probe through the water column to be dissipated, then a second free fall sample was taken. After taking the second sample, the equipment was moved to the next station to be sampled.

It was found that this procedure took about 15 minutes at each station, so that profiles from all four stations could be obtained each hour. The process required two persons, one operating the personal computers and writing field notes in a field log book, the other setting up and dismantling the ADV, profiler and support carriage at each site so that profiles could be taken.

This sampling technique was designed primarily to determine the vertical temperature structure of the water column. It was also hoped that some information of the vertical velocity structure of the water column would be obtained, however subsequent to the investigations, it was discovered that the ADV-1 had been malfunctioning, as discussed in Chapter 4, and none of its readings taken in this manner could be used.

COMBINED FIXED DEPTH AND FREE FALL SAMPLING

Fixed depth sampling was performed by lowering the carriage into the water column to a set depth, allowing the ADV-1 to log for a minimum of 60 seconds, then changing the depth of the carriage and logging again, until three samples had been obtained at that station. Depths at which samples were obtained are presented in Chapter 4, where the process is examined in more detail.

This sampling technique was designed to allow the measurement of turbulence and convection in the water column by the ADV-1 by taking samples with fixed depth, and to also give temperature structure information from the microprofiler by taking the free fall samples. Despite the problems with the ADV-1 malfunctioning, analysis of the turbulence was still possible, however analysis of the convection was not, as is discussed in Chapter 4.

The microprofiler could not be operated during fixed depth readings as the program under which it was operating would fail before the 60 s duration was reached, without allowing the data to be saved. However, since temperatures were also being obtained by the free fall sampling, this was not considered a serious problem.

When the combined free fall and fixed depth sampling routine was employed, sampling was performed by taking the three fixed depth readings, waiting five minutes, then taking a free fall reading. After the free fall reading was taken, the equipment was moved to the next station to be sample. When this mode of sampling was employed, it took approximately 90 minutes to sample from all four stations.

OPERATION OF LONG TERM MONITORING EQUIPMENT DURING THE INTENSIVE MONITORING PERIOD

During the intensive monitoring period, the thermistors were set to record at one minute intervals to allow comparison of temperature readings from the long term and intensive equipment to be made. Unfortunately a malfunction in the DT505 data logger meant that no thermistor data was obtained for the intensive monitoring period.

The meteorologic equipment was set to log all parameters as averages over six minute intervals during the intensive monitoring period; however an error in setting the logger on the first day of investigations meant that no meteorologic data was recorded at the site for the first two days. Fortunately the Macquarie University meteorologic data was available to be used in lieu of the data from the site.

2.6. SUMMARY

The experimental methods used in the field studies to meet the objectives of the overall study have been described. There were two aspects to the study, long term monitoring at sites A and B and intensive monitoring at site B. Details of the techniques used to select the sites have been provided, as have descriptions of the sites, equipment used, installation and monitoring procedures.

Having described the experimental methodology, it is now appropriate to discuss the processes involved in the following chapters.

3. HEAT FLUXES AND STRATIFICATION DEVELOPMENT UNDER LOW WIND CONDITIONS

3. HEAT FLUXES AND STRATIFICATION

Heat fluxes through the air-water interface are important causes of temperature change within the water column in many natural water bodies (Fischer *et al*, 1979). These heat fluxes include shortwave solar radiation, long wave radiation and sensible and latent heat transfers between the water and the atmosphere. The temperature changes they cause have important effects on the hydrodynamics of the water column, potentially causing stratification, mixing and convection.

Other heat fluxes into or out of a water body that may occur include heat transfer through the bed of the water column, groundwater interactions, precipitation and surface water inflows and outflows at different temperatures from the average temperature within the water column. These heat fluxes are either fairly consistent temporally (heat transfer through the bed, groundwater interactions) or are extremely intermittent in their nature (precipitation, surface water inflows and outflows).

A full study of all heat fluxes was beyond the scope of this study, as such, the most pragmatic approach was was to study the air-water interface fluxes only, as they display significant variations on a diurnal basis, occur frequently and predictably enough to be studied comprehensively, and they were expected to have significant effects on temperature stratification in the wetland.

Stratification is the process by which a water body develops density differences with depth. It can result from differences in the physical constituents of the water (such as salt or suspended solids), or from temperature differences. A water body in which less dense water overlies more dense water has a centre of mass below its centre of volume. For this case, the water body has a lower potential energy than if the density was constant with depth.

In this lower energy state more energy is required to provide the same amount of mixing as in a water body where density is uniform with depth; hence stratification markedly affects the transport of constituents due to mixing processes. Where temperature is the cause of stratification, temperature gradients above $1^{\circ}Cm^{-1}$ would be considered highly significant, and will give rise to density differences that can significantly reduce both vertical and horizontal mixing (Imberger and Patterson, 1990).

This chapter examines:

- the observed heat fluxes in open water and vegetated sections of the Manly Dam Site B wetland;
- the expected impacts of these heat fluxes on the temperature structure of the open water and vegetated sections of the wetland;
- the effects that the plant canopy will have on these heat fluxes;
- the changes in temperature that were observed to occur in open water and vegetated sections of the Site B wetland on a day when negligible wind mixing effects occurred;
- whether or not the observed changes in water temperature can be explained in terms of the heat fluxes and plant canopy effects alone.

Heat fluxes considered are: short wave solar radiation, long wave radiation and sensible and latent heat transfers at the air-water interface.

The chapter concludes that temperature changes in the wetland are not fully explained by heat fluxes incident at the water surface, and other heat transfers such as convective motion within the water column must be considered to accurately determine the temperature structure of the water column.

3.1. HEAT FLUXES INCIDENT ON THE WATER SURFACE

Fischer *et al* (1979) identifies four basic heat fluxes incident on water surfaces which affect the temperature of a water body in ways that are hydrodynamically significant. These are:

- Shortwave radiation in the visible spectrum emitted by the sun,
- The nett of long wave radiations emitted and absorbed by the water,
- Sensible heat transfer and
- Latent heat transfer.

These four fluxes are not the only factors which can affect the water temperature. Other factors that need to be considered to perform a thorough heat balance for a water body include inflows and outflows by surface or groundwater, rainfall and convective motion within the water body. Unfortunately these factors could not be examined in detail in this study.

There were no control structures in the wetland so detailed surface inflow and outflow measurement were not feasible at either site, however, it was possible to estimate inflows, outflows and heat exchange by these mechanisms in a rudimentary manner over the long term monitoring period. This is performed in Section 5.

No information on ground water was available for either site and no rainfall occurred during the periods when intensive investigations were performed.

It should be kept in mind that it is not the temperature of the water column itself that is of concern here, rather it is the effects temperature will have on hydrodynamics that is of interest. As such, it is sufficient to examine only those processes that cause significant hydrodynamic effects rather than conducting a complete heat balance.

3.1.1. SHORTWAVE RADIATION AND RESULTING TEMPERATURE STRATIFICATION

In the absence of mixing and advective processes, from Fischer et al (1979) the time rate of change of temperature, T at any location in a water body due solely to shortwave radiation from the sun penetrating the water column can be expressed as:

$$\frac{\partial T}{\partial t} = \frac{-1}{\rho C_p} \frac{\partial \phi}{\partial l_l} \qquad 3.1$$

where C_p is the thermal capacity of water at constant pressure ($Jkg^{-1}C^{-1}$), ϕ is the shortwave radiative flux that penetrates through the water body (Wm^{-2}), l_l is the distance that the light has travelled through the water column and ρ is the density (kgm^{-3}) of water.

The dependence of ϕ on l_l is commonly expressed in exponential form, see for example Henderson-Sellers (1984); this gives the mathematical expression known as Beer's Law:

$$\phi\left(l_l\right) = \phi_s \; e^{-n\, l_l} \qquad 3.2$$

where ϕ_s is the radiative flux that penetrates the surface and η is a decay constant. ϕ_s can have values in excess of 1000 Wm^{-2} under sunny conditions, as will be seen in Section 3.3.

Substituting Equation 3.2 into Equation 3.1 will give a time rate of change of temperature that is depth dependent, which can be expressed as:

$$\frac{\partial T}{\partial t} = \frac{\eta \phi_s}{\rho C_p} e^{-\eta l_l} \qquad 3.3$$

The length l is given by the equation:

$$l_l = \frac{-z}{\cos \theta_t} \qquad 3.4$$

where z is the distance from the water surface, which is defined as positive upwards in the usual manner, necessitating the negative sign, and θ_t is the angle to the vertical of the light transmitted through the water column, as shown in Figure 3.1.

ϕ_s is given by the expression:

$$\phi_s = \tau\phi_i \qquad 3.5$$

where ϕ_i is the radiation incident on the water column and τ is the transmission coefficient, which is a function of the incident and transmitted angles of light to the vertical. At an unvegetated air-water interface, τ is given by Hecht (1987) as:

$$\tau = 4n_s \cos\theta_t \cos\theta_i \left[\frac{\sin\theta_t \cos\theta_i}{\sin(\theta_i + \theta_t)}\right]^2 \qquad 3.6$$

where n_s is the Snells coefficient, θ_i is the incident angle of the radiation to the vertical and θ_t is the transmitted angle. For an air water interface, $n_s = 1.333$. Strictly speaking Equation 3.6 only holds for light with a polarisation perpendicular to the plane of incidence at the interface; however from Hecht (1987), changes in τ with angle of polarisation are minor. Kirk (1983) notes that τ does not change significantly with surface roughness due to surface waves.

θ_t is given by Snells law as:

$$\sin\theta_t = n_s \sin\theta_i \qquad 3.7$$

θ_i is a function of the time of day, time of year and latitude of the site (Meeus, 1979).

In vegetated areas, τ would be expected to be a function of θ_i, θ_t and the density of vegetation.

From tables of density dependence on temperature in fresh water in Fischer *et al* (1979), the rate of change of density due to changes in temperature, α_T, is approximately -0.24 $kgm^{-3}(^{\circ}C)^{-1}$ over the range 20 to 25 °C. Using this value of α_T

gives changes in density accurate to within 0.055 kgm^{-3}.

3.1.2. LONGWAVE AND BLACKBODY RADIATION

All materials with a temperature above absolute zero emit infrared radiation according to the Stefan-Boltzmann law, which can be expressed as:

$$\phi_{lw} = \sigma T^4 \qquad 3.8$$

where ϕ_{lw} is a radiation flux in the infra-red portion of the spectrum, and is hence referred to as the longwave radiation flux, σ is the Stefan-Boltzmann constant which is 5.67×10^{-8} $Wm^{-2}K^{-4}$, and T is temperature (which must be measured on the Kelvin scale for this calculation). When considering the heat balance of a water body, two types of longwave radiation will be significant:

- radiation emitted by water that is transferred to the atmosphere, which will be referred to as blackbody radiation and
- radiation emitted by the atmosphere transferred to the water which will be referred to as longwave radiation.

Since long wave radiation and blackbody radiation always act to oppose one another, it is the nett effect of the two factors that is the important consideration, this is given by:

$$\phi_{lw} = \sigma\left(T_w^4 - T_a^4\right) \qquad 3.9$$

where T_a is the air temperature and T_w is the water temperature. Note that with ϕ_{lw} defined in this way, the flux is considered positive if there is a nett flux from the water column to the atmosphere.

Both longwave and blackbody radiation can be considered as surface phenomenon, since the coefficient of radiative absorption for water in the infrared region of the spectrum is very high, ranging from 200 to 3000 cm^{-1} over different wavelengths in this region of the spectrum (Perry and Chilton, 1973). Such high absorption coefficients ensure that:

- all long wave radiation impinging on the water surface is absorbed within millimetres of the surface; and
- when black body radiation is emitted by water, surrounding water molecules reabsorb the radiation unless the radiating molecule is very close to the surface in which case it escapes to atmosphere.

While extreme values of long wave and blackbody radiation can be quite large, their nett effect in the wetland is typically small, as will be seen in Section 3.3.

Note that in reality, the long wave radiation entering the water column from the atmosphere generally derives from water vapour. Therefore, the temperature used to estimate these should be based on upper atmospheric temperature. However, as these effects are generally small, and this is not a central area of interest in the present study, detailed analysis of long wave radiation and black body radiation is unwarranted and use will be made of the air temperature as recorded at the on site weather station.

Changes in temperature due to nett longwave radiation are given by:

$$\Delta T = \frac{\phi_{lw} \, \Delta t}{C_p \rho \, \Delta z} \qquad 3.10$$

where all terms are as defined earlier. Note that here to be specific, Δz is the depth over which the radiation is absorbed.

3.1.3. SENSIBLE HEAT TRANSFER

Sensible heat transfer is a process (usually turbulent) that takes place at the interface between a water body and the atmosphere. It arises from the temperature difference between the water and atmosphere and may be a heat flux into or out of the water body. From Fischer *et al* (1979), values of sensible heat transfer may be calculated as:

$$H_s = C_s \rho_{air} c_p U_a (T_{air} - T_w) \qquad 3.11$$

where H_s is the sensible heat transfer (defined to be positive when heat leaves the water surface) in Wm^{-2}, C_s is the dimensionless transfer coefficient for sensible heat (1.45×10^{-3}), ρ_{air} is the density of air (1.20 kgm^{-3}), c_p is the specific heat of air (1012 $Jkg^{-1}C^{-1}$), U_a is the wind speed in ms^{-1}, 10 m above the water surface, T_{air} is the air temperature (°C) and T_w is the water temperature (°C). Values of coefficients given here are taken from Fischer *et al* (1979) for conditions of neutral stability in the atmosphere. Imberger and Patterson (1990) found that this approach is succesful for long time scales, as the processes involved tend to be self correcting.

Note that the validity of Equation 3.11 is limited as the value given for C_s is only valid for neutrally buoyant conditions. This is unlikely to be the case at low wind speeds, as the temperature difference between the air and the water will cause the air mass to become either stably or unstably stratified and because C_s is dependant on the roughness of the air-water interface, which is critically dependant on wind speed.

Where a stable stratification develops in the atmosphere, the value for C_s will be decreased as heat exchange is limited by the stratification (Turner, 1973) this may cause C_s to drop significantly at low wind speeds. For example, C_s is 60% lower than its neutral value for a 4 m/s wind speed if the air temperature at 10 m is 4°C above the water temperature (Geernart, 1990). Where unstable stratification arises, buoyancy driven convection will occur, which will cause C_s to be much higher than in the neutrally buoyant case.

These comments on the validity of the value of the dimensionless transfer coefficient will apply equally to the latent heat transfer coefficent discussed below.

It must be acknowledged that the assumption of constant values for transfer coefficients is not strictly valid; however, Imberger and Patterson (1990) note that this approach is generally successful for performing heat budgets over long time scales, as the mechanisms involved are self correcting in the long term.

From Section 3.3, values of sensible heat transfer encountered in this study were usually minor in comparison with other heat fluxes.

Changes in temperature due to sensible heat transfer follow the same form as Equation 3.10.

3.1.4. LATENT HEAT TRANSFER

Latent heat transfer arises from the cooling effect of evaporation on the water body. An expression for latent heat transfer is given in Fischer *et al* (1979) as:

$$H_l = C_l \rho_{air} L_w U_a (Q_o - Q) \qquad 3.12$$

where C_l is the dimensionless transfer coefficient for latent heat under neutrally buoyant conditions (1.45×10^{-3}) and L_w is the latent heat of evaporation of water (2.4×10^{6} Jkg^{-1}). Q is the Specific Humidity 10 m above the water surface; that is, the ratio of the partial pressure of atmospheric water vapour to the total air pressure, corrected for the density difference between water vapour and air. Q_o is the saturation specific humidity. Both Q and Q_o depend on T_{air}. According to Chow *et al* (1989) an emprical expression for Q is:

$$Q = 380\frac{R_H}{p_a}e^{\frac{17.27T_{air}}{237+T_{air}}} \qquad 3.13$$

where p_a is air pressure (101.3 kPa), R_H is the relative humidity and T_{air} is the air temperature in degrees Celsius. Note that Q_o is obtained by taking R_H as 100%, and that $237+T_{air}$ is an empirical term, not a conversion to degrees Kelvin.

As will be seen in Section 3.3, latent heat values in the wetland were generally found to be significantly less than peak shortwave radiation values; however, of an evening, in the absence of solar radiation, it is generally the largest influence on the temperature of the water column, and as it is always a flux out of the water column, it is therefore very significant in causing destratification and mixing due to penetrative convection at night (see Chapter 4).

Changes in temperature due to latent heat transfer again follow the same form as Equation 3.10.

3.2. PLANT EFFECTS ON HEAT FLUXES AND STRATIFICATION

The expected effects of the plant canopy on heat fluxes and stratification are discussed below. Nett longwave radiation has not been discussed here because as will be shown in Section 3.3, its effects are minor.

3.2.1. PLANT EFFECTS ON RADIATIVE HEATING

Radiation entering a plant canopy may be absorbed by vegetation in the canopy, reflected from the vegetation back to the atmosphere, reflected from the vegetation to within the canopy or transmitted through to the ground or water surface (Monteith and Unsworth, 1990). Similar interactions will occur with the components of the vegetation below the water column.

The nature of these processes in the canopy and in the submerged vegetation is quite complex, they depend on the absorption, reflection and transmission properties of the leaves making up the canopy, the number of plants per unit area, the arrangement of the canopy vegetation of these plants, and the angle of incidence of light on the canopy (Monteith and Unsworth, 1990), as shown in Figure 3.1.

No studies could be found in the literature on radiation properties of the canopies of wetland plants; however emergent macrophytes have a canopy architecture that is quite similar to commercially grown crops and there has been much research into the radiation properties of commercially grown crops.

Absorption rates for individual leaves of common crop species are typically 50% of the incoming values, while reflection and transmission rates are typically 25% each (Monteith and Unsworth, 1990). It would be expected then that the combined impact of the large number of leaves present in a canopy of emergent macrophytes may significantly reduce the levels of solar radiation transmitted to the water surface from those incident on the canopy.

Figure 3.1. Transmission Processes

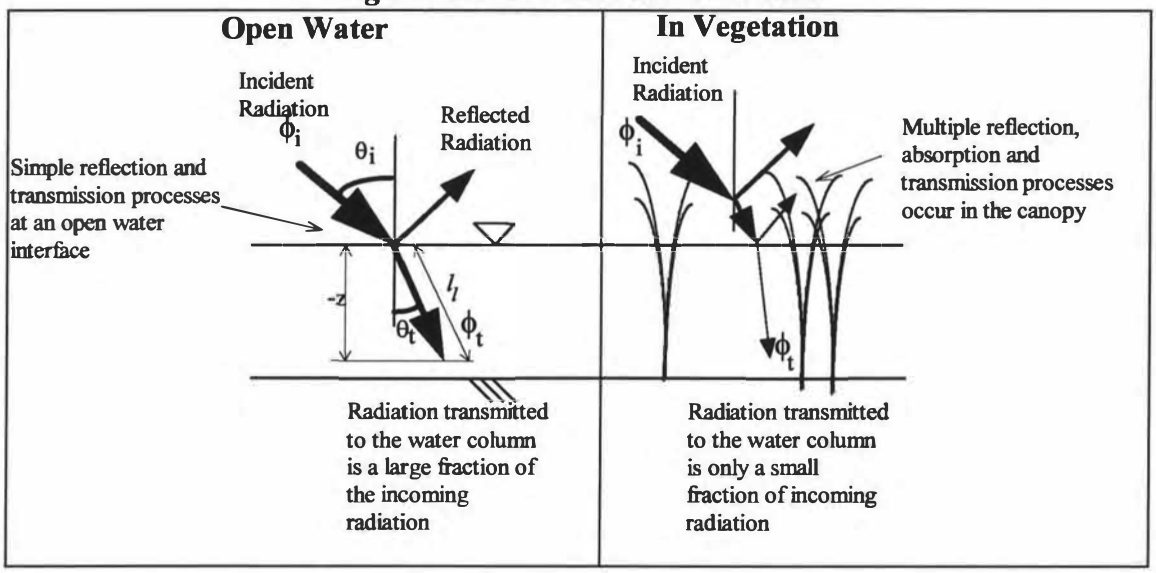

Lower levels of radiation would be expected to significantly reduce the depth averaged temperatures and the extent of stratification in the water column. Evidently as the amount of vegetation in the canopy is increased, these effects will become more apparent.

Of the four types of macrophytes defined in Chapter 1, floating leaf and free floating macrophytes would be expected to have the largest effect on radiation transmission to the water column, as their leaves very efficiently cover the water surface, ensuring that minimal light is transmitted into the water. Emergent macrophytes will be less effective, with multiple reflections and transmissions occurring in the plant canopy, while submergent macrophytes would have little effect on transmission into the water column.

3.2.2. PLANT EFFECTS ON HEAT TRANSFERS AT THE AIR-WATER INTERFACE

From Equations 3.11 and 3.12, the sensible and latent heat transfers respectively, are proportional to the free stream velocity of the air. From Raupach and Thom (1981), air velocities in the plant canopy are expected to be lower than velocities outside the canopy by more than an order of magnitude; therefore sensible and latent heat transfers within vegetated areas are expected to be reduced significantly from their values in open water, when the same air-water temperature difference occurs. However, turbulence in the plant canopy will not be reduced as significantly as the air velocity (Finnigan, 1979), therefore the decrease in heat transfers will not be in direct proportion with the decrease in air velocity.

3.2.3. PLANT EFFECTS ON STRATIFICATION

For the four macrophyte types, floating leaf and free floating macrophytes, effects of vegetation on stratification can be postulated as follows. The effect that floating leaf and free floating macrophytes have on radiation entering the water column was discussed in Section 3.2.1. By physically covering the water surface, these macrophytes will significantly reduce the amount of radiation entering the water column. With the energy source for providing stratification removed, only low rates of stratification can be expected through the water column, except immediately below the water surface, where absorption of radiation by floating plant matter may cause a small layer of higher temperature water to be formed.

Submergent macrophytes would be expected to enhance stratification, as they do not prevent radiation entering the water column, but will act as a barrier to the transmission of light to deep water.

Emergent macrophytes would be expected to display behaviour somewhat between the two extremes portrayed above for the other macrophyte types. The plant canopy would be expected to reduce the amount of incoming radiation, while plant matter within the water column would preferentially absorb radiation in the water column, preventing its transmission to deeper water.

The only previous study that could be found that examined temperature stratification in the presence of vegetation was performed by Dale and Gillespie (1977). They found that stratification in the water column in the presence of submergent vegetation can be significantly greater than in water without vegetation. According to their study, temperature differences of up to 3°C between 20 mm and 600 mm below the water surface can occur in containers of water planted with the submergent macrophyte *Potamogeton richardsonii* under average radiation loadings of 870 Wm^{-2} over 7 hours. Under the same conditions, a tub containing floating algae developed temperature differences up to 4 °C, while no significant temperature difference developed in an open water tub.

Dale and Gillespie (1977) found that the temperature structure of the water was primarily affected by:

- Plant matter above the water surface intercepting radiation, hence reducing the depth averaged temperature in the water column; and

- Plant matter below the water surface preventing light penetrating deeper into the water column, causing temperature stratifications to develop that were higher than in the unvegetated containers.

They considered that the reduction in convection in the water due to the presence of the plants only made a secondary contribution towards enhancing stratification.

Note that in dealing with emergent macrophytes as are present at the wetlands studied, the situation will be complicated by the presence of vegetation above the water column. Vegetation above the water column will reduce the amount of radiation incident on the water column, and will inhibit the heat and momentum transfer at the water surface as outlined above.

In summary, the effects of vegetation on the heat balance in the water column are expected to be quite complex. The primary effect of vegetation will be to reduce the amount of radiation (the dominant heat energy input) entering the water. Secondary effects will include reductions in the surface heat transfers at the water surface and a tendency for higher stratifications to develop due largely to the interception of radiation by vegetation within the water column. Therefore, vegetation effects on the heat balance will depend heavily on biological factors such as the plant type, age, stage in its life cycle, whether it is emergent or submergent and plant density.

3.3. FIELD RESULTS

3.3.1. PLANT CANOPY EFFECTS ON RADIATIVE HEATING

Temporal variability in solar radiation fluxes made analysis of the radiation profiles in the plant canopy difficult at times. Factors causing this variability include:

- changes in the amount of incoming radiation with the time of day;

- the angle of elevation of the sun above the horizon - when the sun is at its highest in the sky, the distance through the canopy that the radiation has to pass is lowest so the radiation reaching a certain level in the canopy will be higher than at other times during the day;
- changes in the incoming radiation due to passing clouds;
- spatial variability in plant density; and
- plant leaves moving with the wind, casting shadows over the radiation sensor on an intermittent basis.

To minimise the effects of transient shading by passing clouds and leaves blowing in the wind, at least two and often up to five radiation readings were taken at 30 s intervals at one height. The readings at a particular height were averaged, then the probe height was changed, giving the profiles shown in Figure 3.2. Figure 3.2 shows the amount of radiation penetrating through the canopy as a fraction of the radiation incident on the canopy, for the seven vertical profiles taken over the afternoon of 22 February 1995.

Figure 3.2. Averaged Canopy Radiation Readings, Station 1, 22 February 1995
Legend shows the time of day at which the profile was taken

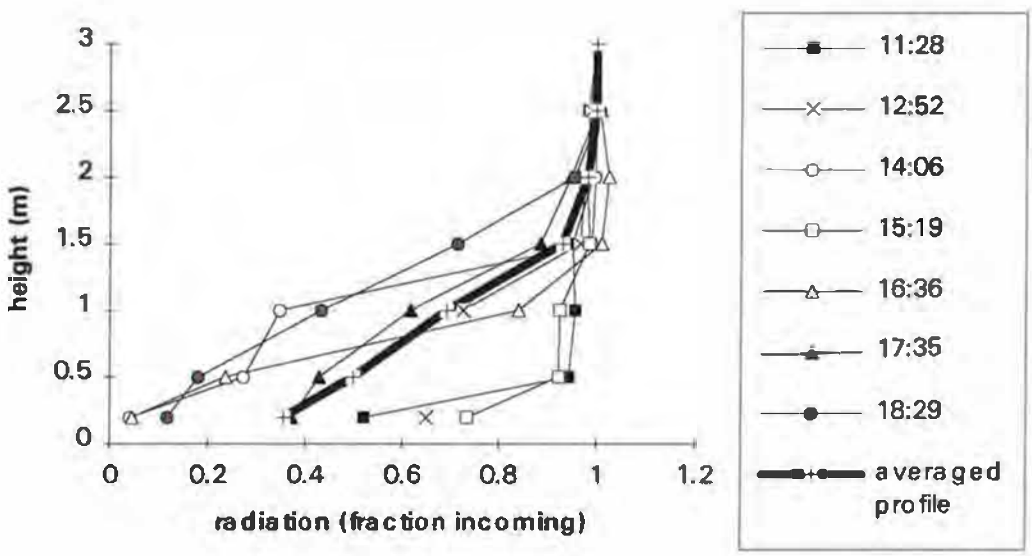

As shown in Figure 3.3, the profiles taken at 1406 and 1636 showed much lower radiation levels at all heights in the canopy than the profiles at other times. This was most likely due to the presence of two large *Typha* stands adjacent to Station 1 shading the instrument at these times.

To account for this variability in shading due to the plant stands, it was necessary to take the time averaged radiation profile over the afternoon to give a profile that is representative of the overall conditions that would apply within the canopy. This average profile is shown as the thick line in Figure 3.2. It was found that there was a linear relationship between the averaged radiation flux and height within the vegetation. This has a correlation coefficient of 0.999, a zero level fractional flux of 0.27 and a rate of decrease in flux of 0.436 m^{-1}.

Figure 3.3. Time Dependence of Radiation at Station 1, 22 February 1995
The legend shows the height in metres above the water level

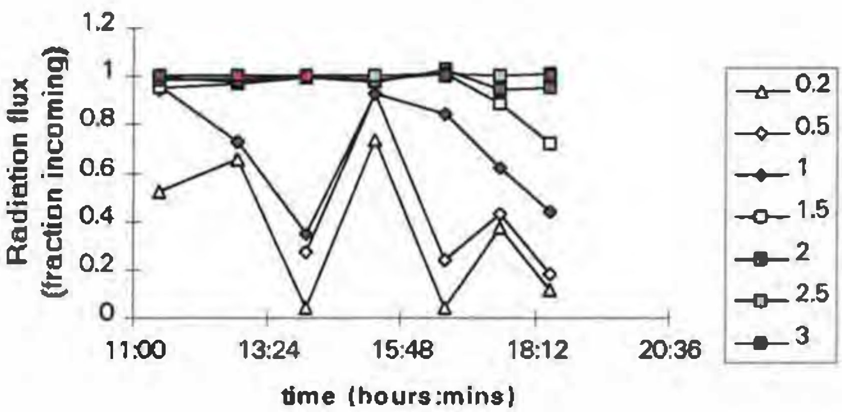

Thus the average percentage of radiation reaching the water surface is 27% of the radiation incident on the surface.

3.3.2. PLANT CANOPY EFFECTS ON AIR VELOCITIES NEAR THE WATER SURFACE

Air velocity profiles were obtained by setting the probe to a particular height for sufficiently long to gather readings through both still and peak gust conditions. The minimum velocities under still conditions and the maximum velocities under gust conditions at each height were then averaged, as shown in Figure 3.4. By performing the sampling in this manner and by taking readings for each profile in quick succession, the effects of non stationarity in the air velocities were minimised

It can be seen from Figure 3.4 that some of the wind profiles show a decrease in velocity with height above the canopy. This phenomenom is not expected to be due to sampling errors, as wind profiles above crop canopies are often observed to show such behaviour (Raupach and Thom (1981).

Two commonly used expressions for velocity profiles in the canopy were fitted to the data, the mixing length model and the constant eddy viscosity model. It was found that the air velocity was well described by the mixing length model used by Cionco (1972) which has the form:

$$\frac{U(z)}{U(h)} = \exp\left[\alpha\left(\frac{z}{h} - 1\right)\right] \qquad 3.14$$

where h is the canopy height, and α is the attenuation coefficient. Cionco (1972) provides a summary of appropriate values for α. A value of $\alpha = 2$ is common for crops such as wheat and should be suitable in the wetland due to the similar structures of *Typha* and wheat plants. However, the model underpredicted velocities in the lower part of the canopy, as shown in Figure 3.4.

The constant eddy viscosity model (see Thom, 1975) was also found to give a good fit to the data, as shown in Figure 3.4. This model is represented by the equation:

$$\frac{U(z)}{U(h)} = \left[1 + \beta\left(1 - \frac{z}{h}\right)\right]^{-2} \tag{3.15}$$

where β is determined empirically. Raupach and Thom (1981) found that β = 1.2 for a "canopy" of rigid vertical cylinders. It is assumed that this value would be suitable for a wetland.

WATER SURFACE MOMENTUM TRANSFER EFFECTS

To calculate shear stresses at the water surface, a logarithmic profile was assumed with the air velocity values obtained at the 0.5 m height (from Figure 3.4 it can be seen that air velocity is fairly constant from 0.5 to 1.0 m). Note that by assuming a logarithmic profile in this situation, the drag force exerted by the vegetation on the air stream is ignored. As a result of ignoring the drag effects of the vegetation, an overestimate of the shear velocity at the water surface will be obtained. The shear velocity in air at the water surface is calculated as:

$$u_a^* = \frac{u(z)k}{\ln\left(\frac{z}{z_0}\right)} \tag{3.16}$$

where u_a^* is the surface shear velocity, u(z) is the velocity at height z, k is von Karman's constant (0.4) and z_0 is the roughness length of the water surface, which can be taken as 3×10^{-6} m in the absence of water waves (Craig and Banner, 1994).

Using the maximum velocity obtained at 0.5 m during the experiments, u(0.5) = 0.5 m/s, gives the shear velocity in the atmosphere within the vegetation as u_{av}^* = 0.017 m/s. To obtain the shear velocity that will apply in the water column, assume that the stress is constant at the interface and note that u* is inversely proportional to the fluid density, so that the shear velocity in the water at the interface is given by:

$$u_w{}^* = \frac{u(z)}{\ln\left(\frac{z}{z_o}\right)}\sqrt{\frac{\rho_a}{\rho_w}} \qquad 3.17$$

where ρ is the fluid density. For an air density of 1.22 kgm^{-3} and a water density of 1000 kgm^{-3}, this gives the shear velocity in the water, within the vegetated area as $u_{wv}* = 0.0006$ m/s.

An estimate for u_{wo}^*, the shear velocity in water for open water can be obtained by assuming a logarithmic profile, based on the maximum wind gust velocity 2.0 m above the water surface. It should be noted that this is not sufficiently high above the plant canopy to be above the boundary layer, so that this value will be an underestimate of the velocity that would apply 2.0 m above the open water. The maximum wind gust velocity 2.0 m above the water surface is 2.0 ms^{-1}, giving $u_{wo}^* = 0.002$ ms^{-1}, which is considerably larger than the above estimate for u_{wv}^*, which, as noted earlier, is an overestimate of the shear velocity in the vegetation.

Figure 3.4. Canopy velocity experiments, Station 1, 6 June 1995

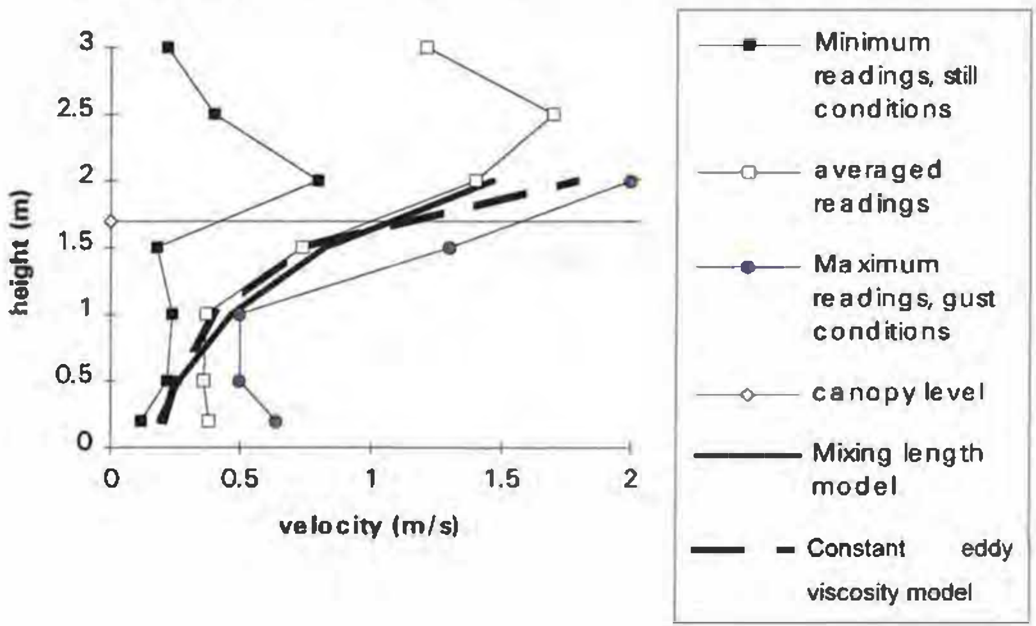

By this argument, it can be seen that wind driven shear in vegetated areas is expected to be much smaller than in open water areas.

3.3.3. METEOROLOGIC CONDITIONS, DAY 95055

Of the field investigations performed, the temperature profiles obtained on Friday 24 February 1995, day 95055, during the intensive field investigations show most clearly the effects of solar radiation on temperature stratification in the wetland. In this section the meteorologic conditions encountered are described, followed by the results of heat flux calculations. Temperature profiles are then given and the results of calculations to assess the affects of vegetation on shading and light absorption.

Figures 3.5a and 3.5b present meteorologic data for day 95055. Figure 3.5a shows that solar radiation was patchy through the morning, but peaked at just over 1000 Wm^{-2} at midday. During the afternoon the radiation dropped away slowly indicating that there was little cloud cover then.

Sunrise was again at around 0630, however the sunset was earlier than day 95054, the radiation probe failing to register any radiation after approximately 1730.

Winds were light through the whole day, as shown by Figure 3.5a. This was especially so from midnight until 0830, with the windspeed remaining below 0.5 ms^{-1}, at 60° from North over this period. Throughout the rest of the day, apart from a brief peak at midday of 2.5 ms^{-1}, the wind speed did not exceed 2.0 m/s and was generally between 1.0 and 1.5 ms^{-1}. The wind direction was mainly towards the South, between 150° from North and 210° from North, but with occasional gusts towards the East at approximately 60° from North. After sunset the wind again dropped to less than 0.5 ms^{-1} at 60° from North until after sunrise the next morning.

Figure 3.5a. Radiation, Wind Speed and Direction, day 95055

Note that the wind direction follows the meteorologic standard, giving the direction the wind is coming from

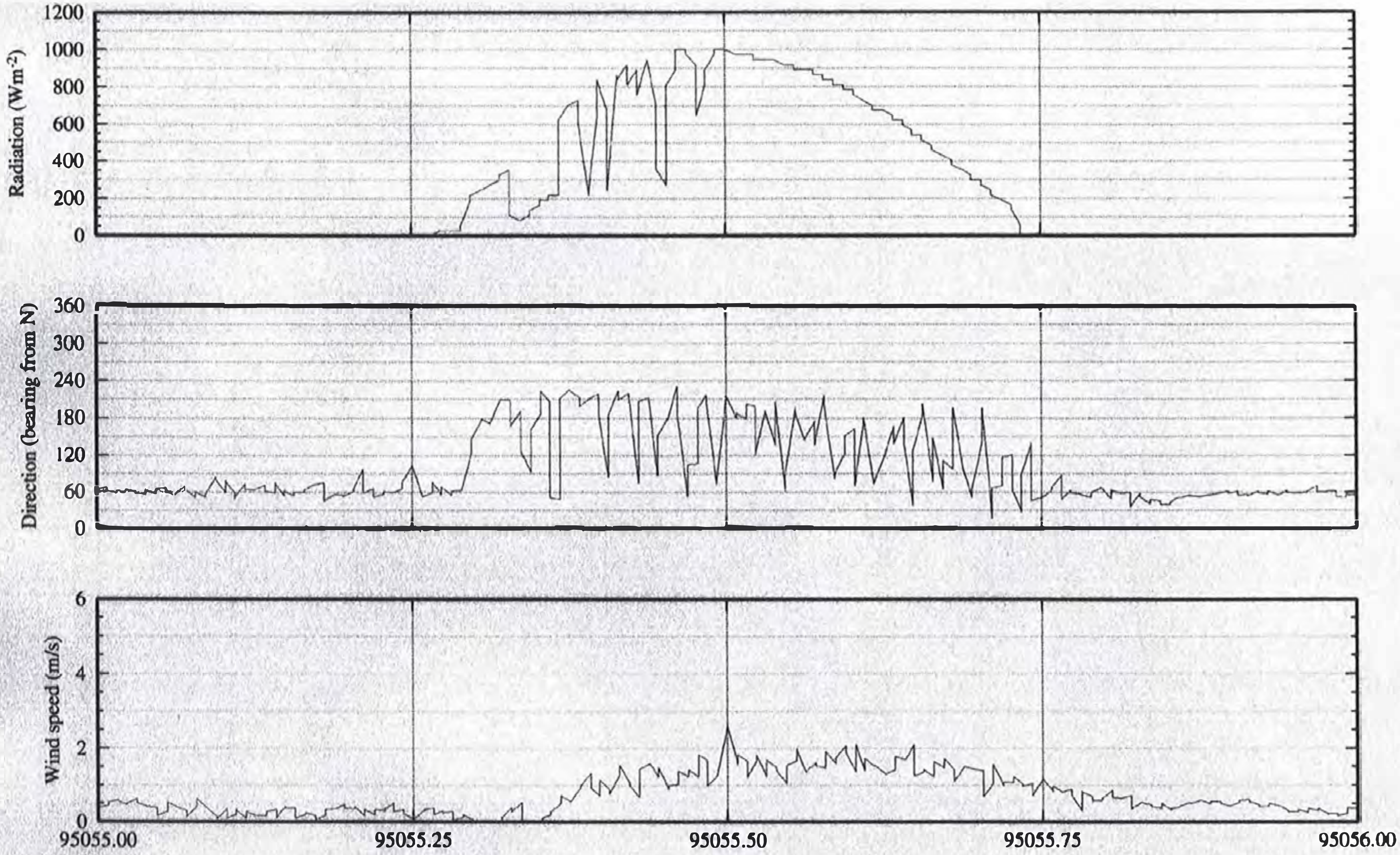

Figure 3.5b. Rainfall, Relative Humidity and Air Temperature, day 95055
Note that no rainfall was recorded

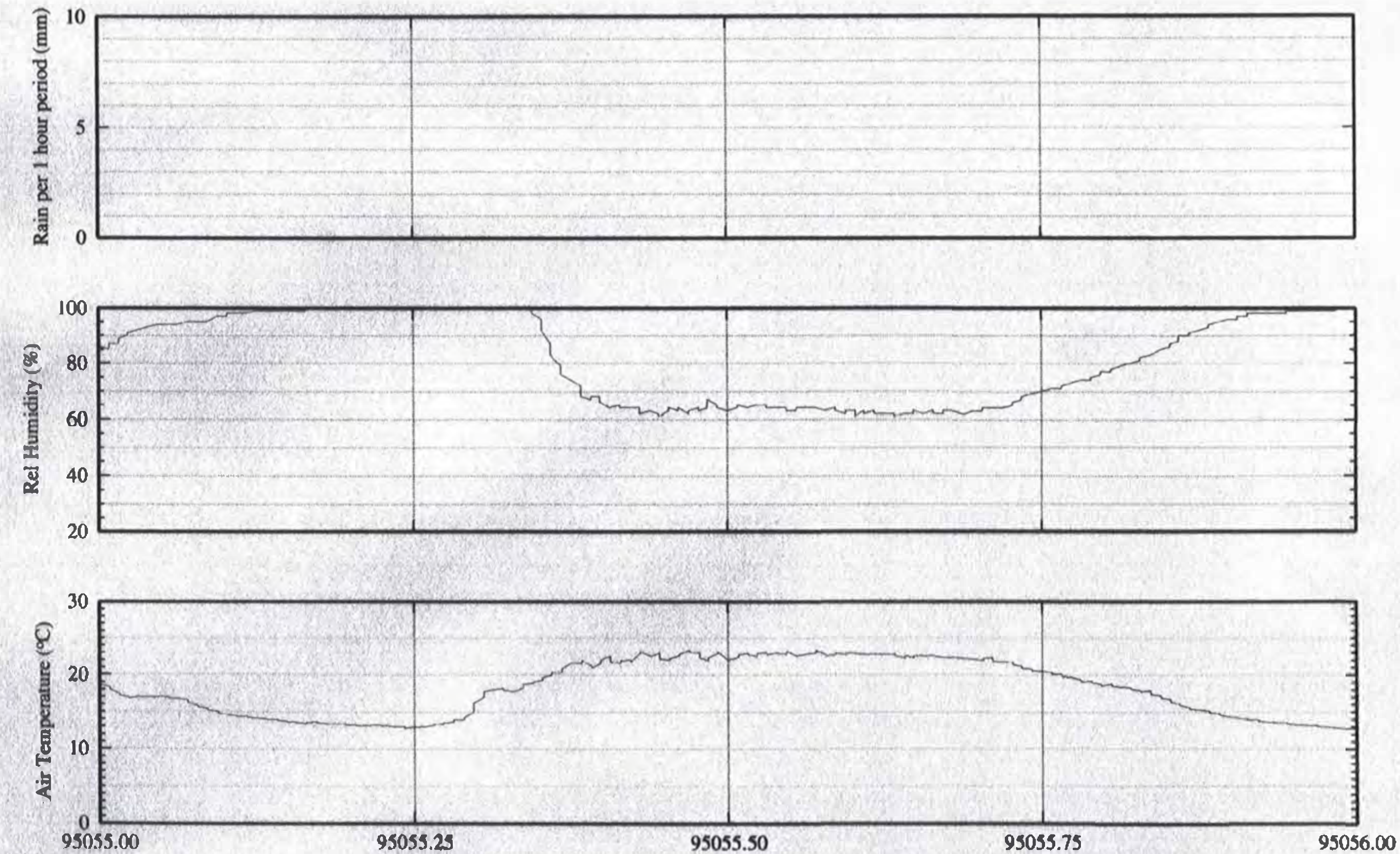

Figure 3.5b shows no rain was recorded on days 95055 and 95056. The relative humidity was quite high at around 100% through the morning of day 95055 until after 0800, then dropped to approximately 65% through the day from 0900 until 1700, when it steadily rose back to nearly 100% at 2200. From 2200 the air was near saturated or saturated until after dawn on day 95056.

The air temperature can be seen on Figure 3.5b to have dropped through the early morning from about 18°C at midnight to about 13°C by 0600. The temperature then rose steadily to reach about 22°C by 0900, then remained fairly constant until about 1700 when it started to fall, dropping gradually to about 13°C by midnight.

These conditions are fairly typical of calm weather in the Sydney area through summer, except that the morning would normally tend to be a bit warmer.

3.3.4. HEAT FLUXES, DAY 95055

Figure 3.6 shows the heat fluxes as positive out of the wetland for day 95055. These were calculated from the meteorologic data shown in Figures 3.5a and 3.5b, using the relationships in Sections 3.1.1 to 3.1.4. Note that in Figure 3.6, no corrections have been made for canopy effects.

Figure 3.6 shows that the heat balance is dominated by the solar radiation. This is despite the fact that black body and long wave radiation are high, since they are of opposite sign and very nearly cancel, as was expected. The nett surface heat transfers (the sum of black body radiation, long wave radiation, latent heat and sensible heat) are of an order of magnitude smaller than the solar radiation throughout the day and thus can be neglected when analysing the build up of stratification given these conditions.

3.3.5. TEMPERATURE PROFILES, DAY 95055

A large number of temperature profiles were obtained using the fp07 fast response thermistor at Stations 1 to 4, starting at 0820 on day 95055 and ending at 0814 on day 95056. These profiles were obtained using the free fall technique as discussed in Chapter 2. Locations of Stations 1 to 4 are given in Figure 2.6.

Figure 3.6. Heat Fluxes, Day 95055

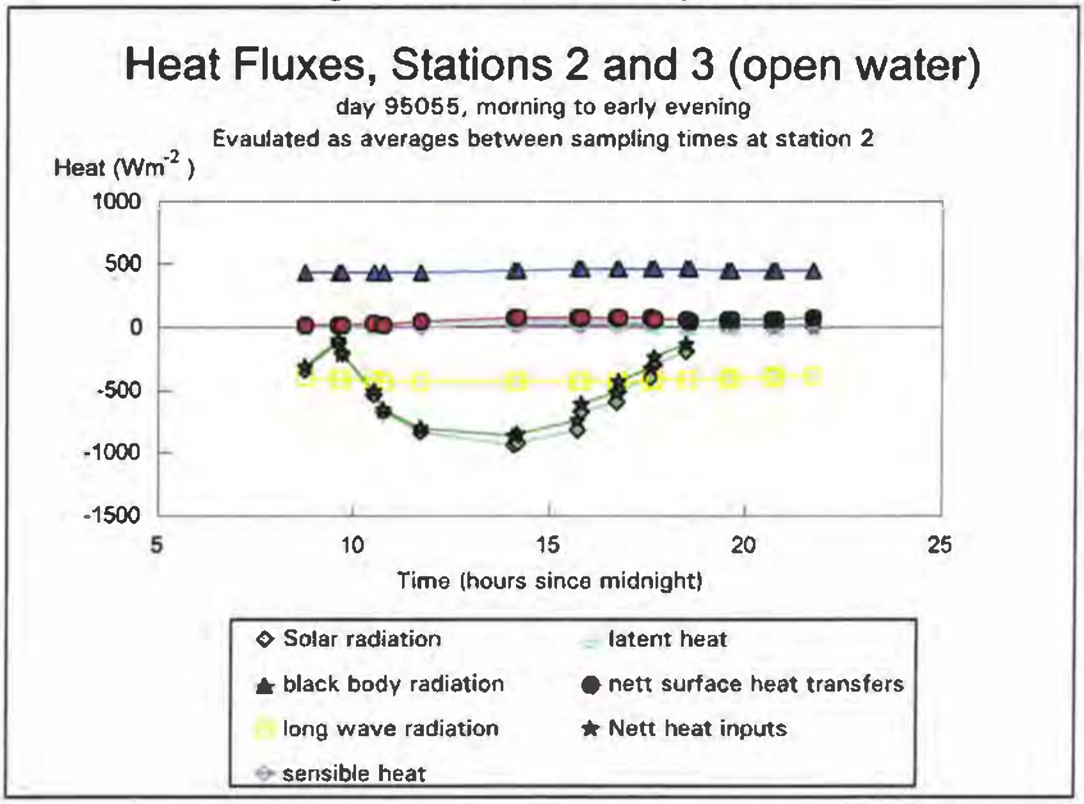

Of interest here are the samples taken through the middle of the day, between 1000 and 1300. Solar radiation during this time was high and winds were low, as seen on Figure 3.5a.

Descriptions of the results of temperature profiling at each station throughout the day is provided below. Figures 3.7a to 3.7d show contour plots of the temperature against time and depth at Stations 1 to 4 respectively.

STATION 1 (IN THE VEGETATED REGION, APPROXIMATELY 10 M FROM THE LAKE)

Figure 3.7a shows time-depth temperature contours and colour images for Station 1. The image reveals that at 0820 when readings commenced, the water temperature at the surface was 21°C and there was a temperature drop between top and bottom of about 1°C. As the day progressed, the surface temperature increased to a peak of 26.7°C at 1354. From 1354 to 1923, the surface temperature gradually fell to 25.2°C, after this time, the temperature fell moderately quickly until midnight.

When readings commenced at 0820 there was no stratification; however, stratification built up until there was a 3.5°C temperature differential between top and bottom at 1124, after which stratification began to diminish. By 1630 conditions were essentially unstratified and remained that way until readings ceased, with a temperature differential of no greater than 0.5°C between top and bottom after 1630.

STATION 2 (IN THE OPEN WATER REGION SURROUNDED BY VEGETATION, APPROXIMATELY 8 M FROM THE LAKE)

Figure 3.7b shows time-depth temperature contours at Station 2. The image shows that at 0840 when readings commenced, the water temperature was 22.7°C and there was a temperature drop between top and bottom of 1.2°C. The surface temperature increased to 27.7°C at 1549 then gradually dropped to 21.7°C at 0554 the next morning. The bottom temperature remained fairly constant until 1044, by which time the water column had developed a temperature differential of 3°C between top and bottom. By 1148, the top-bottom temperature differential had reached 4°C. This level of stratification was still present at 1406 and 1411, however, by 1544 the top-bottom temperature differential had reduced to 1.8°C. Stratification decreased through the afternoon until by 1735 the water was unstratified. The water remained unstratified until the next morning.

Figure 3.7a. Temperature Contours v Time and Depth at Station 1, day 95055

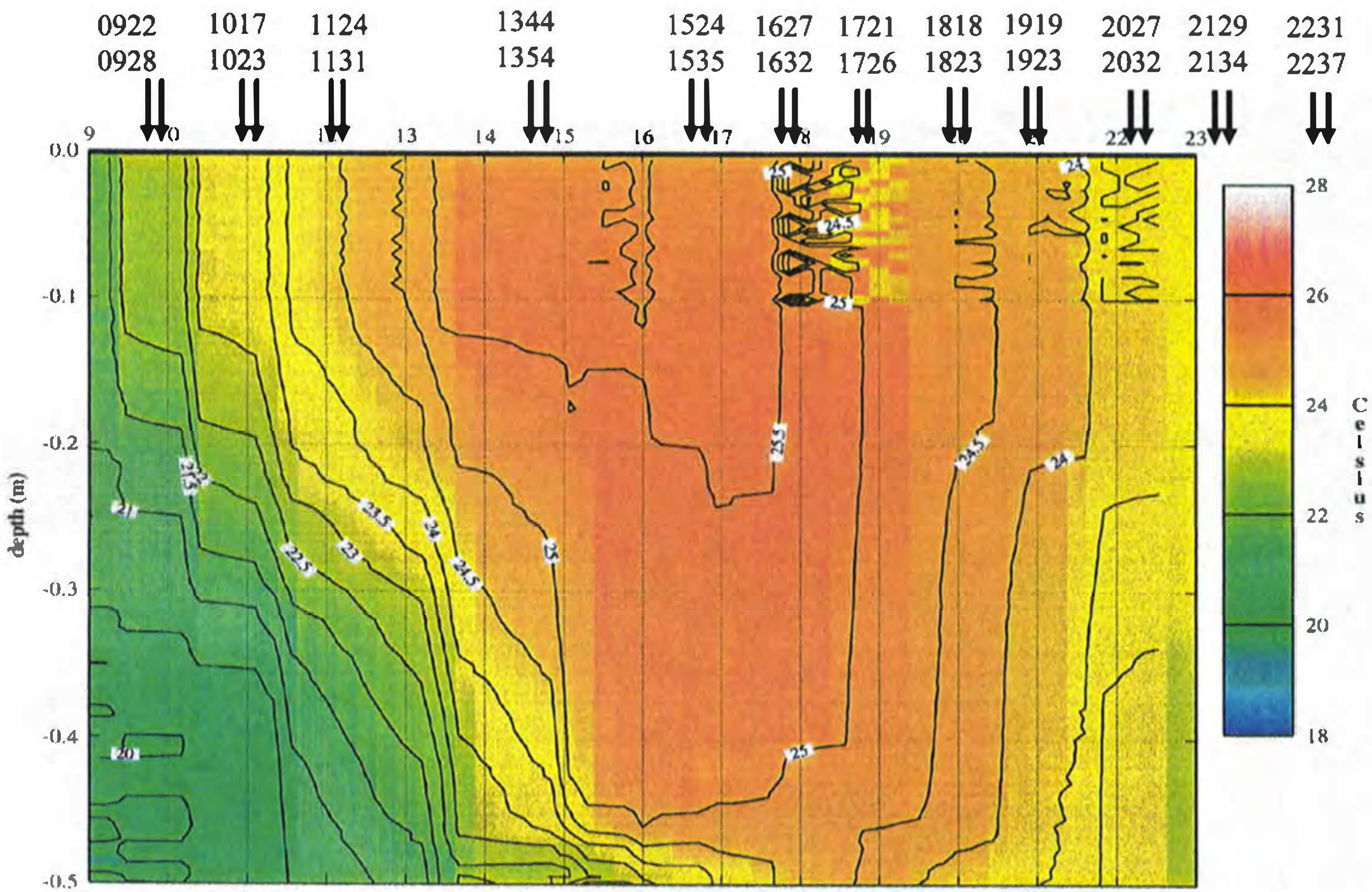

Arrows indicate sampling times

Figure 3.7b. Temperature Contours v Time and Depth at Station 2, day 95055

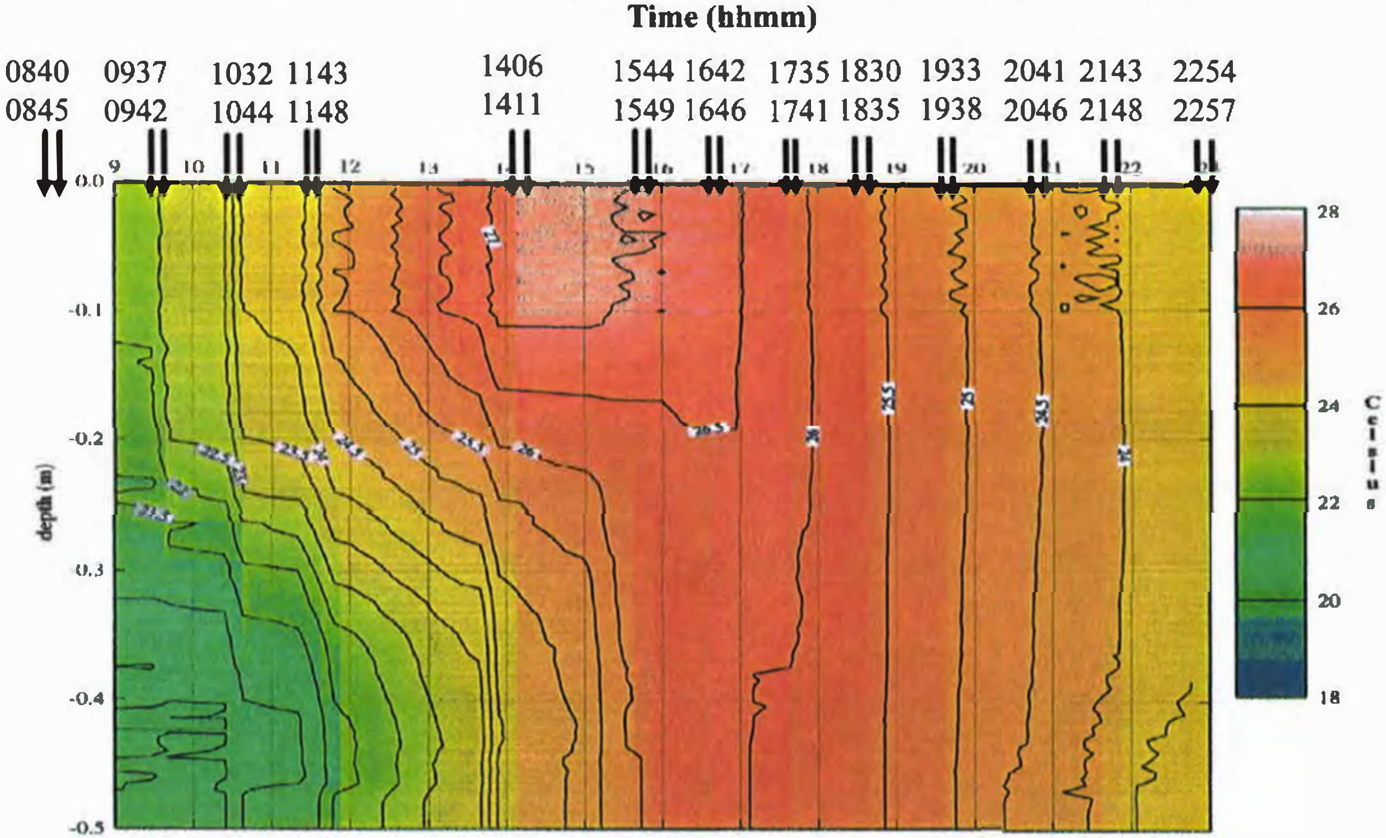

Arrows indicate sampling times

Figure 3.7c. Temperature Contours v Time and Depth at Station 3, day 95055

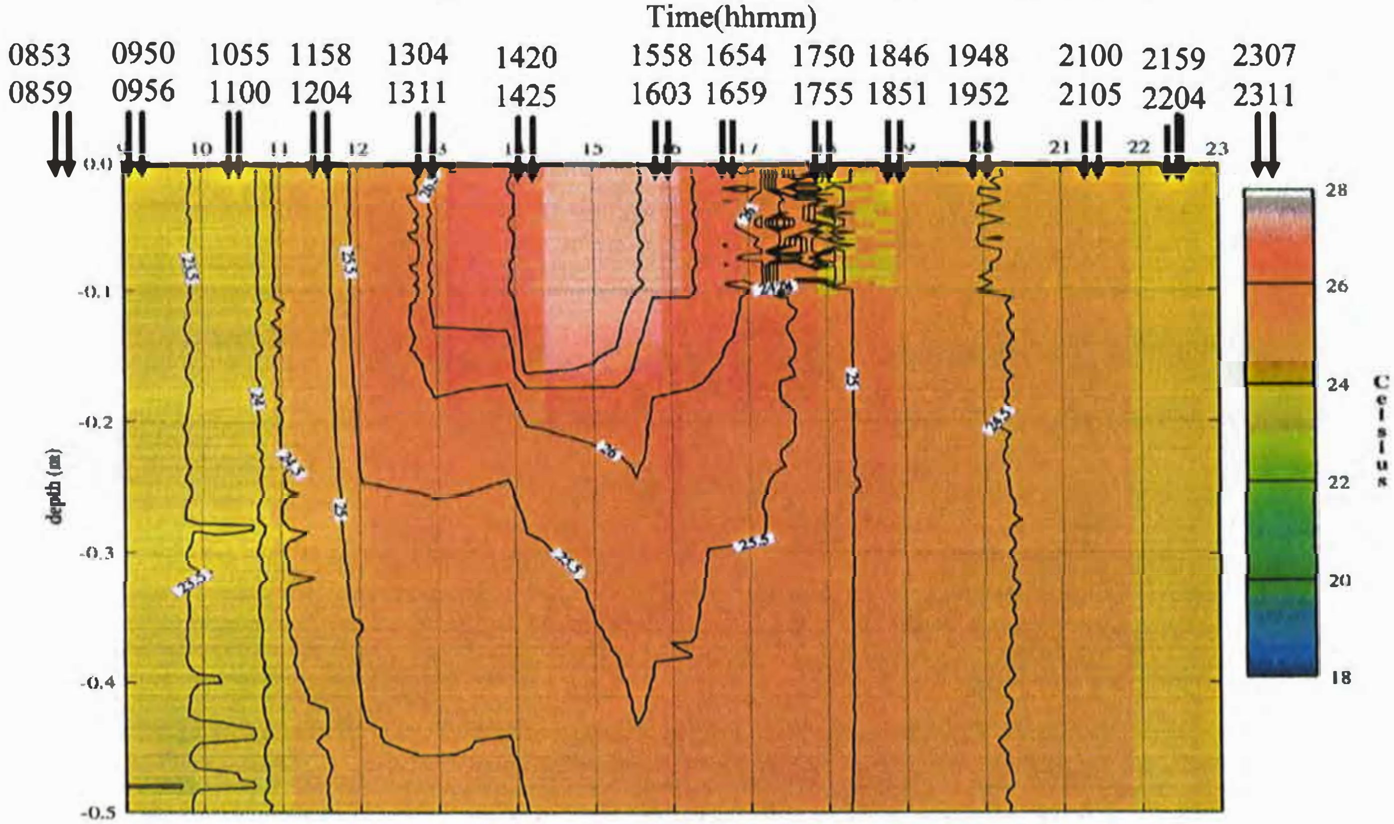

Arrows indicate sampling times

Figure 3.7d. Temperature Contours vs Time and Depth at Station 4, day 95055

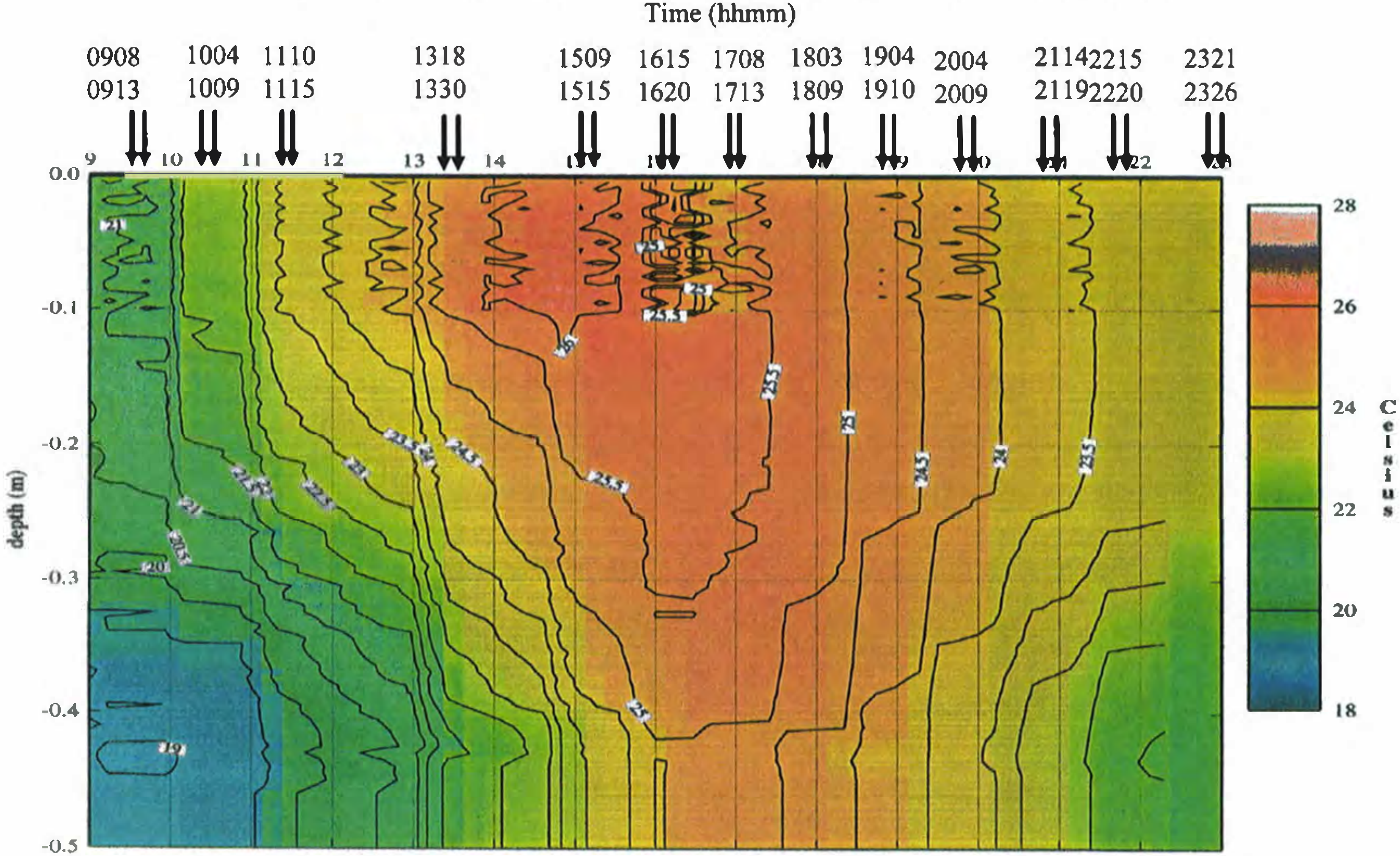

Arrows indicate sampling times

STATION 3 (IN THE LAKE, APPROXIMATELY 10 M FROM THE VEGETATION)

Figure 3.7c shows time-depth temperature contours and colour images at Station 3. The image shows that the water temperature at the surface was 23.2°C at 0853. The initial profile showed a minor temperature increase of 0.3°C over the first quarter of the depth, then a temperature drop of 1.3°C between the peak temperature and the bottom.

Temperatures at Station 3 fluctuated more markedly with depth than at the other stations, probably due to the higher extent of wave action and the influence of wind mixing here, as discussed in Chapter 4.

The surface temperature gradually increased to a peak of 27.6°C at 1420, and remained at about this temperature until 1603. After this, the surface temperature gradually declined eventually reaching 22.8°C by 0431 the next morning.

Through most of the rest of the morning, there was little stratification, until by 1158 a 0.8°C top-bottom temperature difference developed. Unlike at Stations 1 and 2, regions of quite high temperature gradient were noted to develop, the most dramatic of these occurring at 1425, when a temperature drop of 1.2°C was observed over 0.04 m (giving a gradient of 27°C/m) just below the water surface.

Between 1420 and 1425 and between 1603 and 1659 events similar to thermocline deepening can also be observed, whereby a gradual temperature gradient near the surface is transformed to a well mixed layer at a constant temperature overlying a region of quite high temperature gradient.

By 1846 the water column had become quite unstratified and it remained that way until the next morning.

Temperatures at Station 3 were significantly higher than at the other stations, so the possibility of a buoyancy driven exchange between the lake and the wetland had to be accounted for. Such a convection would have caused the warmer water from the lake to enter the wetland as a surface plume flowing towards the North, as discussed in detail in Chapter 5. Furthermore, the wind was blowing from the South throughout the day. This would have given rise to a current heading toward the North in the lake, providing a further driving for any surface current heading towards the wetland.

STATION 4 (IN THE VEGETATION, APPROXIMATELY 15 M FROM THE LAKE)

Figure 3.7d shows time-depth temperature contours and colour images at Station 4. The image shows that at 0908 when readings commenced, the water surface was at a temperature of 20.9°C. This gradually increased until 1509 when the water surface temperature reached 26.6°C, then slowly decreased to reach 20.7°C by 0515 the next morning.

There was apparently a very high degree of turbulence within the water column early in the morning, as temperature fluctuated markedly with depth by up to 0.6°C over 0.02 m (34°C/m). As the day went on, these large fluctuations with depth were not as apparent.

Apart from these large fluctuations, the temperature gradients were generally similar to those at Stations 1 and 2. At 0908, there was a top-bottom temperature decrease of 1.5°C, this increased to 4°C by 1110, then remained between 4 and 4.5°C until 1330. The temperature gradient then decreased until by 1615, there was only a 0.7°C top-bottom temperature difference. As the evening progressed, the water column became quite uniform, except in the bottom half, where stratification developed, reaching a temperature difference of 1.8°C by 2119 and remained at about that level for the whole evening.

3.3.6. TEMPERATURE PROFILE ESTIMATION, DAY 95055

To determine whether solar radiation was responsible for the temperature changes observed in the wetland, two profiles were obtained approximately one hour apart at each station during the morning and in the middle of the day, for day 95055, 25 February, 1995. See Chapter 2 for the details regarding the techniques and equipment used.

Given the first profile, and knowing the incoming radiation over the intervening period, it was possible to calculate an estimate for the second profile, based on heating due to solar radiation. However, as will be seen, heating by the solar radiation alone does not fully explain the temperature changes observed in the water column. As will be discussed, this is most likely due to the effects of convective motions which are discussed in detail in Chapter 5.

If convection is ignored, then the development of the temperature profile with time may be calculated using Beer's law, Equation 3.2 as:

$$T_{E2} = T_{R1} + \frac{\tau\phi\eta t}{\rho C_p} e^{\eta z} \qquad 3.18$$

where T_{E2} is the estimated temperature at the time of the second reading, T_{R1} is the first recorded temperature, τ is the transmission coefficient; ϕ is the incoming solar radiation, η is the coefficient of extinction, t is the time between the two readings, ρ is the water density, C_p is the specific heat of water at a constant pressure and z is the distance from the water surface (positive upwards).

τ and η were used as calibration coefficients in calculating the estimated profiles. Trial and error was used to obtain values for η and τ at each of the stations. Adjusting the transmission coefficient caused the depth averaged temperature to be changed, but only had a small effect on the temperature gradient. Adjusting the extinction coefficient caused the temperature gradient to be changed, but did not drastically change the depth averaged temperature. Values were chosen that gave the closest fit by eye to the second of the recorded profiles.

Fitting was done primarily by ensuring the estimated and recorded profiles were in agreement in the lower part of the water column, where the effects of turbulence and latent heat on the profiles would be minimal. These profiles are shown in Figures 3.8a to 3.8d. A summary of the coefficients used is presented in Table 3.1.

Note that at any one time over the whole day the temperature at Station 3 was higher than at any of the other stations. As will be discussed in Chapter 5, this will lead to a buoyancy driven convection between the lake and the wetland, whereby the warmer lake water will flow into the wetland over the cooler water in the wetland.

Results of the scalings performed in Chapter 5 indicate that for a temperature difference between Station 3 and the other stations of 1°C, as is roughly the case here, the convection would have a velocity of the order of 20 m/hr. At such a speed, the convection could thus easily penetrate the whole area studied, thereby accounting for the slightly greater than estimated increase in temperature observed in the upper portion of the water column at Stations 1, 2 and 4.

Figure 3.8c, at Station 3 shows that while the general form of the profiles are in agreement, the estimated profile significantly exceeds the recorded temperature over the whole depth of the profile. In this case it was difficult to match the estimated and recorded profiles using physically realistic values of the coefficients η and τ.

To have made any further reductions in the temperatures over the whole profile would have required either further reduction in the transmission coefficient, or a different value of the extinction coefficient; however, these would lead to physically unrealistic scenarios as shown below:

Figure 3.8a. Temperature Profiles, Station 1 (vegetated)

$\eta = 5m^{-1}$, $\tau = 0.5$ and solar radiation = 750 Wm^{-2}

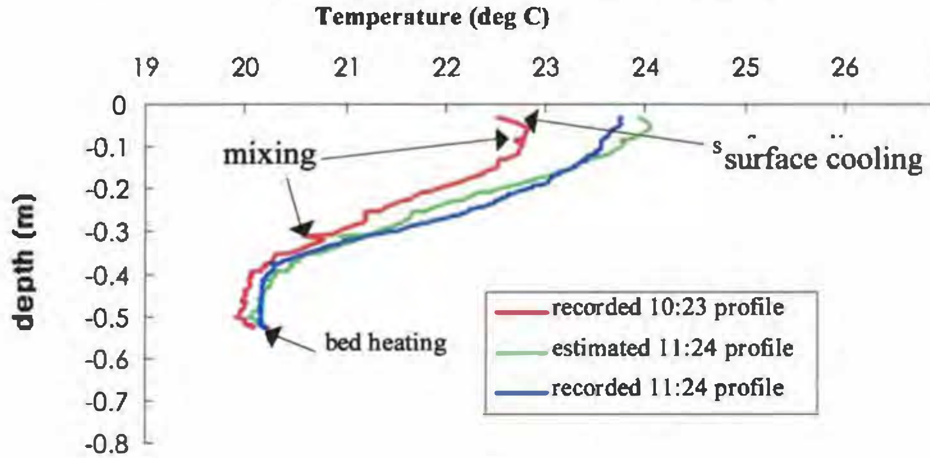

Figure 3.8b. Temperature Profiles, Station 2 (open water)

$\eta = 3\ m^{-1}$, $\tau = 0.5$ and solar radiation = 750 Wm^{-2}

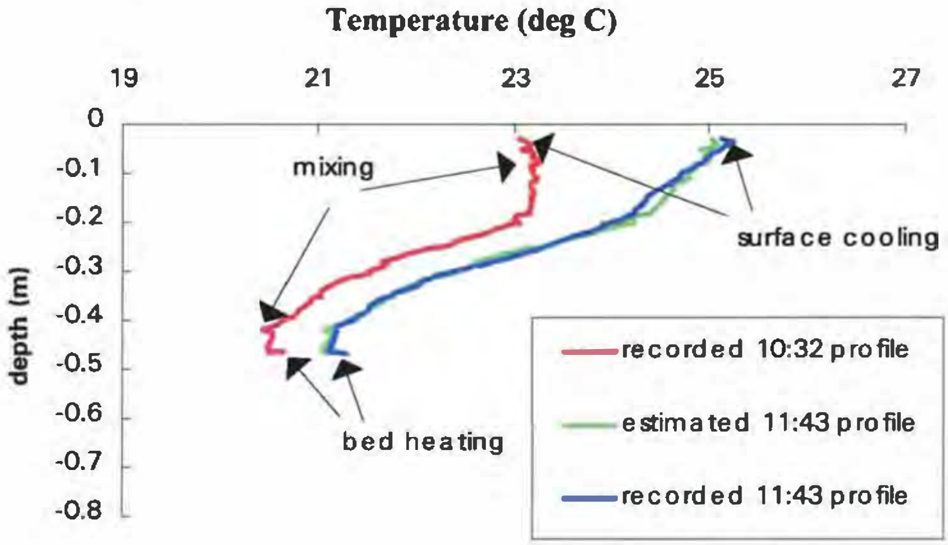

Figure 3.8c. Temperature Profiles, Station 3 (open water)
$\eta = 3\ m^{-1}$, $\tau = 0.9$ and solar radiation = 910 Wm^{-2}

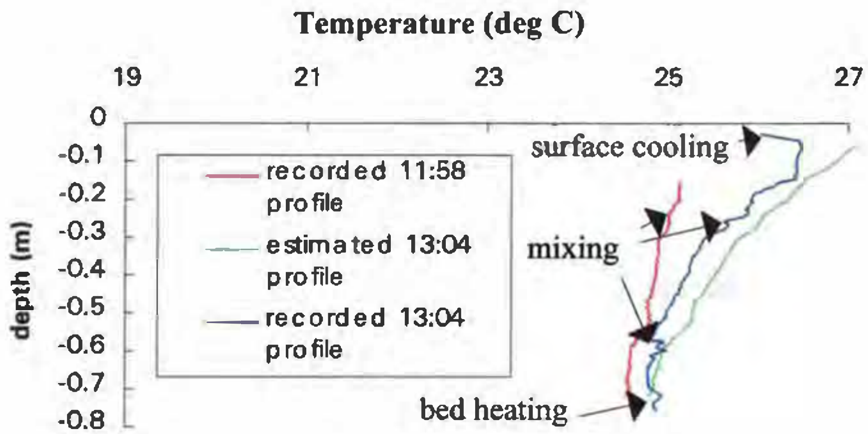

Figure 3.8d. Temperature Profiles, Station 4 (vegetated)
$\eta = 5m^{-1}$, $\tau = 0.8$ and solar radiation = 695 Wm^{-2}

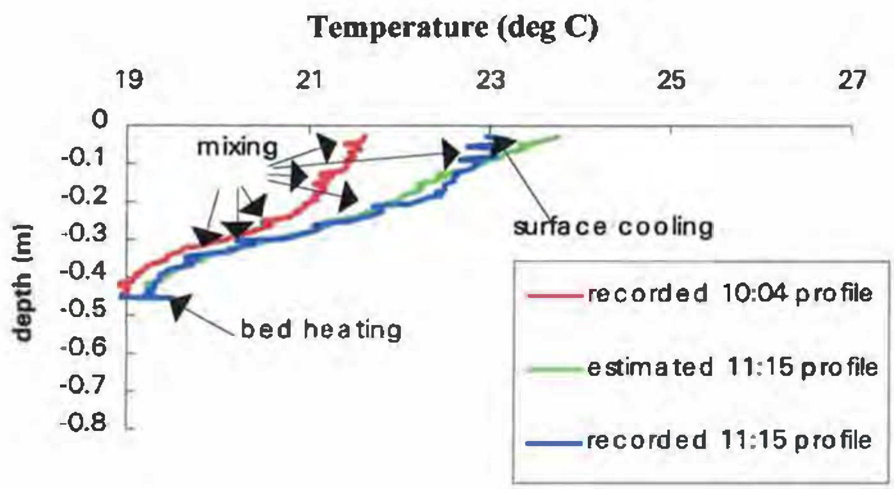

- To have reduced the surface transmission coefficient, τ further would have been unrealistic, since in open water the only physical phenomenon that can prevent transmission of the light at the surface under low wind conditions is reflection of light on surface waves. Reflection is less than 10 % while light is at an angle of incidence of less than 45° (Hecht, 1987), hence τ was set at its lower limit value of 0.9.

- Increasing the coefficient of extinction, η would have increased temperatures close to the water surface, while reducing it would have increased temperatures at depth, both of these being physically unreasonable since the estimated profile already significantly overestimates temperature in these areas.

Figure 3.6 shows that at Station 3 there was a surface heat flux out of the water of approximately 50 Wm^{-2}. Over the 66 minutes between the readings, this would give rise to a 0.5°C temperature decrease for the first 0.1 m of the water column, explaining the temperature drop in the upper portion of the water column.

However the lower than predicted temperatures in the lower portion of the profile cannot be explained by this surface heat loss, so it seems the only other explanation is that exchange with cooler water from the deeper portion of the lake must have occurred.

Important points to note concerning the coefficients shown in Table 3.1 are summarised below.

Table 3.1. Temperature Profile Estimation

Station	coefficient of extinction η (m^{-1})	transmission coefficient τ	Final Average Temperature (°C)	Calculated Final Temperature Gradient (°C/m)
1 (vegetated)	5	0.5	22.0	-9.0
2 (enclosed open water)	3	1.0	23.1	-10.6
3 (open water - lake)	3	0.9	25.4	-2.1
4 (vegetated)	5	0.8	21.3	-7.1

- The calculated transmission coefficients at the vegetated Stations (1 and 4) are consistent with the results of the canopy radiation profiles which revealed that approximately 60% of light is transmitted through the canopy during the middle of the day (see Appendix A.4). Large variations in τ must be expected, due to the heterogeneous nature of the canopy, so it is of no surprise that solar radiation entering the water column at Station 1 is 30% lower than at Station 4.

- When the extinction coefficient η is used as a calibration coefficient, it takes on much greater values in the vegetated area than in the open water. This may be due to vegetation below the water column intercepting the radiation and preventing it penetrating deeper, which is consistent with the findings of Dale and Gillespie (1977); however this finding should be treated with caution as increased stratification could also arise in the wetland due to temperature driven convection, as is discussed in Section 5.

- Much larger temperature gradients developed in the area of open water that was shaded from the wind (Station 2) than developed in the lake (Station 3). Stratification at Station 2 may be enhanced by wind shading from the nearby plant canopy; however as is shown in the next section, mixing rates were found to be quite similar at Stations 2 and 3, so it is likely that the buoyancy driven convections discussed in Section 6 are the cause of the stratifications at Station 2, the open water, sheltered station.

- Temperatures in the lower part of the water column at Station 3 were lower than expected, based on a heat balance performed on this station. The most likely explanation for this is that mixing occurred with cooler waters in the deeper parts of the lake.

Other significant features that can be seen in Figures 3.8a to 3.8d are the marked changes in temperature near the water surface and the bed and a number of "spikes" through the water column.

The large temperature changes near the water surface and the bed are due to heat transfers at these locations. The profiles show that the bed was generally warmer than the water immediately above it, and that surface heat fluxes cooled the water surface. The spikes are indicative of active mixing processes within the water column. Where these features are present in the water column Equation 3.18 will not hold. Mixing processes are discussed in detail in Chapter 4.

3.4. CONCLUSIONS

The dominant heat fluxes that affect the vertical temperature structure of the water column in a free surface wetland containing emergent vegetation have been reviewed. They are shortwave solar radiation, long wave radiation, sensible and latent heats.

Experiments conducted confirm that shortwave solar radiation is generally the most significant of these heat fluxes. Nett black body radiation, sensible and latent heats are generally an order of magnitude smaller than solar radiation. Solar radiation was found to be capable of causing changes in water temperature of up to 2°C hr^{-1}.

Hydrodynamically significant temperature differences developed between vegetated and open water areas of the wetland of the order of 1 to 2°Chr^{-1}; however, by estimating the changes in temperature by heating due to solar radiation, it was found that solar radiation alone did not explain the evolution of the observed temperature profiles.

Plant effects on heat fluxes and vertical water temperature structure were reviewed. From this review the canopy was expected to significantly reduce solar radiation fluxes by directly shading sunlight, and to virtually prevent sensible and latent heat transfers by drastically reducing air velocities in vegetated areas.

From the experiments performed in the canopy of the wetland, it is apparent that the canopy will significantly affect heat and momentum transfers at the air-water interface.

Measurements of air velocities in the canopy show that the mean air velocity profiles agree well with analytical models of velocity profiles in crops. The canopy acts to reduce air velocities to the extent that no significant momentum transfer between the air and the water column is possible within vegetated areas.

Measurements of radiation fluxes in the canopy indicated that for the wetland studied, on average, radiation is transmitted through the canopy with loss in intensity being linear with distance into the canopy, rather than exponential as is the case in dielectric media.

For the day examined, where solar radiation was high, and the wind was low, stratification was strongest from the late morning to early afternoon, but remained significant into the evening. Increased temperature gradients were observed to arise in the vegetated areas, compared with the open water, despite the lower overall temperatures that developed in the vegetated areas.

This enhanced stratification is caused by the combined actions of radiative heating and convective motion between the open water and vegetated areas, as is discussed in Chapter 5.

4. MIXING PROCESSES

4. MIXING PROCESSES

This chapter evaluates the extent of mixing due to turbulence within vegetated and unvegetated sections of the Site B wetlands at Manly Dam. Sources of turbulence examined are wind driven mixing and penetrative convection, which is a heat driven mixing process. Due to the fundamentally different nature of these processes, they have been considered as two separate phenomena within this Chapter. Wind mixing is considered first, then penetrative convection.

In the section on wind mixing, a brief review of concepts important to the area is given first and scaling arguments are presented as necessary, then a review of the effects of vegetation on flows, followed by the findings and interpretations of field observations.

The experimental results were not well suited to analysing penetrative convection, therefore it is only commented on in brief.

4.1. MIXING DUE TO WIND

4.1.1. BACKGROUND

When the air above a water body moves, a transfer of momentum across the air-water interface occurs and motion is induced in the water body. This water movement will cause shear to occur. Shear in turn will lead to turbulence, which causes mixing in the water body.

Air movement above a water body will also cause the propagation of water surface waves. Wind waves themselves only cause mixing when they become steep enough to break due to their own instability. Such wave breaking causes a surface layer of homogenous turbulence to form in large water bodies (Craig and Banner, 1994).

Of more interest here is the wave breaking that occurs after waves traverse the water surface, possibly for quite some distance. In this case, the waves eventually reach shallow water or may encounter an obstacle in the flow and wave breaking will occur. This wave breaking is a highly turbulent process, therefore the generation, propagation and breaking of wind waves may induce mixing in the water column at a location where no wind is immediately present.

There are substantial bodies of literature on:

- the nature of momentum transfers at air-water interfaces (see for example Craig and Banner, 1994, Cheung and Street, 1988) and

- flows within vegetation (see for example Monteith and Unsworth, 1990, Raupach and Thom, 1981).

However, there is only a limited body of literature on mixing and air-water momentum transfers in water bodies containing vegetation (Danard and Murty, 1994, Ackerman and Okubo, 1993 and Anderson and Charters, 1982). Relevant work that has been done in these areas is discussed below.

4.1.2. SCALING OF WIND DRIVEN MIXING IN OPEN WATER

Considering first the case of wind driven turbulence in open water, the Reynolds stress (see for example Tennekes and Lumley, 1972) can be written as:

$$\tau_r = -\rho \overline{u' w'} \qquad 4.1$$

where τ_r is the Reynolds stress, u' and w' are the horizontal and vertical instantaneous turbulent velocities respectively, the overbar represents an averaging function and ρ is the density of the fluid involved. The friction velocity u_* is commonly used to quantify the level of turbulence in a flow (Webster and Hutchinson, 1994). u_* is defined as:

$$u_* = \sqrt{\frac{\tau_r}{\rho}} \qquad 4.2$$

When wind is present above a water body it will give rise to a shear stress on the water surface, which is balanced by the Reynolds stress in the water column (see for example Fischer *et al*, 1979), leading to the expression:

$$u_* \sim \sqrt{\frac{\rho_a}{\rho_w} C_D} U_a \qquad 4.3$$

where ρ_a is the density of air, ρ_w is the density of water and C_D is the drag coefficient.

Cheung and Street (1988) conducted laboratory experiments into turbulence in the surface boundary layer under the influence of wind. They performed experiments over a range of wind speeds from 1.5 ms^{-1} to 13.1 ms^{-1} in water of depth 1.0 m. The surface boundary layer in these experiments developed to between 141 mm and 354 mm depending on the wind speed.

Over the range of wind speeds they investigated, Cheung and Street (1988) found that within the surface boundary layer there were strong correlations between u_* and U_a and between the root mean square velocity fluctuation u_{rms} and u_*, leading to the expressions:

$$u_* \sim 0.0015 U_a \qquad 4.4$$

and

$$u_{rms} \sim 1.8 u_* \qquad 4.5$$

Therefore in open water, it would be expected that the turbulent velocity fluctuations will be three orders of magnitude smaller than the wind speed. As will be seen below, in the field investigations undertaken at Site B, wind speeds were well within the range of the Cheung and Street (1988) experiments; therefore, Equations 4.4 and 4.5 are expected to be valid.

4.1.3. EFFECTS OF VEGETATION ON MIXING DUE TO WIND SHEAR

The four types of macrophytes that occur in wetlands would each be expected to exhibit different effects on mixing. Free floating macrophytes would be expected to transmit shear into the water column, so that movement would be expected to occur in the water column and hence turbulence may arise. However, the presence of vegetation at the water surface, even if free floating, would be expected to reduce the generation of turbulence at the surface. Evidently, with increasing amounts of vegetation on the water surface, mixing will be reduced. The development of motion in the water column below free floating macrophytes is discussed further in Chapter 5.

The presence of floating leaf macrophytes would be expected to greatly reduce mixing in the water column as they would be expected to largely prevent any momentum transfer from the air to the water column, as discussed in Chapter 5.

The presence of submergent macrophytes would not be expected to adversely affect the generation of turbulence at the water surface; however, the presence of such vegetation within the water column would be expected to lead to similar effects to those observed in land based crops, which are briefly discussed below, with increased turbulence at the top of the vegetation and lower turbulence within the vegetation compared to open water. With increasing amounts of vegetation, these effects would be enhanced.

The presence of emergent macrophytes would be expected to reduce the turbulence generated at the water surface, due to the lower air velocities in the plant canopy above the water column. The presence of stems within the water column would be expected to play a similar role to submergent macrophytes.

A number of studies have been performed on mixing in flows through vegetation. These are discussed below.

Danard and Murty (1994) was the only study that could be found that was directly concerned with mixing in emergent macrophytes. They considered the force balance between the drag due to elements in the flow, drag of the water surface on the flow in the air inside the canopy and the drag exerted by the canopy on the free atmosphere and derived an equation for stress at the water surface:

$$\tau_s = \frac{\rho_a C_w C_t U_a^{\ 2}}{C_w + C_D \eta_p H_c d} \tag{4.6}$$

so the friction velocity is given by:

$$u_* = \sqrt{\frac{\rho_a C_w C_t}{\rho_w \left(C_w + C_D \eta_p H_c d\right)}} U_a \tag{4.7}$$

where ρ_a is the air density, C_w is the drag at the water surface, C_t is the drag exerted by the canopy on the flow in the free atmosphere, U_a is the flow velocity in the free atmosphere, C_D is the drag from the plant elements, η_p is the number of plants per unit area, H_c is the canopy height above water level and d is the average stem diameter. From Fischer *et al* (1979), the turbulent velocity should scale with u_*.

Danard and Murty (1994) reported values of $C_w = 2\times10^{-3}$, $C_t = 0.125$ and $C_D = 0.5$. Taking $\rho_a = 1.22$ kgm^{-3}, b-D = 2.5 m, N = 400 m^{-2} and w = 0.01 m, Equation 4.7 gives:

$$u_* \sim 0.0004 U_a \tag{4.8}$$

Comparing this result with Equation 4.4, it would be expected that turbulent velocities in the water column are lower within vegetated areas compared to outside them, by about 60%.

While this analysis appears reasonable, Danard and Murty (1994) reported no data to confirm their model.

Anderson and Charters (1982) performed laboratory experiments on turbulence in flows through *Gelidium nudifrons*, a bush like submergent red alga that grows as a thick matt of branches, 0.5 mm thick in depths of 2 to 30 m off the Coast of California. They performed experiments in which a single plant was placed across a flume and then subjected to constant velocity flows. They found that below a critical flow velocity, an incoming turbulent flow would become laminar, while above the critical velocity laminar flows would become turbulent. They considered that this behaviour was closely analogous to the behaviour of screens in a flow, which are similarly capable of both enhancing and damping turbulence (see for example Groth and Johansson, 1988 and Baines and Peterson, 1951).

Raupach and Thom (1981) and more recently Monteith and Unsworth (1990) present reviews on the micrometeorology of crop environments and the nature of turbulence within crops. Flows through and above a crop are turbulent boundary layer flows involving a rough boundary. Both Raupach and Thom (1981) and Monteith and Unsworth (1990) indicate that turbulence and mean flows reduce drastically from levels above the canopy when descending through the crop from the canopy.

Many of these crop based studies have found plausible relationships for the air velocity profile in the canopy that provide good fits to experimental data. These range from simple analytic models based on mixing length (Cionco, 1972) and constant eddy viscosity (Thom, 1975) assumptions, through to models that balance mean and turbulent kinetic energy, averaged across the canopy to account for wake effects on turbulence (see for example Raupach and Shaw, 1981). Unfortunately none of these models account for shear at the base of the canopy, so they are unsuitable for predicting shear velocities in the water column due to air movement above the canopy.

However, the desire to use such models in the present situation arises due to the need to estimate shear velocities at the water surface. These models do not consider the effects of shear at the base of the canopy, as such they are unsuitable for estimating shear at the air-water interface. The unsuitability of these models was shown in Section 3.3 where the analytic models were found to overpredict velocities just above the water surface within the canopy when applied to data obtained at Site B.

The more complex models were considered not suitable as insufficient data was available for calibrating such a model.

In summary then, from the literature some studies show that mixing would decrease in the presence of vegetation in the water column; however, it appears that it is also possible for mixing to be increased by the presence of vegetation under some circumstances.

4.1.4. FIELD OBSERVATIONS

To determine the effects of wind driven mixing on the water column, data gathered on Thursday 23 February 1994, day 95054 at Site B, using the techniques described in Chapter 2 are examined below. This day was chosen as:

- winds were moderate, so it was expected that some wind driven mixing would be observed and

- solar radiation was low, so it was expected that temperature stratifications would not develop to the extent that mixing would be suppressed.

- Temperature profiles and turbulent velocity measurements were available throughout the day.

4.1.5. METEOROLOGIC CONDITIONS, DAY 95054

Figures 4.1 and 4.2 show the meteorologic conditions for day 95054. Figure 4.1 shows that solar radiation was generally low and fluctuated markedly throughout the day, indicating that the day was occasionally cloudy with some bursts of sunlight. Radiation was first incident on the probe just after 0630 and built slowly until it peaked just after 1330 at 840 Wm^{-2}. No significant radiation was observed after 1818. During daylight hours, the average radiation for the day was 350 Wm^{-2}, and the total radiation load was 15 MJ.

The wind is shown by Figure 4.1 to have been consistently on a bearing of about 220° from 0700 to 1800 from North. The wind speed was moderate just after midnight, between 4 and 6 ms^{-1}, then dropped to 1 to 2 ms^{-1} during the hours before dawn. At about dawn the wind swung back to 220° from North and stayed between 3 and 4 ms^{-1} until about 1700, when the wind speed dropped to 1.5 ms^{-1}. The wind then continued to drop through the evening.

From Figure 4.2, no rain was recorded in the tipping bucket, but the field notes indicate that there was light drizzle in the early morning. Relative humidity was high, over 90% for most of the period from midnight until just after dawn. Just before 0700 the relative humidity started to decline from 100%, reaching 80% at 0730. After 0730 the relative humidity remained between 70 and 85% for the rest of the day.

Figure 4.2 shows the air temperature was initially around 22°C for the first hour after midnight, dropped to between 16 and 18°C until about dawn, then remained quite steady at about 22°C throughout rest of the day, just dropping slightly into the evening.

Figure 4.1. Radiation, Wind speed and Direction, day 95054

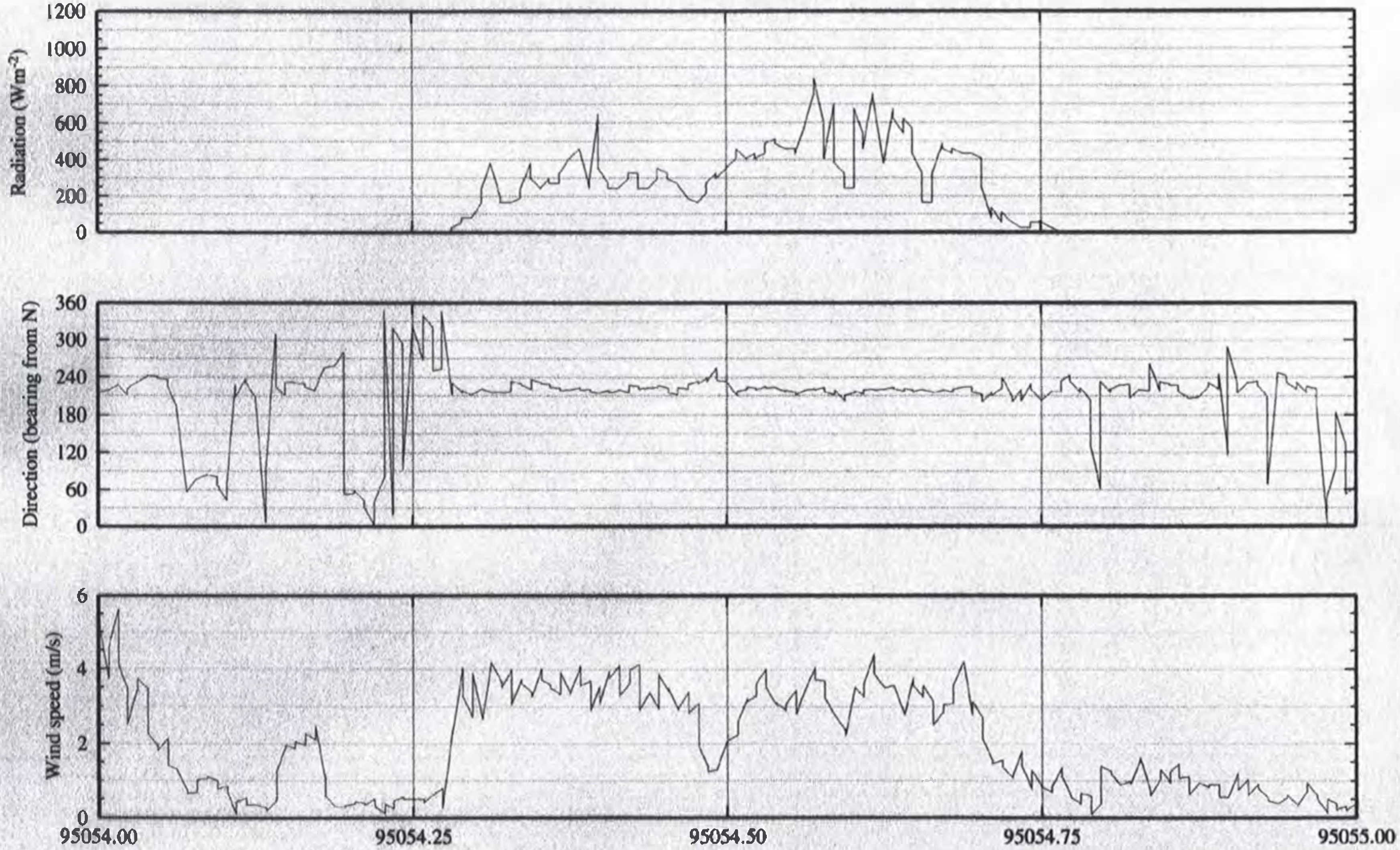

Figure 4.2. Rainfall, Relative Humidity and Air Temperature, day 95054

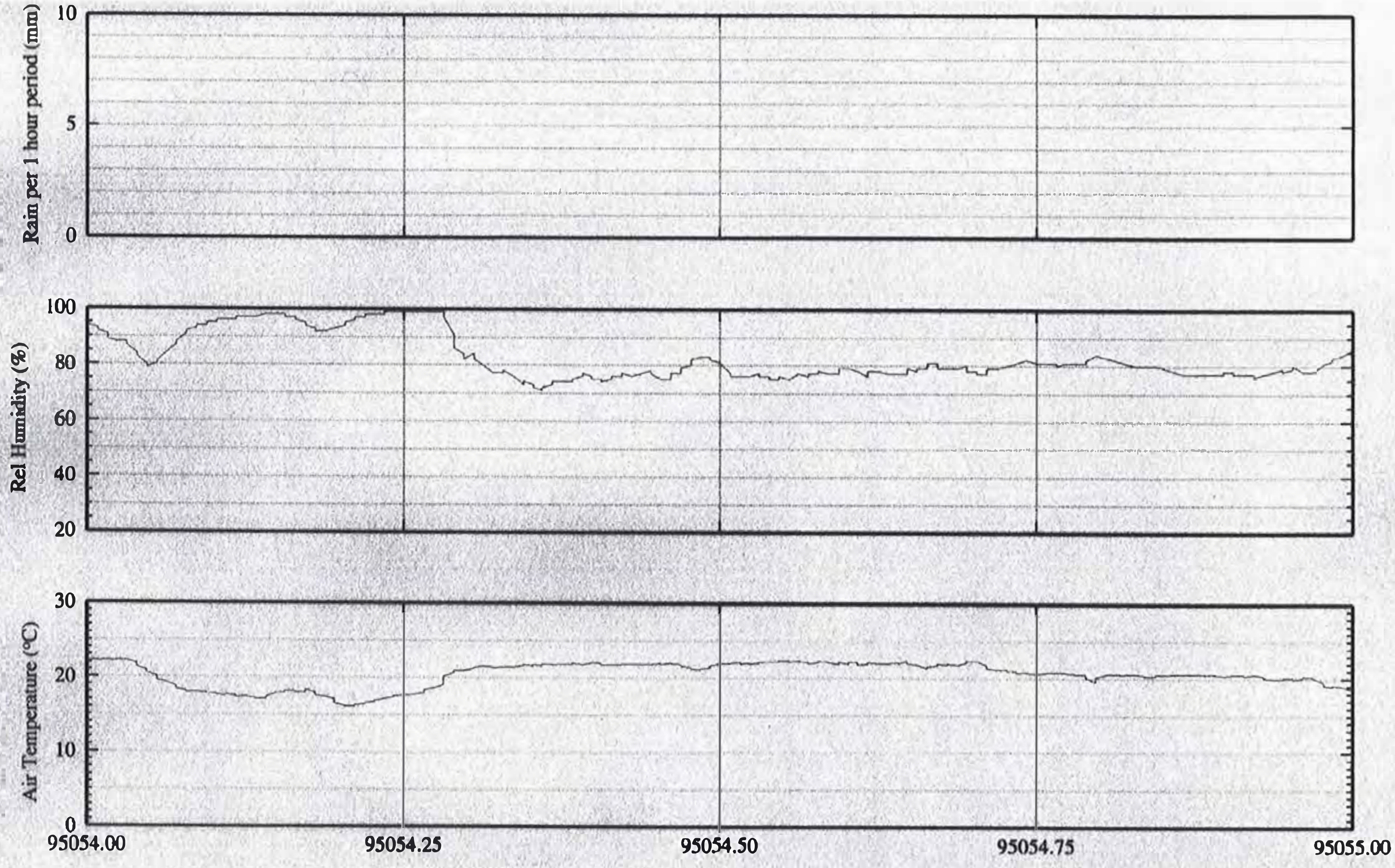

4.1.6. TEMPERATURE PROFILES, DAY 95054

Temperature profiles were obtained between 0630 and 1900 on day 95054 at each of the four stations using the techniques described in Chapter 2. In these profiles, two types of changes with time are important:

- changes of the depth averaged temperature, which indicate whether or not external heating or cooling is taking place, and

- changes of the top to bottom temperature difference, which indicate whether or not mixing is able to overcome the temperature stratification due to external heating.

Temperature differences between the stations are unimportant for analysing mixing processes, however, they may be important in driving convection within the wetland, as discussed in Chapter 5.

Up to five distinct phases of stratifying or mixing behaviour were observed in the water column at Stations 1, 2 and 4. These phases are summarised in Table 4.1, shown on Figure 4.3 and discussed in detail below. The number of these phases that occurred over a single day indicates that within the wetland at the time of measurement there was a fine balance between the external forcings causing mixing and stratification. Plots of temperature against time and at each station throughout the day are also shown in Figures 4.4a to 4.4d.

Importantly, at Station 3, no periods of stratification were observed, despite the much larger increase in the depth averaged temperature at this station over the day. This indicates that in the lake, mixing processes are much more effective at destratifying the water column than in the wetland.

Figure 4.3. Temperature Profiles at Site B, Stations 1 to 4, day 95054

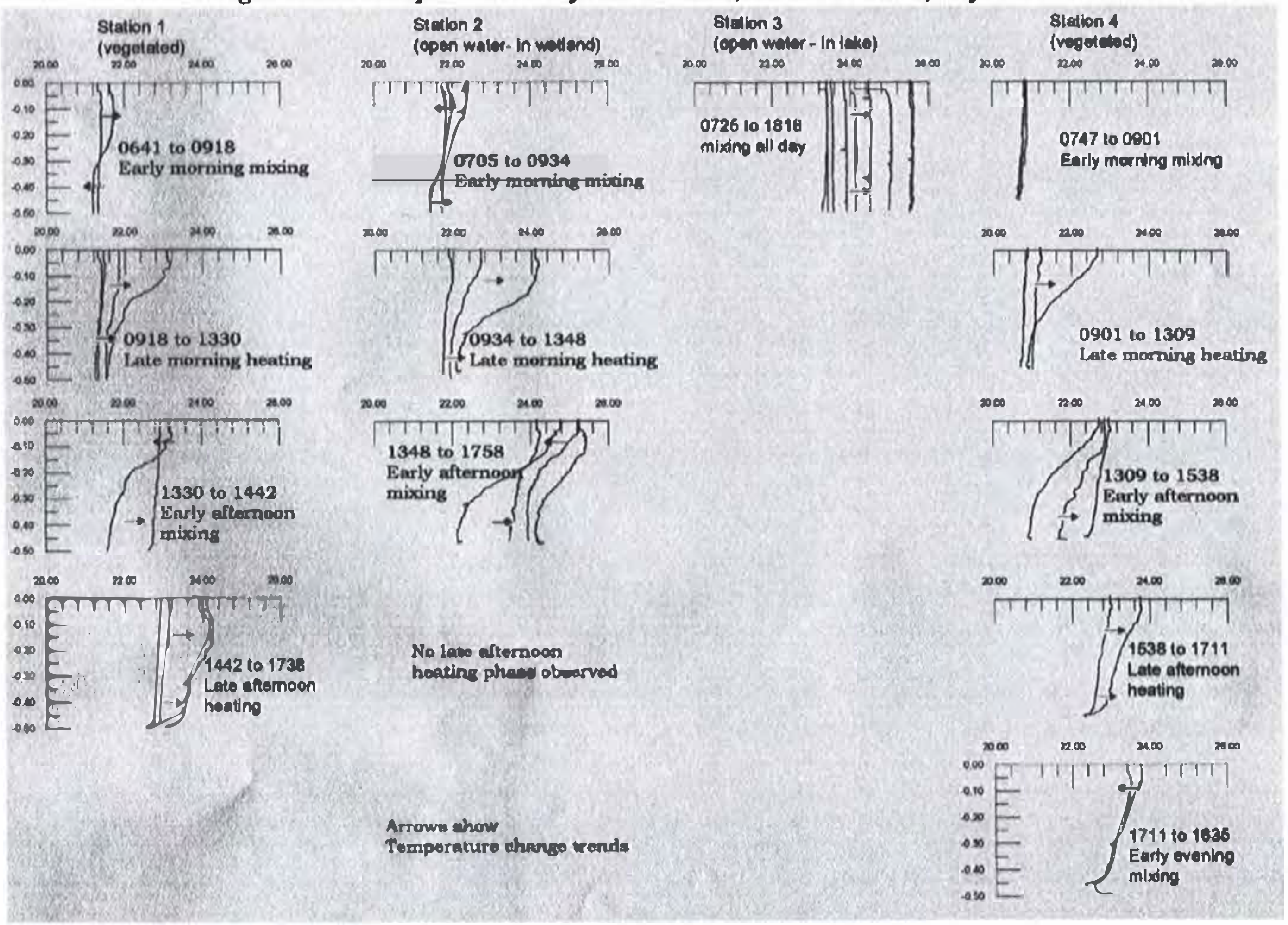

Figure 4.4a. Temperature vs time and depth, Station 1, day 95054

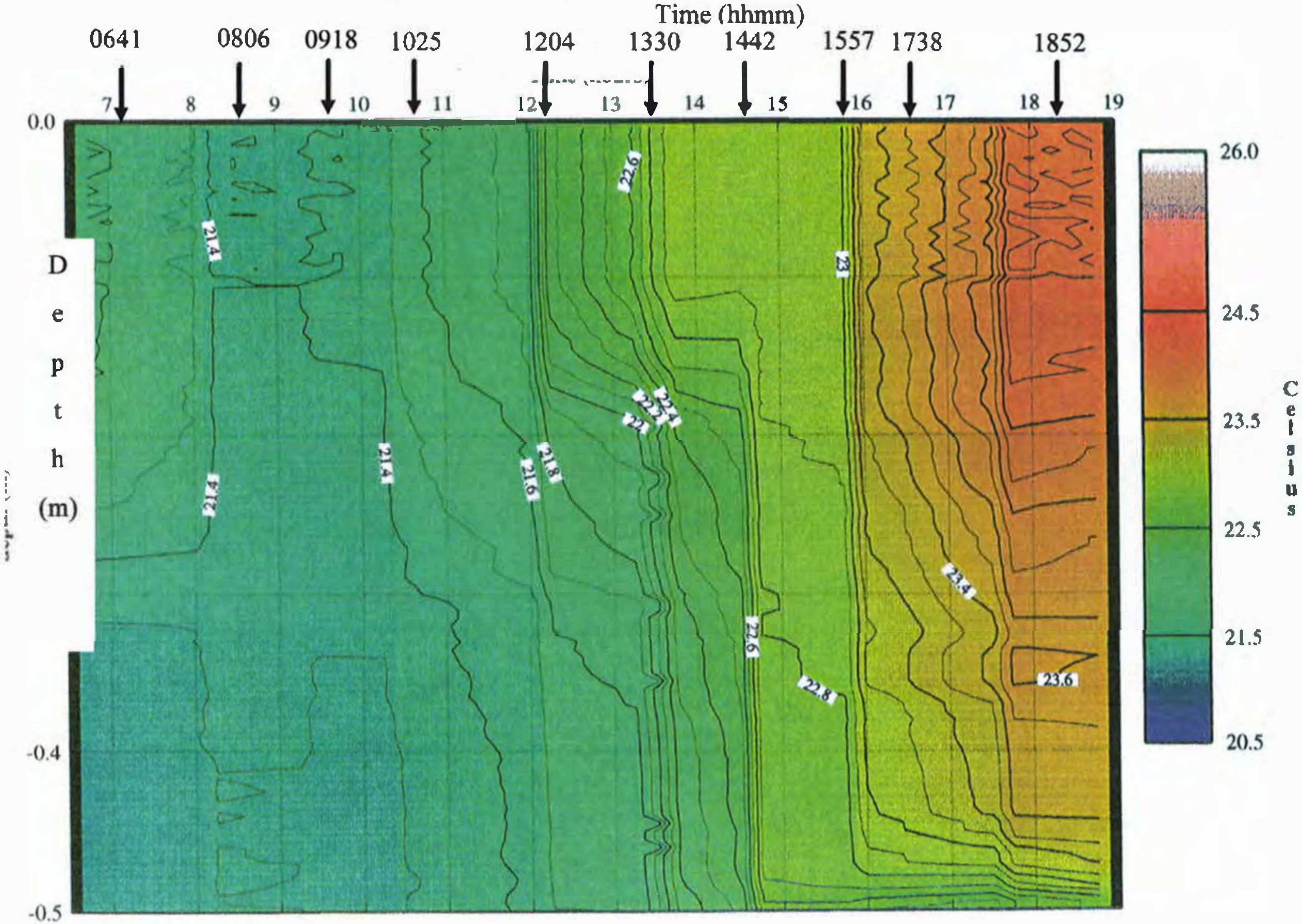

Figure 4.4b. Temperature vs time and depth, Station 2, day 95054

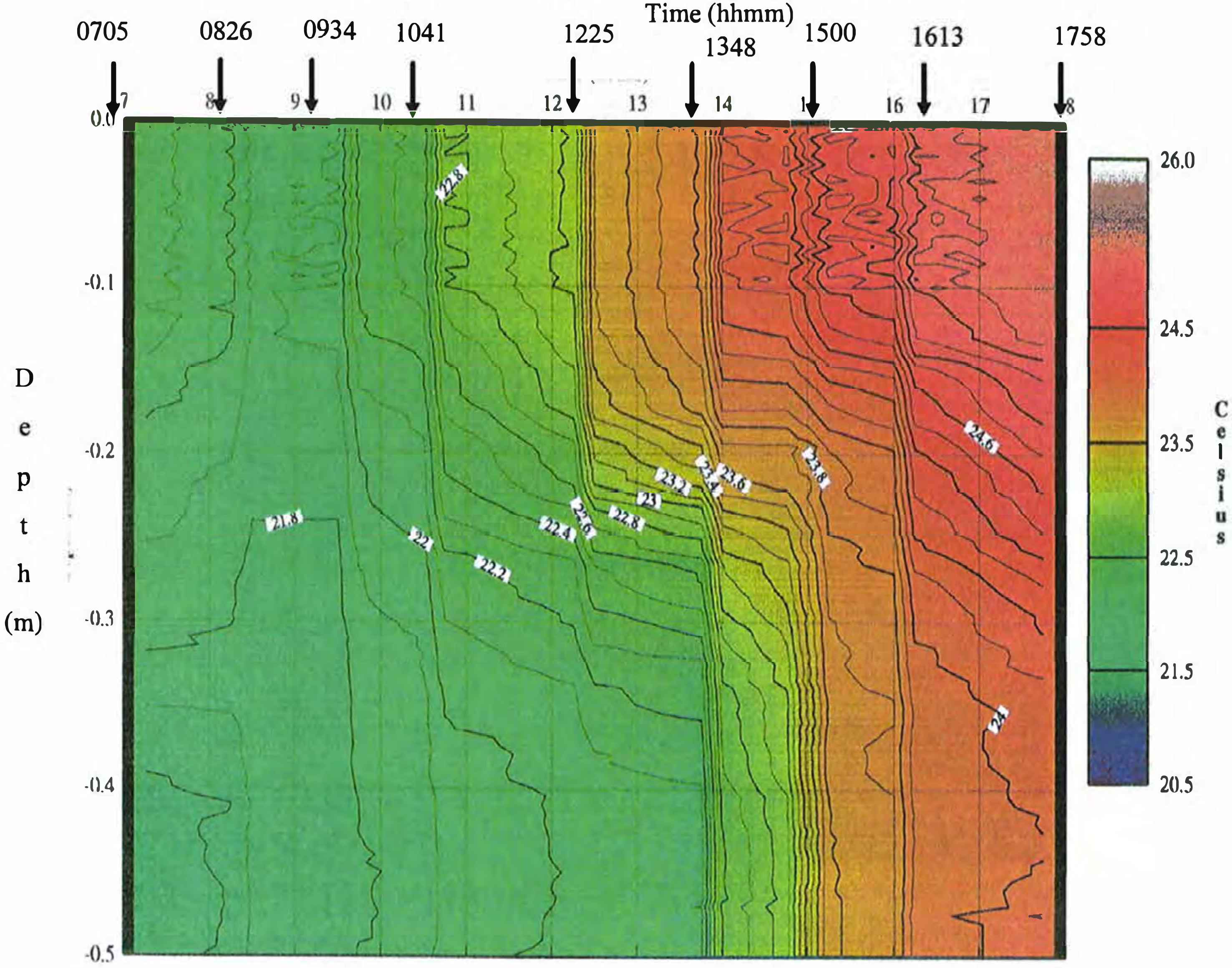

Figure 4.4c. Temperature vs time and depth, Station 3, day 95054

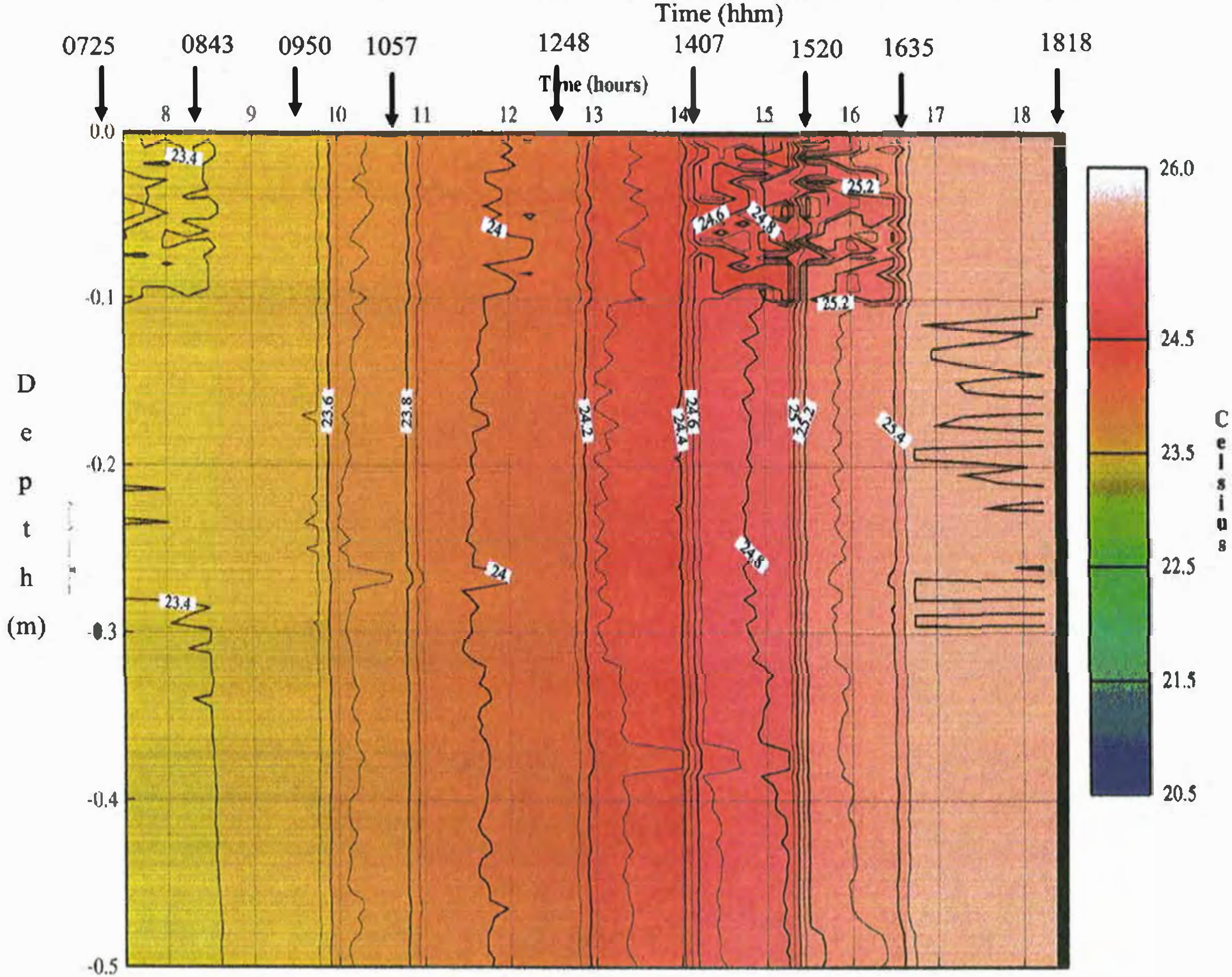

Figure 4.4d. Temperature vs time and depth, Station 4, day 95054

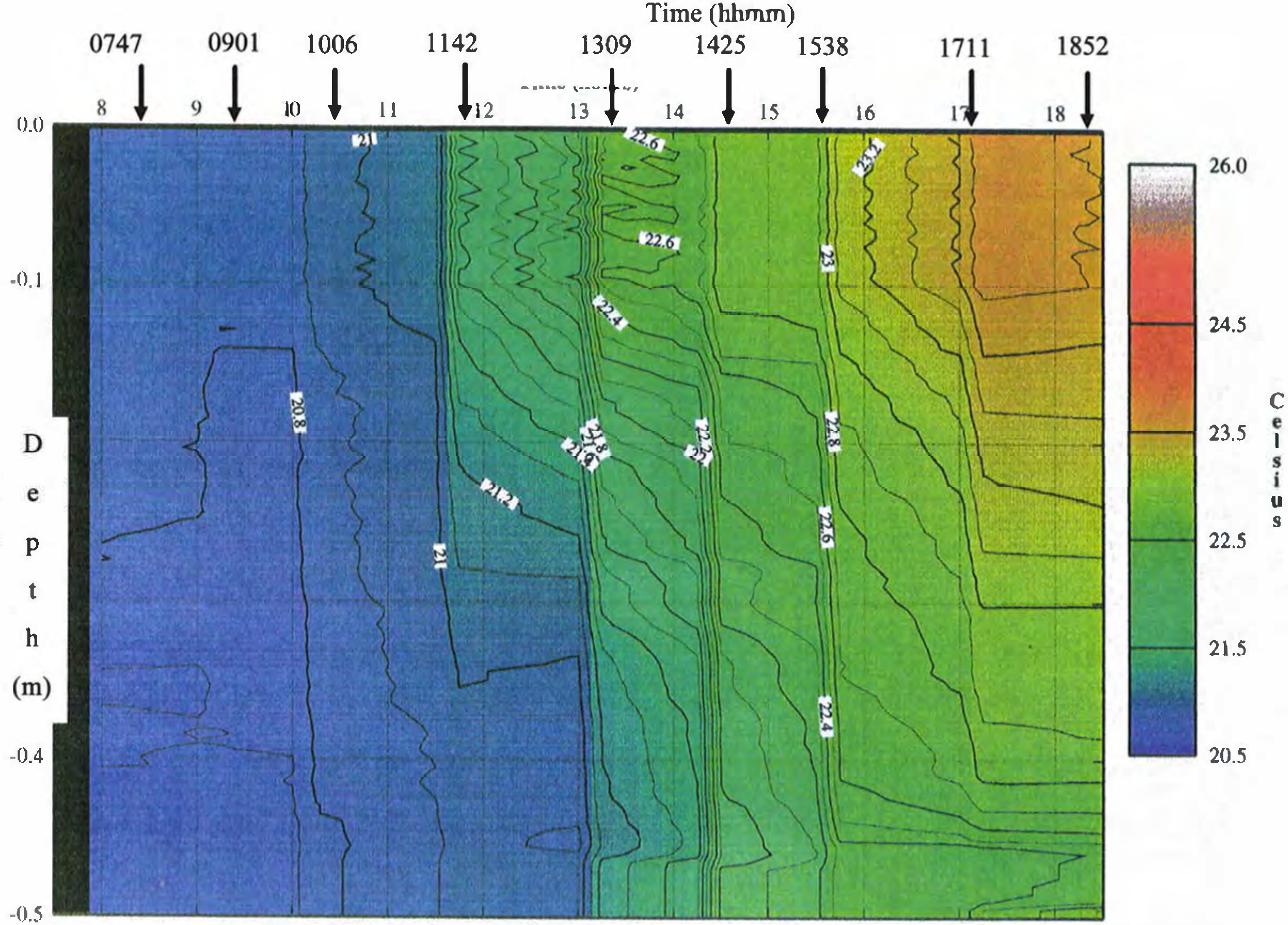

Note that in many areas on Figure 4.3, usually in the upper portion of the water column, wavering contours are present. These wavering contours are caused by changes in temperature of the order of 0.01°C, as measured by the microprofiler. Possible causes of such small changes in temperature would include turbulence, wind at the surface waves, internal waves (where a stratification is present) and noise. These factors are discussed below in the section on the velocity spectra.

Unfortunately the non-stationary nature of the temperature data gathered and the small depth of the water column meant that insufficient data was obtained to allow statistically meaningful temperature spectra to be obtained.

Table 4.1. Summary of Stratification and Mixing Phases

Stations 1 to 4, Site B, 23 February, 1995

All temperatures in °C

Station 1			Station 2			Station 3		Station 4		
Time	$\overline{T}$	ΔT	Time	$\overline{T}$	ΔT	Time	$\overline{T}^*$	Time	$\overline{T}$	ΔT
0641	21.5	0.3	0705	21.9	0.5	0711	23.3	0747	20.8	0.2
Early Morning Mixing			Early Morning Mixing					Early Morning Mixing		
0918	21.5	0.1	0934	21.9	0.2	Mixing		1006	20.8	0.2
Late Morning Stratifying			Late Morning Stratifying					Late Morning Stratifying		
1330	22.5	1.5	1348	22.9	1.7	All		1309	21.9	1.8
Early Afternoon Mixing			Early Afternoon Mixing					Early Afternoon Mixing		
1442	23.0	0.2	1758	24.7	1.3	Day		1538	22.8	0.5
Late Afternoon Stratifying			No late afternoon					Late Afternoon Stratifying		
1852	23.5	0.8	stratifying phase observed			1818	25.6	1711	23.1	1.2
								Early Evening Mixing		
								1835	22.9	0.8

$\overline{T}$: depth averaged temperature

ΔT: difference between top and bottom temperatures

* Temperature constant with depth all day at Station 3.

STATION 1 (VEGETATED, 8 M FROM LAKE)

Figure 4.3 shows that 4 different phases of behaviour occurred through the day at Station 1: an early morning destratification phase; a late morning stratifying phase; an early afternoon destratification phase and another phase of stratifying in the late afternoon. These are discussed separately below.

Early Morning Mixing Phase, 0641 to 0918

Through the early morning from 0641 to 0918, Figure 4.1 shows that the radiation incident on the plant canopy averaged just over 200 Wm^{-2}. Evidently, plant shading significantly lowered the amount of radiation that entered the water column at Station 1 as the depth averaged temperature in the water column remained constant from 0641 to 0918 at 21.5°C.

Over the same period, Figure 4.3 shows that the stratification dropped from 0.3°C over the 0.5 m depth of the water column at 0641 to 0.1°C at 0918. Evidently this destratification resulted from the moderate southerly wind of 3 to 4 ms^{-1} that is shown by Figure 4.1 to have commenced at about the same time as the profiling at Station 1 commenced at 0641. The causes of stratifications in the very early morning encountered at Stations 1, 2 and 4 is most likely buoyancy driven convection, as discussed in Chapter 5.

Late Morning Stratifying, 0918 to 1330

From 0918 to 1330, Figure 4.3 indicates that the whole water column became warmer, probably due to radiative heating and became strongly stably stratified. From Figure 4.1 it can be seen that between 1204 and 1330 the solar radiation load above the canopy became quite strong, averaging approximately 350 Wm^{-2}. The large radiation load caused the average temperature of the water column to increase by 1.1°C from 21.4°C at 0918 to 22.5°C at 1330.

The strong surface heating also gave rise to temperature stratification within the water column. By the time of the 1330 profile, a stable stratification of over 1.5°C over the depth of the water column had developed.

Early Afternoon Mixing, 1330 to 1442

From 1330 to 1442, Figure 4.3 shows that the depth averaged temperature increased by 0.5°C from 22.5°C at 1330 to 23.0°C at 1442; however the extent of stratification reduced dramatically, with the top to bottom temperature difference falling from 1.5°C at 1330 to 0.2°C at 1442.

This reduction in stratification did not correspond to an increase in wind speed, nor a fall in air temperature; however as shown in Figure 4.1, the solar radiation incident on the canopy was significantly lower from 1400 to 1430 than it had been between 1200 and 1330.

It would seem that whereas between 0918 and 1330, the incoming radiation not only heated the water column, but also gave rise to a sufficiently strong buoyancy flux that turbulence was suppressed and momentum driven mixing did not occur. In the absence of strong radiative heating between 1400 and 1430, it is apparent that the wind driven turbulence became strong enough to overcome this buoyancy flux.

Late Afternoon Stratifying, 1442 to 1852

Between 1442 and 1852, Figure 4.3 shows that the depth averaged temperature increased from 23.0°C to 24.0°C and the water column became more stratified with the top to bottom temperature difference increasing from 0.2°C at 1442 to 0.8°C at 1852.

The wavering contours near the water surface on the later profiles, which were taken at 1557 and 1852, again most likely indicate that active mixing is occurring here.

In summary at Station 1, mixing occurred early in the morning, after which stratification built through the day due to either radiative heating (see Section 3) or a convective inflow from the lake (see Section 5). Some event then destratified the water column between the profiles taken at 1330 and 1442, after which, stratification then built up again as it had done through the morning, however not as strongly as in the morning.

STATION 2 (OPEN WATER, 7 M FROM THE LAKE)

Figure 4.3 shows that throughout the day, the water column at Station 2 was generally slightly warmer than at Station 1. As at Station 1 a number of phases can be seen to be present in temperature structure of the water column. These phases are discussed below and comparisons are drawn between behaviour at Stations 1 and 2.

Morning Mixing, 0705 to 0934

From 0705 to 0934, Figure 4.3 shows the depth averaged temperature in the water column at Station 2 was constant at 21.9°C, despite the average solar radiation of 200 Wm^{-2} recorded during this period. Evidently the sun was so low in the sky during this period that the vegetation surrounding Station 2 prevented solar radiation from reaching the water surface directly.

Over the same period, the stratification dropped from 0.5°C over the 0.5 m depth of the water column at 0705 to 0.2°C at 0934. As at Station 1, this destratification was most likely caused by turbulence induced by the southerly wind that arose early in the morning and the apparent absence of significant solar radiation entering the water column due to plant shading.

Late Morning Stratifying, 0934 to 1348

Figure 4.3 shows that during the late morning at Station 2, the average temperature in the water column increased steadily by 1.0°C from 21.9°C at 0934 to 22.9°C at 1348. This is approximately the same rate of increase in temperature as occurred at Station 1 over the same time period.

As at Station 1, the water column at Station 2 became highly stratified after 1330. At Station 2 a top to bottom temperature difference of 1.7°C was recorded at 1348 compared to 1.5°C at Station 1. The increase in average temperature and stratification, especially between 1225 and 1348, can be attributed to the high incident solar radiation and the wind protection provided by the plants surrounding the Station.

Afternoon Mixing, 1348 to 1758

From Figure 4.3 it is evident that from 1348 to 1758, although there was an increase in the depth average temperature from 22.9°C to 24.7°C, there was a slight decrease in stratification, with the top to bottom temperature difference reducing from 1.7°C to 1.3°C. By contrast with Station 1, no late afternoon restratification occurred.

STATION 3 (OPEN WATER IN THE LAKE)

Figure 4.3 shows that water temperatures at Station 3 were much higher throughout the day than at Stations 1 or 2. Furthermore, the near vertical profiles shown on Figure 4.3 at Station 3 throughout the day indicate that the water column was unstratified and well mixed throughout the entire day, not showing stratifying as at Stations 1 and 2.

The water temperature at Station 3 initially was approximately 23.4°C at 0711. As the day went on, the water temperature increased to 25.6°C by 1818.

The lack of stratification at Station 3 compared to Stations 1 and 2 is discussed further in Section 4.2.

STATION 4 (VEGETATED, 13 M FROM THE LAKE)

Comparison of Figure 4.3 shows that temperatures at Station 4 were lower than at the other stations. There was initially little stratification at Station 4, but as at Station 1 and 2, a reasonable stratification had developed by 1300, in this case the temperature difference was about 1.0°C over 0.5 m. Distinct phases of temperature behaviour can be seen throughout the day at Station 4. These phases were similar to those observed at Stations 1 and 2, as described below.

Early Morning Mixing, 747 to 1006

From 0747 to 1006, Figure 4.3 shows the depth averaged temperature in the water column at Station 2 was constant at 20.8°C, and the stratification was constant with a temperature difference over the depth of the wetland of 0.2°C. This invariance in the temperature structure of the water column at Station 4 occurred despite the average solar radiation of 200 Wm^{-2} recorded during this period. Evidently the sun was so low in the sky during this period that the vegetation at Station 2 prevented solar radiation from reaching the water surface directly.

In contrast to Stations 1 and 2, the initial stratification recorded at Station 4 was much lower than at Stations 1 or 2. However the initial reading at Station 4 was taken at 0747, much later than the initial readings at Stations 1 and 2, at 0641 and 0705 respectively. It is therefore difficult to say that there was no initial stratification at Station 4 in the early morning as the profile here was taken much later than at the other Stations. A stratification may have been present early in the morning, but if it had been, evidently wind mixing had destratified the water column by the time of the first sample.

Late Morning Stratifying, 1006 to 1309

Figure 4.3 shows that during the late morning at Station 4, the average temperature in the water column increased steadily by 1.1°C from 20.8°C at 1006 to 21.9°C at 1309. This is approximately the same rate of increase in temperature as occurred at Stations 1 and 2 over the same time period.

As at Stations 1 and 2, the water column at Station 4 became highly stratified in the early afternoon. At Station 4 a top to bottom temperature difference of 1.8°C was recorded at 1309 compared to 1.5°C and 1.7°C at Stations 1 and 2 respectively. As at Stations 1 and 2, the increase in average temperature and stratification, especially between 1142 and 1309, can be attributed to the high incident solar radiation and the wind protection provided by the plants at the Station.

Early Afternoon Mixing, 1309 to 1538

By contrast with the Stations 1 and 2, Figure 4.3 shows that some stratification persisted at Station 4 throughout the whole afternoon; however in the early afternoon, there was some evidence of destratification and therefore mixing as the temperature difference between the top and bottom of the water column dropped from 1.8°C at 1309 to 0.5°C at

1538. This destratification occurred despite a rise in depth averaged temperature of 0.9°C from 21.9°C at 1309 to 22.8°C at 1538.

Late Afternoon Stratifying 1538 to 1711

From 1538 until 1711, Figure 4.3 shows that the water at Station 4 again became warmer and more stratified. There was a significant increase in the average temperature of the water column by 0.5°C from 22.8°C at 1538 to 23.1°C at 1711, over the same period of time the stratification also rose from 0.5°C to 1.2°C.

Early Evening Mixing 1711 to 1835

By contrast with Station 1, Figure 4.3 shows that mixing was observed in the very late afternoon or early evening between 1711 and 1835 at Station 4. Presumably this destratification occurred as much less radiation would have penetrated to the water column at Station 4 as it was much further into the vegetation than the other stations.

During this period of mixing, the stratification dropped from a top to bottom temperature difference of 1.2°C to a top to bottom temperature difference of 0.8°C and the depth averaged temperature dropped by 0.1°C from 23.0°C to 22.9°C.

4.1.7. VELOCITY READINGS, DAY 95054

Velocities were recorded throughout day 95054 at each station using the ADV-1 acoustic doppler velocity probe by the fixed depth sampling method described in Chapter 2. Readings were taken by placing the probe at 3 depths through the water column at each site. Sampling was conducted at the maximum rate possible on the instrument (25 Hz) for a minimum of 60 s; therefore, each time series consisted of at least 2400 measurements. Depths of readings are shown in Table 4.2.

Table 4.2. Depths (in mm) of ADV-1 velocity readings at Stations 1 to 4

	Station 1	Station 2	Station 3	Station 4
Top point	45	40	70*	40
Middle point	290	260	400	230
Bottom point	510	460	760	440
Water depth	520	485	780	455
Bearing to North of velocity signals	218°	242°	324°	356°

* *Readings at the top point at Station 3 were taken 30 mm further below the water surface than at the other stations to ensure that the probe was submerged at all times. This was necessary to account for the higher wave action here.*

Subsequent to the investigations, it was found that a malfunction in the ADV-1 caused cross channel contamination from one of the channels to another. As such, there were only two channels from which reliable data could be obtained for the analysis of turbulent fluctuations. Unfortunately it was not feasible to repeat the experiments after this error in the velocity was found.

Fortunately, the channel gathering data in the horizontal plane was unaffected, so that a fluctuating velocity component in the horizontal could be used for turbulent analysis; however, the other channel from which reliable results were obtained was inclined at an angle of 60° to the horizontal, therefore the vertical fluctuating component could not be examined. All results reported below are for the fluctuating horizontal component of the ADV.

Note that because only one velocity component in the horizontal was able to be measured it was not possible to determine the magnitude nor direction of the mean flow in the horizontal. This introduces the following limitations to these findings:

- It is not possible to report the fluctuating horizontal components aligned, with or normal to the flow, as the direction of the mean flow in the horizontal is not known.

- The power spectra must be plotted as a function of frequency and cannot be plotted as a function of the wave number, as the mean velocity is not known.

- It is necessary to assume that the fluctuating velocity component is isotropic in the horizontal. The validity of assuming the turbulent contributions to the fluctuating velocity signal are isotropic may be argued, but clearly surface waves will be directional and the orientation of the instrument at each of the stations must be considered. Directions of the horizontal velocity signals referenced to North as obtained at each of the four stations are given in Table 4.2.

SPECTRAL TECHNIQUES

The power spectrum in the frequency domain of a stationary, time varying signal is an effective data analysis tool, allowing the effects of physical processes that repeat at different frequencies to be discerned. To distinguish the turbulent fluctuations in the velocity signal from other effects, such as waves and electronic noise, it was necessary to analyse the power spectrum of the velocity time series. Smoothed power spectra were obtained by taking the fast fourier transform (FFT) of the ADV-1 data according to techniques described in Bendat and Piersol (1986).

Preparation of the data was necessary prior to and after applying the FFT to give the best possible results. Techniques applied for data preparation are discussed below, followed by assessment of the spectra obtained.

Data Preparation

Data preparation performed in conjunction with the evaluation of the power spectra consisted of mean removal, windowing, padding, normalising and band averaging.

Mean removal was performed so that only the fluctuating component of the signal would be seen in the spectra. There was no physically expected, nor any clearly apparent trend in the data, under such circumstances detrending is not recommended (Bendat and Piersol, 1986) so no detrending was performed.

The Cooley-Tukey procedure (Bendat and Piersol, 1986) was used to calculate the FFT. This procedure takes advantage of the binary number system used by modern digital computers. However, the Cooley Tukey algorithm can only be used on data sets where the number of samples is equal to a power of 2 (Bendat and Piersol, 1986). To bring the number of samples in the time series up to the next highest power of 2 above the number of samples taken the data set was "padded" with zeroes. Padding is known not to adversely affect the FFT procedure (Bendat and Piersol, 1986).

To reduce leakage in the frequency domain that would occur due to the finite period of time over which sampling was performed a Blackman window was used to taper the time series at either end. The Blackman Window is a commonly used cosine type tapering window given by the equation:

$$f(i) = 0.42 - 0.5\cos\left[\frac{2\pi(i-1)}{n-1}\right] + 0.08\cos\left[\frac{4\pi(i-1)}{n-1}\right] \qquad 4.9$$

where f(i) is the factor by which the i^{th} sample in the time series is multiplied, and n is the number of samples in the data set.

Following mean removal, padding and windowing, the power spectrum in the frequency domain of the fluctuating velocity signal was obtained by taking the FFT of the velocity time series. To smooth the results in the frequency domain, spectral filtering was performed by applying band averaging over the frequency range obtained. To allow resolution of the low frequency readings, while providing sufficient smoothing of the very noisy signals expected at high frequency, band averaging was graded from three spectral values being averaged at the lowest frequencies, to ten spectral values being averaged at high frequency, the geometric rate of increase in band size was 1.2.

From Bendat and Piersol (1982), the accuracy of the estimates of the spectral intensities can be calculated as:

$$\left(1-\frac{2}{\sqrt{n_d}}\right) \leq \frac{\phi_{est}}{\varphi_{95}} \leq \left(1+\frac{2}{\sqrt{n_d}}\right) \qquad 4.10$$

Where ϕ_{est} is the estimated spectral value, ϕ_{95} is the upper/lower confidence limit of the spectral estimate and n_d is the number of spectral values used for band averaging.

Given the above techniques for band averaging, ratios of confidence limit to spectral estimate frequency are plotted as a function of frequency in Figure 4.5, for data obtained at Station 1 on day 95054 at the top of the water column.

From Figure 4.5 it can be seen that except at frequencies below 0.1 Hz, there is a 95% probability that the spectral estimates are within 50% of the calculated values.

To ensure the spectrum represents the correct energy levels in the original signal, as a final step the spectrum was normalised to ensure the area under the spectrum is equal to the variance of the original time series.

Figure 4.5. Confidence Intervals of Spectral Estimates

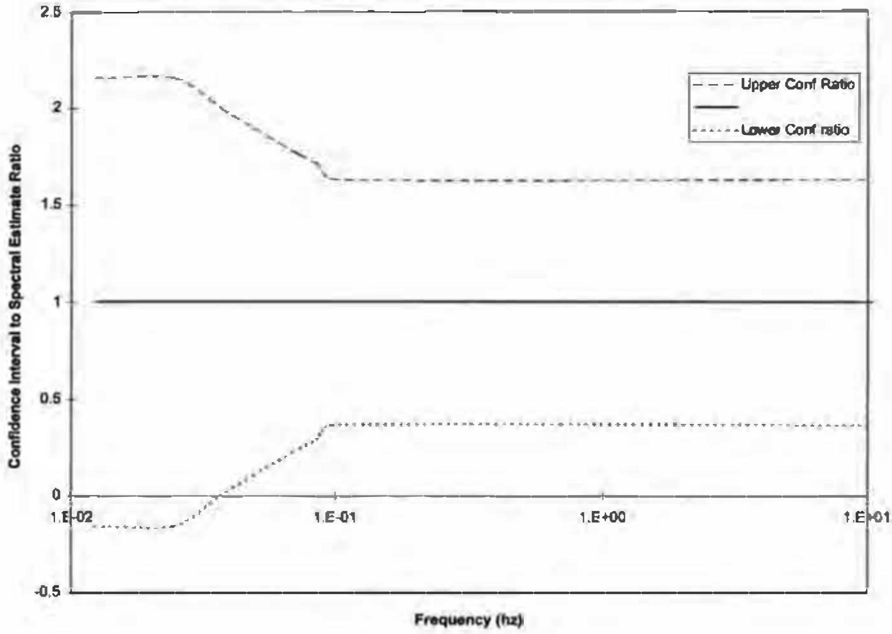

BEHAVIOUR OF THE FLUCTUATING COMPONENT OF THE VELOCITY SIGNALS

Table 4.3 shows the total power, $\overline{u'u'}$ and Root Mean Square (RMS) velocity, $\sqrt{\overline{u'u'}}$, averaged over all readings taken at each station on Thursday 23 February, 1995. Figure 4.6 shows the depth averaged total power $\overline{u'u'}$ at each station plotted against time, again for 23 February 1995. Power and RMS velocity values for each set of readings were calculated as part of the FFT procedures.

No attempt was made to remove components of the signal at different frequencies from the values shown in Table 4.3, they therefore show the combined effects of many factors, as discussed below. If it is assumed that no station is predisposed to more electronic noise than other sites and that sufficient samples were taken at each station to make the levels of noise uniform across all stations, the differences in values shown in Table 4.3 will reflect the differences in levels of velocity fluctuations due to physical processes occurring in the water column.

Table 4.3. Values of Horizontal Power and velocities,

Averaged over all Readings for Thursday 23 February, 1995,

Wind Speed = 1 m/s,

Predicted u_{*unveg} ~ 0.1 cm/s, u_{*veg} ~ 0.04 cm/s (Equations 4.4 and 4.8)

Station	Values over the whole spectra	
	Power (cm^2/s^2)	RMS velocity (cm/s)
1 (veg)	0.116	0.34
2 (open)	0.228	0.48
3 (lake)	0.841	0.92
4 (veg)	0.051	0.23

Figure 4.6 Depth Averaged Spectral Power
(values over the whole spectrum)

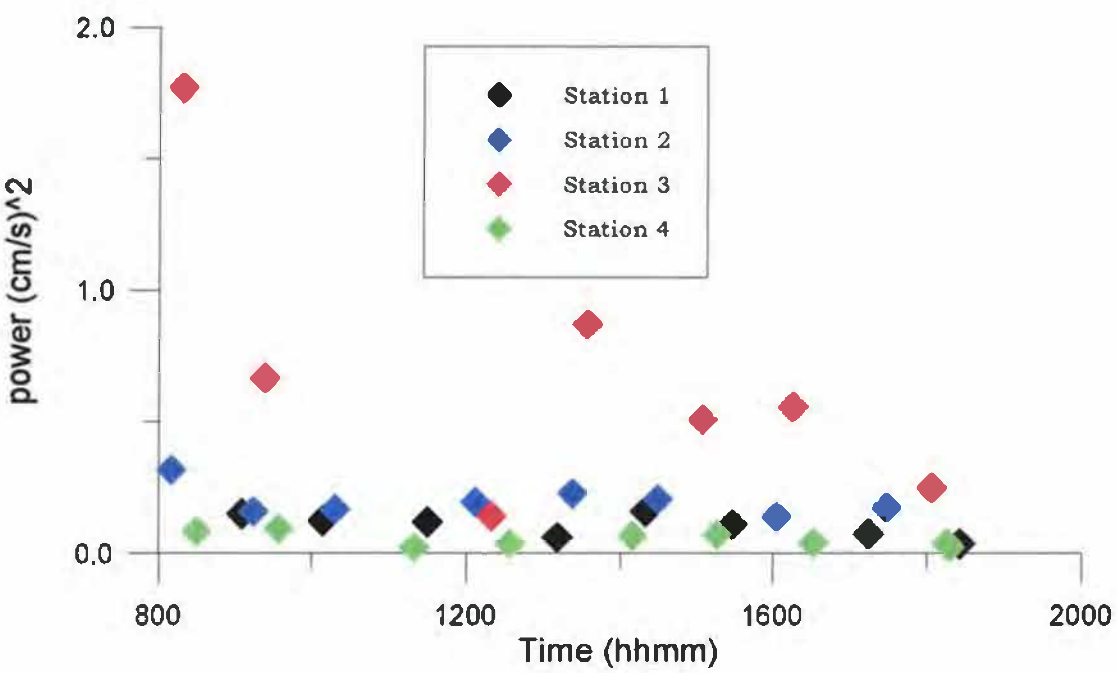

Table 4.3 clearly shows that the time and depth averaged overall power of the fluctuating component of the velocity readings taken is highest at Station 3, followed by Station 2 then Station 1, which have similar levels of power, then Station 4, which clearly has the lowest power. From Figure 4.6, it can be seen this pattern of behaviour is followed throughout the day, the only exception being when the power at Station 3 falls slightly below that at Station 2 just after midday.

Figure 4.6 clearly shows that the velocity fluctuations at Station 3 are non-stationary through the day. At Station 3, the spectral power is high early in the morning, then decreases over the rest of the day. Stations 1 to 4 show no broad changes in depth averaged spectral power through the day.

From Table 4.3 and Figure 4.6 it can clearly be seen that there are generally higher levels of velocity fluctuations in the lake than in the wetland, that velocity fluctuations are marginally higher in open water within the wetland than in vegetated parts of the wetland, and that velocity fluctuations decrease with distance from the lake. However, to determine the extent of mixing caused by these velocity fluctuations it is necessary to examine the processes that give rise to these fluctuations.

A number of previous studies have identified mechanisms responsible for fluctuations of velocity signals in fluid flows. Mechanisms that are relevant to the present study are listed below. It is important to note that not all of these mechanisms cause mixing, as described below.

- **Turbulence** which is an irregular, diffusive, three dimensional, dissipative phenomenon (Tennekes and Lumley, 1972). The diffusive nature of turbulence makes it a cause of active mixing.

- **Surface gravity waves** including wind driven waves (see for example, US Army Core of Engineers, 1984) and seiches which are standing waves caused by wind setup that occur at a resonant frequency for a particular water body (see for example

Hutter, 1984). Of themselves surface waves and seiches are not a cause of mixing but should wave breaking occur, turbulence and mixing will result.

- **Internal gravity waves** that occur across density stratifications within the fluid (see for example Turner, 1972, Gregg and Briscoe, 1979). As for surface waves, internal waves are not a cause of mixing but can break, thereby causing turbulence and mixing.

- **Fossil turbulence** (see Gibson, 1986): because of the dissipative nature of turbulence, if the energy source giving rise to turbulence in a stratified fluid is removed, the turbulence will cease. When the turbulence stops, the irregular, random motion of the turbulence will leave density inversions in the fluid. As the fluid restratifies under the influence of gravity, velocity fluctuations will arise. Such velocity fluctuations are known as fossil turbulence and are a type of internal wave.

- **Noise** in the velocity signal due to limitations of the instrument and sampling techniques used (see for example Bendat and Piersol, 1986).

Figure 4.7 shows smoothed spectral plots of the velocity time series collected between 0850 and 0939 at Stations 1 to 4, Site B. From the preceding section on the temperature structure of the water column, it can be seen that little or no stratification was present at any of the stations during this time period with the exception of Station 2.

Despite the fact that it was difficult to interpret peaks and troughs in individual spectra, from Figure 4.7 there appeared to be a consistent pattern of features in the spectra obtained at each station. Given the 95% confidence limits calculated above, there were three basic features of all the spectra that showed this apparent pattern:

Figure 4.7. Smoothed Spectral Plots obtained at Stations 1 to 4, Day 95054

Plotted as log Spectral Power Intensity in log(cm^2/s^1) vs log Frequency in log(Hz)

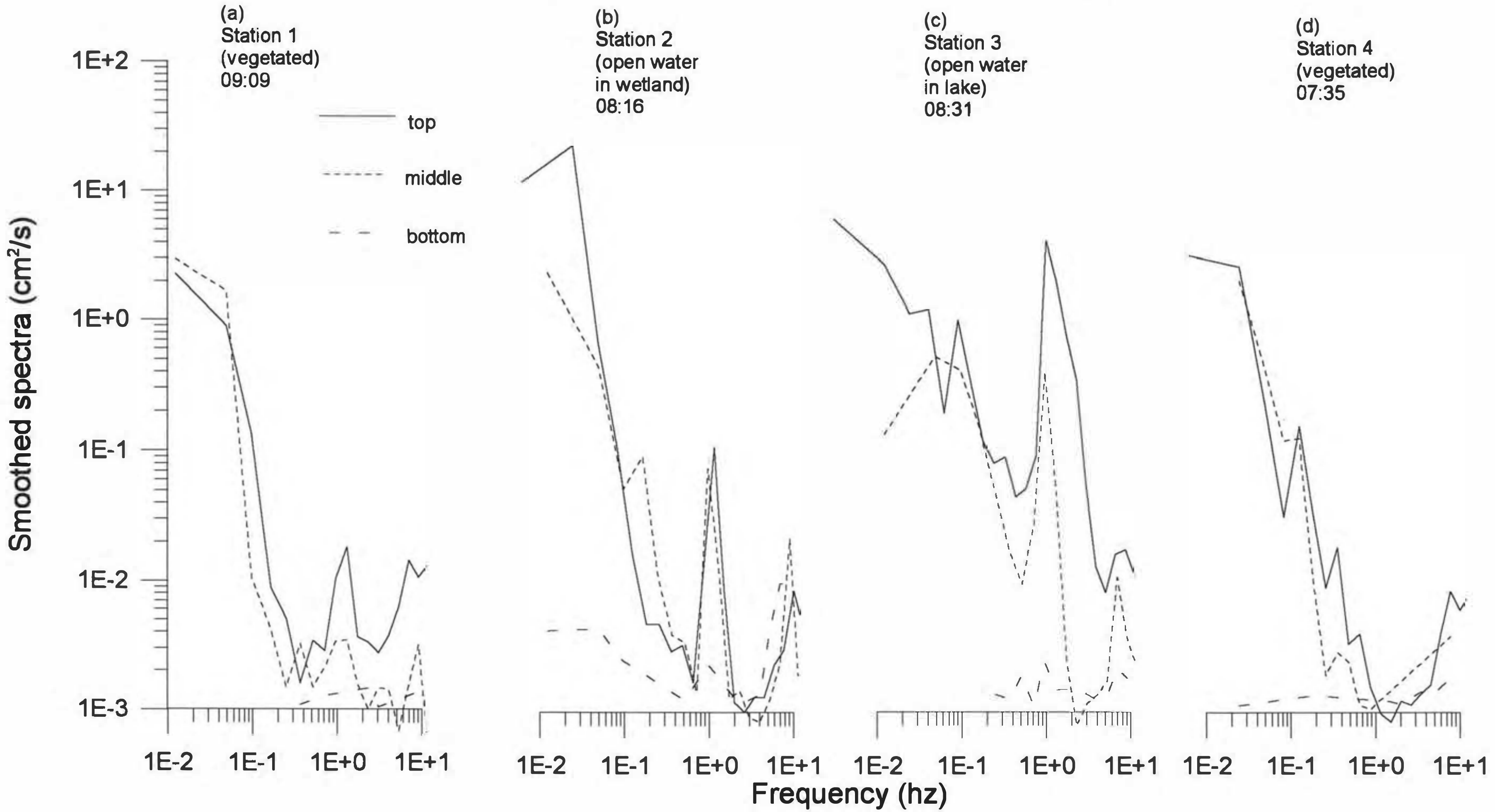

- At low frequency, high spectral intensities were obtained at all stations. These intensities were decreasing with increasing frequency at all stations until about $10^{0.2}$ Hz.

- At mid frequencies between $10^{-0.2}$ and $10^{0.4}$ Hz, all stations showed a local peak in spectral intensity. This peak was highest at Station 3, followed by Station 2, Station 1 and then Station 4.

- At high frequency above about $10^{0.2}$ Hz all stations displayed low levels of spectral intensity that was generally rising with frequency.

These features are consistent with the phenomena mentioned above, as explained below and as shown on Figure 4.8.

TURBULENCE DUE TO WIND DRIVEN SHEAR GIVING RISE TO LOW FREQUENCY VELOCITY FLUCTUATIONS

Turbulence typically occurs over a range of length and time scales, with energy input arising due to the conversion of kinetic energy from the mean flow to turbulence at large length and time scales, then with smaller eddies with faster time scales feeding off these larger eddies, down to the smallest eddies with the fastest time scales where energy is removed by viscous dissipation. This leads to a decrease in power with increasing frequency known as the turbulent energy cascade (see for example Tennekes and Lumley, 1972).

The turbulent energy cascade, characterised by high power eddies at low frequency and low power eddies at low frequency, is consistent with the form of the low frequency behaviour observed in Figures 4.4a to 4.4d; however, evaluation of the frequencies at which this turbulence can occur is needed to ensure that turbulence is a cause of this low frequency behaviour.

It must be acknowledged that other phenomena such as buoyancy driven motions may cause a decrease in spectral power with increasing frequency.

Unfortunately, the need to gather data in a timely manner during the field exercises meant that durations over which sampling was performed were quite short.

In turn, due the short sampling times that were employed, it was not possible to analyse the slopes of the spectra. As spectral slopes could not be assessed, it was not possible to definitively prove whether shear driven turbulence or buoyancy driven convection was causing this pattern in the spectra.

Time Scales cf Turbulent Motion

The largest possible length scale of the eddies is the depth of the water column, while the velocities of the largest eddies must correspond to the wind shear velocity. Thus the lower extreme frequency must scale as:

$$f_l \sim \frac{u_*}{H} \qquad 4.11$$

Where H is the depth of water and u_* as before is the shear velocity A frequently used expression for the highest frequency motions is (see Tennekes and Lumley, 1972), the inverse of the Kolmogorov time scale:

$$f_k = \sqrt{\frac{\varepsilon}{\nu}} \qquad 4.12$$

Figure 4.8. Features of the Smoothed Spectral Plots

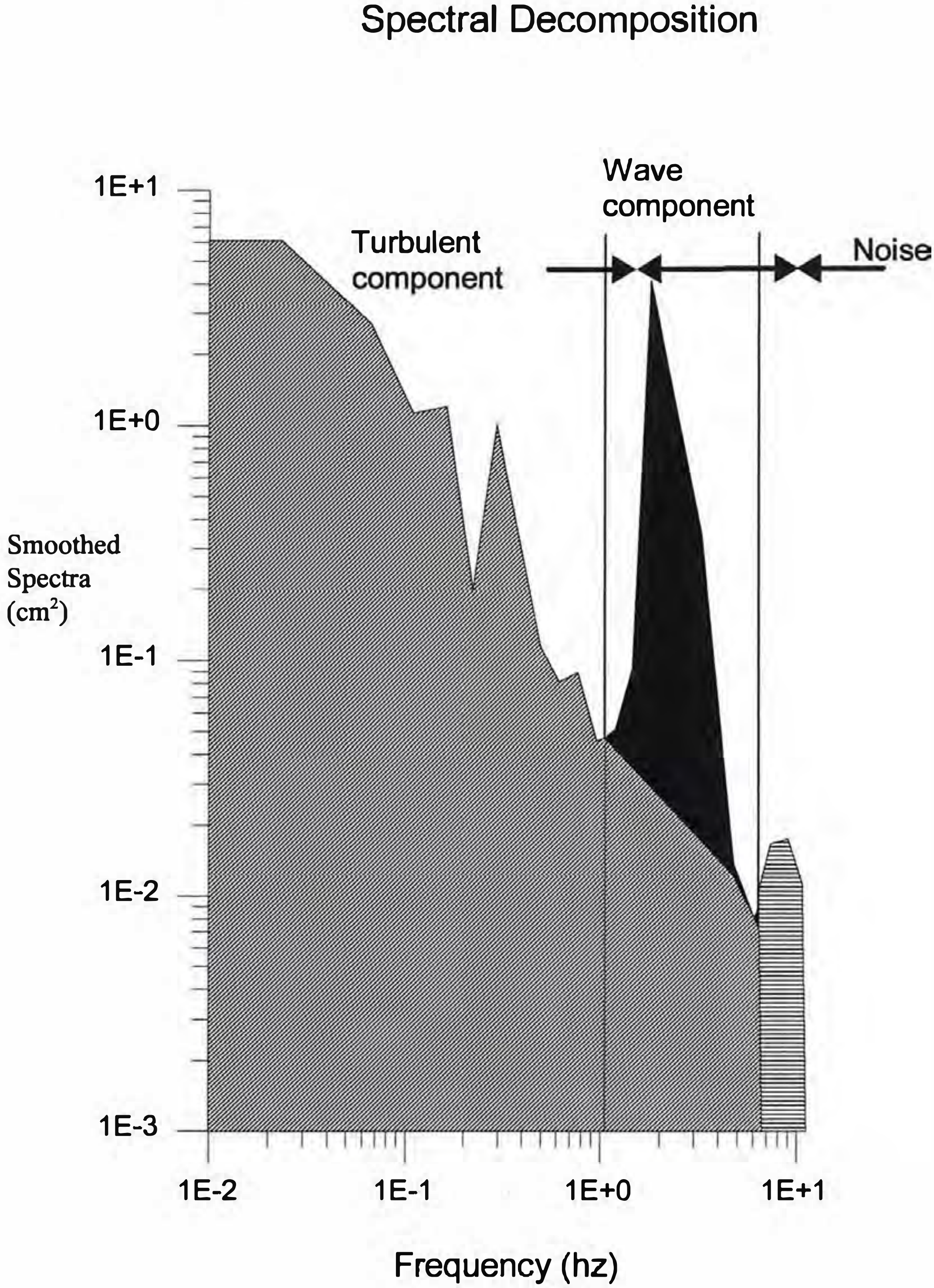

Where ε is the dissipation of turbulent kinetic energy and ν is the kinematic viscosity Thus the frequencies at which turbulence occurs will be between f_l and f_k. Note however that these are not strict limits, merely indicators of the range of frequencies within which turbulence may be present.

From Tennekes and Lumley (1972), assuming a balance between power large scales and dissipation at small scales, the dissipation must be given by:

$$\varepsilon \sim \frac{u_*^3}{H} \tag{4.13}$$

Rearranging Equation 4.12 and substituting into 4.10 gives:

$$f_l \sim \left(\frac{\varepsilon}{H^2}\right)^{\frac{1}{3}} \tag{4.14}$$

and substituting Equation 4.12 into 4.11 gives:

$$f_k \sim \sqrt{\frac{u_*^3}{H\nu}} \tag{4.15}$$

Given values of u_* or ε, the frequency range of the turbulent component of the spectra can be determined. Estimates for u_* in open water can be made from the wind speed according to Equation 4.4. From Figure 4.1, the wind speed was fairly constant at approximately 3.5 m/s during the morning, giving a value of u* = 5.3 mm/s. Resulting estimates of f_l and f_k for each station are reported in Table 4.4.

Measurement of the turbulent dissipation directly is a non-trivial exercise (see for example Oakey, 1982) and could not be performed reliably with the available instruments. However, it is known that ε values in water bodies such as lakes and reservoirs generally fall within the range 10^{-9} and 10^{-5} m^2s^{-3} (Imberger and Ivey, 1991). By using the lower of these ε values, a lower bound estimate was obtained for f_l using Equation 4.14. Similarly, an upper bound estimate for f_k was estimated from Equation 4.15 using the upper bound limit on ε. Resulting values of f_l and f_k at each station are given in Table 4.4.

Table 4.4. Estimates of Upper and Lower Bound Frequencies of Turbulence

Station	Depth (m)	From wind shear $U_a \sim 3.5$ m/s $u^* \sim 0.0053$ m/s		From ε estimates	
				$\varepsilon \sim 10^{-9}$ m^2s^{-3}	$\varepsilon \sim 10^{-5}$ m^2s^{-3}
		f_l (Hz)	f_k (Hz)	f_l (Hz)	f_k (Hz)
1	0.580	0.009	0.51	0.0016	3
2	0.485	0.011	0.55	0.0016	3
3	0.780	0.007	0.44	0.0013	3
4	0.455	0.012	0.57	0.0016	3

Table 4.4 shows that the two estimates for f_l from wind shear values and dissipation estimates are in good agreement. The estimates indicate that the length of time over which measurements was taken (around 1 minute) was too short to detect the lowest frequency turbulent signals.

The two estimates for f_k given in Table 4.4 are quite different in value; however, the sharp drop off observed between 0.1 and 0.25 Hz in the spectra shown in each of the plots on Figure 4.7 occurs between these two f_k estimates, as would be expected of a spectrum arising due to turbulence.

The behaviour of the spectra at low frequency therefore appears to represent the influence of turbulence, with perhaps some influence from internal waves when stratification is present. However, estimation of values of turbulent power or RMS turbulent velocities based on these spectra would not be valid as sampling was not performed for long enough to fully define the turbulent spectra at low frequency.

INTERNAL WAVES GIVING RISE TO LOW FREQUENCY VELOCITY FLUCTUATIONS

In the absence of stratification, internal wave effects are not possible, this is the case for Stations 1, 3 and 4 during the morning stratifying period, as shown in Figures 4.4a to 4.4d. Throughout the parts of the day when stratification is present, internal wave effects are possible. It is therefore desirable to estimate their effects on the spectra. Figure 4.4b shows that at 0934 Station 2 was subject to a top to bottom temperature differential of 0.2°C, so the possibility that internal waves may arise must be examined here because unlike turbulence, internal waves of themselves, unless breaking, do not cause mixing.

Internal waves propagate at frequencies up to the Brunt Väisälä frequency, which is given by the equation:

$$f_b \sim \sqrt{\frac{-g}{\rho}\frac{\partial \rho}{\partial z}} \qquad 4.16$$

where g is acceleration due to gravity, ρ is the ambient density of the fluid and z is distance in the vertical. Taking $g = 9.8\ ms^{-2}$, $\rho \cong 1000\ kgm^{-3}$, a rate of change of density with temperature of $0.24\ kgm^{-3}(°C)^{-1}$ and the temperature difference as 0.2°C over the 0.5 m depth of the water column gives a temperature gradient of $0.4°Cm^{-1}$, a density gradient of $0.096\ kgm^{-2}$ and $f_b = 0.03$ Hz.

From the proceeding argument, it is possible that internal waves may have contributed to the low frequency component of the spectrum shown at Station 2 in Figure 4.7. This may explain why the power values are higher at the sheltered Station 2 than at Station 3 in the lake in the log frequency range of 0.16 to 0.25 Hz, power being between 0.1 and 0.16 cm^2s^{-2} at Station 2 compared to 0.025 to 0.1 cm^2s^{-2} at Station 3. However, clearly there is more mixing occurring at Station 3 than at Station 2 as evidenced by the lack of stratification at Station 3, while Station 2 has a stratification of 0.4°C over the 0.5 m depth of the water column.

WIND WAVES GIVING RISE TO MID FREQUENCY SPECTRAL PEAKS

The local peak in the central region of the spectrum is consistent with the presence of non turbulent surface wave motion, as shown by the following argument.

Wind wave parameters can be estimated as (US Army Core of Engineers, 1984):

$$f_w = 3.5\left(\frac{g^2}{U_a F}\right)^{\frac{1}{3}} \tag{4.17}$$

$$H = 1.6 \times 10^{-3} U_a \left(\frac{F}{g}\right)^{\frac{1}{2}} \tag{4.18}$$

$$C = \frac{g}{2\pi f_w} \tag{4.19}$$

$$L = \frac{g}{2\pi f_w^{\ 2}} \tag{4.20}$$

$$u = \frac{Hg}{2Lf_w}\frac{\cosh[2\pi(z+d)/L]}{\cosh[2\pi d/L]}\cos\theta + \frac{3}{4}\left(\frac{\pi H}{L}\right)^2 C\frac{\cosh[4\pi(z+d)/L]}{\sinh^4[2\pi d/L]}\cos\theta \tag{4.21}$$

where f_w *is the frequency of the wave,* g is acceleration due to gravity, U_a is the wind speed, F is the fetch length across the lake, H is the wave height, C is the wave celerity, L is the wave length, u is the horizontal component of the velocity of a particle that is subject to the wave motion at depth z, in a total water depth of d, with phase θ.

These formulae are valid for non-breaking deepwater waves, in a regime where Stokes second order wave theory is valid.

From Figure 4.1, U_a = 1 m/s and for a southerly wind blowing across the lake towards the wetland, F ≈ 1000 m, giving f_w = 1.6 Hz, H = 16 mm, C = 1.0 m/s and L = 0.6 m. With these estimates, it can be shown that the assumptions that the waves are non-breaking, deepwater waves of Stokes second order type are valid (US Army Core of Engineers, 1984).

Given the crude nature of this estimate, wind waves are a potential cause of the local peak in the spectra at a frequency of around 1 Hz. Wave velocity component predictions at Stations 1, 2 and 4 will be much the same, as these are all in approximately 0.5 m of water. At Station 3, velocity predictions will be somewhat different from the other stations, as here the water depth is 0.78 m. Wave velocity component predictions and associated powers for the top, middle and bottom of the water column are presented in Table 4.5.

Values of the measured wave power over the range of depths at each station are also given in Table 4.5. These values were calculated by integrating the spectral intensity over the range of frequencies making up the peaks shown on the smoothed spectral plots of Figure 4.7.

Table 4.5. Estimates of Horizontal Wave Velocity Parameters

Location	Position	Estimated Velocity Component (cm/s)	Estimated Wave Power (cm^2s^{-2})	Measured Wave Power (cm^2s^{-2})		
				Stn 1	Stn 2	Stn 4
Stations 1, 2 and 4	near surface	0.8	0.6	0.01	0.04	0
	mid depth	0.06	0.04	0.001	0.02	0
	near bed	0.1	0.01	1×10^{-5}	6×10^{-4}	0
Station 3	near surface	0.8	0.64	2		
	mid depth	0.01	10^{-4}	0.1		
	near bed	0.006	4×10^{-5}	4×10^{-4}		

From both the predicted values in Table 4.5 and spectral peak of the observed values in Figure 4.7, the wave velocity at mid depth at Station 3 is appreciably less than that recorded near the surface. This is to be expected because the orbital velocities associated with the wind waves will be attenuated with depth. From Table 4.5, it can be seen that at all depths, the measured wave power at Station 3 is higher than the estimated values. This may indicate that wave power is not the only factor contributing to the spectra in this range, particularly at mid depth, where the measured wave power is three orders of magnitude higher than the estimated wave power.

At Station 2, the spectral peaks recorded at mid depth are of the same order of magnitude as those recorded at the surface; however, the predicted values in Table 4.5 show that the wave velocity at mid depth should be significantly lower than at the surface. This would indicate that some process apart from ordinary wave motion is occurring in the vicinity of Station 2.

At Stations 1 and 4, Table 4.5 and Figure 4.7 both show that wave power was significantly lower at all depths from what would be expected in the absence of vegetation. This result is to be expected, as the vegetation is most likely causing the waves to decay.

These results must be treated cautiously as the limited duration for which recording took place has most likely caused inaccuracies in the spectral peaks. This is confirmed when the magnitude of the wave powers in Table 4.5 are compared to the spectral intensities of Figure 4.7.

Visual observations at the time of the experiments verified that water surface waves were present at approximately this frequency. Furthermore, the waves were observed to be approximately sinusoidal in shape and no wave breaking was observed. It is therefore most likely that the mid frequency peak arose due to small wind waves, which are an orbital, laminar form of motion and therefore there is likely to be little turbulence or mixing associated with this peak.

By taking the cross spectrum of velocity and wave height readings, Kitiagorodskii *et al* (1983) were able to separate the fluctuating velocity spectrum into separate turbulent velocity and wave velocity spectra arising due to wind waves. They found that only a small fraction of the peak in the fluctuating velocity spectrum associated with wind wave activity could be attributed to turbulence. It would therefore be expected that most of the peak in the spectra shown in Figures 4.5a to 4.5d are associated with non turbulent behaviour and therefore do not contribute to mixing.

SEICHING

From Chapter 2 (Methodology) the period of seiches in the lake is approximately 8 minutes, or 500 seconds. This is well below the lowest frequencies for which velocity readings are reported in the spectra of Figures 4.4a to 4.4d, therefore seiching effects can be disregarded here.

NOISE

In Figure 4.7, from about 5 Hz, just after the peak associated with wind waves, to the sampling limit of the instrument at 25 Hz, the smoothed spectral intensities generally rose with frequency. This is characteristic of noise in the spectrum, and is well above the upper level at which, as reported above, turbulence is expected. Velocities observed in this part of the spectrum therefore make no contribution to mixing in the water column.

COMPARISON OF SPECTRA OBTAINED AT STATIONS 1 TO 4

Having established what the different portions of the spectrum represent, it is now possible to qualitatively compare the spectra obtained at each station. Quantitative comparisons of the spectra were not possible because the time series collected were of insufficient length to extend below the lower bound frequencies at which turbulence can be expected, as reported above.

Figure 4.7 shows the components of a typical spectrum obtained. The spectrum is assumed to consist of three regions, as shown in Figure 4.8: a low frequency component due to turbulence, a mid frequency peak at around 1 Hz due to wind waves and a high frequency component due to noise.

Consider Station 3 which was located in the lake. Figure 4.7 shows high spectral intensities over the low frequency turbulent range and the mid frequency surface wave peak.

The other open water station, Station 2, was protected from wind waves to some extent by the vegetation, and this is reflected by the lower peak in the Station 2 spectrum near 1 Hz compared to the Station 3 spectrum. The influence of the vegetation between Station 2 and the lake in reducing turbulence due to wind shear can also be seen by the reduced spectral intensity at frequencies below 0.3 Hz in Figure 4.7 compared to Station 3.

Consequently both wind waves and turbulence are lower at Station 2 than at Station 3, as would be expected, because the plant canopy present here would have reduced the wind shear dramatically.

At Station 4, spectral intensity at both low frequency and mid frequency were significantly lower than at the other three stations. This is easily understood as Station 4 is furthest from the lake, and therefore transport of waves and turbulence into this area are very low.

VARIATIONS IN TURBULENCE WITH DEPTH

Analysis of the depth dependence of turbulence at the four stations provides further evidence that turbulence arises in the vegetated zones by means apart from wind shear. Figures 4.4a to 4.4d show the spectra obtained from horizontal velocity readings at Stations 1 to 4 on the morning of day 95054, at the top, middle and bottom of the water column.

From Figure 4.7, spectra taken at Station 1, in the vegetation clearly show that the turbulence, as represented by the spectral intensities at the low frequency end of the scale are approximately the same at the top and middle of the water column. However, spectral intensities at the bottom of the water column are much lower than at the top or the middle of the water column.

By comparison with Station 1, the spectra obtained in open water at Stations 2 and 3, shown in Figure 4.7 show a trend of decreasing spectral intensity with depth at the low frequency end of the scale from the top to the bottom of the water column. Such a trend is typical of shear driven wind mixing, as the turbulence is generated near the water surface, then mixes vertically down into the fluid where it is dissipated throughout the depth of the water column (see Imberger and Ivey, 1991). Turbulence is therefore strongest near its source at the water surface, and generally becomes weaker with distance from the surface, as reflected in the low frequency spectral intensities shown in Figure 4.7.

Figure 4.7 shows that Station 4, which is vegetated, behaves similarly to Station 1, whereby the turbulence at the top and middle of the water column are of similar orders of magnitude. However, at the bed turbulence is much lower at Station 4 than at Station 1.

The vegetated stations therefore display behaviour that is not consistent with wind driven mixing, indicating that wind driven shear is not responsible for the turbulence that is observed in the vegetation. The most likely cause of turbulence in the vegetated area would seem to be the breakdown of surface waves by energy dissipation due to drag forces on the vegetation. This also explains the lowering of the mid frequency spectral peaks within the vegetated regions where the waves are dissipated. Turbulence resulting from the breakdown of wave orbital velocities in the wakes behind vegetation will occur at a higher frequency than the wave motion itself and will disappear into the noise region of the spectra.

Note that while the wake associated with the motion in the vicinity of the vegetation can be turbulent or laminar; however, in both laminar and turbulent wakes, energy dissipation will occur.

SUMMARY

Smoothed spectra at all stations showed decreasing power with increasing frequency through the range of frequencies in which turbulence can be expected, indicating the presence of turbulence. Furthermore at low frequencies when stratification was present in the water column, higher spectral power values were recorded than when stratification was absent, possibly indicating the presence of internal waves. At mid-range frequencies, a local peak in the spectra was then noticeable that corresponded to the frequency at which wind waves would be expected. Above this peak, the constant or rising spectral values were dismissed as noise in the signal.

A coherent explanation of the experimental findings into turbulence can be summarised as follows:

- Station 3 in the lake, has the highest levels of turbulence and surface waves, as this station is the most exposed to wind. Turbulence at Station 3 appears to result from surface driven wind mixing.

- Station 2, the open water station in the lake has somewhat lower levels of turbulence and surface waves than Station 3 because surface waves on the lake are dissipated by drag on the vegetation between the lake and the open water section in which Station 2 is located.

- Station 1, the vegetated station nearer the lake has somewhat lower levels of turbulence and surface waves than Stations 2 and 3. Turbulence at Station 1 most likely arises due to drag of waves on the vegetation.

- At Station 4, incoming waves and currents from the lake have already been suppressed by drag on vegetation and boundary shear in the shallow sections near the edge of the vegetated area, so little energy remains to allow turbulence to arise. This is shown diagrammatically in Figure 4.9.

4.2. A COMMENT ON PENETRATIVE CONVECTION

Penetrative convection occurs when heat transfer from a water body to the atmosphere cools the surface water causing it to become more dense than the water below it. The surface water is then subject to a negative buoyancy force, hence it descends through the water column, causing vertical mixing. Such conditions may occur during the night following a warm summer day, and may also occur due to changing climatic conditions, such as the advance of a cold front.

Unfortunately, experiments conducted for this study were not well suited to investigating penetrative convection; however, it is expected to be an important cause of mixing in wetlands, hence it is discussed below and the effects of plant presence in the water column on the process are commented on.

Figure 4.9. Mechanisms for the generation of turbulence in the wetland

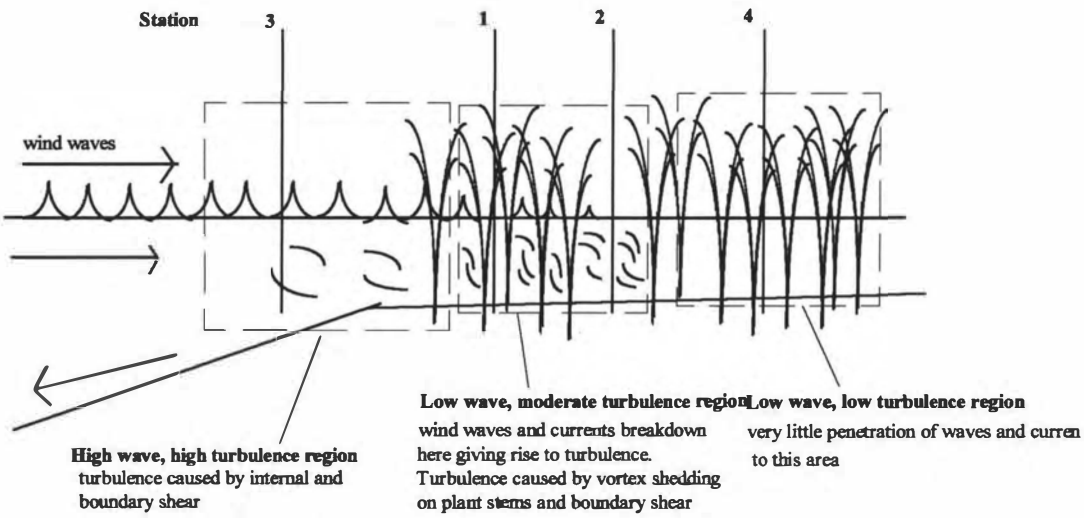

4.2.1. THE PENETRATIVE CONVECTION PROCESS

Thermals are discrete parcels of fluids, with a characteristic dimension much smaller than the water depth, as shown in Figure 4.10. As such, penetrative convection is a markedly different phenomenon from wind mixing, the mechanisms for which are also shown in Figure 4.10. This section sets out the theory of penetrative convection in open water, and the next discusses the likely impacts that plants within the water column would have on this phenomenon. Penetrative convection occurs when the fluid at the surface of a body of fluid is cooled. This cooling causes the fluid at the surface to become unstable as it develops a negative buoyancy, forming thermals which then fall through the water column until they reach a level at which they are neutrally buoyant.

As a thermal falls through the water, it entrains fluid immediately below it and induces a minor potential flow around it, to satisfy continuity. The thermal leaves behind it a wake consisting of the fluid entrained into the thermal and some of the fluid from the thermal itself (Escudier and Maxworthy, 1973 and Turner, 1973).

Figure 4.10. Schematic Representations of turbulent thermals and turbulent eddies

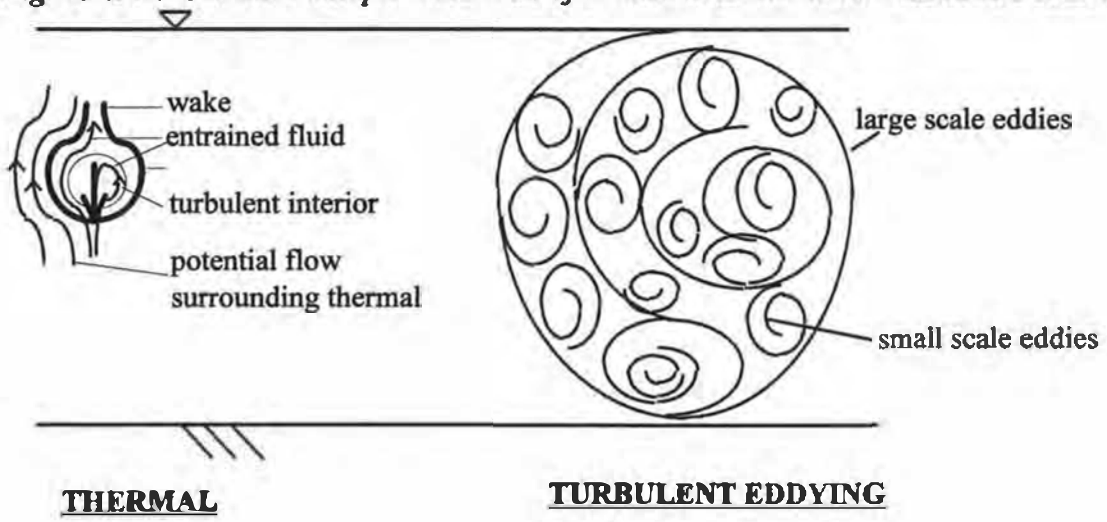

Mixing due to turbulence on the other hand involves motion of the whole water column in eddies ranging in size from the limiting dimension, here the depth down to the Kolmogorov microscale (Tennekes and Lumley, 1972).

From Fischer *et al* (1979), the free-fall velocity of thermals resulting from penetrative convection in an unstratified water body is:

$$u_f = \left(\frac{\alpha_T g H \overline{H}}{C_p \rho} \right)^{\frac{1}{3}} \qquad 4.22$$

where α_T = coefficient of thermal expansion of water by volume ≈ $2x10^{-4}$ °C^{-1}

H = water column depth (m);

$\overline{H}$ = surface cooling rate (Wm^{-2});

C_p = heat capacity of water at constant pressure ≈ 4179 J/kg/°C

Equation 4.22 only applies in the initial stages of the fall of the thermal when viscous, diffusive and entrainment effects can be largely ignored; however, since the depth of water being considered here is only 0.5 m, Equation 4.22 should be valid over the whole depth.

In a stratified water body, these free falling thermals cause a mixed layer to develop as they fall through the water column until they reach a depth of neutral buoyancy. Calculation of the rate at which penetrative convection proceeds requires the computation of the mixed layer development. This is done by an energy balance on the layer. A method for computing the mixed layer development is presented by Fischer *et al* (1979). This energy balance requires that the rate of production of turbulent kinetic energy (P), the rate of change of potential energy (G) due to the mixed layer deepening into the unmixed zone and the rate of dissipation of turbulent kinetic energy ε sum to zero; that is:

$$\frac{dP}{dt}+\frac{dG}{dt}+\varepsilon=0 \qquad 4.23$$

Fischer *et al* (1979) show that this leads to the equation:

$$(C_T^f u_f^{\,2}+\alpha_T \Delta T g h)\frac{dh}{dt}=u_f^{\,3}(1-\frac{2\Phi}{u_f^{\,3}}) \qquad 4.24$$

where C_t^f is the efficiency with which water from the hypolimnion is entrained by falling plumes and mixed to the same state as the epilimnion; it is a calibration coefficient found by Fischer *et al* (1979) to equal 0.5. α is the thermal coefficient of expansion of water; ΔT is the change in temperature across the thermocline; h is the depth of the mixed zone; and Φ is equal to ε divided by the average density. In Fisher *et al* (1979), the bracketed term on the right hand side of Equation 4.24 is assumed constant and was determined to have a value of 0.13.

4.2.2. PLANT EFFECTS ON PENETRATIVE CONVECTION

No previous studies of penetrative convection in a vegetated setting could be found; however effects of plants on mixing due to penetrative convection can be postulated to be as follows.

- In Chapter 3 it was shown that wind speeds are significantly lowered by the presence of a plant canopy consisting of emergent macrophytes. As a result, heat transfers will also be lower at the water surface. Similar effects can be expected in wetlands containing free floating and floating leaf macrophytes. These lower heat transfers will reduce the fall rate of the thermals, u_f from values given by Equation 4.22 or 4.24 as appropriate. The effective rate of dispersion due to the penetrative convection will therefore be lowered. Furthermore, thermals falling through the water column in the presence of plants will experience shear imposed by the no slip condition at the plant surface. The shear force imposed can be expected to slow the fall rate of the thermals even further.
- A reduced length scale of mixing will be imposed by the stem spacing of vegetation within the water column for submergent and emergent macrophytes. This would cause the value of C_{tf} in Equation 4.24 to be reduced. This will be much smaller than the depth. From field observations, distances between plants are generally of the order of 30 mm, whereas water depths are typically of the order of 500 m, so an order of magnitude drop in the length scale of mixing would be expected between open water and vegetated areas.

As the amount of vegetation per unit area increases, all of these effects will be enhanced, reducing the effects of penetrative convection.

4.3. CONCLUSIONS

Two distinct mixing processes will occur in wetlands, wind driven mixing, which occurs due to momentum transfer at the air-water interface and penetrative convection which occurs due to heat transfer at the air-water interface. Both of these processes are expected to be drastically affected by the presence of vegetation in the water column. The nature of wind driven mixing in a wetland has been investigated in some detail here; however, it was only possible to speculate on the nature of penetrative convection in wetlands, as the experimental results were not suitable for analysing this phenomenon.

From the investigations performed, wind was found to cause mixing in both the open water and vegetated sections of the wetland; however, the mechanisms by which mixing occurred differed slightly. In the lake, it seems that turbulence was generated at the water surface, and transported down into the water column. In the wetland, very low air velocities at the water surface prevented turbulence from being generated; however, high levels of turbulence were observed. It seems that wind waves, generated in the lake, were transported into the wetland; once in the wetland, wave motion around the vegetation within the water column apparently generated the turbulence and mixing. As a result, within the wetland, close to the boundary with the lake.

5. CONVECTION PHENOMENA

5. CONVECTION PHENOMENA

Two major causes of convection in natural bodies of freshwater are buoyancy due to density gradients caused by differential heating and shear due to wind action on the water surface (Imberger and Patterson, 1990). Despite an extensive literature search, only one previous study could be found in the literature on buoyancy driven convections in wetlands (Coates and Ferris, 1995) and only one study of wind driven convection in wetlands was found (Danard and Murty, 1994). Note that the term convection is used here to denote horizontal movement in the water column. Penetrative convection, which is a form of buoyancy driven convection operating in the vertical is considered in Chapter 4, rather than here as it results in no horizontal motions.

This chapter firstly reviews the literature on buoyancy driven convection in wetlands giving particular attention to the effects of plants on convection processes. For the previous study performed by Coates and Ferris (1995) there was no vegetation in the water column; for this reason, buoyancy driven flows in open water and of flows through vegetation are examined separately below.

Buoyancy driven convection resulting from differential heating in open water is examined first, largely on the basis of the findings of previous studies. The equations of motion are introduced and relevant scalings are presented.

Following the examination of the open water case, a more comprehensive examination of buoyancy driven convection in vegetation is presented. Again the equations of motion are introduced and scalings are performed; although in greater detail than for the open water case, as there has been little work done in this area previously and because this is the case of particular interest for the present study. Particular attention is paid to the term accounting for drag due to vegetation, as it is this term that distinguishes the vegetated case from the open water case.

In the scaling section, it is found that the buoyancy and drag terms dominate the horizontal momentum equation over the range of conditions expected; however the drag term displays markedly different behaviour under different Reynolds number conditions, ranging from laminar drag at low Reynolds number through a transitional regime to turbulent drag at high Reynolds number. Analytic expressions for the velocity profiles under each of these conditions are obtained. As the horizontal momentum equation was found to be dominated by drag and buoyancy, turbulent and viscous diffusion were neglected in the analysis, therefore the velocity profile expressions will only be valid away from the upper and lower boundaries of the flow, where the non slip and free surface boundary conditions must be obeyed. An exact expression was also obtained for the velocity profile for the non-vegetated case where laminar drag, buoyancy and viscous effects were all accounted for.

Following these analyses, comments on entrainment and wind driven convection are then made.

Finally, the field results are presented. Evidence of buoyancy driven convection was found; however, the velocities were significantly lower than those predicted from the analysis, most likely because the wind was blowing in the opposite direction to the convective motion.

5.1. LITERATURE REVIEW OF BUOYANCY DRIVEN CONVECTION

5.1.2 BUOYANCY DRIVEN CONVECTION IN OPEN WATER

In Chapter 3 it was shown that shading in vegetated areas of the wetland will significantly reduce the amount of radiation incident on the water surface. As such, a temperature differential will exist between vegetated and open water areas, resulting in a density driven exchange between the two areas.

Differential heating and cooling effects occur commonly in natural water bodies. For example, between the main body of a lake and a lake side arm (see Imberger and Patterson, 1990). By day the side arm and the lake are subject to the same heat load from the sun. However the side arm is shallower than the main body of the lake; therefore the side arm undergoes a larger change in temperature than the main body of the lake and a temperature difference arises between the water in these two areas.

Because the water in the side arm is warmer than that in the main body of the lake, it has a positive buoyancy and therefore forms a surface plume, moving out into the main body of the lake above the cooler, denser water of the main body of the lake. Simultaneously, the cooler lake water moves as a plume along the bed into the side arm under the warmer, less dense water in the side arm. This process may be reversed in direction at night as the side arm experiences the same surface cooling fluxes as the lake, but its smaller depth will cause the rate of temperature decrease here to be much higher.

By contrast with an unvegetated side arm, it was shown in Chapter 3 that the vegetated side arm at Site B examined in the field investigations receives a lower radiation input than the main body of the reservoir. This difference in radiation loads between the lake and the side arm is due to shading from the plant canopy and causes water in the vegetated area to be cooler than water in the lake.

Coates and Patterson (1994) examined an unvegetated cavity consisting of a shaded and an unshaded portion subjected to between 64 and 115 Wm^{-2} of heating. They found that the difference in nett heat flux in the water column between the water in the shaded and unshaded portions of the cavity caused significant temperature differences to arise which led to a buoyancy driven convection between the shaded and unshaded portions of the cavity.

The present study differs from the Coates and Patterson (1994) study, because in the site under consideration here, emergent aquatic macrophyte vegetation is present in the side arm. This vegetation not only shades the water column, it also creates drag within the water column, slowing the motions induced. It is therefore necessary to extend the work done by Coates and Patterson (1994) by examining the drag of the vegetation within the water column. This extension is performed in Section 5.2 below.

The equations of motion for a fluid are based on the principles of conservation of mass and conservation of momentum. The principle of conservation of mass must be applied to the fluid itself and to any constituents in the flow such as dissolved salts, heat or suspended sediments. The momentum conservation principle is usually only applied to the fluid itself.

Consider mass conservation first. From Turner (1973), in situations where changes in density within a fluid are small, the fluid may be considered incompressible.

For an incompressible fluid when considering a temporally invariant total mass the equation of conservation of mass in the fluid, otherwise known as the continuity equation, may be written in tensor notation as:

$$\frac{\partial u_i}{\partial x_i} = 0 \qquad 5.1$$

Where $u_i = (u_1, u_2, u_3)$ is the velocity vector and $x_i = (x_1, x_2, x_3)$ is the space vector.

From Fischer *et al* (1979) in the absence of any source or sink terms, the conservation of mass of a flow constituent is generally given as the advection-diffusion equation, which may be written in a conservative form as:

$$\frac{\partial c}{\partial t} + u_i \frac{\partial c}{\partial x_i} = D \frac{\partial^2 c}{\partial {x_i}^2} \qquad 5.2$$

Where c is the concentration of the constituent in the flow, t is time and D is the molecular diffusivity of the fluid. From left to right, the terms in Equation 5.2

represents changes of concentration of the constituent with time, advection of the constituent and diffusion of the constituent.

Turning now to the conservation of momentum, from Turner (1973), the momentum equation for a fluid subject to small variations in density is governed by the Boussinesq Equation, which is commonly written as:

$$\frac{\partial u_i}{\partial t} + u_j \frac{\partial u_i}{\partial x_j} = -\frac{1}{\rho_0}\frac{\partial p}{\partial x_i} + \nu \nabla^2 u_i + \left(1 + \frac{\rho'}{\rho_0}\right) g \delta_{i3} \qquad 5.3$$

where p, the dynamic pressure, is the difference between the local pressure and the hydrostatic pressure, ρ_0 is a reference density , ρ' is the difference between the local density and the reference density, in this case caused by temperature differences, ν is the kinematic viscosity of the fluid, δ_{i3} is 1 for i =3 or 0 otherwise (that is, δ_{i3} is the kronecker delta for j = 3), and g is acceleration due to gravity.

Interpretations of the terms in Equation 5.3 are discussed thoroughly in many fluid mechanics texts (see for example Batchelor, 1967). Considering these terms briefly, from left to right: the first term represents unsteady effects, the second term, advective effects, the third term gives the influence of a pressure gradient on the flow, the fourth term represents the influence of viscosity and the final term represents the effect of buoyancy effects on the flow.

Equations 5.1 to 5.3 provide a valid description of the motion of a fluid and any constituents it contains for a large range of flows. However, these equations are notoriously difficult to solve for velocity, concentration and pressure, either analytically or numerically, for most flows. It is usually necessary to simplify these equations considerably to give a more tractable description of the fluid behaviour.

If the flow is assumed to be two dimensional vertically, then it is simpler to use (u,v,w,x,y,z) notation rather than tensor notation and the continuity equation, Equation

5.1, becomes:

$$\frac{\partial u}{\partial x} + \frac{\partial w}{\partial z} = 0 \qquad 5.4$$

where x is the direction of movement in the horizontal, z is the vertical direction, u is the velocity in the x direction and w is the velocity in the z direction.

The advection-dispersion equation, Equation 5.2, becomes:

$$\frac{\partial c}{\partial t} + u\frac{\partial c}{\partial x} + w\frac{\partial c}{\partial z} = D\left(\frac{\partial^2 c}{\partial x^2} + \frac{\partial^2 c}{\partial z^2}\right) \qquad 5.5$$

For an incompressible fluid, Equation 5.5 can be manipulated into a conservative form and written as:

$$\frac{\partial c}{\partial t} + \frac{\partial u c}{\partial x} + \frac{\partial w c}{\partial z} = D\left(\frac{\partial^2 c}{\partial x^2} + \frac{\partial^2 c}{\partial z^2}\right) \qquad 5.6$$

Note that the dispersive and conservative forms of the momentum and advection diffusion equations will be used interchangeably through the following derivation as convenient.

The vector momentum equation, Equation 5.3, is more easily expressed in terms of the x and z momentum equations which become:

$$\frac{\partial u}{\partial t} + u\frac{\partial u}{\partial x} + w\frac{\partial u}{\partial z} = -\frac{1}{\rho_o}\frac{\partial p}{\partial x} + \nu\left(\frac{\partial^2 u}{\partial x^2} + \frac{\partial^2 u}{\partial z^2}\right) \qquad 5.7$$

and:

$$\frac{\partial w}{\partial t}+u\frac{\partial w}{\partial x}+w\frac{\partial w}{\partial z}=-\frac{1}{\rho_o}\frac{\partial p}{\partial z}+\nu\left(\frac{\partial^2 w}{\partial x^2}+\frac{\partial^2 w}{\partial z^2}\right)-\left(1+\frac{\rho'}{\rho_0}\right)g \qquad 5.8$$

If velocities in the vertical are assumed small then the z momentum equation can be simplified further to give the hydrostatic equation:

$$0=-\frac{1}{\rho_0}\frac{\partial p}{\partial z}-\left(1+\frac{\rho'}{\rho_0}\right)g \qquad 5.9$$

It is simple to integrate Equation 5.9 with respect to z to give an expression for the pressure at depth z as:

$$p=-(\rho_0+\rho')g(z-H') \qquad 5.10$$

where z is the distance a datum with positive z defined as upwards and H' is the height of the water surface locally above the datum. For convenience, the datum here has been taken at the water surface on the edge of the vegetation where x = 0. This is shown diagrammatically in Figure 5.1. Note that in Figure 5.1, H′ is shown with a negative value.

Assuming that temperature and density are invariant in the vertical and that changes in density arise due to changes in temperature, Equation 5.10 can be rewritten as:

$$p=-\rho_0(1+\alpha_T T')g(z-H') \qquad 5.11$$

Where α_T is the thermal expansivity of water, which is approximately a constant when changes in temperature are small (say less than 10°C) and T' is the temperature difference from the reference temperature. Neglecting second order terms and differentiating Equation 5.11 with respect to x, the horizontal pressure gradient is given by:

$$\frac{\partial p}{\partial x}=-\rho_0 g\left(\alpha_T zT_x-S\right) \qquad 5.12$$

Where $S = \frac{\partial H'}{\partial x}$ is the water surface slope and T_x is the temperature gradient in the x direction.

Tennekes and Lumley (1972) note that using the continuity equation, Equation 5.7, the x-momentum equation can be rewritten as:

$$\frac{\partial u}{\partial t}+\frac{\partial u^2}{\partial x}+\frac{\partial uw}{\partial z}=-\frac{1}{\rho_o}\frac{\partial p}{\partial x}+\nu\left(\frac{\partial^2 u}{\partial x^2}+\frac{\partial^2 w}{\partial z^2}\right) \qquad 5.13$$

Figure 5.1. Initial Unsteady Flow Evolution in the Presence of a Buoyancy Driving

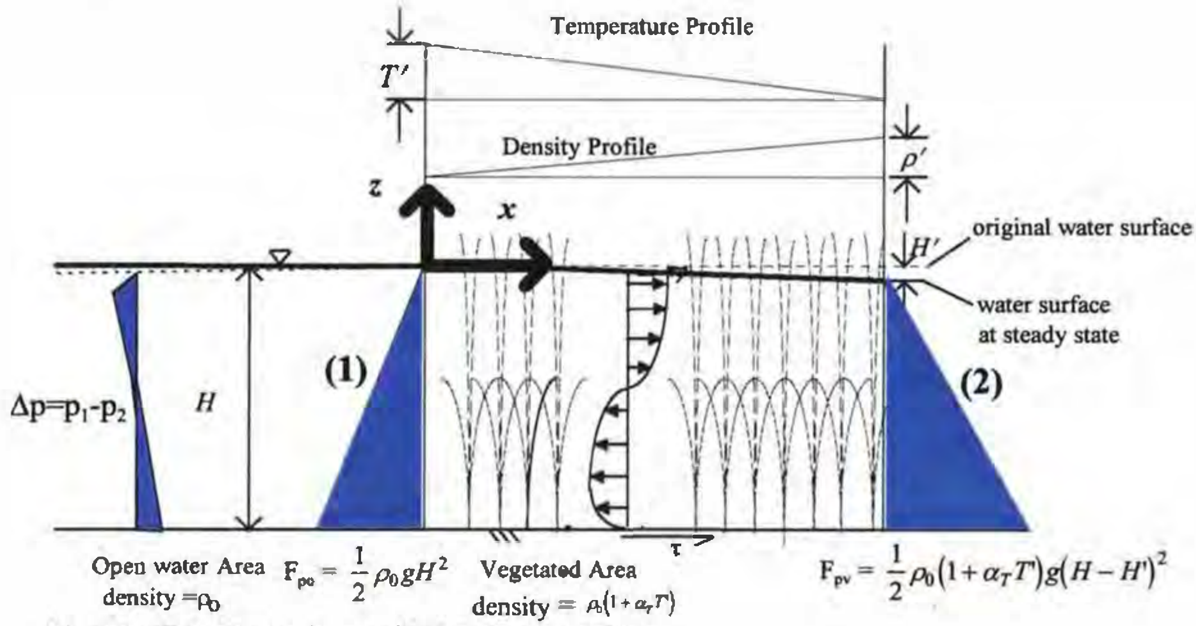

Notes: H' is shown here with a negative value;

α_T is negative for $T > 4°C$; and

in the vegetated area, T' is assumed to be less than zero due to shading.

Equations 5.4 (continuity), 5.6 (conservation of mass of constituent), 5.12 (pressure gradient term) and 5.13 (x momentum) provide a complete description of the flow and movement of constituents within it; however, these equations are highly complex and highly non-linear. Solving these equations usually requires that they be evaluated numerically to a high degree of spatial resolution (Tennekees and Lumley, 1972). It is often necessary to make assumptions about the behaviour of the flow at small scales so that the spatial resolution required to solve the equations becomes more realistic.

To account for the effects of small scale behaviour on the flow at larger scales, the Reynolds decomposition is made between time averaged and fluctuating variables, then the time averages of Equations 5.4, 5.6, 5.12 and 5.13 are taken (see Tennekes and Lumley, 1972). This yields:

$$\frac{\partial \overline{u}}{\partial x}+\frac{\partial \overline{w}}{\partial z}=0 \qquad 5.14$$

$$\frac{\partial \overline{c}}{\partial t}+\overline{u}\frac{\partial \overline{c}}{\partial x}+\overline{w}\frac{\partial \overline{c}}{\partial z}+\frac{\partial \overline{u'c'}}{\partial x}+\frac{\partial \overline{w'c'}}{\partial z}=D\left(\frac{\partial^2 \overline{c}}{\partial x^2}+\frac{\partial^2 \overline{c}}{\partial z^2}\right) \qquad 5.15$$

$$\frac{\partial \overline{u}}{\partial t}+\overline{u}\frac{\partial \overline{u}}{\partial x}+\overline{w}\frac{\partial \overline{u}}{\partial z}+\frac{\partial \overline{u'u'}}{\partial x}+\frac{\partial \overline{u'w'}}{\partial z}=-\frac{1}{\rho_o}\frac{\partial \overline{p}}{\partial x}+\nu\left(\frac{\partial^2 \overline{u}}{\partial x^2}+\frac{\partial^2 \overline{u}}{\partial z^2}\right) \qquad 5.16$$

and

$$\frac{\partial \overline{p}}{\partial x}=-\rho_0 g\left(\alpha_T z\overline{T}_x-\overline{S}\right) \qquad 5.17$$

where overbars represent temporally averaged variables and primes represent fluctuations with time from the mean values. $\overline{u'u'}$ and $\overline{u'w'}$ are known as the Reynolds stress terms and represent the effect of turbulence on the mean flow.

To gain closure in the time averaged equations of motion, it is necessary to relate the Reynolds stress terms to the time averaged properties. This is commonly done (Tennekes and Lumley, 1972) by assuming the Reynolds stresses to be proportional to the time averaged velocity gradients. The coefficients of proportionality are known as the kinematic eddy viscosities, and are generally functions of the flow.

Equation 5.16 can therefore be written as:

$$\frac{\partial \bar{u}}{\partial t}+\bar{u}\frac{\partial \bar{u}}{\partial x}+\bar{w}\frac{\partial \bar{u}}{\partial z}=-\frac{1}{\rho_o}\frac{\partial \bar{p}}{\partial x}+\frac{\partial}{\partial x}\left[\left(K_{Mx}+\nu\right)\frac{\partial \bar{u}}{\partial x}+\left(K_{Mz}+\nu\right)\frac{\partial \bar{u}}{\partial z}\right] \qquad 5.18$$

Where K_{Mx} and K_{Mz} are the kinematic eddy viscosities in the vertical and horizontal directions.

By a similar procedure, Equation 5.15 can be time averaged to give the advection dispersion equation as:

$$\frac{\partial \bar{c}}{\partial t}+\bar{u}\frac{\partial \bar{c}}{\partial x}+\bar{w}\frac{\partial \bar{c}}{\partial z}=\frac{\partial}{\partial z}\left(\left(K_{cx}+D\right)\frac{\partial \bar{c}}{\partial x}+\left(K_{cz}+D\right)\frac{\partial \bar{c}}{\partial z}\right) \qquad 5.19$$

Where K_{cx} and K_{cz} are the eddy diffusivities of the constituent in the vertical and horizontal directions.

Clearly, Equations 5.18 and 5.19 are intractable to analytic solutions. Numerical techniques may be employed in their solution (see for example Tennekees and Lumley, 1972), or further simplifications can be made to the equations through scaling analysis (see for example Patterson and Imberger, 1990).

For the purposes of this study, it is more instructive to examine Equations 5.18 and 5.19 with a scaling approach, as ultimately it is desired to have an understanding of the physics of buoyancy driven flows in vegetation, where the additional physical process of drag must be incorporated into the analysis.

The next section summarises the findings of previous studies that have investigated the scaling of buoyancy driven flows in open water. This is followed by a section where the effects of the vegetation are introduced.

5.1.3. SCALING BUOYANCY DRIVEN FLOWS IN OPEN WATER

A number of previous studies of buoyancy driven convective flows in open water have been performed (see for example Patterson and Imberger, 1980, Patterson and Coates, 1995 and Bohrer, 1996). These studies show that the dimensionless numbers of importance in determining flow regimes are the Reynolds Number R_e, the Richardson Number R_i, the Grashof Number G_r, and the Rayleigh Number R_a. These dimensionless numbers are each considered separately below.

To give an understanding of the nature of the flows expected in wetlands, the ranges of expected values of these dimensionless numbers and the approximate values that could be expected for the particular wetland being considered in the intensive experiments are presented in Table 5.1 Critical values of these numbers and other relevant parameters are also given in Table 5.1.

The Reynolds number is the ratio of the inertial to the viscous effects. It is written as:

$$R_e = \frac{UH}{\nu} \qquad 5.20$$

At low Reynolds number, flows are laminar, at high Reynolds number they are turbulent. From Table 5.1, the Reynolds number for the present case is expected to be 500. Under such conditions, the flow is expected to be laminar (Schlichting, 1955) and the eddy viscosity and eddy diffusivity terms, can be neglected.

The Richardson Number is the ratio of the vertical buoyancy gradient to the velocity shear. It is a parameter that determines the stability of a stratified shear flow (Turner, 1973). For a particular flow, a critical Richardson number may be defined below which the flow will be turbulent. From Fischer *et al* (1979), the Richardson Number is defined as:

$$R_i = \frac{-\frac{g}{\rho}\frac{\partial \rho}{\partial z}}{\left(\frac{\partial U}{\partial z}\right)^2} \tag{5.21}$$

As the convection develops, then the warmer water will gradually move over the top of the colder water, leading to a density stratification in the vertical.

Table 5.1. Typical Dimensionless Parameter Values in Open Water

Parameter	Minimum	Present case (Site B)	Maximum	Units	Reference
U	10^{-4}	10^{-3}	10^{-2}	m/s	Kadlec (1990)
L	0.1	10	100	m	Kadlec (1990)
H	0.01	0.5	1.0	m	Kadlec (1990)
A = H/L	0.0001	0.05	10	dimensionless	calculated from above
g	9.8	9.8	9.8	ms^{-2}	constant
α_T	-2.07×10^{-3}	-2.32×10^{-3}	-2.57×10^{-3}	$kgm^{-3}(°C)^{-1}$	Fischer *et al* (1979)
T	0.1	1	5	°C	Present Study
R_e	0.1	500	10^4	dimensionless	calculated from above
R_i	0.20	1100	13000	dimensionless	calculated from above
G_r	2000	3×10^8	1×10^{10}	dimensionless	calculated from above
P_r	7.14	7.14	7.14	dimensionless	calculated from above
R_a	1400	2×10^9	9×10^{10}	dimensionless	calculated from above
Rac_1	1	1	1	dimensionless	
$Rac_2 = Pr^2$	50	50	50	dimensionless	calculated from above
$Rac_3 = Pr^{16}A^{-12}$	0.46	2×10^{29}	5×10^{61}	dimensionless	calculated from above
$Rac_4 = Pr^{10}$	4×10^8	4×10^8	4×10^8	dimensionless	calculated from above
$Rac_5 = A^{-4/3}$	0.05	0.5	2×10^5	dimensionless	calculated from above
$Rac_6 = A^{-12}$	10^{-12}	4×10^{15}	10^{48}	dimensionless	calculated from above

If it is assumed that heat losses are small, then the temperature difference that develops in the vertical due to this convection must be equal to the temperature difference that was initially present in the horizontal. The Richardson number for the convection in the presence of this stratification can therefore be approximated as:

$$R_i \sim \frac{g\alpha_T T' H}{U^2} \qquad 5.22$$

From Turner (1973), for $R_i > 0.4$, a shear flow will be stable and turbulence will not develop. For Site B (see Table 5.1) R_i is always expected to be greater than 200. This indicates that shear within the water column is unlikely to generate turbulence.

The Grashof Number is the ratio of the buoyancy forcing to viscous damping. From Turner (1973), the Grashof Number is defined as:

$$G_r \sim \frac{g\alpha_T T' H^3}{\nu^2} \qquad 5.23$$

For the present case, from Table 5.1 the Grashof Number is always expected to be very high, indicating that buoyancy will dominate over viscous damping (Monteith and Unsworth, 1990), therefore the flow will initially be unsteady. The unsteady nature of the flow is explored below using a Rayleigh number paramterisation.

The Rayleigh Number is the ratio of the buoyancy forcing to damping by viscosity and diffusion. From Turner (1973), the Rayleigh Number is defined as:

$$R_a \sim \frac{g\alpha_T T' H^3}{D_T \nu} \qquad 5.24$$

where D_T is the diffusivity of heat. Clearly the ratio of the Rayleigh number to the Grashof number is constant for a particular fluid. The constant of proportionality being the Prandtl Number, $P_r = \nu/D_T$.

Patterson and Imberger (1980) performed a detailed scaling of the unsteady natural convection in a cavity of fluid subject to heating at one end and cooling at the other end. Scaling was performed by analysing the time, length and velocities associated with buoyant convection and conduction of heat within the cavity for the case of Prandtl number greater than unity ($P_r = 7.14$ for water).

From Patterson and Imberger (1980), a number of critical Rayleigh numbers may be defined that will determine the nature of the flow. These critical Rayleigh numbers depend only on the Prandtl number of the fluid and the aspect ratio (A_L) of the cavity. They are:

- $Rac_1 = 1$: for $Ra < Rac_1$, the flow will reach a steady state condition whereby heat transfer in the cavity is dominated by conduction. For $Ra > Rac_2$, a steady state will be reached by a combination of buoyant convection and conduction
- $Rac_2 = Pr^2$: for $Ra < Rac_2$, the thermal boundary layers of the flow at the heated and cooled ends of the cavity are comparable to the depth of the cavity. For $Ra > Rac_2$ the opposite will apply.
- $Rac_3 = Pr^{16}A_L^{-12}$: for $Ra < Rac_3$, the time scale for the flow to penetrate through the whole cavity is less than the time scale at which viscosity becomes important. For $Ra > Rac_3$ the opposite will apply and the flow remains inertial until after it has penetrated the entire length of the cavity.
- $Rac_4 = Pr^{10}$: for $Ra < Rac_4$, the flow becomes viscously dominated before the thermal boundary layers at the heated and cooled ends become fully established. For $Ra > Rac_4$ viscosity does not hinder the development of the thermal boundary layers.
- $Rac_5 = A_L^{-4/3}$: for $Ra < Rac_5$, the thickness of the intrusion propagating through the cavity eventually fills the thickness of the cavity before reaching the opposite end. For $Ra > Rac_5$ the intrusion remains distinct until it reaches the opposite end of the cavity.
- $Rac_6 = A_L^{-12}$: for $Ra < Rac_6$, conduction of heat from the intrusion into the core of fluid in the cavity is a significant means of heat transfer. For $Ra > Rac_6$, the intrusion maintains its integrity and thermal diffusivity to the core of the intrusion can be ignored.

For the present case, Table 5.1 shows that the ordering is expected to be:

$$Rac_1 < Rac_2 < Rac_4 < Rac_5 < Ra < Rac_3 < Rac_6.$$

From this ordering it can be seen that heat transfer is expected to be by a combination of conduction and natural convection, that the flow is expected to be partly inertial and partly viscous, that the intrusion is expected to remain distinct from the ambient fluid, despite the fact that it is expected to lose significant heat to the ambient fluid.

One special case in particular is worth considering, that where the flow is assumed steady state, invariant in the x direction and with buoyancy balancing viscosity. This case occurs for $Rac_1 < Rac_2 < Rac_5 < Rac_6 < Ra < Rac_3 < Rac_4$ and is examined in detail below.

5.1.4. LAMINAR-VISCOUS FLOWS IN THE ABSENCE OF VEGETATION

In the absence of drag, if the flow is assumed to be steady state and invariant in x, then the x-momentum equation (Equation 5.18) reduces to a balance between the viscous term and the buoyancy term. The following equation results:

$$0 = g(\alpha_T T_x z - S) + \nu \frac{\partial^2 U}{\partial z^2} \qquad 5.25$$

Equation 5.25 is easily solved by integrating twice with respect to z, following Hutchinson (1957). Using the free shear and non-slip boundary conditions, and by imposing the zero nett flux condition over the depth of the water column, the constants of integration and the water surface slope S can be solved for. This yields a velocity profile given by a cubic polynomial in z as:

$$U = \frac{g\alpha_T T_x}{\nu}\left(-\frac{z^3}{6} - \frac{3z^2 H}{16} + \frac{H^3}{48}\right) \tag{5.26}$$

5.1.5. SUMMARY

From the above literature review, it can therefore be seen that the scales of motion involved in buoyancy driven convection in open water have been explored to quite some degree of detail in previous studies. However, the effects of vegetation within the flow on buoyancy driven convections have not been examined in such detail. It is therefore appropriate now to consider the effects of vegetation on the flow.

5.2. LITERATURE REVIEW OF FLOW THROUGH VEGETATION

As stated above, the only previous study found in the literature of buoyancy driven flows within wetlands was that by Coates and Ferris (1995); however this study was a laboratory experiment involving free floating macrophytes. For the case of free floating macrophytes, there is virtually no vegetation in the water column, apart from that immediately below the surface.

For wetlands containing floating leaf macrophytes, buoyancy driven flows would be expected to develop in a similar manner to that observed in free floating macrophyte wetlands, due to the shading of the water column provided by the vegetation.

For both free floating and floating leaf macrophyte wetlands, as the amount of vegetation per unit area increases, the effects of buoyancy driving would be expected to be enhanced, as the amount of shading would be expected to increase.

In wetlands containing only submergent macrophytes, the presence of the macrophytes would increase absorption of radiation in the upper portion of the water column. A buoyancy driven convection would then be expected to develop in the opposite direction from that indicated above, as adjacent water in the open water would be cooler near the surface, but warmer near the bed than in the vegetated zone.

From Chapter 3, in a wetland containing emergent macrophytes, differential heating between open water and vegetated areas can be significant. Unlike floating leaf and free floating macrophyte wetlands, where emergent macrophytes are present, the drag on the vegetation within the water column would play a significant role in retarding the flow. For this reason, convection for the present case is expected to be significantly different from that examined by Coates and Ferris (1995). It is therefore necessary to review studies of drag due to vegetation first, then to consider how these drag forces will affect buoyancy driven convections.

5.2.1 DRAG EFFECTS OF VEGETATION ON FLOWS

For emergent macrophytes, both differential heating and drag due to vegetation within the water column are expected to be significant. As both the buoyancy driving and the drag will increase as the amount of vegetation per unit area is increased, it is unclear whether buoyancy driven convections will strengthen or weaken with increasing vegetation per unit area.

The elements within a vegetated region will cause any flow to be three dimensional and highly complex when considered on the length scales of the individual elements within the vegetation. However where the length scales of interest are many times larger than the scale of the individual elements, Wilson and Shaw (1977) showed that by averaging the x-momentum equation in the horizontal, a tractable equation for the mean flow can be obtained.

To distinguish between spatial averaging, as performed here, and temporal averaging, as is usually performed for turbulent analysis (see for example Tennekes and Lumley, 1972), the following analysis will use the convention <a> to represent a horizontal average of the quantity a, a" to represent local variations in a from the horizontal average, ie a" = a - <a> and A to represent a spatial and temporal average of a.

Before continuing, it is necessary to mention an important difference between temporal and spatial averaging - the non commutative nature of the differential of the horizontal averaging operator being used, which is discussed in detail by Raupach and Shaw (1982), that is, generally $\langle \partial a/\partial x_i \rangle \neq \partial \langle a \rangle/\partial x_i$. This non commutative nature of the operators arises because of the presence of the plant elements within the region over which averaging is being performed.

Adopting this convention and assuming the buoyancy effects remain invariant under averaging, following Wilson and Shaw (1977) Equation 5.13 can be averaged over time and space to give:

$$\left\langle \frac{\partial \bar{u}}{\partial t} \right\rangle + \left\langle \bar{u}\frac{\partial \bar{u}}{\partial x} \right\rangle + \left\langle \bar{w}\frac{\partial \bar{u}}{\partial z} \right\rangle + \left\langle \frac{\partial \left(\overline{u''u''}\right)}{\partial x} \right\rangle + \left\langle \frac{\partial \left(\overline{u''w''}\right)}{\partial z} \right\rangle + \left\langle \frac{\partial \left(\overline{u'u'}\right)}{\partial x} \right\rangle + \left\langle \frac{\partial \left(\overline{u'w'}\right)}{\partial z} \right\rangle = -\frac{1}{\rho_o}\left\langle \frac{\partial \bar{p}}{\partial x} \right\rangle - \frac{1}{\rho_o}\left\langle \frac{\partial \overline{p''}}{\partial x} \right\rangle + \nu\left\langle \nabla^2 \bar{u} \right\rangle + \nu\left\langle \nabla^2 \overline{u''} \right\rangle \qquad 5.27$$

All terms in Equation 5.27 are analogous to terms in Equation 5.16 except for the fourth, fifth, ninth and eleventh terms from the left of Equation 5.27, which represent the effects of the vegetation on the mean flow.

The fourth and fifth terms from the left of Equation 5.27 are referred to as the dispersive flux terms. They arise from gradients in spatial correlations in fluctuations in a vertical plane and horizontal velocities from their spatially averaged values (Raupach and Thom, 1981). These terms can clearly be seen to be analogous to the Reynolds stress tensor, with the difference that they are still expected to arise in fully laminar flows. Raupach and Thom (1981) report that attempts to measure the dispersion flux have so far been unsuccessful. The dispersive flux will not be considered further here, as its measurement has so far not been possible (Raupach and Thom 1981) and as numerous studies including Raupach and Thom (1981) and Naot *et al* (1996) have successfully modelled flow through vegetation without consideration of the term.

The ninth and eleventh terms from the left in Equation 5.27 represent the effects of pressure drag and viscous drag respectively due to the vegetation elements (Wilson and Shaw, 1977). Given this interpretation of these terms, assuming the flow is two dimensional in the vertical and that changes of velocity in the z direction are much greater than changes in the x direction it is possible to greatly simplify the x-momentum equation to give the expression:

$$\frac{\partial U}{\partial t}+U\frac{\partial U}{\partial x}+W\frac{\partial U}{\partial z}=-\frac{1}{\rho_o}\frac{\partial P}{\partial x}+\nu\frac{\partial^2 U}{\partial z^2}-\frac{\partial \tau_{rs}}{\partial z}+f_D \qquad 5.28$$

Where $\tau_{rs} = \left\langle \overline{u' w'} \right\rangle$ is the Reynolds Stress divided by the density; and

$f_D = -\frac{1}{\rho_o}\left\langle \frac{\partial \overline{p''}}{\partial x} \right\rangle$ is the (negative) acceleration of flow due to drag.

The other terms in Equation 5.28 have their usual meaning. The form of the equation has also been simplified by using U and P to represent the temporally and spatially averaged velocity and pressure respectively.

To solve Equation 5.28 it is necessary to consider further the Reynolds stress, drag and pressure terms. These are considered in the following sections. Emphasis is placed on the analysis of the drag term, as this is the term that most distinguishes flows in vegetation from flows where no vegetation is present.

5.2.2. THE REYNOLDS STRESS TERM

Raupach and Thom (1981) reviewed the work of a number of previous studies of flows in crop canopies that investigated the nature of τ_{rs}. They report that a number of previous studies had used momentum diffusion models to relate τ_{rs} to the mean velocity field and a limited number of studies had used TKE budget approaches. TKE budget approaches were found to give better predictions of flows in the canopy than the local diffusion models; however they are more computationally complex and require numerical solutions. Naot *et al* (1996) also used a TKE budget to calculate τ_{rs} in partly vegetated channels, and thereby model their hydrodynamic behaviour. In the present study, TKE budget approaches are of little use in the present context which is aimed simply at scaling the effects of the different processes occurring and will not be considered further, rather a local diffusion model will be used.

Local diffusion models are based on the assumption that τ_{rs} is proportional to the velocity gradient (Raupach and Thom, 1981) as is commonly assumed in simple turbulence models such as for boundary layer flows (see for example Schlichting, 1960), that is:

$$\tau_{rs} = K_M \frac{\partial U}{\partial z} \qquad 5.29$$

where K_M is the momentum diffusivity due to turbulence, otherwise known as the turbulent eddy viscosity. Raupach and Thom (1981) report that a number of studies have successfully modelled flows in plant canopies using various relationships for K_M. These studies all used commonly accepted turbulent eddy viscosity expressions. They include:

- K_M assumed constant (for example, Landsberg and James, 1971)
- K_M assumed proportional to velocity (Cowan, 1968).
- K_M assumed to take a mixing length form, with the mixing length taken as constant within the flow (for example Cionco, 1965)

Substituting Equation 5.29 into Equation 5.28 gives:

$$\frac{\partial U}{\partial t}+U\frac{\partial U}{\partial x}+W\frac{\partial U}{\partial z}=-\frac{1}{\rho_o}\frac{\partial P}{\partial x}+\nu\frac{\partial^2 U}{\partial z^2}+\frac{\partial}{\partial z}\left(K_M\frac{\partial U}{\partial z}\right)+f_D \qquad 5.30$$

It should be noted that the advection-diffusion equation can be treated similarly to the momentum equation to give the advection-dispersion equation for transport of a constituent in a flow through vegetation as:

$$\frac{\partial C}{\partial t}+U\frac{\partial C}{\partial x}+W\frac{\partial C}{\partial z}=\frac{\partial}{\partial z}\left((K_{cz}+D)\frac{\partial C}{\partial z}\right) \qquad 5.31$$

Where C is the temporally and spatially averaged concentration of the constituent and K_{cz} is the dispersive flux of the constituent in the vertical direction.

5.2.3. THE VEGETATIVE DRAG TERM

The magnitude of the total drag force F_D exerted on a body by an oncoming flow with constant velocity is commonly given by the equation:

$$F_D=-\frac{1}{2}C_D\rho AU^2 \qquad 5.32$$

where C_D is the drag coefficient, ρ is the ambient fluid velocity, A is the frontal area of the body, that is, the projected area of the body normal to the plane through which the velocity acts and U is the mean velocity of the approaching flow. F_D acts in the opposite direction to the velocity as indicated by minus sign.

The drag coefficient is generally a function of the Reynolds number based on the stem diameter, R_{es} (see for example Batchelor, 1967), which is commonly defined as:

$$R_{es}=\frac{Ud}{\nu} \qquad 5.33$$

where d is the stem diameter and ν is the kinematic viscosity. Drag to Reynolds number relationships for various simple, smooth bodies are shown in Figure 5.2.

Given the physical similarity between flow through vegetation and flow through cylinders, to analyse flow through vegetation it is useful to review the results of studies of flows past single cylinders and through arrays of cylinders. These studies provide quite conclusive results despite not quite representing the physical situation of interest. Studies that have attempted to measure drag due to vegetation directly are then analysed. These studies are not so conclusive, but do represent the physical situation of interest.

DRAG OF A SINGLE CYLINDER IN A FLOW OF INFINITE EXTENT

The C_D-R_{es} relationship for a single cylinder in an infinite flow normal to the long axis of the cylinder is well understood (see for example Justesen, 1987). For such a flow, the frontal area is the cylinder diameter multiplied by its height.

Figure 5.2 shows that the drag coefficient for a cylinder is approximately 1 over a large range of Reynolds numbers from 500 to 200 000. At stem Reynolds number less than 1, the drag coefficient varies inversely proportionally with R_{es}.

EFFECTS OF ROUGH CYLINDERS

Justesen (1987) presents data showing that the sudden drop in C_D from 1 to 0.3 shown on Figure 5.2 at $R_{es} \cong 3\times10^5$ occurs at much lower Reynolds number for rough cylinders; however, even for the roughest surfaces, the rapid drop in C_D always occurs above $R_{es} = 10^4$. Apart from this variation, Justesen (1987) found that cylinder roughness has little effect on the drag coefficient.

Figure 5.2. Drag Coefficient to Stem Reynolds Number Relationship
from Luketina (1996)

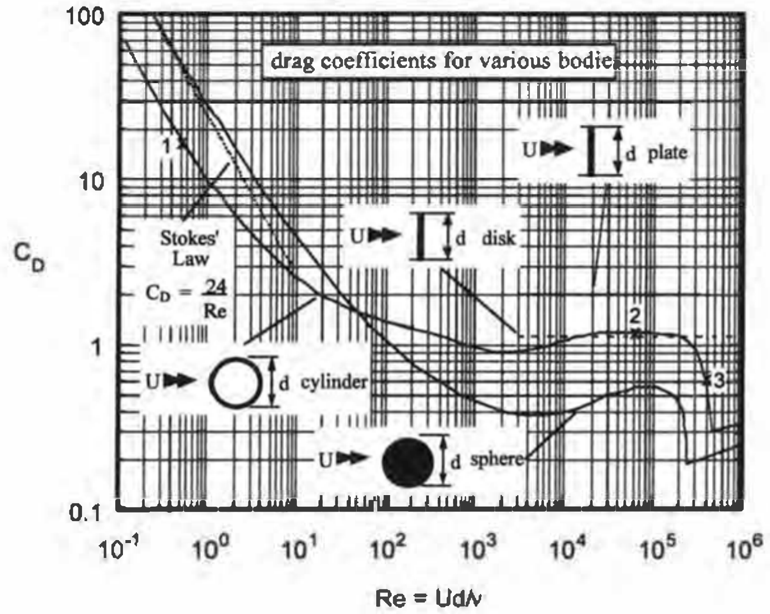

ARRAY EFFECTS

Steady drag coefficients within an array of cylinders were reported by Chen (1987) for stem Reynolds number between 2×10^4 and 1.4×10^5. These experiments were conducted at stem Reynolds numbers higher than expected in the wetland, they demonstrate that caution is required in assessing drag coefficients in an array of cylinders, as they may differ markedly from the single cylinder case.

For the first row in the array, C_D was between 4.5 and 5.5 (decreasing monotonically with increasing Reynolds number). For the second row, C_D was between 0.22 and 0.01. C_D was between 0.4 and 0.5 for the third row, then between 0.5 and 0.7 for the 4th row. The average of C_D over the first four rows is 1.6 which is very similar to the value for an isolated cylinder in the same Reynolds number range. It is apparent then that within the first few rows of an array, C_D varies markedly, the overall drag behaviour will be quite similar to that of an isolated cylinder.

STUDIES OF DRAG DUE TO VEGETATION

A number of problems are encountered when dealing with previous studies of drag in flows through vegetation. Some of the more fundamental problems are:

- Inconsistent results in determining drag coefficients, because of experimental difficulties in determining drag forces and frontal areas of vegetation, roughness and array effects in different vegetation types and dynamic effects caused by the flexibility of vegetation at high Reynolds numbers. Kadlec (1990) found that such problems lead to a scatter in data between different studies of more than an order of magnitude.
- Studies of drag in vegetation have not always parameterised drag using the conventional drag relationship, making comparison of the results of these studies with others difficult (Kadlec, 1990).
- Studies in crop micrometeorology (such as Raupach and Thom, 1981) account for the dispersive flux and drag terms separately; however, studies in wetlands and vegetated channels do not account explicitly for the dispersive flux term, therefore any effects from this term are lumped in with the drag term. It is therefore difficult to compare the results of such studies.
- Lack of detail reported on the physical structure of the vegetation. Many studies (for example Kadlec, 1990; Raupach and Thom, 1981) do not consider the structure of the vegetation, such as the number of plant stems per unit area, and average stem diameters. Without such basic information to describe the flow, it is difficult to compare the results of different studies and to relate the results of these studies to the present study.

Important studies of drag due to vegetation, include the following:

- Finnigan (1979) reported drag coefficients for air flow through a wheat field.
- Raupach and Thom (1981) reviewed previous studies of drag due to individual canopy elements. They reported that individual canopy elements behave similarly to isolated cylinders, and that at high Reynolds number array effects are quite

important. As drag due to isolated cylinders and array effects have already been reviewed, there is no further need to comment on this area.

- Naot *et al* (1996) analysed the hydrodynamics of partly vegetated channels, formulating a k-ε turbulence model and comparing its results to experimental studies of flow through partially vegetated open channels.

Of these studies, the work of Finnigan (1979) and Raupach and Thom (1981) have been reviewed by Naot et al (1996). The findings of this train of literature is examined below.

Naot *et al* (1996) used conventional drag theory to model the drag term, with two distinctions. Firstly they included a dimensionless shading coefficient, S_f (not to be confused with the friction slope, which is represented by the same symbol). S_f is a function of the spatial distribution of the plant stems. From Schlichting (1962), for randomly distributed rods, S_f can be written as:

$$S_f = 1 - d\sqrt{\eta_p}\left(1 - 0.5\sqrt{d}\,\eta_p^{\frac{1}{4}}\right) \qquad 5.34$$

where d is the plant width or diameter as appropriate and η_p is the number of plants per unit area. From Raupach and Thom (1981), S_f takes values between 0.25 and 1.0, depending on the Reynolds number of the flow and crop type. With the addition of the S_f term, the expression for the drag force per unit mass in the vegetated area becomes:

$$f_D = -\frac{1}{2} C_D \, d\eta_p S_f U^2 \qquad 5.35$$

As stated earlier, the drag coefficient, C_D is a function of the Reynolds number as shown in Figure 5.2. From Naot *et al* (1996) C_D can be crudely approximated as:

$$C_D = \begin{cases} 1 & 10^3 < R_e < 10^5 & \text{Turbulent drag} \\ \left(\dfrac{10^3}{R_e}\right)^{\frac{1}{4}} & 3 < R_e < 10^3 & \text{Transitional drag} \\ \dfrac{10}{R_e} & 0 < R_e < 3 & \text{Laminar drag} \end{cases} \qquad 5.36$$

Note that in the literature the terms "vegetation resistance" and "vegetative resistance" are used commonly in the literature to describe the contribution of vegetation to head loss in a flow. Use of these terms has been avoided here since the physical phenomena that cause the head loss are viscous and form drag, regardless of whether or not the drag equation is used to quantify these losses. Therefore the term drag is used exclusively below to avoid confusion.

Kadlec (1990) performed a balance between the pressure and drag terms for flows through a wetland driven by surface slope alone (ie no buoyancy forcing). This involved neglecting the Reynolds stress term, τ_{rs}, the inertial term and the unsteady term in Equation 5.30, and assuming that boundary shear stress is negligible. However, rather than using the drag relationship for the drag term, Kadlec (1990) adapted an expression first used by Horton (1938) to give:

$$\frac{Q}{b} = UH = KH^{\beta}S^{\alpha} \qquad 5.37$$

Where Q is the flow rate, b is the width of the wetland, H is the depth of flow, S is the energy line slope and K, α and β are empirical coefficients. Kadlec (1990) showed that the results of all previous studies could be re-expressed in the form of Equation 5.37 giving rise to a relatively narrow range of constants.

The use of Equation 5.37 was justified on the grounds that

- The rate of head loss per unit length (that is, the slope of the energy line, which is equal to the bed slope and the slope of the water surface in the case of uniform flow) and depth of flow are the only dependant variables that can change with changing specific flow (flow per unit width).

- Most other expressions for drag due to vegetation can be expressed in this manner.

There are a number of serious drawbacks to the approach taken by Kadlec (1990). These are:

- The equation leads to awkward units for the calibration coefficient, *K*, which takes the dimensions of $L^{2-\beta}T^{-1}$; it is therefore important to specify the units of measurement used when quoting *K* values.
- The equation does not account for stem density or stem diameter, thereby limiting its widespread application. Furthermore Kadlec (1990) quotes no values of stem density or diameter, so the repeatability of his experiments is questionable.
- Determining head loss in the field to determine water surface profiles requires very high precision surveying equipment. Kadlec (1990) does not report the equipment nor the techniques used for the surveying undertaken. This makes it difficult to assess the amount of error associated with the reported values of K, α and β.
- Only 16 sets of measurements were used to determine the values of the three parameters, K, α and β for the Houghton Lake wetland. These sets were obtained by measuring the flow rate over all combinations of depths of 50 mm, 100 mm, 200 mm and 300 mm and slopes of 10^{-3}, 10^{-4}, 10^{-5} and 10^{-6}. This represents a limited set of readings upon which to fit the parameters.
- The values of the parameters, K, α and β that Kadlec gives for equivalence to the Darcy-Weisbach, Mannings and laminar shear flow equations do not appear to be consistent with the original equations.

For these reasons, Kadlec's (1990) approach has not been considered further and the standard drag term from Equation 5.32 will be used here.

5.3 THE EFFECTS OF VEGETATION ON BUOYANCY DRIVEN CONVECTION

In the previous sections, buoyancy driven convection in open water and the effects of vegetation on flows were examined through literature reviews. It is now possible to consider the case of buoyancy driven convection with vegetation present. This will be done by performing scaling analysis, based on the literature examined above.

Substituting the conventional drag expression (Equation 5.32) into Equation 5.28 and rearranging the viscous and turbulent diffusivity terms gives:

$$\frac{\partial U}{\partial t}+U\frac{\partial U}{\partial x}+W\frac{\partial U}{\partial z}=g\left(\alpha_T T_x z-S\right)+\frac{\partial}{\partial z}\left[\left(K_M+v\right)\frac{\partial U}{\partial z}\right]-\frac{1}{2}C_D S_f \eta d U^2 \qquad 5.38$$

Clearly while Equation 5.43 gives a detailed description of the flow, it would be instructive to gain a better understanding of the physics of the flow by performing a scaling analysis on the equation to determine which terms, and therefore which processes are important. This is performed below.

5.3.1. SCALING BUOYANCY DRIVEN FLOWS THROUGH VEGETATION

Patterson and Imberger (1980) performed a scaling of the equations of motion for buoyancy driven flow in open water. This scaling has already been considered in Section 5.1.3. That scaling was based on the conventional two dimensional form of the continuity, advection-dispersion and momentum equations, Equations 5.4, 5.6 and 5.7 respectively, with the pressure term given by Equation 5.12 under the assumption that the slope S is negligible.

Using the length, time and velocity scales from Table 5.1, it was found that for the Manly Dam Site B wetland, heat transfer would be expected to occur by a combination of conduction and convection, with the convection being partly inertial and partly viscous.

For buoyancy driven flow in vegetation, the x momentum equation is given by Equation 5.38 rather than by Equation 5.7, so the Patterson and Imberger (1980) analysis is invalid, because of the presence of the drag term. It is therefore necessary to perform a new scaling analysis using Equation 5.38 as the x-momentum equation so that the drag term can be included in the analysis.

To perform the scaling analysis thoroughly, it would also be necessary to scale the advection-dispersion equation for temperature from Equation 5.19; however, it is the velocity field within the water column that is of primary interest here, not the temperature field so the approach adopted has been to assume the temperature field as a known independent variable and to treat the velocity as dependent on the temperature.

To assess the behaviour that will develop according to Equation 5.38, it is assumed that velocity, length and time scales representative of the flow behaviour on a large scale can be found that are invariant under the differential operator. Furthermore, it must be assumed that:

- the heat transfer from solar radiation to the water column and the consequent convection that occurs are both steady state processes,
- momentum transfer in the vertical does not play a significant role, and
- other factors that could cause convection, such as wind are negligible (an assessment of the effects of wind on convections observed is performed later in Section 5.5.2).

These conditions are quite restrictive, however, it must be recognised that the aim of this work is to determine the dominant processes that take place in the wetland, as few investigations have previously been performed in this area. It is therefore beyond the scope of this study to investigate these processes in detail.

Considering these simplifications, the following equation results:

$$\frac{U_s}{t_s} + \frac{U_s^2}{L} + \frac{W_s U_s}{H} = g\left(\frac{\alpha_T T' z}{L} - S\right) + \left(K_M + \nu\right)\frac{U_s}{H^2} + f_D \qquad 5.39$$

Where the s subscript represents a scaled value, L is the (horizontal) length scale and H is the (vertical) depth scale. Simplifications that can be made to Equation 5.39 include the following.

- From continuity, $W_s/H \sim U_s/L$, allowing the second and third terms from the left to be combined.
- The maximum value for the buoyancy term is obtained by taking $z = 0$.

Using these simplifications in Equation 5.39 yields:

$$\frac{U_s}{t_s} + 2\frac{U_s^2}{L} = -g\left(\alpha_T \frac{HT'}{L} - S\right) + \left(K_M + \nu\right)\frac{U_s}{H^2} + f_D \qquad 5.40$$

Note that the estimate of the second term from the right, which represents the effects of dissipation due to turbulence and viscosity, is somewhat more prone to error than the others, as it is based on a double derivative, while the other terms are based on single derivatives.

Table 5.2 presents values for the parameters in Equation 5.40. Using these parameter values, values for the terms in Equation 5.40 can be estimated. These estimated values are given in Table 5.3. From Table 5.3 it can be seen that the magnitude of each term can vary widely. Estimates of the drag term from the different studies vary widely; however it can clearly be seen that the estimates of the drag term generally dominate the other retarding terms.

It can therefore be expected that the drag term will provide the balance to the buoyancy term in Equation 5.40 and the unsteady, advective and viscous terms may be neglected. Equation 5.40 can therefore be simplified to a balance between drag and buoyancy. This simplification is performed below, followed by an assessment of the flow development as a balance between viscosity and buoyancy, the terms that would dominate in the absence of vegetation.

Table 5.2. Expected Typical Parameter Values For Flows in Wetlands

Parameter	Minimum	Present case	Maximum	Units	Reference
U_s	10^{-4}	10^{-3}	10^{-2}	m/s	Kadlec (1990)
t_s	60	3600	10^{5}	s	Scales of interest
L	0.1	10	100	m	Kadlec (1990)
H	0.01	0.5	1.0	m	Kadlec (1990)
A	0.0001	0.05	10		
g	9.8	constant		ms^{-2}	
S	10^{-6}	10^{-4}	10^{-3}	dimensionless	Kadlec (1990)
α_T	-2.07×10^{-3}	-2.32×10^{-3}	-2.57×10^{-3}	$kgm^{-3}(°C)^{-1}$	Fischer *et al* (1979)
T'	0.1	1	5	°C	Present Study
η_p	10	300	1000	m^{-2}	Present study
d	0.001	0.006	0.01	m	Present Study
S_f	1.0	0.91	0.77	dimensionless	Equation 5.34
ν	10^{-6} constant			m^2s^{-1}	Fischer *et al* (1979)
D_T	1.4×10^{-7} constant			$°Cs^{-1}$	Fischer *et al* (1979)
R_e (stem)	0.1	6	10	dimensionless	calculated from above
R_e (depth)	1	500	10^{4}	dimensionless	calculated from above
K_M	10^{-7}	10^{-5}	10^{-3}	m^2s^{-1}	Raupach and Thom (1981)
R_i	0.20	1100	13000	dimensionless	calculated from above
G_r	2000	3×10^{8}	10^{10}	dimensionless	calculated from above
P_r	7.14	7.14	7.14	dimensionless	calculated from above
R_a	1400	2×10^{9}	9×10^{9}	dimensionless	calculated from above
C_D	5.5	7	80	dimensionless	Figure 5.2

Note that the high C_D term occurs under the low R_e condition and vice versa

An assessment of the special case of creeping flows in vegetation is also performed, as this combines the low reynolds number drag and viscous cases, and an exact solution of the equation of motion under these conditions is possible.

5.4.1. BUOYANCY - DRAG BALANCE

With only buoyancy and drag accounted for, Equation 5.40 becomes:

$$\frac{1}{2}C_D S_f \eta_p d U^2 = g(\alpha_T T_x z - S) \tag{5.41}$$

This equation is easily solved for U, yielding:

$$U = \sqrt{\frac{2g(\alpha_T T_x z - S)}{C_D S_f \eta_p d}} \tag{5.42}$$

Table 5.3. Expected Orders of Magnitude of Terms in the Scaled Momentum Equation

(Equation 5.40) Given the expected parameter values from Table 5.2

Term		Minimum (ms^{-2})	Present case (ms^{-2})	Maximum (ms^{-2})
Unsteadiness	U_s/t_s	10^{-9}	10^{-7}	10^{-6}
Advection	$2U_s^2/L$	10^{-10}	10^{-7}	10^{-3}
Buoyancy	$-g\alpha_T\left(\frac{HT}{L}-S\right)$	10^{-8}	10^{-4}	10^{-1}
Drag Naot *et al* (1996)	$\frac{1}{2}C_D S_f \eta_p d U^2$	10^{-9}	10^{-6}	10^{-4}
Viscous	$\nu U_s/H^2$	10^{-10}	10^{-8}	10^{-4}

In Equation 5.42, C_D is dependant on the Reynolds number and therefore on the velocity, so this equation is not strictly explicit. Using Equation 5.36 for C_D gives three relationships for U in the fully laminar ($R_e < 3$), transitional ($3 < R_e < 1000$) and fully turbulent regimes ($R_e > 1000$). From Table 5.3, it is expected that for the present case, flows in the wetland will fall into the transitional regime.

In the laminar regime, this gives:

$$U = \sqrt{\frac{2g(\alpha_T T_x z - S)}{\frac{10v}{Ud} S_f \eta_p d}} \qquad 5.43$$

which is easily rearranged to give:

$$U = \frac{g(\alpha_T T_x z - S)}{5vS_f \eta_p} \qquad 5.44$$

Interestingly, this expression is independent of the stem diameter. Knowing that this expression only holds for $R_e < 3$ gives the criterion for laminar flow as:

$$\frac{g(\alpha_T T_x z - S)d}{v^2 S_f \eta_p} < 15 \qquad 5.45$$

Using the expression for C_D from Equation 5.36 in the transitional regime in Equation 5.47 gives:

$$U = \sqrt{\frac{2g(\alpha_T T_x z - S)}{\left(\frac{1000v}{Ud}\right)^{0.25} S_f \eta_p d}} \qquad 5.46$$

which is easily rearranged to give:

$$U = \left[\frac{2g(\alpha_T T_x z - S)}{(1000v)^{0.25} S_f \eta_p d^{0.75}}\right]^{\frac{4}{7}} \qquad 5.47$$

From Equation 5.36, in the turbulent regime $C_D \cong 1$, when substituted into Equation 5.42 this gives:

$$U = \sqrt{\frac{g(\alpha_T T_x z - S)}{S_f \eta_p d}} \qquad 5.48$$

Knowing that this expression holds for $R_e > 1000$ gives the criterion for turbulent flow as:

$$\frac{g(\alpha_T T_x z - S)d}{v^2 S_f \eta_p} > 5 \times 10^5 \qquad 5.49$$

So for the three regimes, the expression for U is:

$$U = \begin{cases} \sqrt{\dfrac{2g(\alpha_T T_x z - S)}{S_f \eta_p d}} & \dfrac{g(\alpha_T T_x z - S)}{S_f \eta_p d} > 5 \times 10^5 \quad \text{Turbulent drag} \\ \left[\dfrac{g(\alpha_T T_x z - S)}{(1000vd^3)^{\frac{1}{4}} S_f \eta_p}\right]^{\frac{4}{7}} & 15 < \dfrac{g(\alpha_T T_x z - S)}{S_f \eta_p d} < 5 \times 10^5 \quad \text{Transitional drag} \\ \dfrac{g(\alpha_T T_x z - S)}{5vS_f \eta_p} & \dfrac{g(\alpha_T T_x z - S)}{S_f \eta_p d} < 15 \quad \text{Laminar drag} \end{cases} \qquad 5.50$$

The profiles described by Equation 5.50 are shown in Figure 5.3. The profile due to the laminar viscous-buoyancy balance in the absence of vegetation that was developed in Equation 5.26 is also shown on Figure 5.3 for comparison.

From Equation 5.50, the following points are noteworthy:

Figure 5.3. Expected Velocity Profiles arising due to Lateral Buoyancy Differences in a vegetated water body for the cases of a laminar drag on vegetation balancing buoyancy, transitional drag on vegetation balancing buoyancy and turbulent drag on vegetation balancing buoyancy (all given by Equation 5.50, with $S = -\alpha_T T_x H/2$) and a laminar viscous to buoyancy balance without vegetation (Equation 5.26).

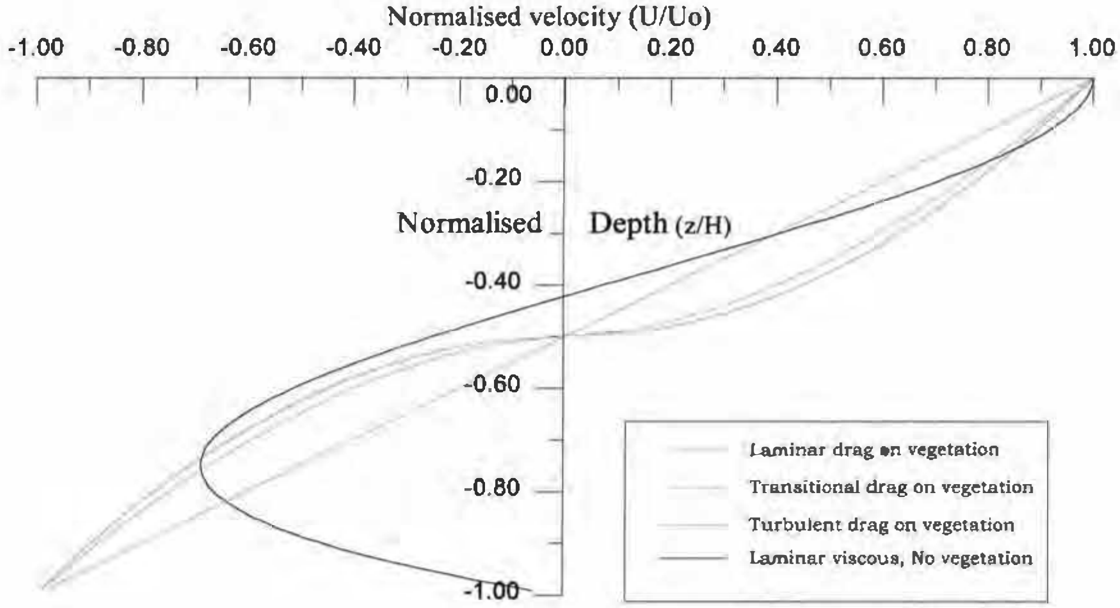

Notes

- The laminar inviscid, transitional and turbulent profiles violate the non-slip and free boundary conditions as turbulent and viscous diffusion were ignored in their derivation. These profiles are therefore invalid near the upper and lower boundaries
- Comparison of the magnitudes of the velocities in different profiles cannot be made from this figure as the velocities are normalised against the surface velocity for each profile.

- It should be remembered that S_f is the shading factor from the drag term and is not to be confused with the friction slope.
- The velocities given by Equation 5.50 appear to decrease as the number of plants per unit area is increased, due to increasing drag. This is misleading as the temperature gradient arises from the shading provided by the vegetation, and hence the number of plants per unit area so the two effects will cancel to some degree.
- To satisfy continuity, the integral of the velocity over the depth of the water column should be zero. If no external water surface slope is imposed on the problem, then the value of S can be adjusted to ensure that continuity is met. By integrating U over the range $z = -H$ to $z = 0$ for any of the expressions in Equation 5.50, it is easily shown that for each of these cases $S = -\alpha_T T_x H/2$.

- Clearly, none of the velocity profiles given in Equation 5.50 meet the non slip and free shear boundary conditions at the bed and the water surface respectively. These profiles therefore only provide a limited description of the flow and will not be valid near the bed or the water surface.

- Note that as the flow evolves according to Equation 5.26 or 5.50, warm water will flow over the top of cold water, inducing a temperature gradient in the vertical. Rigorous treatment would then require that stratification effects be included in the analysis; however, this is beyond the scope of the present study, which is restricted to defining only the primary mechanisms of fluid motion in a wetland. While stratification may play a role in the fluid motion, that role is expected to be secondary to the primary mechanisms of buoyancy and drag.

- From Figure 5.3 it can be seen that the non-slip condition has a dominant influence on the flow over the lower 20% of the profile. Over the rest of the depth, all the profiles show reasonable agreement, given the different bases on which they have been derived, except that the depth at which the velocity is zero in the laminar viscous profile is somewhat higher than for the other profiles. It is therefore expected that Equation 5.50 will provide reasonable estimates of the velocity profile from $z = -0.8H$ to $z = 0$.

5.4. FIELD OBSERVATIONS

The most dramatic observations of buoyancy driven convection were made on the evening of Monday 20 February, 1995, Julian day 95051. For this reason this day was chosen for analysis of buoyancy driven despite the absence of meteorologic data on that day (buoyancy driven convection was much less evident on other days of the intensive monitoring period).

To define the context in which these observations were made, the meteorologic conditions that applied on that day are described first, followed by descriptions of the temperature profiles obtained at Stations 1 to 4 respectively. Finally, convections indicated by these temperature profiles are then discussed.

5.4.1. METEOROLOGIC CONDITIONS

Unfortunately meteorologic conditions were not available at the site on for Monday 20 February, 1995, as the logger for the meteorologic station was inoperable. However, meteorologic data was available for the period at Macquarie University and are shown in Figures 5.4 and 5.5. A comparison of meteorologic data at Macquarie University and Manly Dam is contained in Appendix A.4, and despite limitations, the data appears to be acceptable for the purposes of this analysis.

The meteorologic conditions show that on day 95051, solar radiation was low throughout the day, especially in the afternoon. Wind was from the south east, between 1 and 3 ms^{-1} throughout the day from 0600 until just before 2100. In fact from 1100 until 1800, the wind was above 2.0 ms^{-1}. After 2100, the wind remained below 1.0 ms^{-1} for the rest of the evening, blowing from a north westerly direction until 0800 the next morning.

As discussed in Appendix A.4 neither the wind direction nor wind speed readings at Macquarie University and Manly Dam are well correlated; however, observations at Manly Dam during the investigations on day 95051 indicate that winds were strong through the afternoon and died off into the evening, as observed at Macquarie University and the ORS. The wind direction at Manly Dam however was noted to be from a South-Easterly direction during the day, while Figure 5.4 shows it to have been from a South Westerly direction. The difference here is probably due to local topographic effects as the wetland was in a low-lying area with hills to the North East and South West. It therefore seems that winds on day 95051 at the site were moderate to strong and from a Southerly direction.

Figure 5.4. Radiation, Wind Speed and Direction days 95051 to 95052
From Macquarie University Data

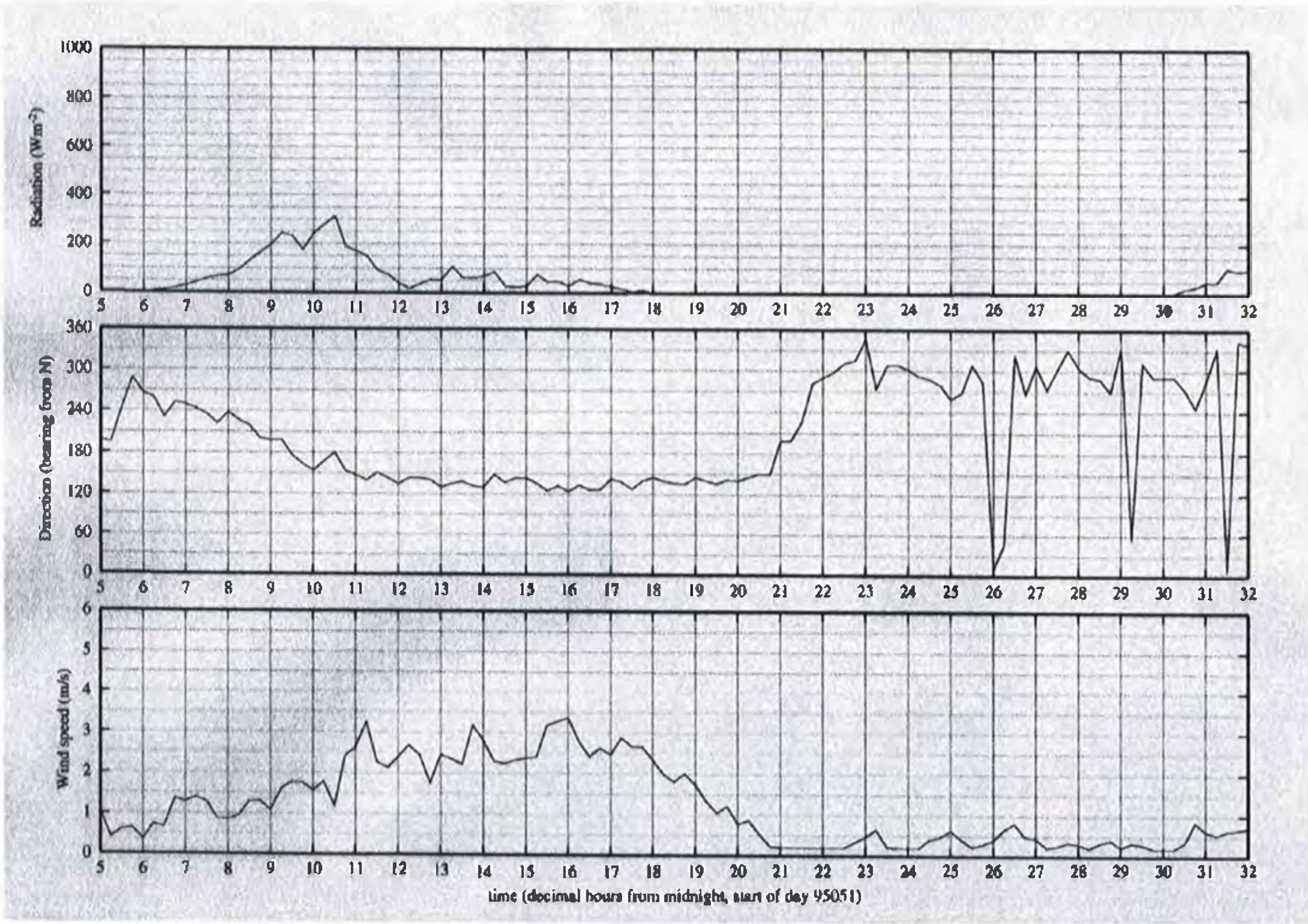

Figure 5.5. Air Temperature, Relative Humidity and Rainfall day 95051 to 95052 from Macquarie University Data

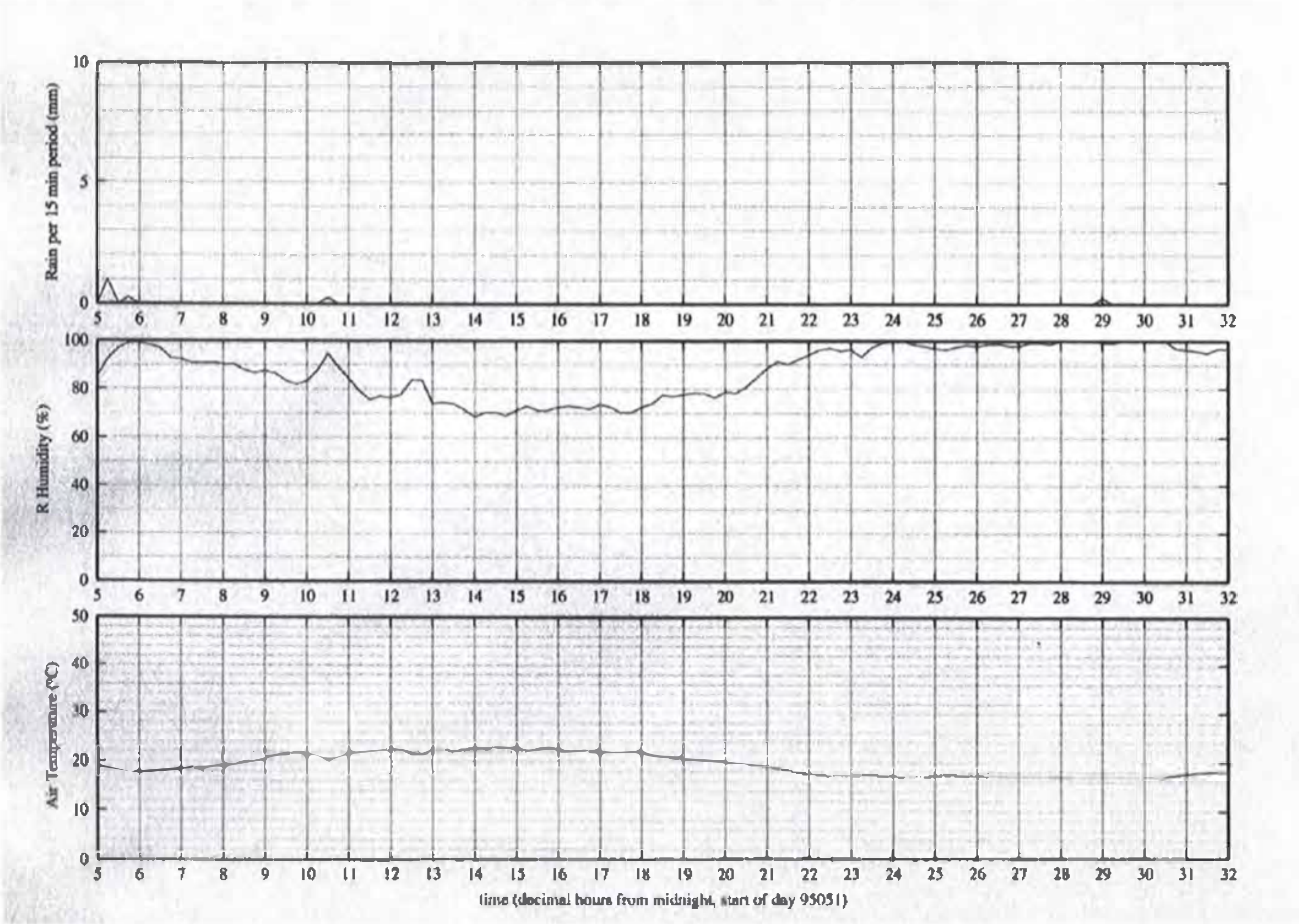

Temperature profiles were taken at Stations 1 to 4 from 1337 in the afternoon, until dawn the following morning, as described in Chapter 2. The data from these profiles is presented as contours and colour images of temperature plotted against time and depth in Figures 5.6a to 5.6d and as temperature vs depth plots in Figure 5.7.

Descriptions of the temperature behaviour observed at each Station are provided below.

5.4.2. TEMPERATURE PROFILES, STATION 1 (VEGETATED)

Figure 5.6a shows clearly that through the afternoon, in the vegetation Station 1 was unstratified; however, as the evening progressed the water column went from an unstratified to a stratified state. Furthermore, the water at the surface became progressively warmer from 2000 until about 0330 am, rising by approximately 1.0°C. This is despite a drop in air-temperature of 3°C recorded at Macquarie University. Between 0330 am and 0700, the surface water cooled by about 0.4°C, after which it began to rise with the morning sun. Meanwhile at the base of the water column, the water cooled through the evening by about 0.8°C until 0430. The temperature then rose by about 0.4°C until just before 06:00. It then dropped again by about 0.4°C between 0430 and 0730. Features of the stratification are summarised in Table 5.4. Table 5.4 also contains calculations of the features of the buoyancy driven convection, as predicted by the scaling performed earlier in this chapter.

5.4.3. TEMPERATURE PROFILES, STATION 2 (OPEN WATER, IN WETLAND)

Figure 5.6b shows that as the evening progressed, the water column at Station 2 initially cooled, until 2000, after which the water at the surface slowly became warmer until about 0200, after which it remained fairly constant until 0400, then fell by about 0.3°C until 0630, then began to rise again with the morning sun.

Figure 5.6a. Temperature vs Time and Depth Station 1, day 95051

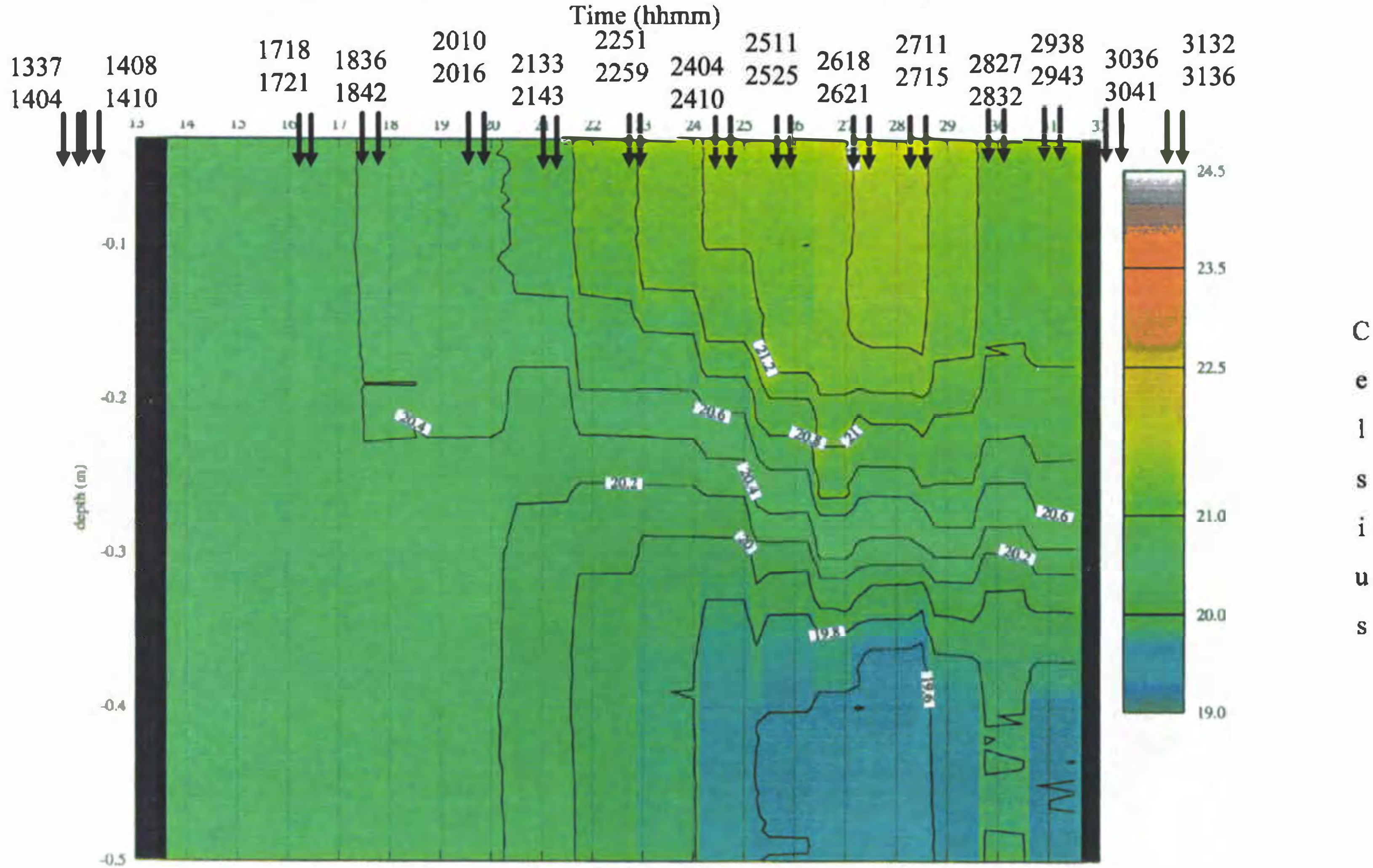

Figure 5.6b. Temperature vs Time and Depth Station 2, day 95051

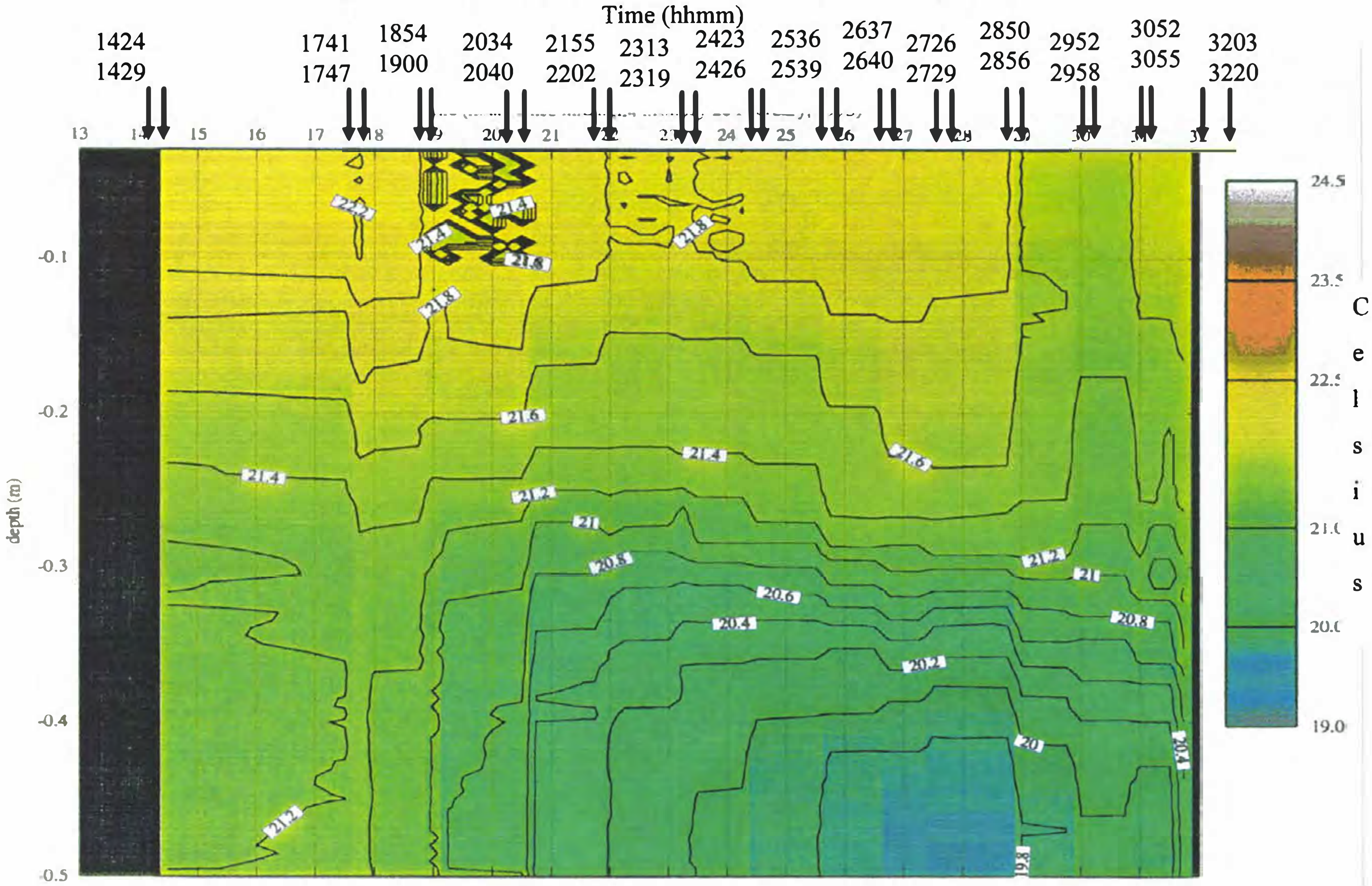

Figure 5.6c. Temperature vs Time and Depth Station 3, day 95051

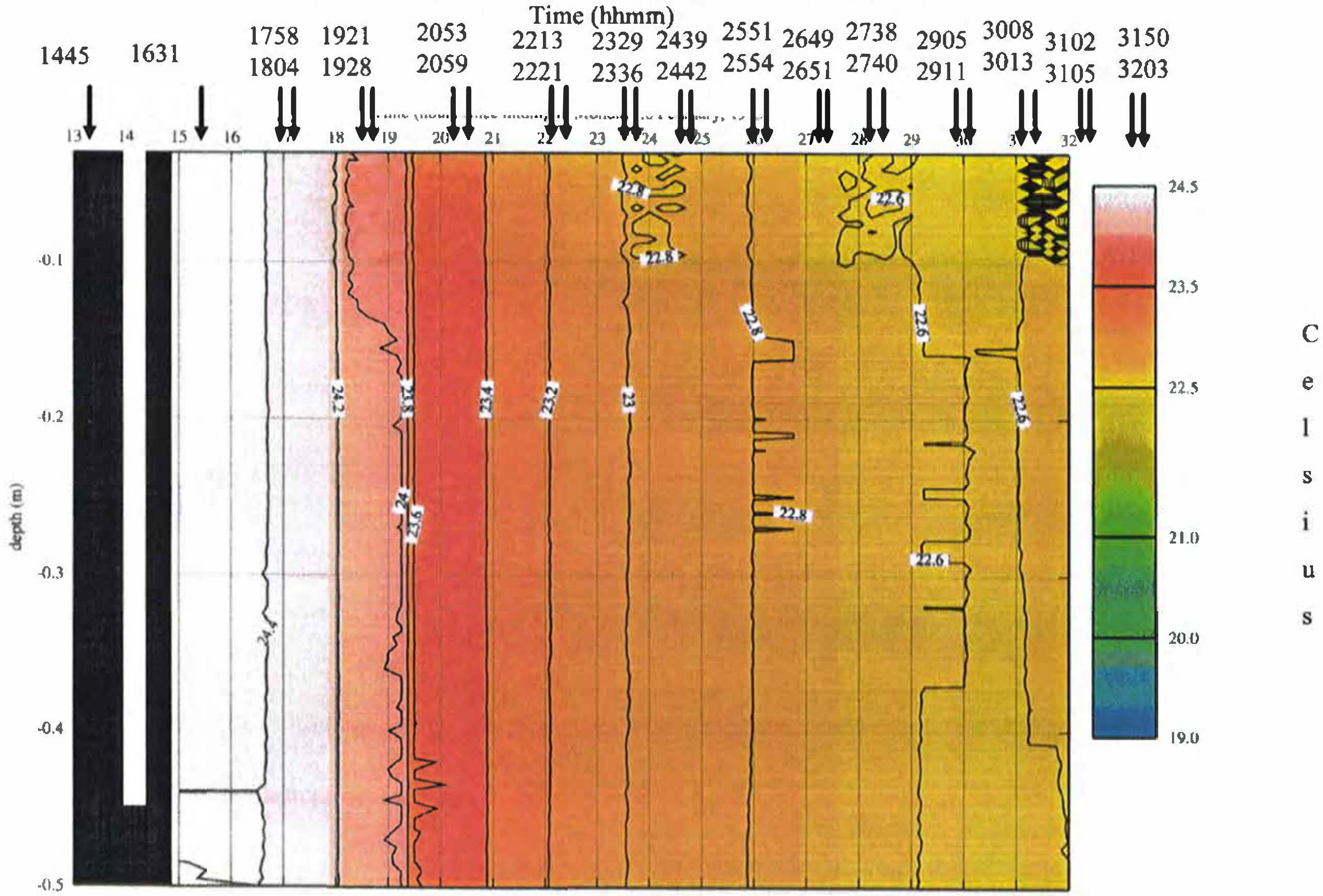

Figure 5.6d. Temperature vs Time and Depth Station 4, day 95051

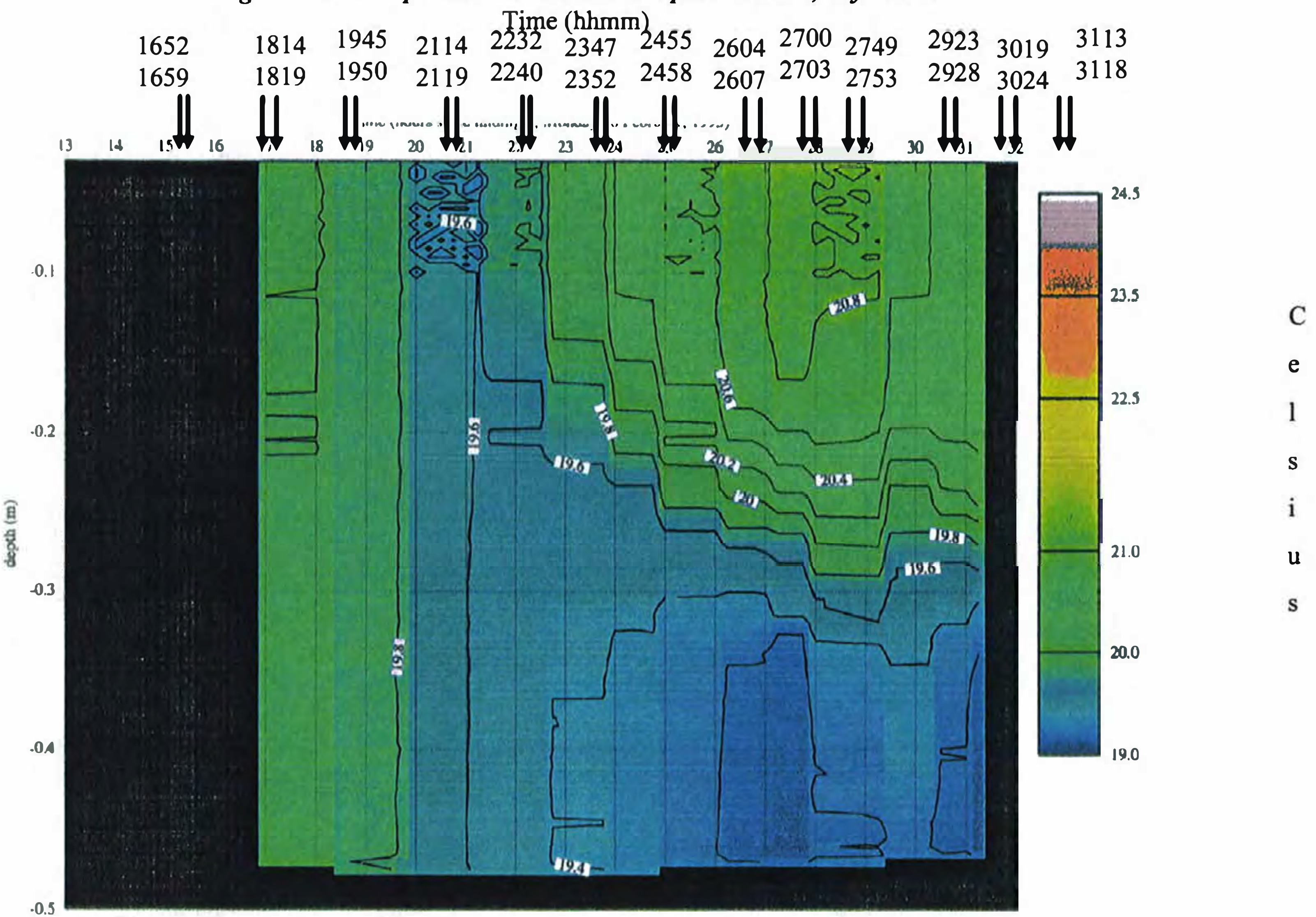

Figure 5.7. Temperature Profiles at all Stations day 95051

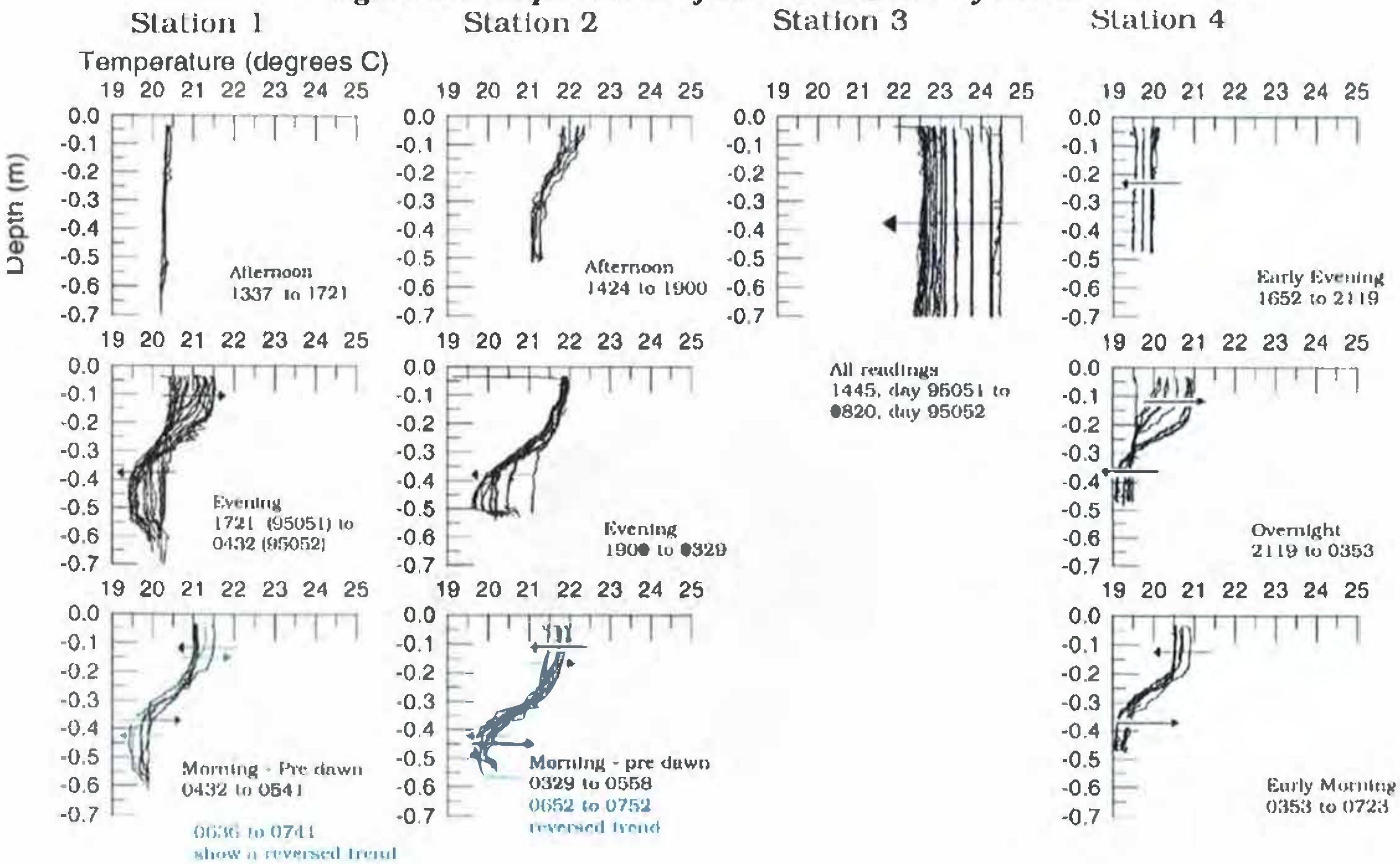

At the base of the water column, the water cooled by about 1.5°C between 1800 and 0430 am, then warmed by about 0.2°C between 0430 and 0630, then cooled again by about 0.4°C between 0630 and 0800. As for Station 1 it seems that it was not until the high winds recorded at Macquarie subsided that the buoyancy driven interchange was observable, as it had previously been masked by the turbulent mixing arising due to the dissipation of the wind waves.

5.4.4. TEMPERATURE PROFILES, STATION 3 (OPEN WATER IN LAKE)

Figure 5.6c shows that in the lake, Station 3 remained unstratified throughout the evening, cooling by about 1.8°C between 1600 and 0600.

Throughout the period for which temperature profiles were taken, the temperature at Station 3 was always significantly higher than readings taken at the other stations. The temperature difference between Station 3 and the other stations was highest in the late afternoon: at 1700, the temperature at Station 3 was quite uniform at approximately 24.4°C At Stations 1, 2 and 4, the depth averaged temperatures were lower than the Station 3 temperature by approximately 4.0°C, 2.8°C and 4.7°C respectively.

By 30 hours after midnight, day 95051 (that is, at 0600, day 95052), the temperature at Station 3 had dropped to 22.6°C. At Stations 1, 2 and 4, the depth averaged temperatures were lower than the Station 3 temperature by approximately 1.1°C, 1.6°C and 2.6°C respectively.

5.4.5. TEMPERATURE PROFILES, STATION 4 (VEGETATED)

From Figure 5.6d the temperature structure in the vegetated region furthest from the lake, Station 4 evolved in a similar manner to Stations 1 and 2, displaying the following characteristics listed below.

- The water column was essentially unstratified from 1700 until a slight stratification became evident at 2200, when the surface water began to warm. Prior to this, the water column had cooled by about 0.4°C over the whole depth.

- Between 2100 and 0400, the water at the surface became warmer by about 1.3°C, while the water at the base cooled by about 0.4°C. From 0400 to 0700, the surface water cooled by about 0.3°C.
- From 0400 to just before 0600, the water at the base warmed by about 0.2°C, then from 0600 to 0700, it cooled again by about 0.2°C.

As at Station 1, at Station 4 the buoyancy driven interchange was not observed until the late evening. Again, the buoyancy driven interchange was not observed earlier, as mixing by the breakdown of wind waves would have broken down any stratification that would have indicated the presence of such a convection.

5.5. CONVECTIONS BETWEEN THE LAKE AND THE VEGETATION

As stated above, significant temperature differences arose between the lake and the wetland. It is expected that these temperature differences will lead to significant buoyancy driven convections between these two areas. Buoyancy driven convections and potential convections due to other mechanisms are described below.

5.5.1. BUOYANCY DRIVEN CONVECTION

Figures 5.6a to 5.6d show that the profiles taken through the evening at each station form a similar pattern. At Stations 1, 2 and 4, three distinct regions can be clearly seen in each profile, an upper layer with a slight stratification, or at times unstratified, a layer at mid-depth that is quite stratified, and in which the stratification rate remains quite consistent throughout the evening, and a lower region which is generally unstratified.

Details of the development of temperature profiles, expected convections due to buoyancy driving and dimensionless numbers between Stations 1 and 3 and Stations 4 and 3 on the evening of day 95051 are summarised in Table 5.4. Richardson Numbers, and Entrainment coefficients were also calculated. As was expected, the Richardson Numbers were high enough that the assumption that entrainment could be neglected can be seen to be valid.

As Station 2 was situated in open water, the buoyancy-drag form of the momentum equation would not be valid and this station was therefore not included in the analysis.

It seems most likely that the lower water temperatures resulted from a flow coming from the upstream creek. Upstream of the wetland, the valley becomes quite narrow and is very well shaded by trees, the water temperature upstream of the monitoring positions was observed during field work to be colder further up the creek than where the observations were taken.

Velocities were calculated by the buoyancy-drag balance with the transitional Reynolds number relationship. All dimensional parameters fell into the ranges expected from the scaling so no further comment on these is required.

With the expected intrusion velocities being 12 mms^{-1} at Station 1 and 9 mms^{-1} at Station 4, it would be expected that water from the lake would be advected to Station 1 in approximately 11 minutes and to Station 4 in approximately 24 minutes.

These travel times appear to contradict the temperature readings shown in Figures 5.6a to 5.6d. These figures show that the water in the wetland at Stations 1, 2 and 4 always remained cooler than the water in the lake at Station 3, despite the movement of water from the open water area into the wetland in a fairly short time frame.

If it is assumed that the velocity estimate is correct and surface cooling is the cause of the heat loss, then within 15 minutes, the temperature of the plume moving into the vegetated area must be lowered by approximately 3.4°C.

Table 5.4. Features of Temperature Profiles at Stations 1 and 4, day 95051

(evaluated by inspection cf Figures 5.6a to 5.6a)

average stem width = 6 mm, plant density = 300 m^{-2}

Station	**1**	**4**
Approximate thickness of the upper, mixed layer (mm)	150	170
Approximate thickness of the middle, stratified layer (mm)	200	140
Approximate thickness of the mixed, lower layer (mm)	150	90
Distance from open water (m)	8	13
Approximate middle layer stratification (°C/m)	10	13
Temperature difference with Station 3 at sunset 1900, just below water surface (°C)	3.8	4.2
Rayleigh Number	8×10^9	8×10^9
Grashof Number	6×10^{10}	6×10^{10}
Prandtl Number	7.14	7.14
Aspect Ratio	0.063	0.038
Horizontal temperature gradient from the edge of the vegetation to the station (°C/m)	0.48	0.32
Velocity estimate for the Drag-Buoyancy balance (m/s) just below surface	0.012	0.009
Stem Reynolds Number	54	48
Richardson Number	11	9
Entrainment E	2×10^{-4}	2×10^{-4}
Time of first sign of surface heating t_i	2010	2232
Temperature difference with Station 3 at t_i	3.0°C	3.0°C
Time of peak surface temperature t_p	0427	0349

Assuming the specific heat of water to be 4179 Jkg^{-1}(°C)$^{-1}$, and the plume to be 150 mm thick, then the rate of heat loss through the water surface would be 3300 Wm^{-2}, which is clearly not possible.

Heat loss may also be possible through the plant stems. With 300 stems per square metre over the 150 mm plume thickness and the average stem diameter being 6 mm, the stems contribute a surface area of 1.7 m^2 per square metre of the wetland. If it is assumed that heat transfer occurs at the same rate through the plant stems as through the water surface, a rate of heat loss through the water surface and stems of approximately 1200 Wm^{-2} would be required, which is still unreasonably large.

Possible causes for the discrepancy between the velocity predictions and the observed temperature behaviour are:

- the presence of some other convective process arresting the velocities in the wetland due to the buoyancy driven flow;,
- the presence of some mixing process which was vigorous enough to drastically reduce the temperature of the upper layer, but was not strong enough to overcome the stratification between the upper and lower layers;
- three dimensional effects - as the profiles were only obtained at single points, it is difficult to say whether or not these profiles are representative of the average behaviour of the wetland over its full width;

Processes that may have affected the buoyancy convection between the lake and the wetland giving rise to these causes are:

- wind driven convection due to the light wind from the North that was present throughout the evening; and
- surface and internal seiche motions in the lake caused by the wind through the afternoon.

5.5.2. WIND DRIVEN CONVECTION EFFECTS

Data from the Macquarie University Meteorologic Station shows that throughout the evening a light wind of approximately 0.3 m/s was present throughout the night, coming from a North Westerly direction. The presence of such a wind would give rise to a convection in the lake, in a direction away from the wetland. From Tsahalis

(1979), the surface velocity in open water due to wind is commonly given as:

$$U_s = 0.03U_A \qquad 5.51$$

where U_s is the surface velocity in the water and U_A is the wind speed. With the recorded wind speed through the evening of approximately 0.3 ms^{-1}, surface water velocities of the order of 0.009 ms^{-1} or 9 mms^{-1} can be expected in the lake. This velocity estimate is the same order of magnitude as the expected velocities due to buoyancy driven convection, so it is most likely that wind driven convection in the lake was the mechanism responsible for arresting the buoyancy driven flows in the wetland.

To account for wind effects in the equations of motion, a surface stress is generally applied as a boundary condition in the x-momentum equation. Due to the lack of meteorologic data available at the site on the day when data was collected, a thorough analysis of this scenario is unjustified here.

5.5.3. SEICHING EFFECTS

Seiching may have been responsible for the behaviour observed in the wetland at Stations 1, 2 and 4 in the early hours of day 95052, around 30 hours after midnight day 95051. During this time, Figures 5.6a, b and d show that Stations 1, 2 and 4 experienced a brief increase and then decrease in temperature near the bed of the wetland and the reverse behaviour near the surface. From Chapter 2, first order seiches are expected to have a period of 8 minutes.

The temperature profiles at Station 3 show that stratification was absent in the side arm throughout the period, therefore no internal seiching would have been possible.

5.6. COMMENTS ON TEMPERATURE PROFILES IN THE AFTERNOON

From Table 5.4, it is interesting to note that despite the temperature difference between Stations 1 and 3, there was no apparent increase in temperature due to buoyancy driven convection until 2010. Furthermore, the strong southerly winds that were present should have increased the speed at which the interchange propagated into the vegetated area; however, there is no evidence of any interchange based on the temperature profiles alone.

The strong southerly wind would not only have transported a flux of water into the vegetated area, it would also have resulted in wind waves on the lake that would have propagated across the lake from the South towards the wetland. As detailed in Chapter 4, the energy associated with these waves would then have been transformed into turbulent energy in the vegetated area. The turbulence would then have been responsible for mixing in the vertical.

When the wind stopped, the source of turbulence in the vegetated area would have been removed so that vertical mixing could not persist. Changes in temperature with depth through the afternoon and evening were then observed to take place in the vegetated area. These consisted of a warming of the water near the surface and a cooling of water near the bed. These temperature changes are a clear sign of convection, as they have taken place despite the absence of any heat fluxes.

This convection most likely occurred due to temperature driven buoyancy forcing between the vegetated area and the open water area. This can be seen as there are only two alternative types of convection that are possible, both of which are unfeasible. The unfeasible types of convection are:

- **wind driven convection,** which could not have been responsible for the convection observed as the wind was travelling in the opposite direction to the direction of the convection; and
- **convection due to an inflow from the creek,** could have caused an inflow to the

wetland of water at a different temperature to that within the wetland. For example, had the inflow been cooler than the water in the wetland, a cooler layer would have been formed at the bed, while the overlying water would have remained at the same temperature (if mixing effects are ignored). Such a mechanism could not have been responsible for the convection observed as water near the bed cooled, while that near the surface heated, indicating that water was moving in opposite directions near the surface and near the bed.

The lack of wind velocity readings at the site on day 95051 makes it difficult to confirm that this was the sequence of events that took place; however, it does provide an explanation that is consistent with the observations made.

It therefore seems most likely that the buoyancy driven convection was occurring throughout the afternoon and may even have been enhanced by the wind action. However, mixing in the vegetated area due to the turbulence generated by waves arising from the Southerly winds would have masked this effect. The situation is shown diagrammatically in Figure 5.8.

5.7. SUMMARY OF PLANT EFFECTS ON CONVECTION

From this chapter, the presence of vegetation within a wetland can be seen to cause significant convection. This occurs as canopy shading leads to buoyancy driven convection between open water and vegetated sections of the wetland. Furthermore, the vegetation affects the flow by its presence in the water column, causing drag, and hence introducing another term into the equation of motion.

In vegetated areas, under the conditions examined, the momentum balance was found to be dominated by the drag term and the buoyancy driving term. Velocities calculated by scaling arguments from this momentum balance are expected to be of the order of 0.01 m/s. These buoyancy driven flows are expected to be the most significant feature of flows in the vegetated areas.

Experiments conducted in the wetland indicate that these buoyancy driven flows must occur, as they are the only possible cause of the increased water temperatures observed during night-time investigations. However, the estimated velocity of the plume of water entering the vegetated area from the open water area was too high to explain the rate of temperature increase observed. It appears that wind driven convection in the lake away from the wetland arrested the flow, giving it more time to lose heat to the atmosphere and providing an additional method for mixing the incoming plume with the ambient fluid, thereby further reducing its temperature.

Figure 5.8. Sequence of events observed on day 95051

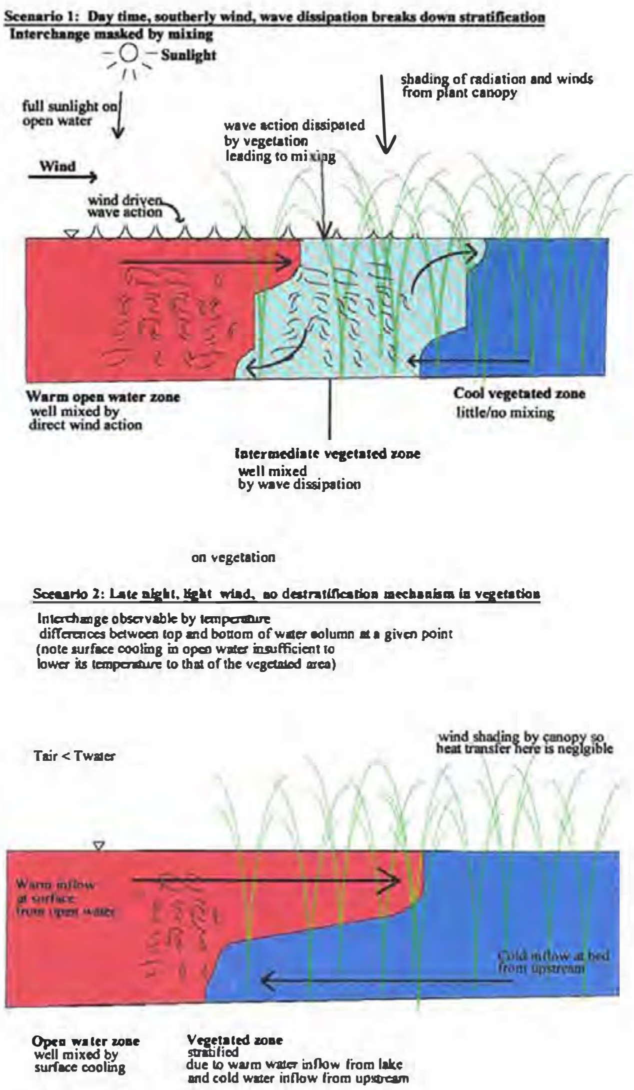

6. SEASONALITY AND SITE DEPENDENCY

6. SEASONALITY AND SITE DEPENDENCY

It is well known that changing conditions with season and site can cause marked variations in the hydrodynamics, water chemistry and biology of lakes and other inland water bodies, see for example Hutchinson (1957), Imberger and Patterson, (1990) and Uhlmann, (1979). Seasonal variations of water chemistry in wetlands have often been reported (Brodie, 1990, Bavor *et al*, 1992) and many species of wetlands vegetation are known to display perennial behaviour (Sainty and Jacobs, 1988). However, no evidence could be found in the literature that previous investigations had been undertaken into the effects of season on hydrodynamics in wetlands.

From the results of the intensive investigations (see Chapters 2 to 5), under summer conditions, features of the hydrodynamic behaviour of the wetland at Site B were:

- faster rates of heating due to solar radiation in open water than in vegetation;
- faster rates of cooling by night in open water than in vegetation;
- higher depth averaged temperatures in open water than in vegetation throughout the whole diurnal cycle;
- buoyancy driven flows between open water and vegetation, with flow from open water into the vegetation at the surface, due to the higher temperatures in the open water than in the vegetation and flow from the vegetation to the open water at the bed due to the lower temperatures in the vegetation;
- wind driven mixing in the open water under winds from any direction due to direct wind driving;
- wave breaking in the vegetated region causing mixing in the vegetated areas when wind blows across the open water towards the vegetated zone;

With changing meteorologic conditions at different times of the year, it is desirable to know what changes can be expected to occur in these patterns. The following points are of particular interest.

- To what extent do the magnitudes of vertical and horizontal temperature gradients change with season?

- Over how many diurnal cycles can buoyancy convections persist through the night during different seasons?
- How frequently do conditions arise that would break down or unstable buoyancy convections? Does the frequency with which such breakdowns occur change with season?
- Are the features noted above that were observed during the intensive monitoring period observed in other wetlands?

In an attempt to answer these questions, long term monitoring was conducted at two sites in Manly Dam Reserve using techniques discussed in Chapter 2. This allowed the effects of site location and seasonality on stratification and buoyancy driven convection to be examined.

Behaviour at the first site, Site A, is only examined briefly, using data gathered on three consecutive days in July 1994. Behaviour at the second site, Site B is described in more detail by analysing data obtained between March 1995 and June 1996.

This approach was taken because widely fluctuating water levels during monitoring at Site A often caused thermistors near the surface to be left stranded out of the water, so the data from this site was generally less reliable than at Site B. However, inclusion of some of the results from Site A allows comparison of the behaviour at the two sites to be drawn.

6.1. SITE A INVESTIGATIONS

This section is based largely on Waters and Luketina (1995), which was written as part of the author's studies for this thesis. In that paper, the lead author was responsible for choosing the processes to be studied, reviewing literature; field techniques, data collection, data analysis and interpretation of results.

6.1.1. SUMMARY OF INVESTIGATIONS AT SITE A

Full details of investigations conducted for long term monitoring investigations at Site A, including site description, equipment specifications and techniques employed are discussed in Chapter 2. A summary of these details is provided below.

Site A is a small wetland, approximately 0.5 m deep and 150 m^2 in area, that is directly connected to Manly Dam. Investigations were conducted here from June 1994 to December 1994, before low water levels forced the site to be abandoned. A full meteorologic station was deployed at the site, as were 16 thermistors, which measured water temperature in three distinct regions of the wetland: an open water region, a region consisting of the emergent macrophyte *Schoenoplectus validus* and a region consisting of the emergent macrophyte *Typha Orientalis*, as was shown in Figure 2.4. Water level data for the dam was also available.

Varying water levels at Site A during the investigations often caused the thermistors to be left stranded above the water level. This led to many periods in the data set where data quality was low, which was a principal reason for abandoning the site for the deeper wetland at Site B. However results obtained at site A over a period of three consecutive days of monitoring are reported as many hydrodynamic features observed at Site B were also observed at Site A and it is known that for this period, all probes were submersed at their correct depths.

Reporting at least some results from Site A that show similar features to the results at Site B demonstrates that the Site B results are not particular to that site alone, but instead appear to be general features of hydrodynamic behaviour of wetlands.

6.1.2. SOME RESULTS OF INVESTIGATIONS AT SITE A

Figure 6.1 presents readings of solar radiation, wind speed and air temperature for 24 to 26 June 1994. Radiation loadings were low as it was mid-winter, peaking at around 500 W/m^2 on all three days. Daylight hours were limited, being less than 10 hours each day.

Hourly average wind speeds throughout the three days being considered were moderate on the first day, but generally low on the following two days. Winds followed the same basic pattern on each day, decreasing from midnight to lows around 3 to 5 kmh^{-1} during the early morning then strengthening through the day. Wind speed peaked at 13 kmh^{-1} on the first day and 9 to 10 kmh^{-1} on the other two days. On the first day, wind speed generally remained over 10 kmh^{-1} until midnight, while on the other two days the wind speed remained under 10 kmh^{-1} and had dropped to less than 5 kmh^{-1} by 6:00 pm (about dusk).

Hourly average air temperatures correlated well with wind speed, with lows of 4 to 6 °C in the early morning, rising to 17 °C each day, then falling though the afternoon and evening. Note that under the still conditions of the second and third days, air temperatures dropped rapidly at about sunset.

Figure 6.2 presents readings of water temperature at depths 100 and 400 mm below the water surface in the three sections of the wetland at Site A. Differences between these top and bottom temperature readings indicate that temperature stratification occurs in the water column at all three locations. The three zones display markedly different patterns of growth and decay of stratification. Furthermore, the temperature differences between the open water zone and the two vegetated zones indicates that a buoyancy driven convection most likely exists between the open water and each vegetated section.

Figure 6.1. Time Series of Meteorological Factors

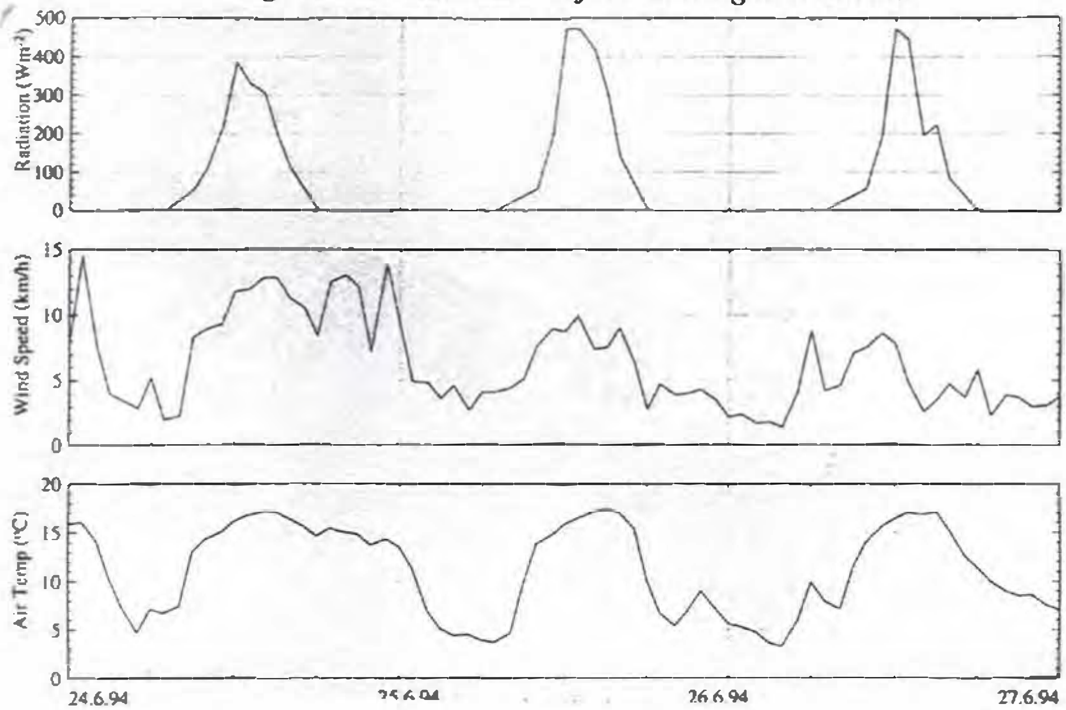

***Figure 6.2. Temperature in Open Water,* Schoenoplectus *and* Typha**

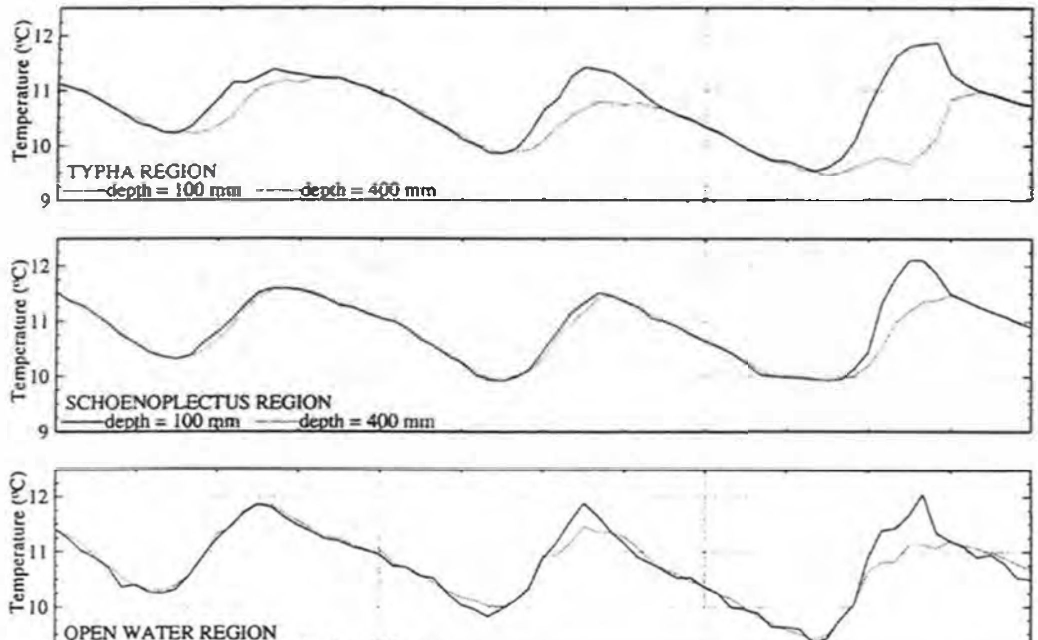

STRATIFICATION DEVELOPMENT AND DECAY

Some degree of stratification arose on each of the three days in the *Typha* zone. Peak daily temperature difference between the higher and lower probes exceeded 0.5 °C on each day, and exceeded 2 °C in the afternoon of the third day.

No stratification occurred in the *Schoenoplectus* zone until the third day, when stratification was short lived, with a temperature difference between the probes of 0.5 °C.

The open water zone did not stratify on the first day, stratified very briefly on the second day, then displayed some stratification in the afternoon of the third day, with a peak temperature difference between the probes of 0.8 °C.

The differences in behaviour of the two vegetated zones in comparison with the open water zone can be explained as follows: the *Typha* has a canopy that extends to almost 2 m out of the water column; however, as the plants had lost most of their foliage though winter senescence, radiation was still able to penetrate well into the water column. Furthermore, the *Typha* stand is somewhat open, with plant stems typically growing at 200 to 500 mm centres, so the amount of radiation that reaches the water column in this area is not significantly reduced. However, the presence of the canopy will significantly buffer the wind immediately above the water surface, so that wind mixing will be significantly reduced here and thus the water column in the *Typha* stratifies easily, as there is a reasonable radiation loading reaching the water surface, but little wind mixing to prevent the growth of stratification.

By contrast with the *Typha* zone, in the *Schoenoplectus* zone there was a very high number of plants per unit area, with plant stems at 10 mm centres or closer; as such very little light penetrates to the water surface, so little stratification can develop.

BUOYANCY DRIVING BETWEEN ZONES

Considering now differences in temperatures between locations, distinct differences can be seen between the open water and vegetated areas. By day the open water generally reaches higher temperatures than the vegetated areas, while by night the open water temperature becomes lower than the temperature in the vegetated areas.

This is particularly noticeable on the morning of the third day, day 94177, where the temperature in the open water drops to 9.4°C, while the temperature in the Schoenoplectus regions experiences a low of approximately 10°C.

Such temperature differences between zones will lead to convective motions between the areas experiencing the temperature differences, as described in Chapter 5.

SUMMARY

It can be seen that even in mid-winter, significant temperature stratification can develop within sections of a wetland. The stratification is dependant on the type of plants within the wetland. During winter, stratification builds up slowly through the day, but decays rapidly at night. This is most apparent in planted sections of the wetland containing plant types with an open structure such as *Typha*. In areas with plants that have a very close structure, such as *Schoenoplectus*, stratification is limited as little light penetrates though the canopy to the water column. In open water areas, the build up of stratification is hindered by wind mixing, but may still develop.

Temperature differences between water in different regions can develop as the open water region is more exposed than the vegetated regions and therefore receives more sunlight by day, and is cooled more rapidly at night. Such temperature differences are significant as they can cause buoyancy driven convection between the regions.

6.2. SITE B INVESTIGATIONS

Due to drought conditions applying over the spring of 1994 and summer of 1994 to 1995, it was necessary to relocate long term monitoring equipment to Site B, as the water level in the dam fell by approximately 800 mm, leaving the bed of Site A above the water line.

Site B and the nature of the investigations undertaken here are described in detail in Chapter 2. The site was located in a long, narrow drowned creek bed that drains into Manly dam from the North. The average depth of water in the wetland was approximately 1.0 m.

Investigations here took place between 13 February 1995 and 3 June 1996. At the commencement of the investigations at Site B, the wetland had a mean depth of approximately 400 mm. Following water level rise after intense, sustained rainfall which returned the water levels in the dam to their normal operating height in early March, the mean depth was approximately 1100 mm.

The site is directly connected to the lake and consists of two zones: a region dominated by the emergent macrophyte *Typha orientalis*, and a small somewhat sheltered open water region that is separated from the lake by the *Typha*.

Equipment used at Site B was the same as at site A; however the different nature of the site led to a different pattern of deployment for the thermistors.

The thermistors were deployed in four assemblies, two assemblies were deployed in the *Typha*, designated as Stations 1 and 4, one assembly was deployed in the sheltered open water section, designated as Station 2 and the remaining assembly was deployed in the open water directly connected to the reservoir, designated as Station 3, as shown on Figure 2.7 in Chapter 2.

This pattern of deployment was chosen to provide data which can be used to:

- determine the influence of the lake dynamics on stratification and mixing in the wetland;
- investigate differences between stratification and mixing in the vegetated and unvegetated areas;
- assess the variability of stratification and mixing within a planted area; and
- determine the effect of the lake on hydrodynamics within the wetland.

DATA QUALITY MANAGEMENT

A number of problems were encountered during the collection of data for the long term investigations at Site B. These problems and the ways in which they were handled are discussed in the points below.

- For the period 27 February, 1995 to 20 March, 1995, thermistor data was unable to be recovered from the datataker due to an error in the configuration of the logger.
- For the period 25 May 1995 to 1 June, 1995, data from the meteorologic station was unable to be recovered due to a battery failure.
- Between 25 May 1995 and 8 June 1995, no thermistor data was available due to a battery failure in the datataker.
- The thermistor 100 mm below the surface at Station 1 was found to be malfunctioning on 11 July 1995. It was subsequently discovered that it had been malfunctioning since its deployment. As detailed below, at each of the other stations a thermistor was deployed 100 mm below the surface, while it was only at Station 2 that a thermistor was deployed 50 mm below the surface. To maintain uniformity across the stations, it was therefore decided to move the thermistor from 50 mm below the surface to 100 mm below the surface. Hence prior to 11 July 1995, at Station 1 no temperature readings were available at 100 mm below the water surface, and after July 1995, no temperature readings were available at 50 mm below the surface.

- On 16 August 1995, the float at Station 1 was found to be 50 mm out of the water at Station 1. This problem was rectified, however it was necessary to discard all temperature readings from the thermistor 100 mm below the surface at Station 1 prior to 16 August.
- Between 10 October 1995 and 19 December 1995 temperature readings were found to fluctuate widely, often taking unreasonable values well outside the range of expected readings (9°C to 30°C). The cause for these fluctuating temperature readings was not discovered. The most likely cause was an electronic error in the datalogger as the logger was reset and the battery changed on both of these dates - the error introduced on 10 October was evidently corrected on 19 December when the previous logging schedule was overwritten.
- The anemometer was inoperable due to an electrical fault from 10 March 1995 until 28 April 1995, as such no wind speed data, sensible or latent heat fluxes nor nett heat balances could be calculated for this period.
- Subsequent to the investigations, it was found that the wind vane had been operating incorrectly from 15 April onwards. The wind direction data over most of the period was therefore invalid and therefore none of the data is reported here.

Due to these data gaps, data is reported here for the period 20 March, 1995 to 3 June, 1996; apart from two gaps in the data from 25 May, 1995 to 8 June 1995 and from 10 Oct 1995 to 19 December 1995, as noted above.

6.3. SEASONALITY OF HYDRODYNAMIC BEHAVIOUR

6.3.1. METEOROLOGIC FORCINGS

Basic meteorologic parameters are shown in Figure 6.3 Heat fluxes into and out of the water column for Station 3 are shown in Figure 6.4 with fluxes out of the water shown as positive. Formulae for the calculation of sensible heat, latent heat and nett long wave radiation were given in Chapter 3.

Figure 6.3. Meteorologic Parameters for Site B, April 1995 to June 1996

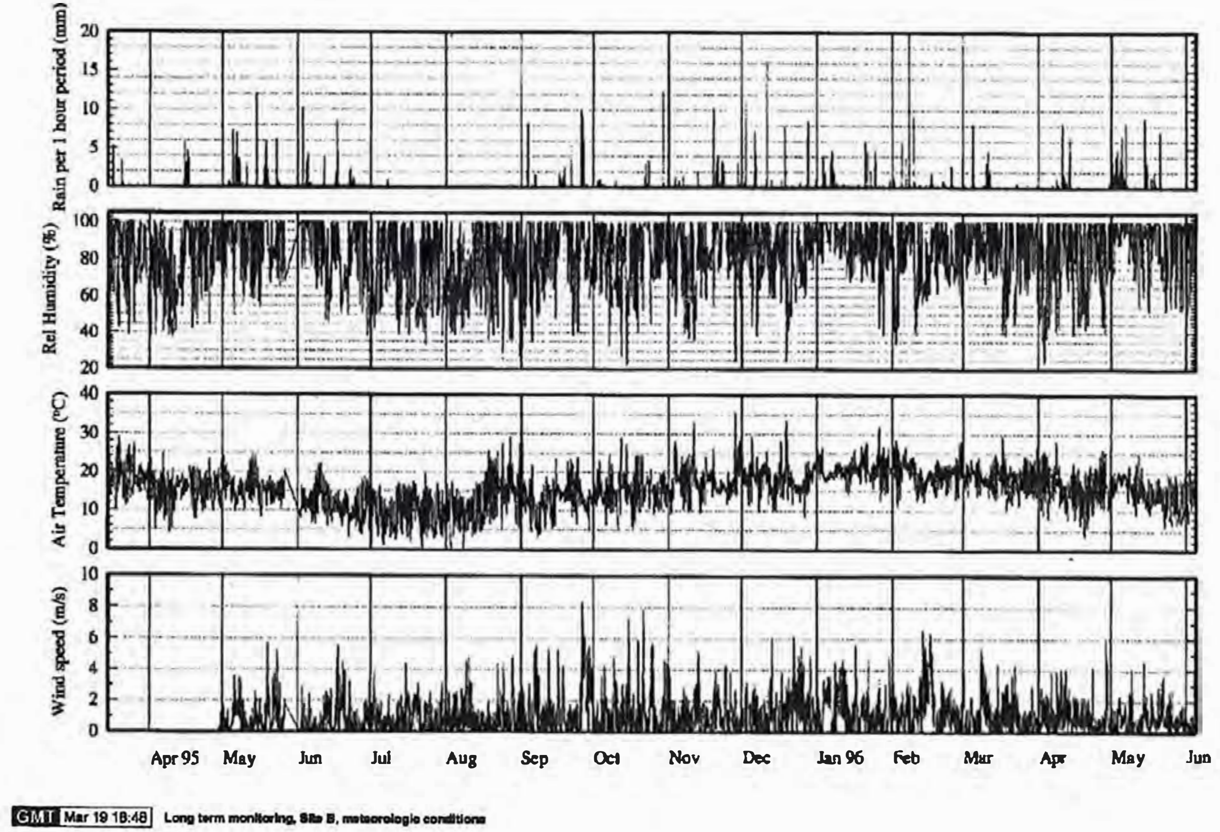

Figure 6.4. Surface Heat Fluxes at Site B, April 1995 to June 1996

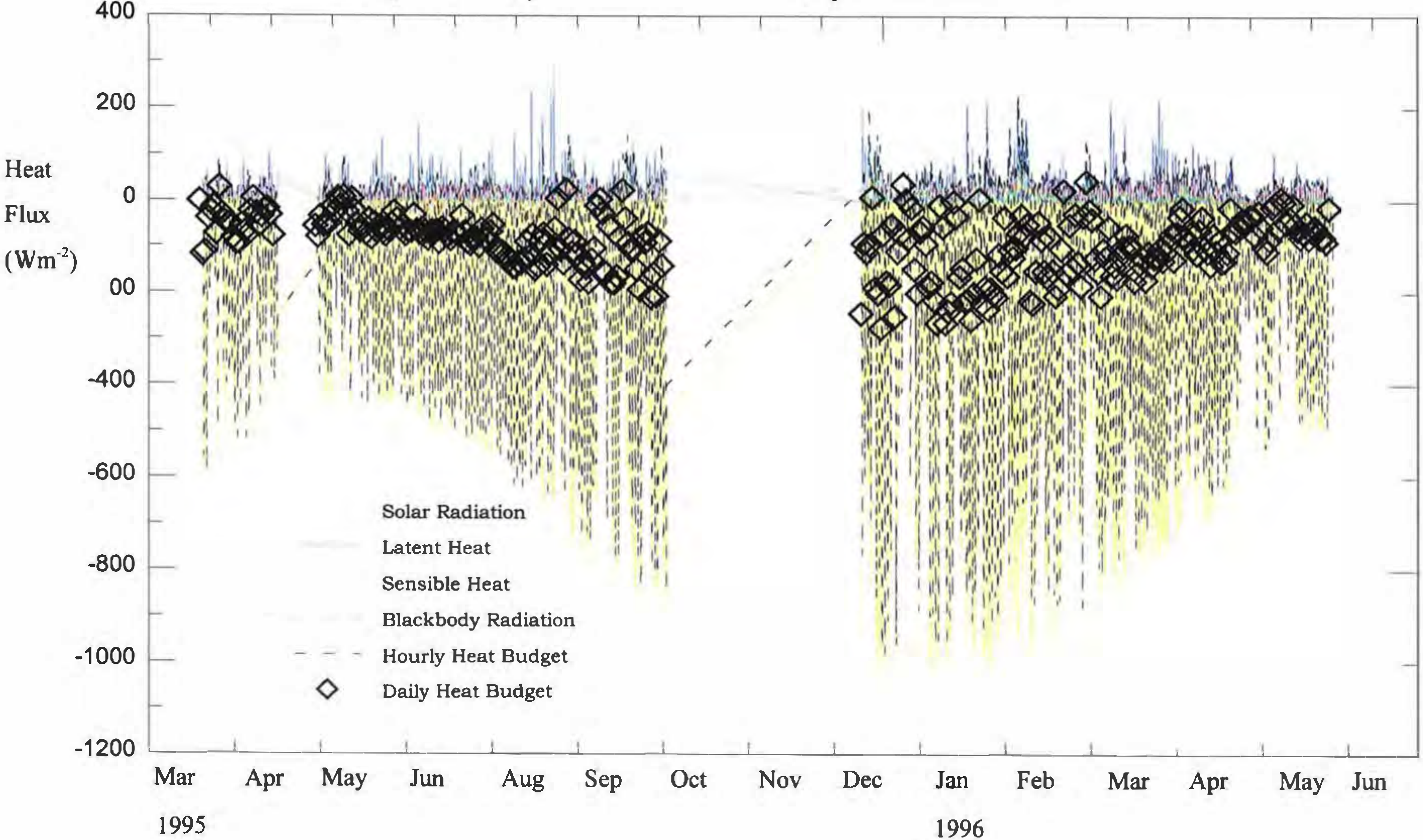

Solar radiation values were obtained by direct measurement from the meteorologic station. Gaps in the meteorologic and heat transfer time series are discussed in Appendix A.5.

Calculations for sensible heat and latent heat require values for water temperature and wind speed to be known. It would not have been valid to calculate these at the stations within the wetland as the wind speed at these stations was unknown due to the influence of the plant canopy. Calculations of sensible and latent heats were therefore only made for Station 3 in the lake, using the water temperature 100 mm below the water surface.

The daily average surface heat budget in Figure 6.4 shows that there is a nett influx of heat to the water column throughout the year of around 100 to 200 Wm^{-2}. This is higher than expected from other studies that have performed more detailed analysis of surface heat budgets such as those performed for Wellington Reservoir in Western Australia (Imberger and Patterson, 1990) and Lake Tahoe (Myrup et al, 1979).

In particular, Wellington Reservoir has an annual nett surface heat influx of approximately 80 Wm^{-2} and is subject to strong predominant winds (Imberger and Patterson, 1990), whereas winds at Manly Dam are generally only minor (Chapter 6). From these differences in prevailing winds between the two lakes, it would be expected that the annual average heat transfer entering the water surface at Manly Dam would be somewhat greater than at Lake Wellington.

For the wetland to be in a steady state over the long term, other heat fluxes must also be significant, such as stream inflows, rainfall, the transfer of heat from the warm, shallow waters of the wetland to the cooler deeper waters of the main lake and thermal conduction into the bed of the wetland. Taking these fluxes into account gives the heat balance of the wetland as:

$$0 = H_{SF} + H_B + H_R + H_I + H_O \qquad 6.52$$

Where all fluxes are assumed positive when heat is transferred out of the wetland, H_{SF} is the nett surface heat flux, which from above is of the order of -100 to -200 Wm^{-2}, H_B is the heat flux through the bed, H_R is the heat flux due to rainfall, H_I is the heat flux associated with surface water inflows, H_O is the heat flux associated with nett outflows to the lake. The nett change in the heat of the wetland due to these processes is assumed to be approximately zero over a full year.

Of these fluxes, Wetzel (1982) found that typically the heat flux through the bed is likely to be of the order of only 2 Wm^{-2} and is therefore expected to be only a very minor component of the total heat budget. Without any temperature data for the bed of the wetland, it is not possible to further examine this flux.

The heat fluxes due to inflows, outflows and precipitation can be estimated based on the rainfall, temperature data and catchment information. The heat flux due to rainfall will be:

$$H_R = \rho_W C_p i.\Delta T/t \qquad 6.1$$

where H_R is the heat flux due to rainfall (Wm^{-2}), ρ_W is the density of water, C_p is the heat capacity of water, i is the rainfall depth, ΔT is the difference between the temperature of the rain and that of the water in the wetland, averaged over the time interval of concern, and t is that time interval.

Manly Hydraulics Laboratory (1995, 1996) report that rainfall for the year April 1995 to March 1996 was 1048 mm for the Manly region so with t = 1 year and the other parameters taking their usual values, it can be seen that $H_R = 0.13\Delta T$. The temperature of the rainfall was not measured; however, it is extremely unlikely that ΔT would be outside the range of ±20°C, therefore H_R is likely to be within ±3 Wm^{-2}, and is expected to be only a very minor component of the total heat budget.

Due to their similar natures, it is convenient to consider the heat fluxes due to inflows and outflows together. Due to the small size of the wetland, the assumption was made that the inflow is approximately equal in magnitude to the outflow. Therefore, the nett heat flux due to inflows and outflows can be expressed as:

$$H_I + H_O = \rho C_p Q(T_O - T_I) \qquad 6.2$$

where Q is the average outflow (equal to the negative inflow), T_O is the average temperature of the outflow and T_I is the average temperature of the inflow. Each of these terms is considered separately below.

The outflow Q can be estimated as a fraction of the rainfall over the year, multiplied by the area of the catchment upstream of the wetland. From above, the annual rainfall for the wetland was 1048 mm. The catchment area was measured as approximately 580 000 m^2 from the Department of Land and Water Conservation 1:25 000 maps for Sydney Heads (9130-2-N) and Parramatta River (9130-3-N). From Chow et al (1989), as the catchment consists largely of heavy clays and impervious rock, the fraction of rainfall converted to runoff is expected to be 0.8. With these figures, the expected average runoff rate, and hence Q is expected to be 490 000 m^3/year or 0.015 m^3/s.

In Chapter 5, evidence was presented that inflows to the wetland occur as low temperature intrusions at the bed of the wetland. If this is the case then the inflow temperature can be approximated by the temperature near the bed of the wetland at Station 4. Figure 6.5b below shows that the near bed temperature at Station 4 is 16°C when averaged over the year from April 1995 to March 1996. By a similar argument, water leaving the wetland must pass by Station 3. From Figure 6.6, at Station 3, the wetland is generally well mixed at Station 3, therefore, the temperature of outflows from the wetland can be approximated by the depth averaged temperature at Station 3, which is 18°C.

Given the above values for outflow rate, temperatures of inflow and outflow and surface area of the wetland, $H_I + H_O$ is approximately 130 kW.

In summary then, the heat budget of the wetland is dominated by two heat fluxes: the nett surface heat flux of -100 to -200 Wm^{-2} and the nett heat outflow from the wetland of approximately 130 kW. A_W, the surface area of the wetland, was found by survey to be approximately 1 000 m^2, therefore the nett surface heat flux of the wetland is between -100 and -200 kW. These two estimates give a reasonable balance, when the uncertainties involved in their derivation are considered.

6.3.2. DIURNAL AND SEASONAL VARIATIONS IN WATER TEMPERATURES

Figures 6.5a and b show time series of the temperatures obtained at all thermistors arranged by depth. Figure 6.5b also shows the depths of water at Station 1.

From these figures, differences in temperature between Station 3 in the lake and Stations 1, 2 and 4 in the wetland dramatically reveal the effects of shading in the vegetated area. The extent of convective motion can also be seen from these figures.

NEAR SURFACE TEMPERATURE VARIATIONS

From Figures 6.5a and 6.5b, the water temperatures 50, 100 and 150 mm below the surface clearly show large diurnal fluctuations at all stations throughout the year of up to 10°C. These diurnal fluctuations were much higher at the open water Stations (2 and 3) than at the vegetated Stations (1 and 4).

Figure 6.5a. Temperatures Near the Top of the Water Column, April 1995 to June 1996 at Site B

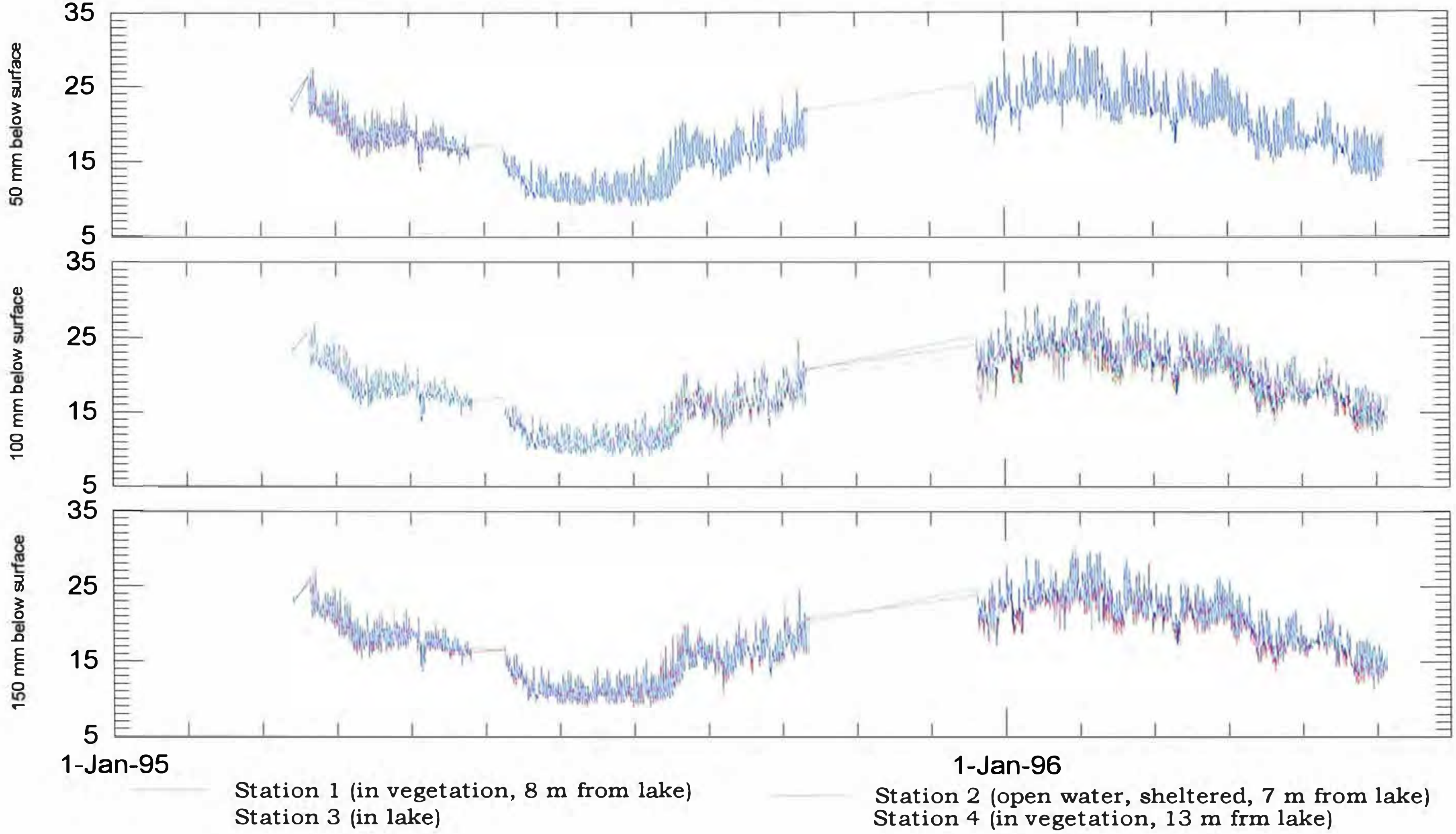

Figure 6.5b. Water Levels and Temperatures Near the Bed of the Water Column, April 1995 to June 1996 at Site B

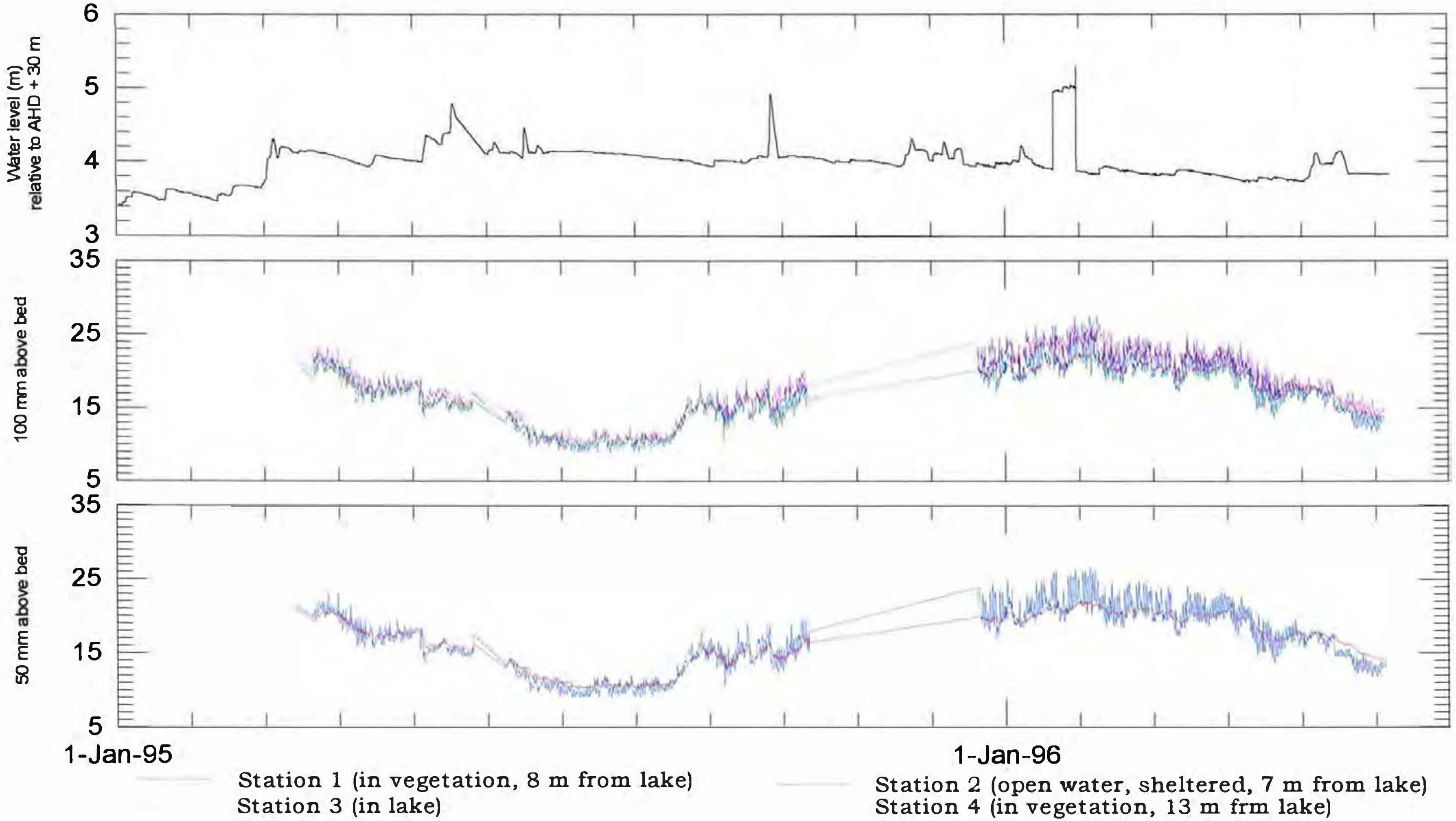

Lower diurnal at Stations 1 and 4 were expected, since from Chapter 3, the plant canopy was found to significantly reduce solar radiation fluxes and surface heat fluxes. The diurnal fluctuations can also be seen from Figures 6.5a and 6.5b to have been especially high through summer at all stations. Again this is a result that was expected, due to the larger diurnal fluctuations in the surface heat budgets through summer shown on Figure 6.4.

The higher fluctuations in temperature observed near the water surface at the open water stations (2 and 3) led to much higher peaks in water temperatures there than occurred at the vegetated stations (1 and 4).

Minima in water temperatures were very similar at all stations. This was to be expected as the buoyancy driven convection between the lake and the wetland would have acted to reduce any temperature differences between these areas.

NEAR BED TEMPERATURE VARIATIONS

Diurnal variations in water temperature near the bed were not as large as at the water surface. This can be seen by comparing the time series for the probes 50 and 100 mm above the bed with the probes 50, 100 and 150 mm below the surface in Figures 6.5a and 6.5b.

Figures 6.5a and 6.5b show that through the summer, water temperatures 50 and 100 mm above the bed in the open water stations (2 and 3) were consistently higher than those at the vegetated stations (1 and 4). This was the case despite the diurnal variations in temperature that occur at all stations. Again, this was to be expected because of the shading influence of the plant canopy, provided that this effect is more important than wind sheltering, which is probably true considering the low winds at the site.

In winter, diurnal variations in water temperatures 100 mm above the bed at all stations follow similar trends to those near the water surface, examined above. However, the water temperature 100 mm above the bed at Station 3 is clearly higher than at the other stations as shown on Figure 6.5b. This is especially significant when it is considered that the probe at Station 3 is much lower in the water column than the probes at the other locations, due to the greater depth of water at Station 3.

In winter, water temperatures 50 mm above the bed at Stations 1 (vegetated) and 2 (open water) show a marked difference in behaviour from the cases examined above. Throughout the year near the water surface and 100 mm above the bed, water temperatures are generally higher in the open water stations (2 and 3) than in the vegetated stations (1 and 4), which implies that the depth averaged temperatures at Stations 2 and 3 (open water) are higher than those at Stations 1 and 4. However the water temperatures 50 mm above the bed plotted on Figure 6.5b are consistently higher at Station 1 (vegetated) than at Station 2 (open water). In fact from Figure 6.5b, it can be seen that through May 1996 the temperature 50 mm above the bed at Station 1 remained nearly one degree above the temperature at Station 2 continuously for over half the month. These results are surprising, as it was expected that plant canopy shading would cause the water temperatures to be lower at Station 1 (vegetated) than at Station 2 (unvegetated).

It may be argued that latent heat is a possible mechanism by which the thermistor at Station 2 (open water) near the bed shows a lower temperature than the thermistor at Station 1 (vegetated). However, latent heat will cause penetrative convection, destratifying the whole water column and causing the temperature over the whole depth to decrease. Consequently, if latent heat loss were causing temperatures near the bed at Station 2 to be lower than at Station 1, it would also be expected that the depth averaged temperature would be lower at Station 2 than at Station 1.

As discussed below, Figure 6.8 shows that this scenario does not occur, rather, the depth averaged temperature is generally higher at Stations 2 (open water) than at

Station 1 (vegetated); therefore, latent heat is not a potential source of the observed temperature differences between the thermistors near the bed at Stations 1 and 2.

Potential causes for the temperature differences between Stations 1 and 2 are examined in the following section.

VERTICAL TEMPERATURE STRATIFICATION

The extent of vertical temperature stratification can be seen by examining Figures 6.6 and 6.7. These figures show the degree of stratification observed:

- near the water surface (from 50 mm below the water surface to 100 mm below the surface and from 100 mm below the water surface to 150 mm below the water surface);
- through the water column (from 100 mm below the water surface to 100 mm above the bed); and
- near the bed of the wetland (from 100 mm above the bed to 50 mm above the bed).

Each of these cases are discussed seperately below.

Near the water surface, Figures 6.6 shows that significant positive vertical temperature differences of up to 3°C can develop in both open water and vegetated areas. Figure 6.7 shows that the temperature gradients corresponding to these temperature differences can reach up to 60°Cm^{-1}, although they generally do not exceed 20°Cm^{-1}. These surface stratifications are always diurnal, reflecting the diurnal cycles of solar heating by day and atmospheric cooling by night.

Through the water column, from near the surface to near the bed of the wetland, Figure 6.6 shows that temperature differences of up to 10°C can occur. Figure 6.7 shows that the temperature gradients are much smaller than near the water surface, never exceeding 20°Cm^{-1}, and generally being less than 10°Cm^{-1} (the distance between the probes is much greater than for the probes near the water surface). Significant features that can be seen from Figures 6.6 and 6.7 are summarised below.

- By contrast with the stratifications near the surface, stratification through the water column quite often lasts significantly longer than the diurnal cycle. This is expecially so through the summer months from late September to March. The longest lived of these stratifications occur at Station 4, where through January the stratification is maintained for over half the month.
- The highest stratifications develop at Station 4, then stations 1 and 2, while the lowest stratifications occur at Station 3.
- Negative stratifications occur on occasion at Station 4, especially through the winter months from April to August, but occasionally through summer as well. These stratifications were observed to last through the diurnal cycle, especially from April to June. Neither the length of time for which negative stratifications occurred, nor the magnitude of these stratifications were as large as for the positive stratifications; however the frequency with which they occurred was similar.

Inspection of Figure 6.6 shows that for Station 1 the temperature 50 mm above the bed was often higher than at 100 mm above the bed for intervals much longer than a day, especially through winter. The times at which these temperature inversions occurred near the bed at Station 1 corresponded well to the times at which temperature inversions occurred from near the surface to near the bed at Station 4.

Note that similar temperature inversions were observed in the temperature profiles taken during the intensive field investigations (see Chapter 5).

Figure 6.6. Vertical Temperature Differences April 1995 to June 1996 at Site B

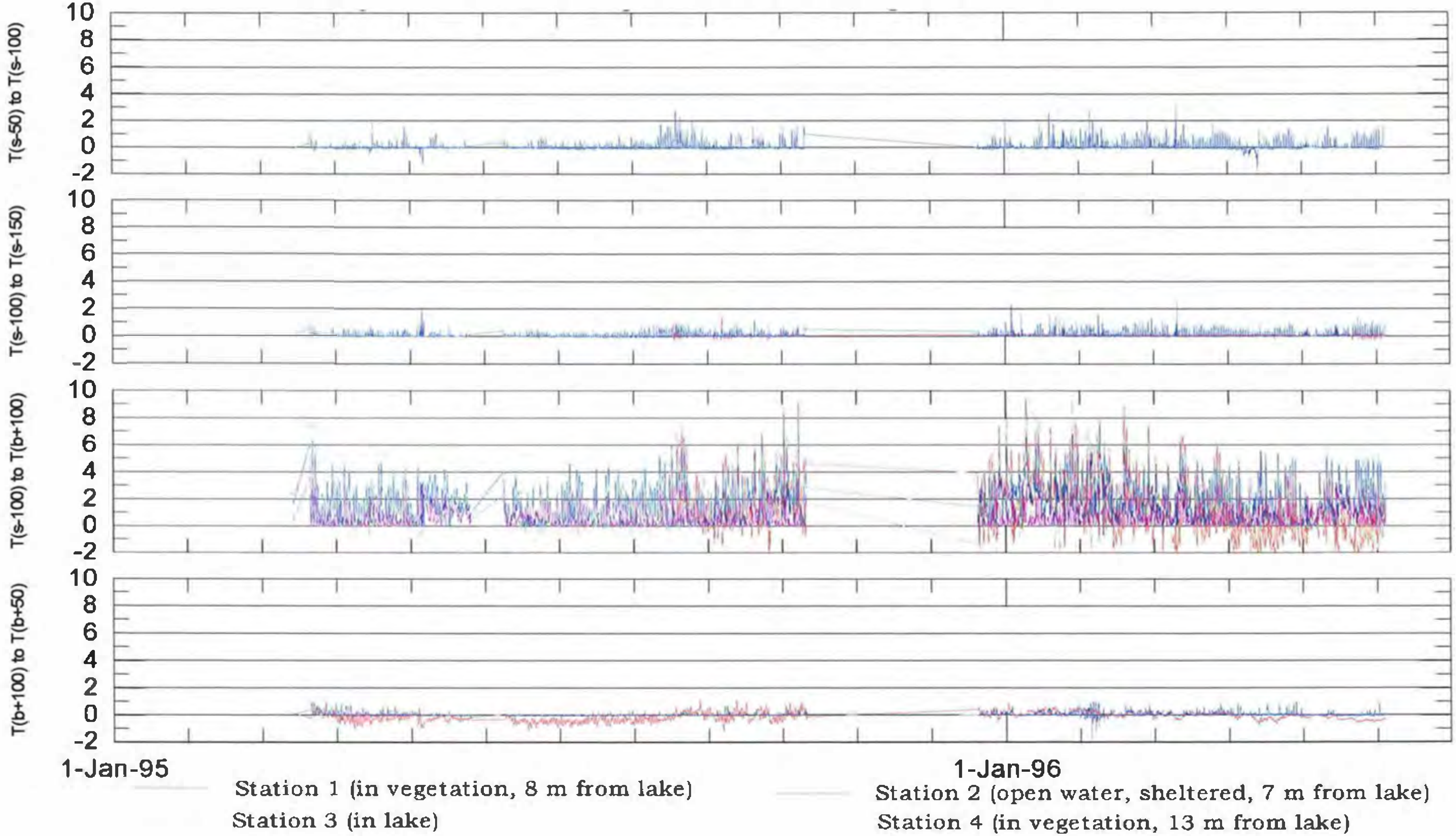

Figure 6.7. Vertical Temperature Gradients, April 1995 to June 1996 at Site B

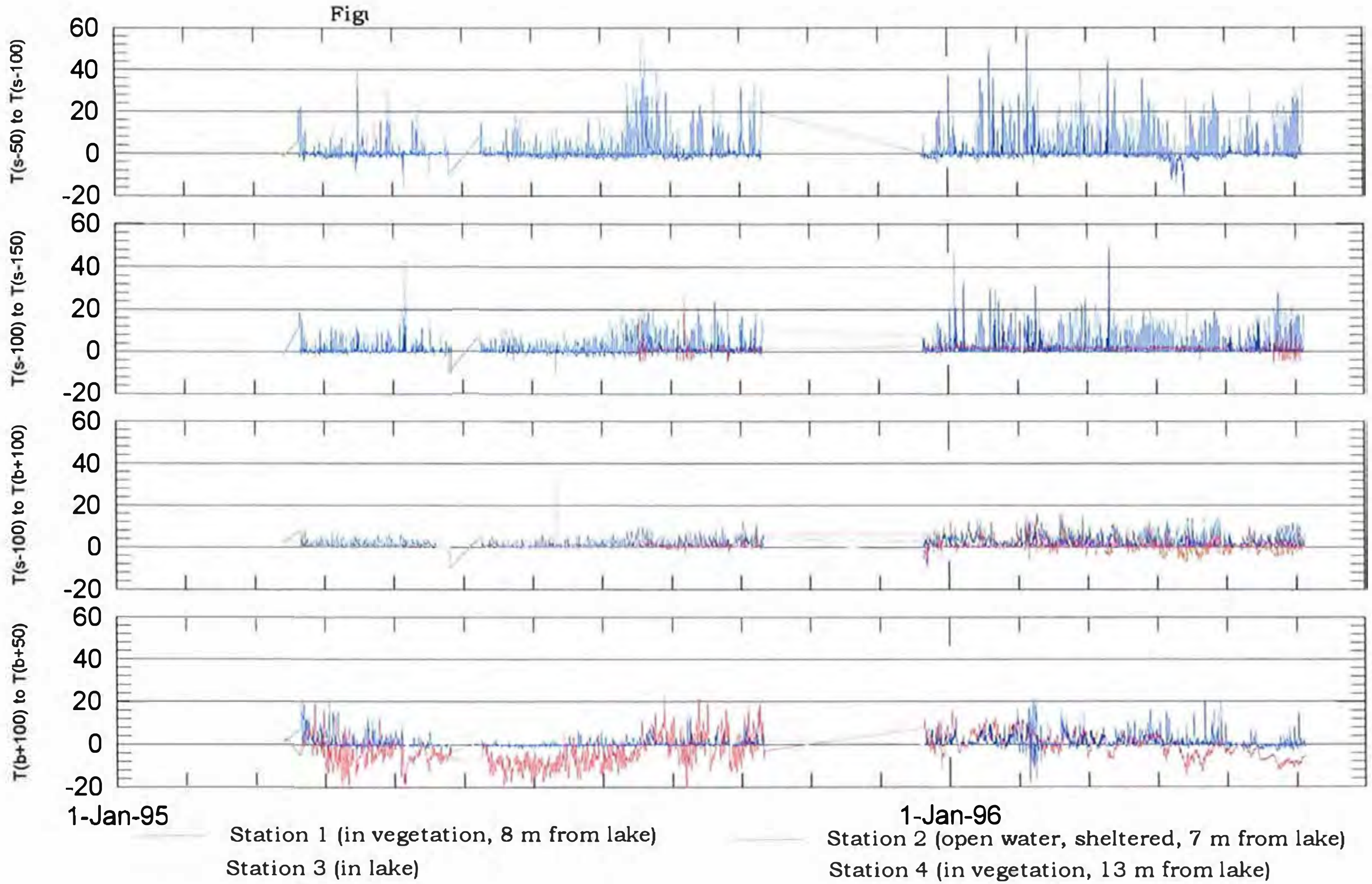

From Turner (1973), temperature inversions such as these will be stable when the Raleigh Number, $R_a < 657$, that is for:

$$R_a = \frac{g\alpha \Delta T d^3}{\kappa \nu} < 657 \qquad 6.3$$

Where: g is acceleration due to gravity (9.8 ms^{-2});

α is the expansivity of water (2×10^{-4} $°C^{-1}$);

ΔT is the change in temperature observed, here ~ 1°C;

d is the depth over which the change in temperature occurs, here ~0.004 m;

κ is the thermal diffusivity of water ($1.42\times10^{-5} m^2s^{-1}$); and

ν is the kinematic viscosity of water ($1\times10^{-6} m^2s^{-1}$).

Using the values given above for these variables gives $R_a = 2\times10^6 >> 657$, indicating that the temperature differences observed are too large to be stable against convection. The occurrence of such a temperature inversion would therefore require the presence of an additional stratifying mechanism, such as salinity or the presence of particulates, to keep the inversion stable.

Wetzel (1983) notes that stable layers with elevated temperatures near lake beds are common, generally being formed in the following manner:

- inflows of saline groundwater and the liberation of salts and dissolved organic compounds from the bed often cause a discrete dense layer of water to be formed at the bed.
- the density of this layer largely prevents mixing with the less dense water overlying the layer, so if the layer is exposed to a source of heat, an inverse temperature gradient forms.

It is also possible that water flowing into the wetland from the upstream creek could contain significant levels of salts or colloids. Such salts and colloids could come from the upstream catchment, or may result from the decay of vegetation on or just above the bed of the wetland.

Radiative heating is a possible heat source for this high density layer immediately above the bed; however the layer may already have an elevated temperature if it results from the inflow of saline groundwater with high temperature (Wetzel, 1983).

From the above it appears that in the vegetated zone, there is a layer of water within which a significant temperature inversion exists, and where mixing is restricted. The layer is over 100 mm thick at Station 4 (the station furthest from the lake), is between 50 and 100 mm at Station 1, but is not observed at all at stations 2 or 3. The most likely explanation for the difference in the depth of this layer is that mixing was less energetic at Station 4 and therefore the layer would be more likely to stay intact here.

The presence of this temperature inversion may also explain why the temperature at Station 1 was higher than at Station 2, as commented on in the previous section.

The presence of such a density stratification would provide additional buoyancy driving to the convection between the wetland and the lake.

DEPTH AVERAGED TEMPERATURES

Figure 6.8 shows the depth averaged temperature at each station. These were calculated by averaging over all available temperature data from the different depths at each station. Two periods of data can be seen where conditions stay quite consistent over many weeks. These occur in summer, (December to March), and winter, (late June to August). Autumn (April to early June), and Spring (mid August to December) appear to be transitional periods.

It is quite clear from Figure 6.8 that seasonal variations in depth averaged temperature are larger than diurnal ones. The depth averaged temperature at each station responds to seasonal conditions quite similarly across all stations.

On a diurnal scale, depth averaged temperature variations are much higher at Station 2 than the other stations. This is surprising as it was thought that Station 3 would be subject to higher diurnal temperature fluctuations than the other stations due to its exposed location. Evidently, as the depth of water is smaller at Station 2 than at Station 3, it is more sensitive to the daily fluctuations in heat fluxes, despite the fact that the surface heat fluxes here were expected to be lower.

LATERAL, DEPTH AVERAGED TEMPERATURE DIFFERENCES

Figure 6.9 shows time series of the lateral differences in depth averaged water temperatures from Station 3 (in the lake) to Station 1 (vegetated 8 m from the lake), Station 2 (open water, protected, 7 m from the lake) and Station 4 (vegetated 13 m from the lake). These lateral temperature differences are of great significance, since as shown in Chapter 5, they can cause convection between the open water and vegetated zones.

Throughout the summer (December to February), Figure 6.9 reveals the following points.

- Depth averaged temperatures at Stations 1, 2 and 4 in the wetland were generally colder than at Station 3 in the lake typically by 1 to 4°C.
- Lateral depth averaged temperature differences to Station 3 were highest in magnitude at Station 4 (vegetated 13 m from lake), reaching -5°C, then at Station 1 (vegetated, 8 m from lake), then Station 2 (open water, 7 m from lake).
- Water in the lake (Station 3) rarely became colder than water in the vegetation (Station 1 and 4).
- Periods of many weeks at a time could pass where the water in the vegetation (Stations 1 and 4) remained continuously colder than the water in the lake (Station 3).

Figure 6.8. Depth Averaged Temperature, April 1995 To June 1996 At Site B

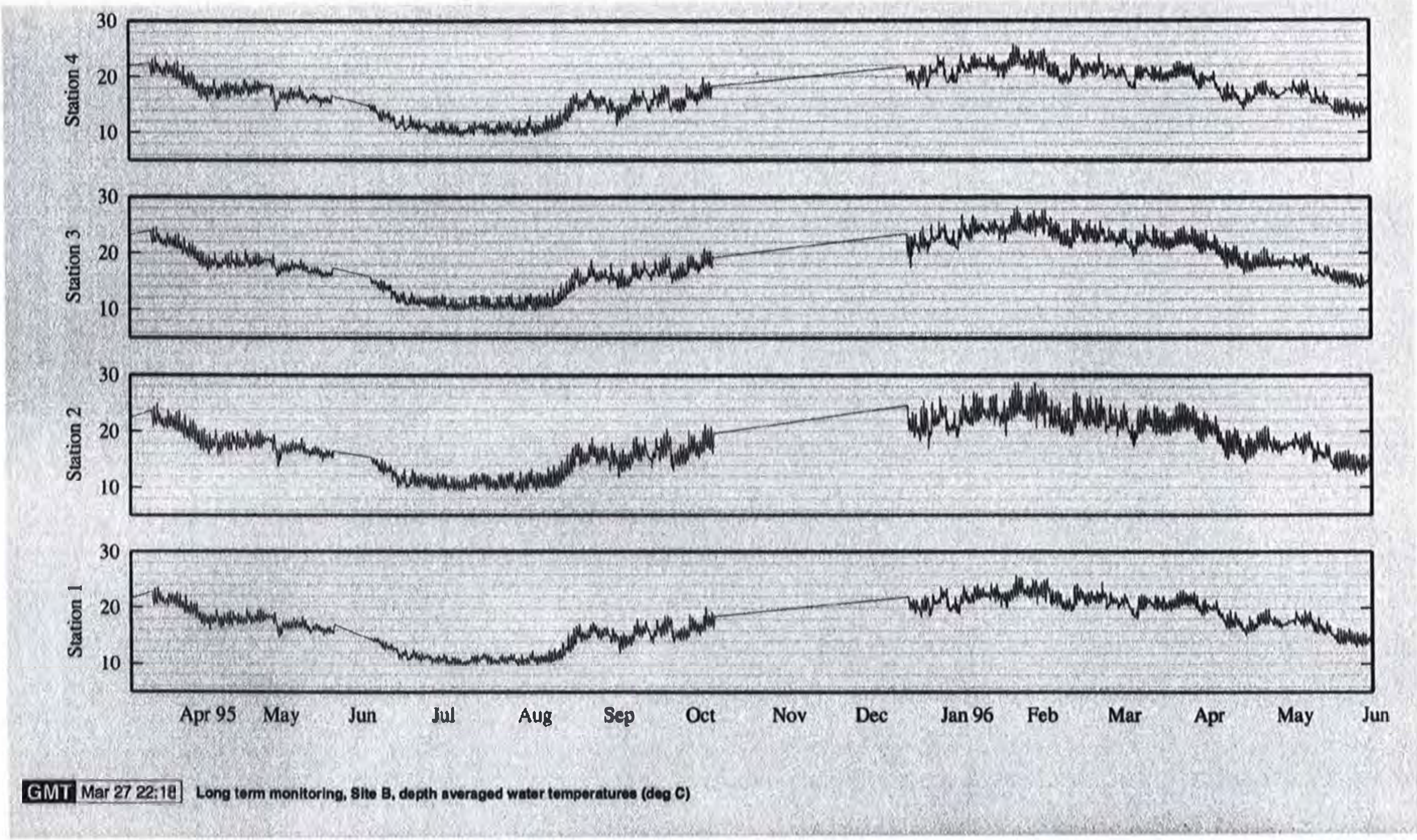

Figure 6.9. Lateral Depth Averaged Temperature Differences

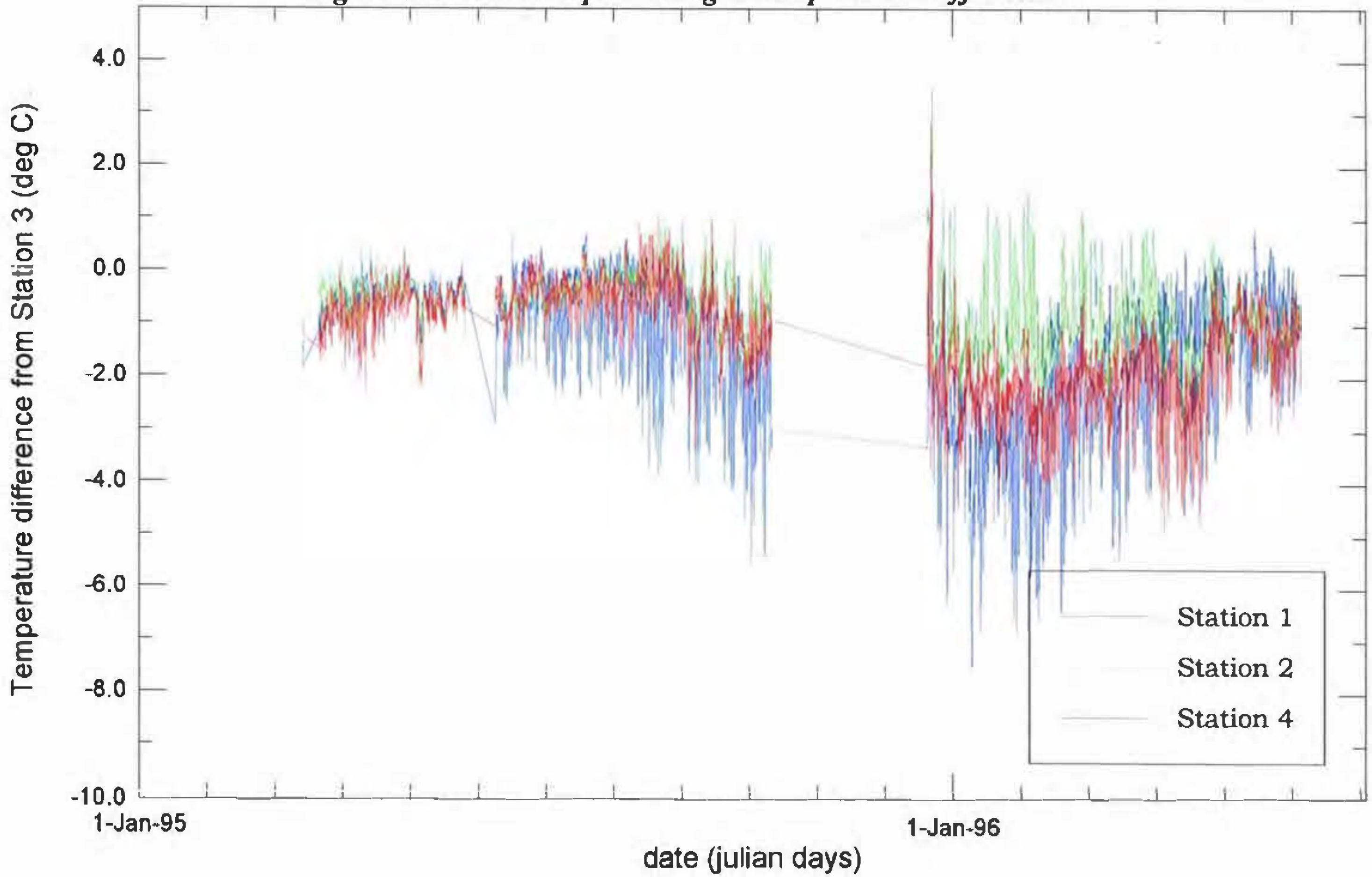

- Diurnal fluctuations in lateral temperature differences with Station 3 were highest at Station 2 (open water, 7 m from the lake) reaching up to 5°C here, then Station 4 (vegetated 13 m from the lake), reaching up to 4°C, then Station 1 (vegetated 8 m from the lake).
- It was not unusual for the lake water (Station 3) to become colder than the water at Station 2 (open water, protected).
- As the water at Stations 1, 2 and 4 was generally significantly colder than at Station 3, strong convection is to be expected, whereby warm lake water would flow in over the top of the cooler water in the wetland, which will flow out into the lake along the bed.
- These convections will be maintained throughout the night and into the next day over periods of weeks to months at a time.

During winter (June to August) Figure 6.9 reveals the following points.

- Depth averaged temperatures at Stations 1, 2 and 4 were generally lower than at Station 3, typically by 0.2 to 0.5°C. This is a marked contrast with the strong temperature differences of between 1 and 5°C reported above for the summer conditions.
- As for the summer conditions, lateral depth averaged temperature differences to Station 3 were highest in magnitude at Station 4, reaching, then at Station 1, then Station 2.
- Water in the lake (Station 3) was often colder than water at Stations 1, 2 and 4. This provides a contrast with the summer conditions where the water in the lake rarely became colder than the water in the vegetated areas (Stations 1 and 4), but is in agreement with the finding for summer that the lake water is often colder than the water in the open water protected area (Station 2).
- By contrast with the summer conditions the water in the vegetation (Stations 1 and 4) did not remain continuously colder than the water in the lake (Station 3) for periods of more than about one week.
- Unlike the summer conditions, diurnal fluctuations in depth averaged lateral temperature differences with Station 3 were much the same at Stations 1, 2 and 4

and were much smaller than the summer conditions, typically being only 1 to 1.5°C.

- By contrast with the summer conditions, convection between the lake water (Station 3) and the other stations is expected to be weak because large depth averaged water temperature differences between these areas were not present.
- When these weak convections do occur, they will follow a diurnal cycle, whereby during the day, the water temperature in the lake will become greater than the water temperature in wetland. The warm lake water will then flow in over the top of the cooler water in the wetland, which will flow out into the lake along the bed. By night, as the lake cools to a lower temperature than the wetland, this convection will be stopped and possibly reversed. The cooler lake water will then flow in underneath the warmer water in the wetland, which will flow out into the lake at the surface.

6.3.4. DIMENSIONLESS ANALYSIS AND BUOYANCY DRIVEN CONVECTIONS

To augment the long term analysis, velocity estimates for buoyancy driven convection were calculated according to the equations given in Chapter 5. Discussion and the results of these calculations are presented below.

BUOYANCY DRIVEN VELOCITIES

Figure 6.10 shows estimates for the daily maximum, average and minimum velocities that would arise due to the temperature differences between the lake and the wetland, based on the temperature data obtained from Stations 1 and 3, estimated using Equation 5.50.

Figure 6.11 shows estimates for the daily average velocities between the lake and the wetland based on the temperature differences between Stations 1 and 3, and between Stations 3 and 4.

A much greater degree of variability in convection can be seen in winter than summer and at times the convective velocity becomes negative. When the convective velocity is negative, the buoyancy forcing is in the reverse direction from that generally expected; that is, the water in the wetland is warmer than that in the lake. Warm water will therefore flow out of the wetland into the lake as a surface flow, while the cooler lake water will flow into the wetland at the bed. This would most likely occur under conditions where rapid surface cooling occurs, causing the lake to lose heat at a faster rate than in the more sheltered wetland.

These reversals only occur sporadically and the magnitudes of the velocities under these conditions show that reversed flows are generally weaker than those in the forward direction.

RICHARDSON NUMBERS

Figure 6.12 shows the Richardson Number as a time series throughout the long term studies. Richardson Numbers were calculated using the Equations given in Chapter 5. From Figure 6.12, it can be seen that the Richardson Number is generally greater than 0.4, so that the wetland is expected to be stably stratified for most of the year. Unstable conditions only apply fleetingly, whereas stable conditions persist for long periods of time, for example from mid January to mid February.

6.4. SUMMARY

The most significant finding of the long term field experiments in the wetlands at Manly Dam is that solar radiation fluxes in summer are sufficiently large to ensure that convective motions between the lake and the wetland are sustained through the whole day and night. These motions consist of warm lake water flowing into the wetland over the top of cool water from the wetland which flows into the lake.

Figure 6.10. Estimated Buoyancy Driven Velocities, April 1995 to June 1996 at Site B

Station 1: Maximum, Average and Minimum Daily Values

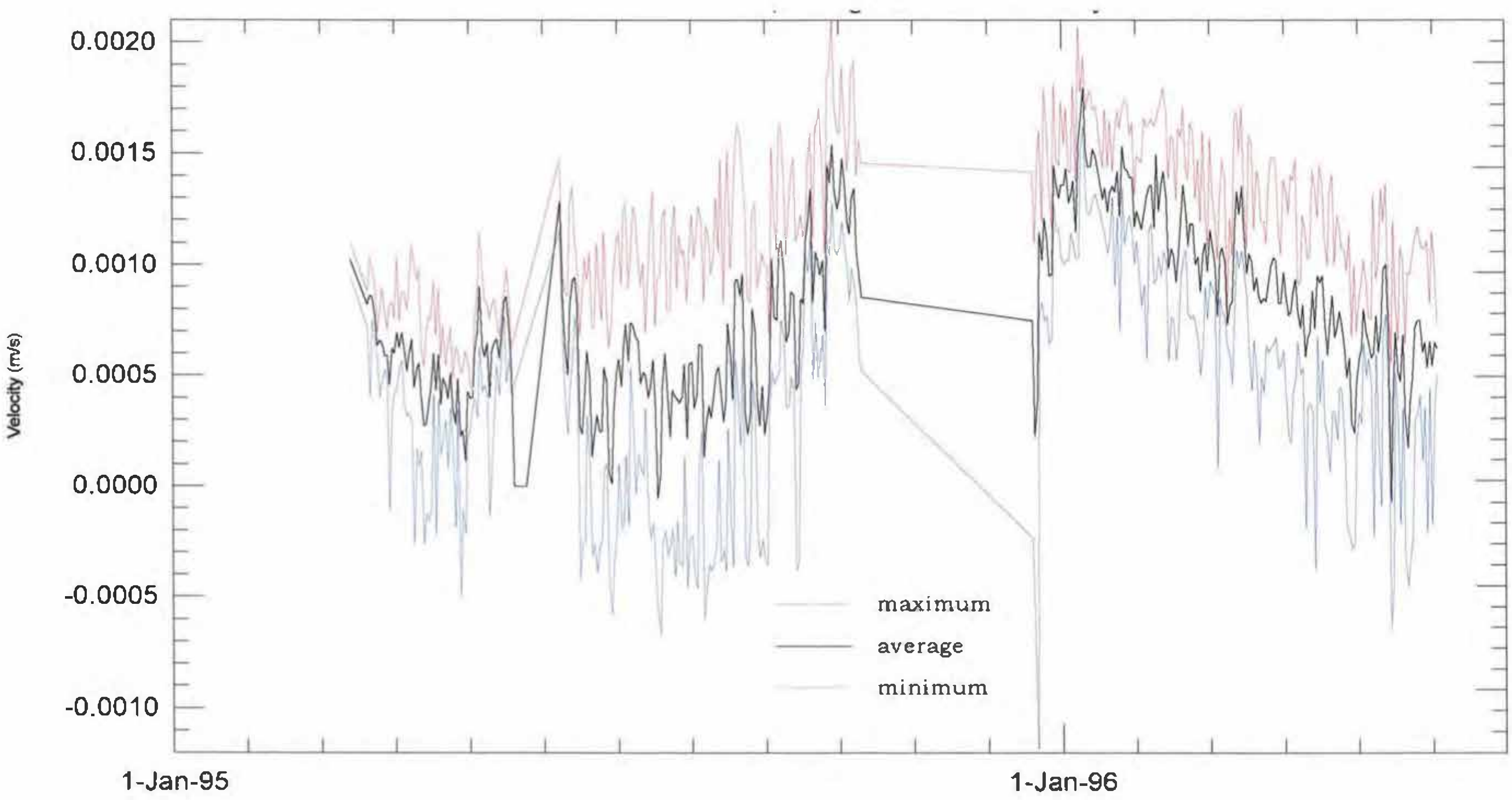

Figure 6.11. Estimated Buoyancy Driven Velocities, April 1995 to June 1996 at Site B
Stations 1 and 4: Average Daily Values

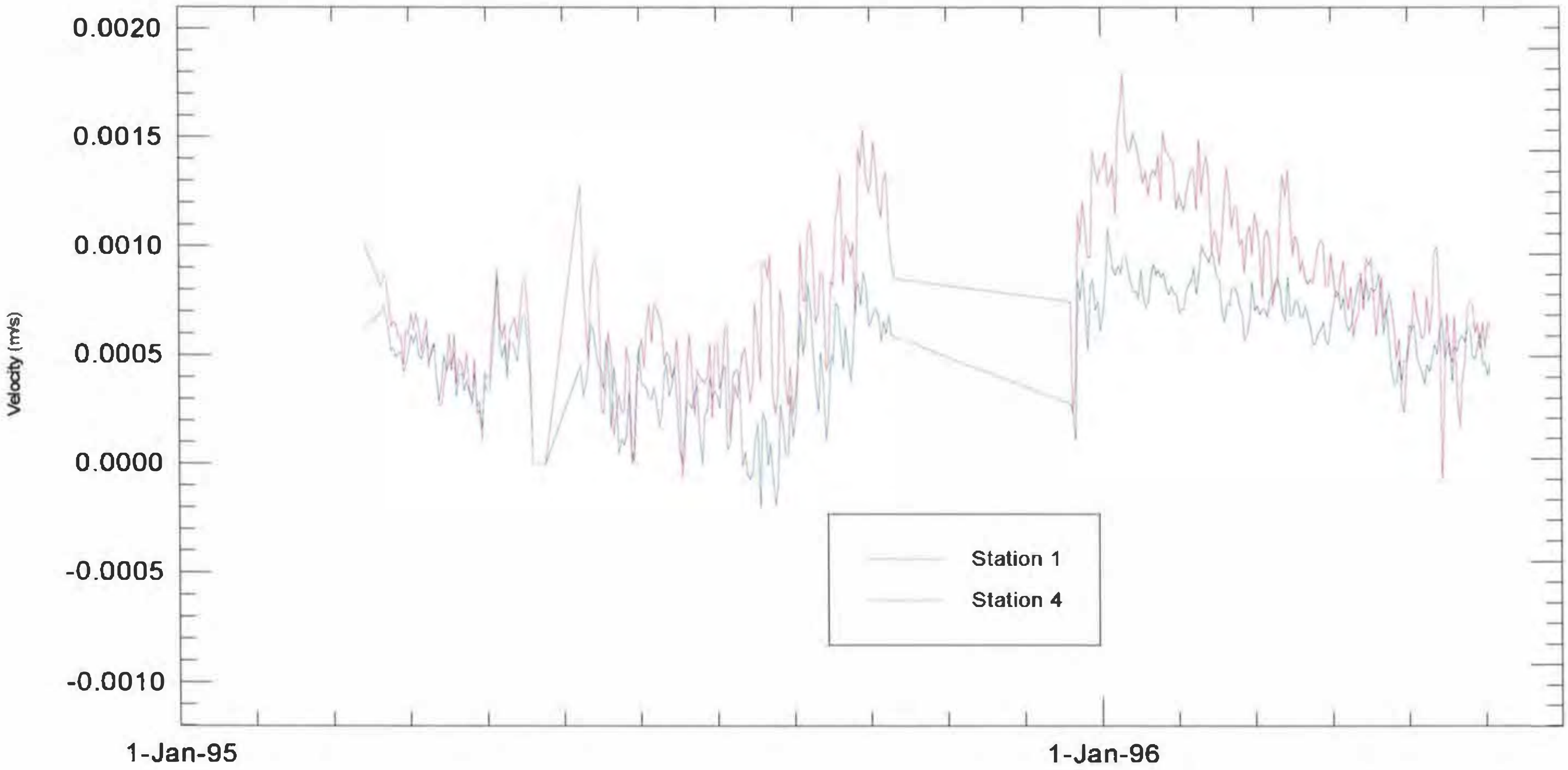

Figure 6.12. Richardson Number Time Series, April 1995 To June 1996 At Site B

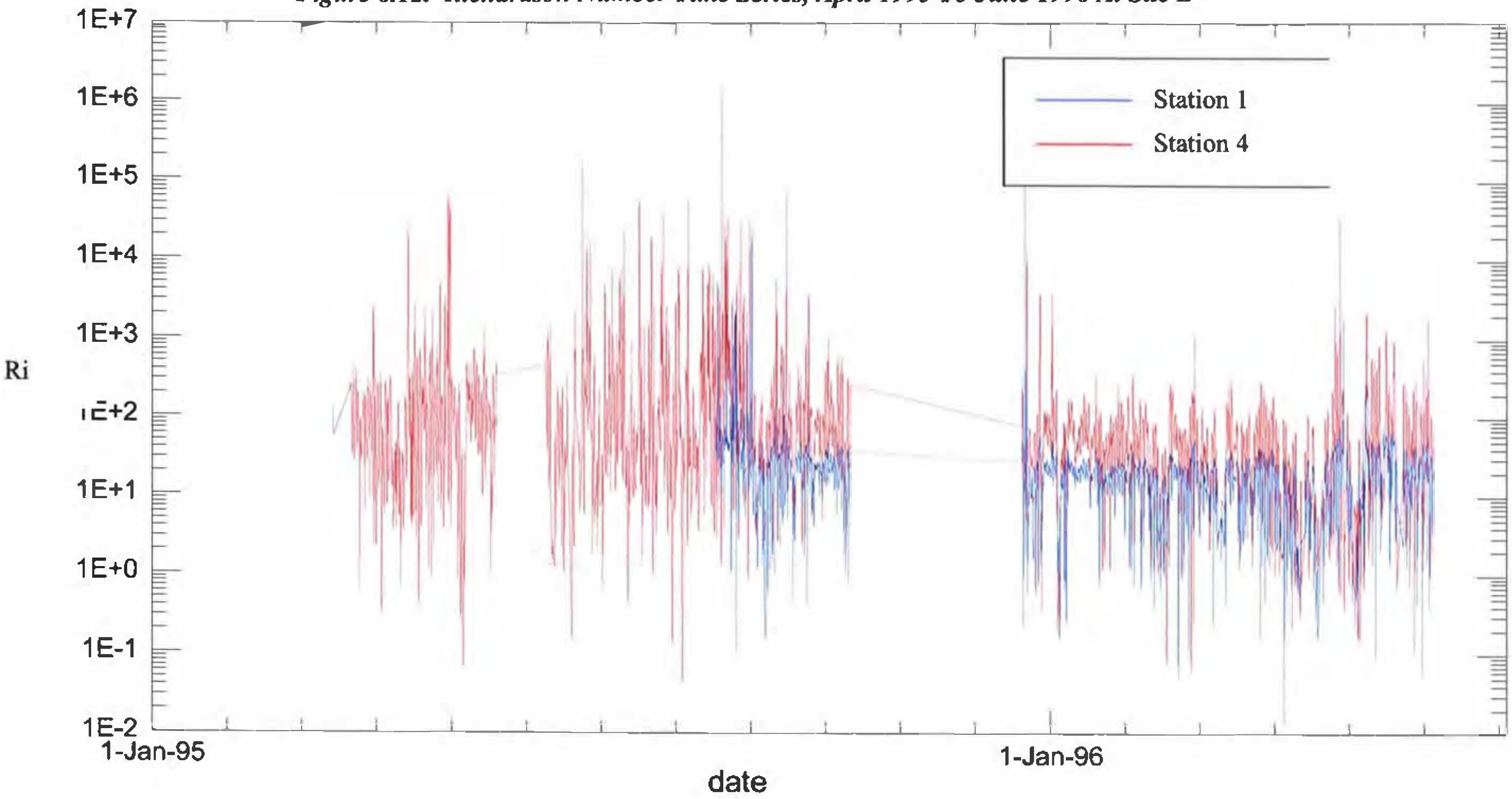

In winter, radiation fluxes through the day are large enough to establish convective motions by day in the same manner as the sustained convections that occur through summer. However, the radiation fluxes in winter are not sufficiently large to maintain these convective motions through the night, and in fact a reversal in convection will occur by night, whereby the lake water becomes cooler than the water in the wetland, thus the warmer water of the wetland flows out into the lake over the cooler lake water which flows into the wetland.

Other findings of significance are as follows.

- Large positive temperature stratifications occur throughout the year in both open water and vegetated areas. These were observed in both wetlands studied, even in winter. Positive stratifications were generally observed to be diurnal in winter at all stations and in summer at the open water stations. In summer in the vegetated areas, positive stratifications often persisted for many days at a time.
- The bed of the wetland was observed to act as a significant heat source in vegetated areas. Inverse temperature gradients developed near the bed, most likely due to heating at the bed. These inverse gradients can be sustained for many days, indicating that mixing in these areas is restricted. These density stratifications possibly arise due to dissolved salts or colloidal materials suspended in the lower part of the water column. The depth of this layer was found to increase with distance from the lake, probably because the amount of mixing reduces with distance from the lake.

7. IMPLICATIONS OF HYDRODYNAMICS ON WETLAND ECOLOGY

7. IMPLICATIONS OF HYDRODYNAMICS ON WETLAND ECOLOGY

This chapter contains a discussion of the expected effects of the hydrodynamic processes of Chapters 3 to 6 on wetland ecology. These effects will have particular implications for the design of constructed wetlands, but also more generally for the management and maintenance of any water bodies containing aquatic plants.

To demonstrate the ways in which wetland hydrodynamics will affect other issues in wetlands, in this chapter the implications of the processes of stratification, mixing and convection for water quality are discussed. Where appropriate, the implications of the field results on water quality are discussed with consideration given to previous studies performed in wetlands or similar environments demonstrating the importance of these processes on water quality and ecology.

Following the discussion on the implications of processes, a classification scheme has been developed in an attempt to allow the effects of hydrodynamic processes on wetlands ecology to be more easily understood.

7.1. IMPLICATIONS OF STRATIFICATION

From Chapters 3 and 6, two important features of stratification in emergent macrophyte wetlands can be seen.

- Differences in temperature of the order of 1°C from the top to the bottom of a 0.5 m deep wetland can occur quite commonly. These temperature differences are generally higher in vegetated than unvegetated zones.
- The combined actions of radiative heating, convection between open water and vegetated zones and surface driven mixing processes cause stratification to build up and decays on daily or shorter time scales.

These two features have important consequences for chemical and biological processes. Stratification of the water column may lead to the formation of anaerobic conditions at the bed of the wetland, while when the water is unstratified, aerobic conditions should persist throughout.

The formation of oxygen deficient zones at the bed of shallow lakes containing macrophyte vegetation is a well established phenomenon (Wetzel, 1983),. Here diurnal cycles of plant photosynthesis and respiration, combined with microbial decay processes commonly cause changes in DO concentration of 4 to 6 mg/L. Diurnal patterns of temperature stratification and destratification and consequent effects on the transport of DO in the vertical may therefore have serious consequences on biological activity at the bed of the wetland.

Temperature differences arising from stratifications may have a minor impact on the metabolic rate of organisms within the water column and on kinetics of water chemistry processes. More importantly, these temperature differences will markedly affect the rate at which mixing in the vertical direction within the water column can occur. This is an important consideration when it is noted that the microbial activities responsible for wastewater treatment processes within a wetland display large degrees of variation across the wetland, with microbial activity being highest at the bed of the wetland (Hatano *et al*, 1992).

The presence of stratification may restrict the rate at which chemical constituents are made available to the sites of microbial activity, especially dissolved oxygen, which is discussed in more detail in the next section.

Behaviour under stratified conditions is expected to significantly affect the oxygen and phosphorus cycles in the wetland. An oxygen demand will exist at the bed of the wetland due to the presence of humus; however, under stratified conditions, the oxygen demand may exceed the rate at which it can be supplied due to the much lower rates of mixing, so anaerobic conditions would be expected to develop at the base of the wetland. This in turn may allow the release of phosphorus from bed sediments (Mulhern and Steele, 1988).

As the time scales of stratification and destratification cycles are of the order of one day or less, the persistence of anaerobic conditions will only be shortlived, so that stratification is not expected to have consequences as serious as in lakes, where stratifications may persist for many months at a time.

7.2. IMPLICATIONS OF MIXING PROCESSES

In Chapter 4 it was shown that meteorological factors cause significant mixing processes to occur in the water column of the wetland. One of the primary effects of mixing processes is to provide a flux of dissolved oxygen (DO) into the water column from the surface. As a general rule, the presence of dissolved oxygen is desirable within a water body to maintain aerobic conditions allowing fish and other macro and micro organisms to survive. Anaerobic conditions are generally undesirable; however, cycles of aerobic and anaerobic conditions may cause cycling of nutrients, especially Nitrogen (Metcalf and Eddy, 1976).

Note however, that in reality the situation is far more complicated than has been presented above. Even with a flux of DO through the water column, organisms may not receive sufficient oxygen for other reasons such as fine scale mixing processes or organism physiology (Webster, 1997). An adequate supply of light, carbon and other nutrients may also place limits on organisms (Wetzel, 1982).

Attached microbial growth populations show large variations throughout an individual wetland, especially in the vertical (Hatano, Frederick & Moore, 1992). As such, the efficiency of the overall treatment process will depend on mixing in the water column of the wetland. Mixing in the vertical will be especially important to examine the extent to which incoming pollutants, initially in the water column, may be brought into contact with the soil, where microbial activity is highest.

It was shown in Chapter 4 that the presence of open water areas give rise to mixing in both the open water itself, by direct mixing, and in nearby vegetated areas by the generation of wind waves and their subsequent transport into the vegetated areas, where they break, thereby causing mixing. Furthermore, it was shown in Chapter 4 that penetrative convection arises in open water to a much greater degree than in vegetated areas, providing another mechanism for mixing, enhancing DO transfer into the water column.

It is apparent then that to encourage aerobic conditions within the wetland, it is important that large areas of open water be present and that large, thick stands of vegetation should be avoided to prevent these areas becoming stagnant.

7.3. IMPLICATIONS OF CONVECTIVE PROCESSES

The main impact of convective processes in wetlands is expected to be through the enhanced transport of nutrients through the vegetated zone which can have drastic effects on the ecology of a wetland. In addition to the transport of nutrients, convective processes can also play an important role in the distribution of organisms within a water body. These processes are described below.

Knoppers (1994) reports the results of field studies of a coastal wetland known as Ninigret Pond. This is a small wetland within the Rhode Island Salt Ponds in Rhode Island, USA. It contains various macrophytes and filamentateous macroalgae. Enhanced nutrient exchange due to lateral convection was considered to be a major factor contributing to eutrophication of one of the wetlands after it was permanently opened to the Atlantic in the mid 1950's. Prior to its opening, the wetland was inhabited by the two macrophyte species *Potamogeton* sp. and *Ruppia* sp. After the opening, *Zostera* sp. gradually invaded and replaced the other two species in the pond. Changes in the species of macroalgae in the wetland were also noted.

Convective transport can also play an important role in the distribution of suspended aquatic flora and fauna species. Chong *et al* (1996) report that in the Klang Strait in Malaysia, penaied prawn larvae hatched in deep waters are carried by shoreward currents towards the fringes of the strait. Large numbers of prawn larvae then become trapped in the mangroves along the fringes of the strait.

Webster (1990) and Webster and Hutchinson (1994) showed that the non neutral buoyancy of phytoplankton species can lead to heterogenous distributions of these species in lakes subject to wind driven convection. They found that the distribution of phytoplankton within a lake will be quite different under low and high wind speeds.

Buoyancy driven convection between the open water and vegetated zones of the wetland provides a potential mechanism for moving water between the two zones. From a design perspective, this has two possibilities: firstly by designing the wetland so that large open water zones are present, with only small amounts of vegetation scattered sporadically throughout the open water, the vegetated area will remain aerobic at all times. This will be so because temperature differences will develop between the open water and vegetated areas giving rise to a convective flow between the two areas under most conditions.

Such a design could be performed by ensuring the time taken by the water to circulate through the vegetated zone is less than the time taken for biochemical processes to use up the available oxygen.

The second case is somewhat more speculative: by placing a long side arm of vegetation alongside an open water area, the travel time for convection to reach the other end of the side arm could be made so long that biochemical processes use up all oxygen as it travels into the vegetated zone, ensuring that anaerobic conditions occur within the vegetated zone. Under such conditions with aerobic and anaerobic zones present in the water column, it may be possible to develop a

Nitrification/Denitrification cycle, hence promoting Nitrogen removal.

7.4. EUTROPHICATION ISSUES

It has been acknowledged for some time now that stratification, convection and mixing processes play important roles in the dissolved oxygen, phosphorus and nitrogen cycles of inland water bodies subject to eutrophication (Bowmer, 1981). Furthermore, recent studies have found that certain micro-organisms apparently use the stratification of the water column to their own advantage. It is now understood that cyano-bacteria, one of the species responsible for blue-green algae blooms, are able to regulate their buoyancy to regulate their position in the water column depending on the relative amounts of nutrients and light available (Sanderson *et al*, 1992).

By utilising this mechanism, under high nutrient conditions with little mixing, the cyano-bacteria are able to float just below the water surface, thereby gaining the maximum possible light for their own use, but preventing light or dissolved oxygen penetrating further into the water column. Under worst case conditions, this can lead to a blue green algal bloom, which may cause devastating effects on the ecology of the water body and posing a health threat to humans, stock and native animals using the water body as a source of drinking water.

Disregarding the impacts of wetlands species on the chemistry and biology of the water column, the physical presence of aquatic macrophytes in the water column is expected to affect cyano-bacterial growth in a number of complex ways. Firstly, the presence of the plant canopy will lower the amount of radiation entering the water column. Secondly, the enhanced stratification and reduced rates of mixing in the water column are likely to give the buoyancy regulating cyano-bacteria an advantage over other species, thereby encouraging an algal bloom.

Considering these mechanisms for algal growth and the results of Chapter 4, it is evident then that sufficient areas of open water should be made available in the wetland. This will have the following effects.

- Mixing will occur in the vegetated sections of the wetland by the breakdown of wind waves on the vegetation, thereby enhancing the transport of dissolved oxygen into the water column and mixing the cyano-bacteria away from the water surface, thereby breaking down, or preventing the build up of a blue green algal bloom.
- Temperature stratifications in the water column will break down, so the comparative advantage held by the self regulating cyano-bacteria will be removed.

7.5. CLASSIFICATION OF WETLANDS

From the preceding chapters, it is known that convection between the open water and vegetated areas occurs. Convections appear to occur with distinctive diurnal patterns, and the presence of lateral temperature differences between the open water and vegetation areas is a potential cause of these convections.

For convection driven by lateral temperature differences, it is possible to propose a classification scheme for the thermal state of wetlands based on the diurnal and seasonal patterns of these temperature differences. However, it must be acknowledged that such a classification scheme can only be considered very preliminary at this stage, as the role of wind driven convection must also be considered.

If it is assumed that other wetlands will show similar behaviour, with lateral stratifications being significant and leading to significant buoyancy driven convections, then a classification system should be based largely on the patterns of lateral temperature stratification and convection. This classification can only be tentative until further research confirms to what degree lateral stratifications and convections occur in wetlands generally.

To maintain consistency with previous studies, it is useful to consider the classification scheme first proposed by Forel in 1904 as described by Wetzel (1983) for classifying the thermal state of lakes.

The thermal structure of lakes are generally dominated by the presence or absence of stable one dimensional vertical thermal stratification (see for example Imberger and Patterson, 1990, Wetzel, 1983); however, as has been seen in the earlier chapters, in a wetland the lateral nature of the temperature structure can be of vital importance to its hydrodynamics. It is apparent then that while some similarities will exist between the thermal nature of lakes and wetlands, there will also be marked contrasts.

In this subsection, Forel's thermal classification system for lakes is described, followed by the development of a thermal classification for wetlands.

7.5.1 FOREL'S THERMAL LAKE CLASSIFICATION SYSTEM

Forel's system for lake classification is based on the thermal structure of the water column of a lake. The system is applicable to any lake where changes in density occur solely due to temperature. The classification is based on the number of times per year that a lake is mixed to its full depth. This classification scheme allows chemical and biological features of a lake to be more easily understood (Wetzel, 1983).

An important consideration in the classification of lakes is whether the temperature is above or below the maximum density point of water at approximately 4°C. Below this temperature, α_T, the rate of change of density with temperature is positive, and above it, α_T is negative.

In the classification below, the familiar case of decreasing temperature with depth will be referred to as an ordinary stratification, while increasing temperature with depth is referred to as an inverse stratification. When the temperature in the lake is above 4°C, an ordinary stratification will be stable and mixing in the vertical will be severely restricted. For water temperatures less than 4°C, an inverse stratification will be stable and mixing in the vertical will be severely restricted.

The descriptions below of lake types are drawn from Wetzel (1983). These are given below in order of increasing average lake temperature. They are summarised in Table 7.1.

AMICTIC LAKES

Amictic lakes have water temperatures between 0°C and 4°C. They are permanently covered in ice and therefore display stable inverse thermal stratifications. They are only very rarely or never subject to destratification or mixing events as surface mixing is prevented by the permanent cover of ice. Such lakes only occur at the poles or at extreme altitude.

COOL MONOMICTIC LAKES

In Cool monomictic lakes stable inverse thermal stratifications occur throughout the year, except for one period in summer when heating by solar radiation raises the temperature near the water surface, causing the stratification to become unstable. During this mixing annual period the water temperature at the surface may rise above 4°C, but not for long enough to stratify significantly. Again these lakes typically occur at high latitude or high altitude and typically are covered by a layer of ice through the winter.

COOL POLYMICTIC LAKES

In Cool Polymictic lakes, weak stable ordinary temperature stratifications develop and decay on a frequent basis. They occur at high latitude or high altitude in high wind environments that display little seasonal change in air temperature. These lakes typically have temperatures at or slightly above 4°C. The frequency with which these lakes are destratified means that the stratifications that do occur are only weak.

DIMICTIC LAKES

Display distinct patterns of summer and winter stratification, with mixing in spring and autumn. During summer the water temperature throughout the depth of the lake is at 4°C or higher and ordinary stable stratification occurs. During winter all water in the lake is at 4°C or lower, an ice layer may be present at the surface and an inverse stable stratification occurs.

Strong mixing occurs in Dimictic lakes in spring and autumn when the transition is made between the summer and winter stratifications. In spring this occurs as the water near the surface is heated by solar radiation, up to a temperature of 4°C. With this heating the water becomes denser than the water below it and falls through the water column, entraining surrounding fluid and thereby raising the temperature throughout the water column until the entire water column is at a temperature of 4°C. After this point, further heating near the surface causes the density of the water here to fall and the stable summer stratification develops.

In autumn the process is reversed, surface cooling causing the water temperature at the surface to a temperature of 4°C. With this cooling, the water again becomes denser, falling through the water column, causing mixing until the temperature throughout the lake is 4°C. Further surface cooling causes the density of water near the surface to fall and the stable winter stratification develops.

Such lakes are common in cool temperate zones.

WARM MONOMICTIC LAKES

Lakes in warm temperate climates commonly have water temperatures greater than 4°C throughout the year. Such lakes are termed monomictic. They have a stable stratification through summer, when radiative heating causes an ordinary stratification to develop; however through winter, surface cooling is sufficient to destratify the entire lake. The temperature of such lakes may drop below 4°C through winter; however no stable stratification occurs. No ice layer develops on the surface of such lakes.

OLIGOMICTIC LAKES

In tropical climates lake stratification may be sustained for many years, only destratifying under abnormally cold conditions. Such lakes are termed Oligomictic and always have water temperatures much greater than 4°C.

WARM POLYMICTIC LAKES

As for Cool Polymictic lakes, in Warm Polymictic lakes ordinary temperature stratifications develop and decay on a frequent basis and the frequency with which these lakes are destratified means that the stratifications that do occur are only weak. These lakes display weak stable ordinary temperature stratifications. They occur at low latitude in the tropical zone.

7.5.2. THERMAL CLASSIFICATION OF WETLANDS

The earlier chapters of the present study have demonstrated that wetlands display changes in behaviour on a relatively short times scale compared to lakes. Drastic changes in the thermal structure of the wetland can occur a number of times per day, as opposed to a number of times per year in a lake. Furthermore, as seen from the earlier chapters, the dominant feature of the thermal structure of the wetlands is the strong lateral stratification and resultant buoyancy driven fluxes that can develop between open water and vegetated regions.

A twofold classification is required to account for both diurnal and seasonal features of convections due to lateral stratification. This has been done below by defining a number of possible *Diurnal Convection States* that describe the nature of the convections occurring in a particular wetland within the diurnal cycle, and by defining *Seasonal Convection Classes* that describe the states occurring in a wetland as the seasons change.

Table 7.1. The Forel Classification for Lakes

Type	Mixing Frequency	Mixing Season	Ice Cover	Locations
Amictic	Never	None	Permanently covered in ice	High latitudes, high altitudes
Cool+ Monomictic	Once per year	Summer	Ice covered except in summer	High latitudes, high altitudes
Cool+ Polymictic	Frequently	Any	May be ice covered in winter	High latitudes, high altitudes, high wind environment
Dimictic	Twice per year	Spring, Autumn	May be ice covered in winter	Cool temperate climates
Warm* Monomictic	Once per year	Winter	No ice cover	Warm temperate climates
Oligomictic	Rarely	Winter	No ice cover	Tropical climates
Warm* Polymictic	Frequently	Any	No ice cover	Tropical climates

+ *Cool* indicates that the average lake temperature is between 0 and 4°C.

* *Warm* indicates that the average lake temperature is above 4°C

7.5.3. DIURNAL CONVECTION STATES IN WETLANDS

It was found in Chapter 6 that the wetland at Site B, displayed significantly different diurnal behaviour in summer and winter. In summer, the difference between solar radiation heat fluxes in the lake and in the wetland was large enough to cause the temperature in the lake to be higher than the temperature in the wetland throughout both the day and the night. In winter it was found that the temperature in the lake was higher than that in the wetland by day, but by night, the lake became cooler than the wetland.

In Chapter 5 it was found that the convection resulting from these temperature differences persisted into the evening and remained in the same direction both by day and by night. By contrast, as discussed in Chapter 6, it can be assumed that during winter the diurnal reversal in the temperature difference between the lake and the wetland will cause similar reversals in the convections between the lake and the wetland.

It is apparent then that:

- convection may occur in either direction; and
- under some circumstances the convection may be sustained over a full diurnal cycle, while under other circumstances there may be a reversal in the direction of the convection.

The direction of convection is most easily defined in terms of the direction in which the surface water moves between the open water and the vegetation. It is therefore useful to define nominal directions for *ordinary* and *reversed* directions of convection, and to define the diurnal nature of the convection as *monoconvective* or *diconvective*. These terms are defined below.

When the buoyancy driving causes the surface water to move from the open water area to the vegetated area, this will be termed *ordinary convection*. Under warm conditions (when the water temperature is greater than 4°C), this will occur if the temperature in the vegetated area is less than that in the open water. Under cool conditions (when the water temperature is less than 4°C), this will occur if the temperature in the vegetated area is higher than that in the lake.

When the buoyancy driving causes the surface water to move from the vegetated area to the open water area, this will be termed *reversed convection*. Under warm conditions (when the water temperature is greater than 4°C), this will occur if the temperature in the vegetated area is greater than that in the open water. Under cool conditions (when the water temperature is less than 4°C), this will occur if the temperature in the vegetated area is lower than that in the lake.

If the direction of the convection remains the same throughout the diurnal cycle, then the convection is said to be *monoconvective.* If the direction of the convection changes between the two possible directions of convection, then the convection is said to be *diconvective.*

Under most conditions, the thermal state of the wetland and the nature of convection in it, can therefore be described in terms of its average absolute temperature (*warm* or *cool*), the direction of convection (*ordinary* or *reversed*) and whether or not the convection is sustained throughout the full diurnal cycle or not (*monoconvective* or *diconvective*). A number of possible states that can be seen to arise from these conditions are described below, along with the *Aconvective* and *Wind Driven* States.

Cool Ordinary Monoconvective

For a wetland in which the temperatures in both open water and vegetated regions are less than 4°C and where the water temperature in the open water is lower than that in the vegetation, ordinary convection will occur. Such a condition may occur if the open water section of a wetland is subject to high rates of surface cooling. If such a condition is maintained over a full diurnal cycle, then the wetland can be said to be in the Cool Ordinary Monoconvective state.

Cool Reversed Monoconvective

For a wetland in which the temperatures in both open water and vegetated regions are less than 4°C, and where the water temperature in the open water is higher than that in the vegetation, ordinary convection will occur. Such a condition may occur if the open water section of a wetland is subject to radiative heating. If such a condition is maintained over a full diurnal cycle, then the wetland can be said to be in the Cool Reversed Monoconvective state.

Cool Diconvective

In a Cool Diconvective state, the temperature in both the open water and vegetated sections of the wetland are less than 4°C, both surface cooling by night and radiative heating by day in the open water section are strong enough to cause convections.

Aconvective

Conditions will arise under which it is expected that convection will not take place in a wetland, such a state will be referred to as aconvective. Two Aconvective states will be possible, these will be termed Aconvective States I and II and are described below:

In *Aconvective State I*, the dimensions of the vegetated area are far in excess of the dimensions of the open water area, or the vegetation density is so large that drag exerted by the vegetation is excessive, making the convection into the vegetated zone negligible.

In *Aconvective State II,* the water temperature in the open water is less than 4°C, while the temperature in the vegetated region is greater than 4°C so that despite a temperature difference, no significant density difference is present. Such a state is very finely balanced and is therefore expected to only occur as a transitory state between other states, as described below.

Warm Diconvective

In the Warm Diconvective state, temperatures are greater than 4°C in both the open water and vegetated areas. Heating by day causes ordinary convection and cooling by night causes reversed convection. This is the state that the Site B wetland was found to be in through winter.

Warm Ordinary Monoconvective

Temperatures are greater than 4°C in both the open water and vegetated regions for the Warm Monoconvective state. Heating by day causes ordinary convection, the temperature difference is sufficiently large that the convection is maintained through the evening. This is the state that the Site B wetland was found to be in through summer.

Warm Reversed Monoconvective

Temperatures are greater than 4°C in both the open water and vegetated regions for the Warm Monoconvective state. Cooling by night causes reversed convection, the temperature difference is sufficiently large that the convection is maintained through the day.

Wind Dominated Convective

Under high wind conditions, wind driven convection may dominate over temperature driven convection, despite the thermal state of the wetland. Conditions under which the wetland would enter this convective state are uncertain.

SEASONAL THERMAL BEHAVIOUR

Having defined a system of convective states for wetlands, it is apparent that as seasons change, the convective state of the wetland may also change. This was seen to be so in Chapter 6 for the Site B wetland which was *Warm Ordinary Monoconvective* in Summer and *Warm Diconvective* in winter.

With the definition of nine convective states in the previous section, it can be seen that there is the potential for a diverse range of seasonal behaviours under different climactic conditions. Clearly the patterns of behaviour with season are analogous to the Forel system for classification of lakes. Some examples of such patterns are shown in Figure 7.1.

Figure 7.1: Examples of Seasonal Thermal Behaviour in Wetlands

<table>
<tr><th>Climate</th><th colspan="2">Expected Thermal Behaviour for Subtropical Wetlands (eg Manly Dam Site B)</th><th colspan="2">Expected Thermal Behaviour for Temperate Wetlands</th></tr>
<tr><th>Season</th><th>Day</th><th>Night</th><th>Day</th><th>Night</th></tr>
<tr><td rowspan="3">Spring</td><td>Warm Ordinary Convection</td><td>Indeterminate</td><td>Indeterminate</td><td>Indeterminate</td></tr>
<tr><td colspan="2"></td><td colspan="2"></td></tr>
<tr><td colspan="2">Transitional</td><td colspan="2">Transitional</td></tr>
<tr><td rowspan="3">Summer</td><td>Warm Ordinary Convection</td><td>Warm Ordinary Convection</td><td>Warm Ordinary Convection</td><td>Warm Reversed Convection</td></tr>
<tr><td colspan="2"></td><td colspan="2"></td></tr>
<tr><td colspan="2">Warm Ordinary Monoconvective</td><td colspan="2">Warm Diconvective</td></tr>
<tr><td rowspan="3">Autumn</td><td>Warm Ordinary Convection</td><td>Indeterminate</td><td>Indeterminate</td><td>Indeterminate</td></tr>
<tr><td colspan="2"></td><td colspan="2">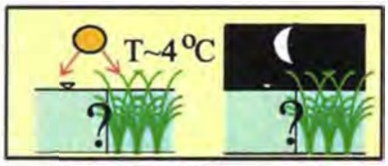</td></tr>
<tr><td colspan="2">Transitional</td><td colspan="2">Transitional</td></tr>
<tr><td rowspan="3">Winter</td><td>Warm Ordinary Convection</td><td>Warm Reversed Convection</td><td>Cool Reversed Convection</td><td>Cool Ordinary Convection</td></tr>
<tr><td colspan="2">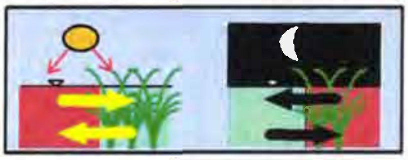</td><td colspan="2"></td></tr>
<tr><td colspan="2">Warm Diconvective</td><td colspan="2">Cool Diconvective</td></tr>
</table>

- *Red (warmer) and dark blue (colder) indicate the temperature difference between the open water and vegetated regions, not the temperature in an absolute sense.*
- *Arrows indicate the direction of water movement, question marks indicate the wetland is in a transitional state and flow may be in either direction.*
- *It was found in Chapter 6 that the Manly Dam Site B wetland followed the behaviour expected for subtropical conditions; however, the expected behaviour for temperate conditions is untested and is presented here merely as a hypothetical case to demonstrate the principles involved.*

7.6. SUMMARY

Of the hydrodynamic processes identified as occurring in wetlands, transient vertical temperature stratifications and enhanced mixing in the vicinity of open water regions will have minor effects on water quality and the ecology of wetlands, most likely causing brief periods of aerobic and anaerobic conditions to arise. Lateral temperature stratifications and buoyancy driven convections between open water and vegetated areas will have significant effects on the transport of constituents between these areas. The importance of these lateral stratifications leads to a classification system for wetlands based on the diurnal patterns of lateral stratification. This classification is based on whether or not the convections are sustained throughout the full diurnal cycle or not, whether the water temperature is above or below the maximum density temperature of water (4°C) and whether the convection is wind driven or buoyancy driven. Changing conditions with season will most likely cause changes in the patterns of lateral stratification and convection, a number of potential cycles of such seasonal changes have been demonstrated.

8. RECOMMENDATIONS

8. RECOMMENDATIONS

Recommendations that arise as a result of this study fall into two categories:

- recommendations for techniques to allow natural and constructed wetlands to be better managed to bring about improved water quality through understanding hydrodynamic processes within the wetlands; and
- recommendations for further research into water quality and hydrodynamic processes in wetlands.

These two categories of recommendations are treated separately below.

8.1 RECOMMENDATIONS FOR IMPROVED DESIGN AND MANAGEMENT OF WETLANDS

A number of ways in which the design and management of wetlands can be improved can be seen from this study. These are listed below.

- Give consideration to the class of the wetland being considered.
- Adequate amounts of open water zones should be incorporated into the design of wetlands to allow wind mixing and buoyant convections to take place between the open water and vegetated areas.
- Plant densities should be assessed regularly and selective harvesting should be performed if necessary to prevent vegetation from becoming too thick to allow mixing and buoyancy driven interactions to occur. This will ensure that sufficient levels of dissolved oxygen are able to be transported into the vegetated sections of the wetland to allow aerobic conditions to be maintained.
- Consideration should be given to incorporating temperature and velocity profiling to determine diurnal and seasonal patterns of mixing and buoyancy driven convections in wetlands where water quality monitoring is needed. This will allow other water quality parameters to be understood in the context of the hydrodynamic processes occurring within the wetlands.

8.2 RECOMMENDATIONS FOR FUTURE RESEARCH

Areas of research that can be identified as a result of performing this study include the following.

- Perform field studies to determine profiles of shortwave radiation, velocity and temperature at the air-water interface of vegetated sections of wetlands containing different types of vegetation to assess the radiation, momentum and heat transfer across the interface.
- Perform studies of buoyancy driven convections in wetlands subject to different climactic conditions and different configurations of open water and vegetated zones to allow them to be classified into the different types listed earlier.
- Perform studies to determine fluxes of heat and water across the sediment water interface to determine the cause of the heat source at the wetland bed and to better define the heat budget of the water column.
- Perform more detailed studies of wind driven convection, wave breaking and wave dissipation processes within the vegetated sections of a wetland, so that the classification scheme detailed above can be broadened to include wind effects. Sufficient velocity and temperature readings should be taken to allow the full turbulent spectra to be defined.
- Perform temperature and velocity profiling of the Manly Dam wetland or a similar wetland through one or more diurnal cycles during winter, autumnal and spring conditions to better define the diurnality of buoyancy driven convections throughout the different seasons.
- In the wetlands at Manly Dam, or similar wetlands, perform sampling further back from the lake to determine how far away from the lake mixing due to wave breaking is experienced and how far convective motions travel into the wetland.
- Develop appropriate numerical models of the hydrodynamic processes that have been found through this study to occur in wetlands.
- Confirm whether salinity is the cause of the reverse temperature stratifications at the bed of the wetland, as this would severely restrict interactions between the bed and the open water.

- Determine whether or not the thermal classification system proposed has significance to wetlands ecology and water quality.
- Determine the effects of the three dimensional nature of flows in the wetland. According to this thesis, it has been assumed that flows are two dimensional in the vertical, this will not necessarily be so, and the three dimensionality of flows may be highly significant.
- Determine the effects of variations in wind stress in the vicinity of the vegetation on circulation patterns.

9. CONCLUSIONS

9. CONCLUSIONS

This thesis has examined the effects of vegetation on the hydrodynamics of two wetlands adjacent to a reservoir. Heat fluxes, stratification, turbulent mixing by wind and penetrative convection, convection between vegetated and open water zones and seasonal behaviour have been considered.

Effects of these processes on wetland limnology have also been considered and recommendations arising from the study have been made.

Heat transfers were found to be significantly reduced in vegetated areas by shading due to the plant canopy. The canopy reduced solar radiation levels and lowered wind speeds at the air-water interface, thereby reducing sensible and latent heat transfers at the air-water interface.

Large temperature induced density stratifications can develop within the wetland due to diurnal solar radiation forcings and due to convection between open water and vegetated areas. These stratifications are large enough to be hydrodynamically significant; they arise throughout the year; however, given the shallowness of the wetland, little work is required to fully mix the water column, therefore mixing events may occur frequently so the wetland may go through cycles of stratification and decay on time scales shorter than one day.

Both wind mixing and penetrative convection have significant effects within the wetland. However vegetation has a different effect on each of these processes. The presence of vegetation causes wind waves that have been generated in the open water to degenerate, thereby acting as a source of turbulence. Near the edge of the vegetated zone, higher levels of turbulence are encountered than in the open water, however moving further into the vegetated zone, less turbulence is seen as the waves are not able to penetrate very far into the vegetation.

The effects of vegetation on penetrative convection are much simpler. The plant canopy in vegetated areas causes the wind velocity across the water surface to be very low here, hence sensible and latent heat fluxes are also low, so there is no driving mechanism for penetrative convection. Hence the effects of penetrative convection are expected to be substantially reduced within vegetated areas of wetlands.

The presence of a plant canopy extending above the water surface was found to reduce the depth averaged water temperatures in vegetated areas by reducing the amount of radiation entering the water column. This was found to cause lateral density differences and hence buoyancy driven convection to develop between open water and vegetated areas. A scaling analysis revealed that these buoyancy driven convections are likely to reach steady state quickly and a balance between the buoyancy driving and drag due to vegetation will be established. For the Site B Manly dam wetland, convective velocities of the order of 0.01 ms^{-1} would be expected.

The velocity scales of the buoyancy driven convection were large enough to bring an intrusion of warm water from the lake into the vegetated area in a comparatively short time. While temperature rises due to buoyancy driven convection from the open water were observed in the vegetated area, the temperature in the vegetated section never rose to the same level as in the lake and the rate of temperature rise observed was lower than predicted by the buoyancy - drag balance.

A wind in the opposite direction to the buoyancy driving was present throughout the period for which this convection was observed, so it was concluded that a wind shear on the water surface would have partly arrested the convection. With the convection partly arrested, water entering the vegetated area from the lake would be slowed sufficiently for its temperature to be lowered by surface cooling to the rises of temperature that were observed.

By comparing the results of the studies at Sites A and B, it was found that there is some generality to these results as similar behaviours were observed at both sites.

Stratifications sufficiently large to affect the hydrodynamics of the wetland occurred at both sites, and long term studies at one site revealed that they occur throughout the year.

A most significant finding of the long term study was that the horizontal temperature structure showed marked differences between summer and winter conditions. Through winter, lateral temperature differences between the vegetated and open water locations arose by day due to shading from solar radiation in the vegetated areas. By night, the open water cooled at a faster rate than the vegetated area, so the lateral temperature differences between the open water and vegetated areas reversed sign. Buoyancy driven convections would therefore be in opposite directions by day and by night.

In summer it was possible for large temperature differences between vegetated and open water zones to be sustained for many weeks at a time. These temperature differences indicate that through summer, buoyancy driven convections may occur uninterrupted over many weeks.

A surprising finding of the long term monitoring was that throughout much of the winter, and some of the summer, the bed of the wetland can act as a significant heat source, causing higher temperatures in the vicinity of the bed than higher up in the water column, despite the buoyancy that such warm water would have. It is apparent that the water very close to the bed is stagnant. The most likely cause of these reverse temperature stratifications is increased salinity at the bed due to saline groundwater intrusions or biochemical reactions at the bed causing a stable density stratification despite the higher temperatures here. These higher temperatures at the bed most likely arise due to radiative heating of the bed.

From the study a number of implications of hydrodynamics on wetlands ecology can be postulated. Temperature differences between open water and vegetated areas would be expected to have significant impacts on water quality by providing a buoyancy driving for convection between these areas. Such convections would most likely play a significant role in the transport of dissolved oxygen and other constituents through the wetland.

Vertical stratification and mixing processes will most likely not have as significant effect, as these processes are quite transient, with cycles of stratification and mixing occurring diurnally or more frequently.

Given the importance of temperature differences between open water and vegetated areas, a classification scheme is proposed which is largely based on these temperature differences and their patterns of occurrence on diurnal and seasonal cycles. It is argued that such a classification should have a significant bearing on the water quality and ecology of the wetland.

10. REFERENCES

10. REFERENCES

Ackerman JD and Okubo A (1993), "Reduced Mixing In A Marine Macrophyte Canopy" *Functional Ecology*, Vol 7, pp 305 - 309

Anderson SM and Charters AC (1982) "A Fluid Dynamics Study Of Seawater Flow Through *Gelidium Nudifrons*" *Limnology and Oceanography*, Vol 2, No 3

Baines WD and Peterson EG (1951), "An Investigation Of Flow Through Screens" *Transactions, ASME, Vol 73 pp 467 - 480*

Batchelor (1967), *An Introduction To Fluid Mechanics*, Cambridge University Press

Bavor HJ, Andel EA, Schulz TJ and Waters MT (1992), "Byron Bay Constructed Wetlands Research Program. Progress Review – November 1992," *University Of Western Sydney - Hawkesbury, Water Research Laboratory Report.*

Beer T (1983) *Environmental Oceanography*, Pergamon Press.

Bendat JS and Piersol AG (1986), *Random Data: Analysis and Measurement Procedures*, Second Edition, John Wiley and Sons

Böhrer B (1996), "Convection In A Long Cavity With Differentially Heated End Walls" Submitted To *Journal Of Fluid Mechanics*

Bowmer, KH (1981), "Nutrient Enrichment Eutrophication" In *Waterplants Of New South Wales* By Sainty, GR and Jacobs SWL, Water Resources Commission, NSW.

Brodie, GA (1990), "Constructed Wetlands For Treating Acid Drainage At Tennessee Valley Authority Coal Facilities", In *Constructed Wetlands In Water Pollution Control, Proceedings Of The International Conference On The Use Of Constructed Wetlands In Water Pollution Control*, Eds Cooper, PF and Findlater, BC, Pergamon Press.

Carter GD, Scolaro G, Elford D and Luketina DA (1985) "Vertically Rising Microstructure Profiler (RMP)", *Environmental Dynamics Report ED-85-098*, University Of Western Australia

Chen SS (1987), *Flow Induced Vibration Of Circular Cylindrical Structures*, Hemisphere Publishing Corporation

Cheng D (1993), *Water Quality Management Plan For Manly Dam*, University Of Technology, Sydney

Cheschier GM (1987), "Hydrology of Wetland Buffer Areas for Pumped Agricultural Drainage Water", in DD Hook (ed) *The Ecology and Management of Wetlands,* Croom-Helm

Cheung TK and Street RL (1988) "The Turbulent Layer In The Water At An Air-Water Interface", *Journal Of Fluid Mechanics*, Vol 44, pp 133 - 151

Chong VC, Sasekumar A and Wolanski, E (1996), "The role of Mangroves in retaining Penaied Prawn Larvae in Klang Strait Malaysia", *Mangroves and Salt Marshes*, Vol 1, No 1.

Chow VT, Maidment DR and Mays LW (1989), *Applied Hydrology*, Elsevier Press.

Cionco RM (1972), "Intensity Of Turbulence Within Canopies With Simple and Complex Roughness Elements", *Boundary Layer Meteorology,* Vol 2, pp 453 - 465

Coates MJ and Ferris JM (1994) "The Radiatively Driven Natural Convection Beneath A Floating Plant Layer", *Limnology and Oceanography Vol 39, pp 1186-1194*

Coates MJ and Patterson JC (1993) "Unsteady Natural Convection In A Cavity With Nonuniform Absorption Of Radiation", *Journal Of Fluid Mechanics* Vol 253, pp 131-161

Collier, RD (1982), "Calibration With Confidence: The Assurance Of Temperature Accuracy", In *Temperature - Its Measurement and Control In Science and Industry*. Vol 5, Part 2, pp1311 To 1315. American Institute Of Physics

Cowan (1968), "Mass, Heat and Momentum Exchange Between Plant and their Atmospheric Environment", *Q J R Meteorologic Society*, Vol 94, pp 318-322

Cowardin, LM, Carter V, Folet FC, La Roe ET (1979), *Classification Of Wetlands and Deepwater Habitats Of The United States*, US Department Of The Interior, US Fish and Wildlife Service.

Craig PD and Banner ML (1994), "Modelling Wave-Enhance Turbulence In The Ocean Surface Layer", *Journal Of Physical Oceanography,* Vol 24(12), pp 2546-2559

Dale HM and Gillespie TJ (1977), "The Influence Of Submersed Aquatic Plants On Temperature Gradients In Shallow Water Bodies" *Can J Bot* Vol 55, pp 2216 - 2225

Danard MB and Murty TS (1994), "Storm Surge Mitigation Through Vegetation Canopies", *Natural Hazards*, Vol 9, pp 155 - 166

Eberdorfer A (1994), "Tracer Studies In An Artificial Wetland", Dissertation Submitted To The Universitat Bodenkultur, Vienna

Escudier MP and Maxworthy T (1973) "On The Motion Of Turbulent Thermals", *J Fluid Mech*, Vol 61, No 3, pp 541 - 552

Finnigan JJ (1979), "Turbulence In Waving Wheat, I Mean Statistics and Honami", *Boundary Layer Meteorology*, Vol 16, pp 181 - 211

Fischer H B, List EJ, Koh RCY, Imberger J, Brooks NH (1979), *Mixing In Inland and Coastal Waters*, Academic Press.

Gill AE (1982), "Atmosphere Ocean Dynamics", *International Geophysics Series*, Vol 30.

Gibson CH (1986), "Internal Waves, Fossil Turbulence and Composite Ocean Microstructure Spectra", *J Fluid Mech*, Vol 168, pp89 - 117

Goldsmith F.B, C.M. Harrison and A.J. Morton: (1986) "Description and Analysis Of Vegetation", In *Methods In Plant Ecology*, Edited By Moore P.D. and S.B. Chapman, Blackwell Scientific Publications

Gregg MC and Briscoe MG (1979), "Internal Waves, Finestructure , Microstructure and Mixing In The Ocean", *Reviews Of Geophysics and Space Physics*, Vol 17, No 7.

Groth J and Johansson AV (1988), "Turbulence Reduction By Screens", *J Fluid Mech*, Vol 197, pp 139 - 155

Hammer DE and Kadlec RH (1986), "A Model for Wetland Surface Water Dynamics" *Water Resour Res*, Vol 22, No 13.

Hatano K, Frederick DJ, and Moore, JA (1992), "Microbial Ecology Of Contructed Wetlands Used For Treating Pulp Mill Wastewater" *Wetlands Downunder*, International Specialist Conference On Wetlands Systems In Water Pollution Control.

Hecht E (1987), *Optics*, Addisson-Wesley

Henderson-Sellers B (1984), *Engineering Limnology*, Pitman Publishing.

Horton RE (1938) "The Interpretation and Application of Runoff Plant Experiments with Reference to Soil Erosion Problems", *Proc Soil Soc of America*, No 3

Hutchinson, GE (1957), *A Treatise On Limnology, Volume 1, Geography, Physics and Chemistry*, John Wiley and Sons

Hutter (1984), "Linear Gravity Waves, Kelvin Waves and Poincare Waves, Theoretical Modelling and Observations" *Hydrodynamics Of Lakes*, Springer Verlag

Imberger J and Ivey GN (1991), "On The Nature Of Turbulence In A Stratified Fluid. Part II: Applications To Lakes". *Journal Of Physical and Oceanography*, Vol 21. American Geophysical Union.

Imberger J and Patterson JC (1990), "Physical Limnology", *Applied Mechanics*.

Justesen, (1987), Institute Of Hydrodynamic and Hydraulic Engineering, Technical University Of Denmark, Series Paper No 43

Kadlec RH (1991), "The Hydrology of Overland Flow in Wetlands" *Chem Engrg Commun.* Vol 9, pp 331 - 344

Kadlec RH (1993), "Flow Patterns In Constructed Wetlands", *Proc Hydraulic Engineering '93*, ASCE National Conference On Hydraulic Engineering. American Society Of Civil Engineers

Kadlec, RH and Hey DL (1992), "Constructed Wetlands For River Water Quality Improvement" *Wetlands Downunder*, International Specialist Conference On Wetlands Systems In Water Pollution Control.

Kadlec, RH (1990) "Overland Flow In Wetlands: Vegetation Resistance" *Journal Of*

Hydraulic Engineering, Vol 116, No 5

Kirk JTO (1983), *Light and Photosynthesis in Aquatic Ecosystems*, Cambridge University Press.

Kitaigorodski SA, Donelan MA, Lumley JL and Terray EA (1983) "Wave Turbulence Interactions In The Upper Ocean. Part II: Statistical Characteristics Of Wave and Turbulent Components Of The Random Velocity Field In The Marine Surface Layer" *Journal Of Physical Oceanography*, Vol 13, pp 1988 To 1999

Knoppers B (1994), "Aquatic Primary Production In Coastal Lagoons" *Coastal Lagoon Processes*, Edited By Kjerfve B, Elsevier Oceanography Series, 60, Elsevier Science Publishers

Landsberg JJ and James GB (1971) "Wind Profiles in Plant Canopies: Studies on an Analytic Model" *J Appl Ecol,* Vol 8, pp 729 - 741

Lewandowski, JA, Sobey, RJ and Goodwin, P (1993) "A Hydrodynamic Model For A Tidal Wetland". *Proc Hydraulic Engineering '93*, ASCE National Conference On Hydraulic Engineering. American Society Of Civil Engineers

Luketina DA (1996): *Lecture Notes, Environmental Fluid Mechanics*. Unpublished Document, School Of Civil Engineering, University Of New South Wales

Manly Hydraulics Laboratory (1995): *Coastal Rainfall Annual Summary, 1994-1995* NSW Department of Public Works and Services, MHL Report 730

Manly Hydraulics Laboratory (1996): *Coastal Rainfall Annual Summary, 1995-1996* NSW Department of Public Works and Services, MHL Report 776

Maslen PG and Schulz TJ (1995), "The CRC Advanced Constructed Wetland Project, An Australian Cooperative Research Scheme", *AWWA 16th Federal Convention, Proceedings*, Vol 1, pp 421 - 428

Meeus J (1979), *Astronomical Formulae for Calculators*, Monografieen Over Astronomie en Astrofysia, Uitgegeven Door Volkssterrenwacht Urania VZW en Vereniging Voor Sterrenkunde VZW

Metcalf and Eddy Inc. (1976), *Wastewater Engineering Treatment, Disposal, and Reuse,* Second Edition, Mcgraw Hill.

Monitor Sensors (1993) *Automatic Weather Monitoring Stations: Installation and Cperating Manual,* Monitor Sensors.

Monteith and Unsworth (1990), *Principles Cf Environmental Physics*, Arnold

Myrup LO, Powell TM, Godden Da and Goldman CR (1979) "Climatological estimate of the average monthly energy and water budgets of Lake Tahoe, California - Nevada". *Water Resources Res* Vol 15, pp1499-1508

Naot D, Iehisa N and Nakagawa H (1996), "Hydrodynamic Behaviour of Partly Vegetated Open Water Channels", ASCE Journal of Hydraulic Engineering, Vol 122, No 11.

NSW Department Of Public Works and Services, Manly Hydraulics Laboratory, (1996) *Water Level Data Collection Instruments*, http://www.mhl.nsw.gov.au/www/water_data_how .html

Oakey, NS. (1982) "Determination Of The Rate Of Dissipation Of Turbulent Kinetic Energy From Simultaneous Temperature and Velocity Shear Miscrostructure Measurements", *J Phys Oceanogr*, Vol 12, pp 256-271

Patterson J and Imberger J (1980) “Unsteady Natural Convection in a Rectangular Cavity”, *JFM* Vol 1, Part 1

Perry RH and Chilton CH (Eds) (1973), *Chemical Engineers Handbook*, Mcgraw Hill,

Raupach MR and Shaw RH (1982), "Averaging Procedures For Flow Within Vegetation Canopies", *Boundary Layer Meteorology,* Vol 22, pp 79 - 90

Raupach MR and Thom AS (1981), "Turbulence In and Above Plant Canopies", *Ann Rev Fluid Mech* Vol 13, pp 97 - 129

Roig LC (1994), *Hydrodynamic Modelling Of Flows In Tidal Wetlands*, Phd Thesis, University Of California, Davis

Sainty, GR and Jacobs, SWL, (1988), *Waterplants In Australia*, Australian Water Resources Council

Sanderson BG, Webster IT and Humphries SE (1992), “Chaotic Solutions for irrandiance regulated buoyant motion of cyanobacteria”, *Limnol. Oceanogr.* 37(8).

Schlichting, H (1951), *Boundary Layer Theory*, Mcgraw Hill

Swanson, P (1995), "Reducing The Impact Of Urbanisation On Streams Using Energy-Efficient Systems", *AWWA 16th Federal Convention, Proceedings*, Vol 2, pp 789- 796

Tennekes H and Lumley JL (1972), *A First Course In Turbulence*, MT Press, Cambridge Massachusetts

Thermometrics (1986) *Thermistor Sensor Handbook* Thermometrics Inc

Thom AS (1975), "Momentum, Mass and Heat Exchange Of Plant Communities" In

Monteith JL (Ed) *Vegetation and The Atmosphere. Volume 1: Principles*, Academic Press

Tsahalis DT (1979), "Theoretical and Experimental Studies of Wind and Wave Induced Drift" *JPO,* Vol 9, pp 1243-1251.

Turner J S (1973), "Buoyancy Effects In Fluids" In *Cambridge Monographs On Mechanics and Applied Mathematics*, Cambridge University Press.

Uhlmann, D, (1979), *Hydrobiology*, John Wiley and Sons

US Army Core Of Engineers (1984), *Shore Protection Manual Volume 1*, Department Of Army, US Government Printing Office

Waters MT and Luketina DA (1995), "The Importance Of Meteorologic Influences On Mixing In Wetlands", *Proceedings AWWA Federal Convention, Sydney 1995*

Waters MT Luketina DA and Ball JE (1994), *Wetland Hydraulics Scaling Analyses. Part 1: External Influences On Mixing Processes* Water Research Laboratory Research Report RR185

Webster IT (1990), "Effect Of Wind On The Distribution Of Phytoplankton Cells In Lakes", *Limnol. Oceanogr.* Vol 35, pp 989-1001

Webster IT (1997), "Examiners report on Thesis Submitted for the Degree of Doctor of Philosophy, Effects of Vegetation on the Hydrodynamics of Freshwater Wetlands"

Webster IT and Hutchinson PA (1994), "Effect Of Wind On The Distribtion Of Phytoplankton In Lakes Revisited", *Limnol. Oceanogr.* Vol 39, No 2

Western AW (1994), *The Behaviour Of Salinity and Density Stratified Flows In The*

Wimmera River, Australia, Phd Thesis, University Of Melbourne

Wetzel G (1982), *Limnology*, Saunders

White G, Smalls IC and Bek P (1992), "Carcoar Wetland - A Wetland System For River Nutrient Removal", In *Wetlands Downunder - International Specialist Conference, Wetland Systems In Water Pollution Control, Proceedings,* IAWQ.

Wilson and Shaw (1977), "A Higher Order Closure Model For Canopy Flow", *J Appl. Meteorol.* Vol 16, pp 1198- 1205

APPENDICES

APPENDIX A. EQUIPMENT SPECIFICATIONS

A.1. Meteorologic Equipment

The meteorologic equipment is shown in Figure A1. All probes and the data logger were obtained from Monitor Sensors, and were factory calibrated before deployment, except for the tipping bucket raingauge, which was calibrated by the author as described below. From the Monitor Sensors Installation and Operating Manual (Monitor Sensors, 1993), the equipment had the following characteristics:

Figure A.1. Meteorologic Equipment and Data Recording Equipment
Photograph taken looking East with Open Water Thermistors on the left, Meteorologic Station and Data Logger Housing on the Scaffolding

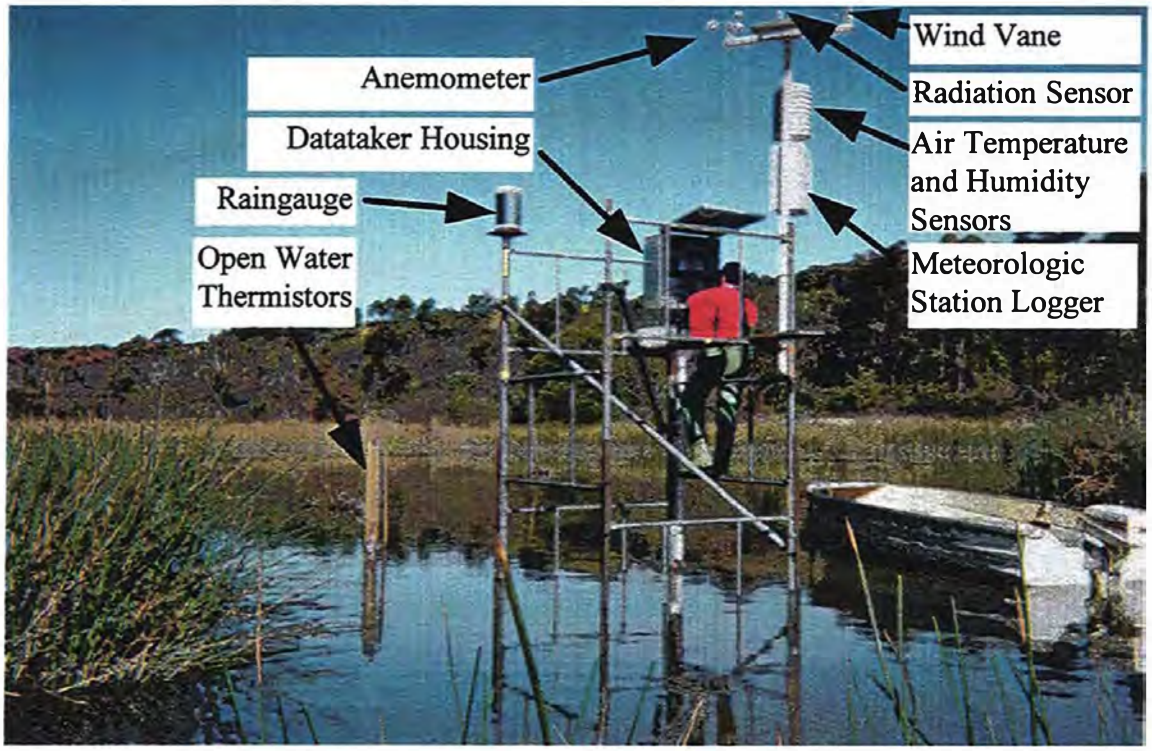

The data logger used was a model GL-128, which received pulsed digital inputs from the sensors. It had 8 input channels, of which 7 were used. Signals from inputs had a minimum pulse width of 40 ms and a maximum square wave frequency of 12.5 Hz. A

6V, 2.6 Ah sealed lead acid battery with a 0.5 W solar panel for battery recharge. Memory was stored as CMOS with 216 kb capacity. Downloading was performed by RS232 full duplex communications with a T1850 Toshiba laptop PC, operating Monitor Sensors software "logger". Data format was 8 bit ASCII, with no parity and 1 stop bit.

Relative humidity was sensed with a HD-01 coreci cracked chromium sensor. The device has an accuracy of 5 % over a range of 5 to 95 % relative humidity, with a hysteresis of less than 1 %. Response time to reach 95 % of the true value is 1 minute. The electronics of the instrument are sealed in a plastic tube of 25 mm diameter and 150 mm length, with the sensor element protruding from one end. It is powered by a 5 V regulated source and draws about 500 μA. Factory calibration involved preconditioning the sensor between 10 and 30 % for 8 hours, then cycling the sensor between 17.7 and 80.2 % for 24 to 48 hours.

Temperature was sensed using a TDC-01A digital temperature sensor, which consists of a diode connected to a transistor and a voltage to frequency converter. Factory calibration involved logging the sensor against a temperature standard for 28 hours, while the temperature was cycled over the range of 0.3 to 46.2 °C.

The HD-01 and TDC-01A probes were mounted in a SS-04B sensor shelter. The shelter was constructed of spun aluminium louvres coated with white ultraviolet stabilised polyester baked powder coat to minimise absorption of solar radiation. The undersides of the louvres are blackened.

Rainfall was measured using a tipping bucket raingauge, model RGD-01, with a 0.2 mm tip bucket and 203 mm collector funnel. Tips are recorded by the bucket tilting, which causes a magnet to close, then open a reed switch. The RGD-01 was calibrated using a Hydrological services tipping bucket calibration device. Adjustments were made to the stops supporting the buckets until the number of tips for 20 mm of rainfall was within the range of 95 to 105 tips. Care was taken at the time of installation to ensure that the tipping bucket was installed on a level surface.

A model AND-02-10 anemometer was used to measure wind speed. The anemometer had a stall speed of 0.3 m/s and a maximum wind speed of 200 km/h. An inductive pickup is actuated by the rotation of a small magnet attached to the shaft of the anemometer. With this equipment, a count is recorded for every 4 revolutions that is, every 10 m of wind run.

Solar radiation is measured by a SRD-02 digital solar radiation sensor, which is cosine corrected for angles of incidence up to 80°. Factory calibration involved logging the sensor against a standard for 1 hour while the radiation varied from 62 to 1065 W/m^2.

The wind direction sensor was a WDD-03 vane type sensor which produces two square wave outputs with frequency proportional to sine and cosine of the angle of the wind direction, relative to North.

To verify the factory calibrations of the meteorologic sensors, meteorologic data was compared with data from the Macquarie University weather station as described in Appendix A.5.

A.2. Thermistors

The thermistors were thermistor assemblies, model number A727E-P60BA252M-L60M, obtained from Thermometrics. The thermistor beads themselves were encased in a stainless steel case. A two wire, shielded cable 60 m long transmitted the signal to the data logger, which was situated on the scaffolding where the meteorological equipment was deployed, as shown in Figure A.1. This shielded cable ensured that there was minimum noise in the cable.

In operation, signals from the thermistors were recorded as resistance across the bead, logged by the DT505 logger. Temperature-resistance calibration of the thermistors is discussed in Appendix B.

The thermistors were deployed vertically, wrapped in 2 mm thick PVC tubing which terminated 10 mm behind the tip. The PVC tubing ensured that if there was significant temperature stratification, minimal heat transfer along the stainless steel housing would result.

A.3. Data Logger

Data from the 16 thermistors and the pressure transducer were recorded using a DT505 datataker data logger, obtained from Data Electronics. The DT505 has 10 analog channels, plus an expansion module, giving it the capacity to log an extra 10 analog channels. Channel selection is by relay multiplexer, ensuring that cross channel interference is non-existent and that damage due to lightning strikes or other unforeseen high input voltages are minimised.

Power was supplied by a 6 V, 4.2 Ah battery, and memory was stored on a 1 Mb memory card. The logger was down loaded at weekly intervals by RS232 communications at 9600 baud to a laptop PC.

A.5. Water Level Recorder

Water levels in the dam were obtained from a water level recorder installed and maintained in Manly Dam by the NSW Department of Public Works and Services Manly Hydraulics Laboratory. The recorder is floatwell system, made up of a float connected to an optical shaft encoder (NSW DPWS, 1996). Readings are taken every 10 seconds for 160 seconds, averaged, then stored on the quarter hour at Australian Eastern Standard Time.

APPENDIX B. EQUIPMENT CALIBRATIONS

This appendix presents the details of calibrations performed on:

- the platinum resistance thermometer used to calibrate the thermistors;
- the thermistors used in the long term monitoring;
- the fp07 thermistor in the microprofiler used in the intensive experiments; and
- the pressure transducer in the microprofiler.

B.1. Platinum Resistance Thermometer Ice Point Resistance

CONTEXT

Accurate measurement of water temperatures in the field was achieved by the use of 16 thermometrics thermistors, specifications for which are given in Chapter 2. To ensure the accuracy of these thermistors relative to each other over the range of 5°C to 30°C, it was necessary to calibrate them against an independent standard thermometer. The standard thermometer used was a Leeds and Northrup Platinum resistance thermometer (PRT).

According to Collier (1982), To ensure that the thermistors were calibrated to an accuracy of 0.1°C or better, it was necessary to ensure the PRT had an accuracy of 0.01°C or better. This was done by ensuring the resistance of the PRT was in accordance with its quoted resistance of 100.000 Ω at when immersed in an ice-bath at 0.00°C, using techniques presented by Collier (1982).

AIMS

- To determine the resistance of the Leeds and Northrup model 8078 portable precision temperature bridge Platinum Resistance Thermometer (PRT) at 0.00 °C in water in its uncalibrated state.

- To recalibrate the PRT to its nominal resistance of 100.000 Ω at 0.00 °C, by adjustment of the "Ice Point Set Value" while in an ice-water bath.

METHOD

1. Fill a container with crushed ice, ensuring that the ice is tightly packed throughout.
2. Fill the pore spaces between the ice chips with water, until overflowing, taking care to ensure there are no air voids in the mixture.
3. Insert the PRT to its proper insertion depth, ensuring good contact between the probe and the ice chips.
4. Allow at least 15 minutes for the ice-water bath to reach thermal equilibrium (5 minutes after the initial iteration).
5. Record the resistance of the PRT to the nearest 0.001 Ω,
6. Adjust the zero point set of the PRT as necessary to give a resistance reading of 100 Ω, noting the values of the Ice Point Set before and after the adjustment is made.
7. Repeat steps 3 to 7 until the PRT consistently reads 100.000 Ω, without adjustment to the "ice point set" between readings.

RESULTS

Two separate calibrations were performed, as reported below. The first was cut short as high ambient temperatures caused excessive amounts of ice to melt, so the accuracy of the temperature was in doubt. The second was performed under cooler ambient conditions so that ice melt was minimised.

Calibration 1

Time mins	Initial PRT Resistance Ω	Ice Point Set Value		Temperature, °C
		Before Immersion	After Immersion	
23	100.036	440	548	0.09
30	99.998	548	545	0.00

Calibration 2

Time mins	Initial PRT Resistance Ω	Ice Point Set Value		Temperature, °C
		Before Immersion	After Immersion	
17	99.999	545	539	0.00
20	100.000	539	539	0.00
37	100.000	539	538	0.00
57	100.000	538	538	0.00
65	100.000	538	538	0.00

Conclusions

After displaying some instability at the ice point in the first calibration, the PRT showed high stability of resistance at the ice point. It is therefore expected that the PRT will be highly stable and a good reference thermometer, suitable for the calibration of other temperature devices to a resolution of 0.01°C.

B.2. Long Term Thermistor Rising Temperature Calibrations

In order to use the thermistors for temperature measurement, it was necessary to determine the temperature-resistance relationship of each individual thermistor over the range of temperatures expected in the field. Temperature-resistance relationships for thermistors are quite non-linear, however they are generally well described by polynomial relationships fitted to calibrated data (Thermometrics, 1986).

The 16 thermistors used were calibrated prior to installation in the field, then verified on two separate occasions, after deployment at Site A, prior to deployment at Site B, and at the end of the long term experiments. On each of these occasions, identical techniques were employed as described below.

AIM

Determine the resistance of the 16 thermistors over the range 5 to 30 °C.

APPARATUS

- Leeds and Northrup PRT, model - 8078 portable precision temperature bridge
- 16 Thermometrics thermistors: part code A727E-P60BA252M-L50M, with zero power resistance of 2500 Ω, labelled A to P, each with 60 m of cabling.
- DT505 Data logger and expansion module

METHOD

The methods for the calibration and verification experiments followed the same format. The only difference between them was that it was necessary to perform polynomial fits to the temperature-resistance data for the calibration experiment, whereas for the verification experiments, it was merely necessary to compare the predicted temperature from the resistance measurement made, against the actual temperature.

1. Place the holding plate in the container and insert the PRT, the reference thermometer and the thermistors to their proper insertion depths.
2. Place ice in the container and fill the container with water to the overflow level
3. Start the mixer and allow mixing to proceed until all ice melts and the temperature

throughout the container is uniform

4. Record the temperature readings of the digimulti probes.
5. Record the resistance of the PRT to the nearest 0.001 Ω
6. Record the resistances of the thermistors the DT505 logger
7. add 5 or 10 l of water as required to raise the water temperature by between 1 and 2 °C (when water temperature is too high to allow heating in this way, insert electric water heater coil)
8. Repeat steps 3 to 8 (excluding 7 after the first reading is taken) until a reading of over 30 °C is achieved.
9. Construct the 6th order polynomials to fit the temperature - resistance curves for each thermistor

RESULTS

Figures B.1a to B.1p show the results of the calibrations for all 16 thermistors, labelled A to Q respectively. Results are shown as plots of temperature vs resistance over the range 5 to 34°C. Coefficients of the polynomial fits for each thermistor are also shown on these figures.

Table B.1 shows the results of the verification performed on the thermistors on 10 July 1996.

CONCLUSIONS

All thermistors displayed a high degree of stability, both when resistance measurements were repeated at one temperature, and when the temperature was changed, so that a second calibration was not deemed necessary prior to commencing field work. Despite this stability, each thermistor displayed its own unique resistance - temperature relationship, so that thermistors cannot be interchanged, and care is required to ensure that the correct temperature -resistance relationship is used for each thermistor.

Verification of the thermistors was performed after the thermistors were retrieved from the field, using the same techniques as were employed for the thermistor calibration. The results of this verification experiment are shown in Table B.1.

Table B.1 indicates that a drift of less than 0.09°C was experienced by each of the thermistors, over a range of 14.5°C to 29.0°C, except thermistors A and C.

Temperature drifts in thermistors A and C were 0.1°C and 0.2°C respectively. Inaccuracies of this order at thermistors A and C were able to be tolerated as these were the thermistors used for measuring air temperatures at Stations 1 and 4.

Figure B.1.a. Temperature-Resistance Relationship for Thermistor A

Thermistor Calibration

Y = M0 + M1*x + ... M8*x^8 + M9*x^9	
M0	79.931
M1	-0.038875
M2	9.6581e-06
M3	-1.2826e-09
M4	6.7401e-14
R	0.99991

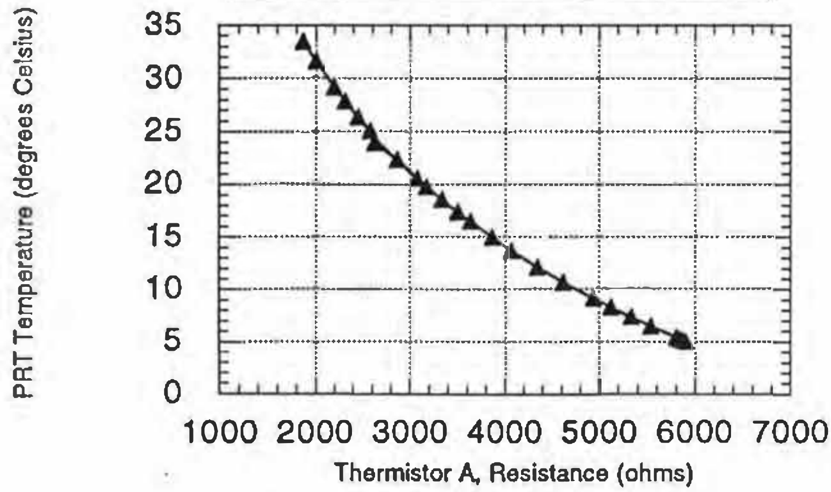

Figure B.1.b. Temperature-Resistance Relationship for Thermistor B

Thermistor Calibration 11:01:13 AM 17/5/94

$Y = M0 + M1*x + ... M8*x^8 + M9*x^9$	
M0	74.599
M1	-0.032367
M2	7.1016e-06
M3	-8.5795e-10
M4	4.1938e-14
R	0.99997

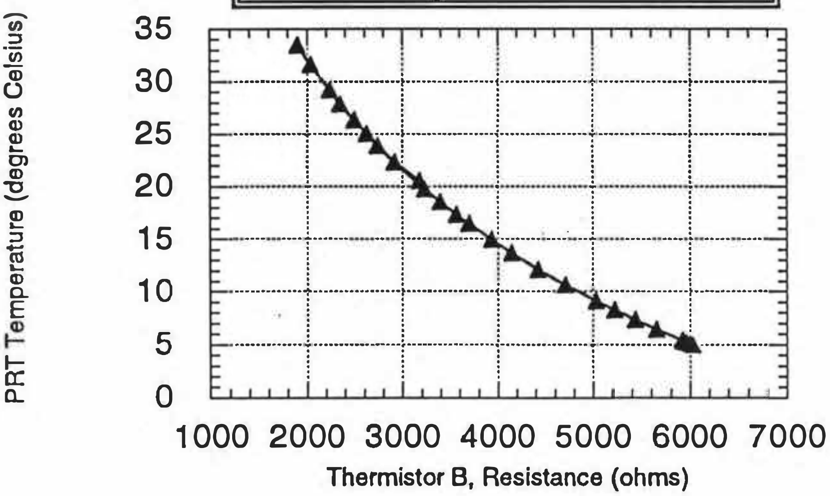

Figure B.1.c. Temperature-Resistance Relationship for Thermistor C

Thermistor Calibration 11:01:13 AM 17/5/94

$Y = M0 + M1*x + ... M8*x^8 + M9*x^9$	
M0	74.953
M1	-0.038735
M2	1.01e-05
M3	-1.4377e-09
M4	8.2301e-14
R	1

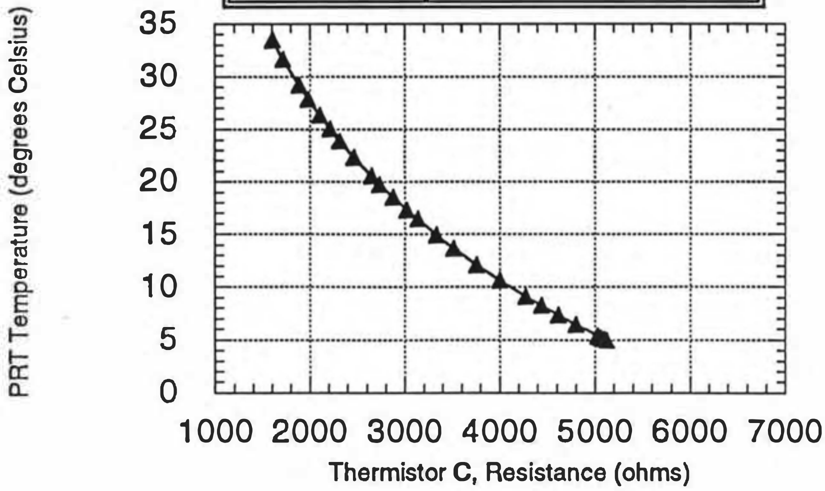

Figure B.1.d. Temperature-Resistance Relationship for Thermistor D

Thermistor Calibration 11:01:13 AM 17/5/94

$Y = M0 + M1*x + \ldots M8*x^8 + M9*x^9$	
M0	75.484
M1	-0.035168
M2	8.2622e-06
M3	-1.0601e-09
M4	5.4743e-14
R	1

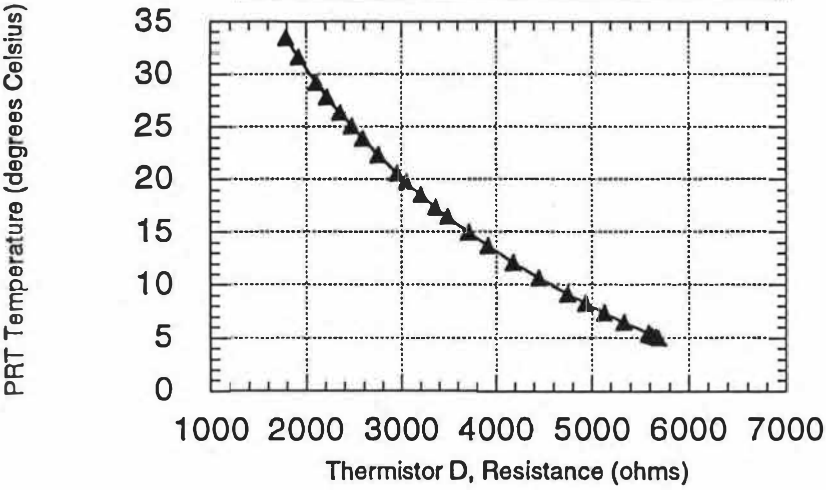

Figure B.1.e. Temperature-Resistance Relationship for Thermistor E

Thermistor Calibration 11:01:13 AM 17/5/94

Y = M0 + M1*x + ... M8*x^8 + M9*x^9	
M0	75.964
M1	-0.034603
M2	7.9293e-06
M3	-9.9301e-10
M4	5.0087e-14
R	1

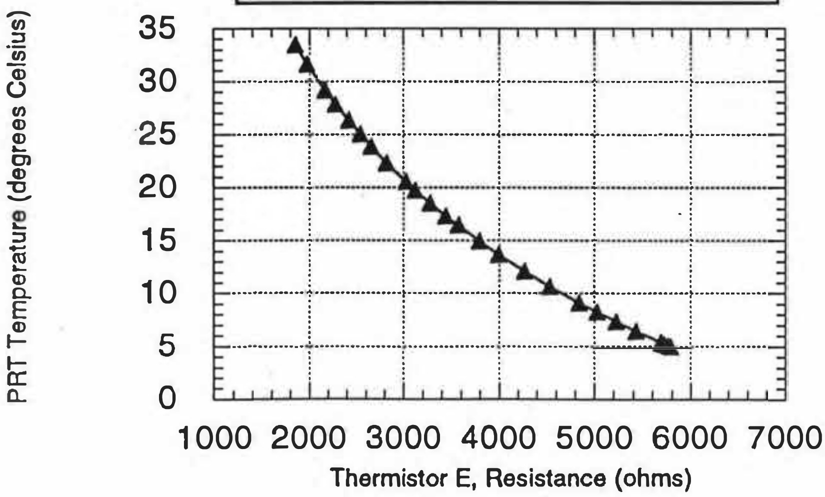

Figure B.1.f. Temperature-Resistance Relationship for Thermistor F

Thermistor Calibration 11:01:13 AM 17/5/94

Y = M0 + M1*x + ... M8*x^8 + M9*x^9	
M0	76.012
M1	-0.034969
M2	8.1032e-06
M3	-1.0252e-09
M4	5.2203e-14
R	1

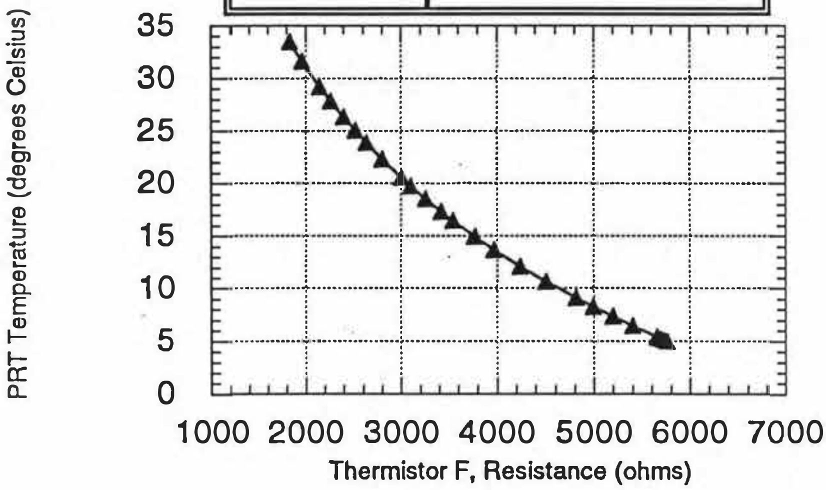

Figure B.1.g. Temperature-Resistance Relationship for Thermistor G

Thermistor Calibration 11:01:13 AM 17/5/94

$Y = M0 + M1*x + \ldots M8*x^8 + M9*x^9$	
M0	77.615
M1	-0.037213
M2	9.0261e-06
M3	-1.1891e-09
M4	6.2762e-14
R	0.99999

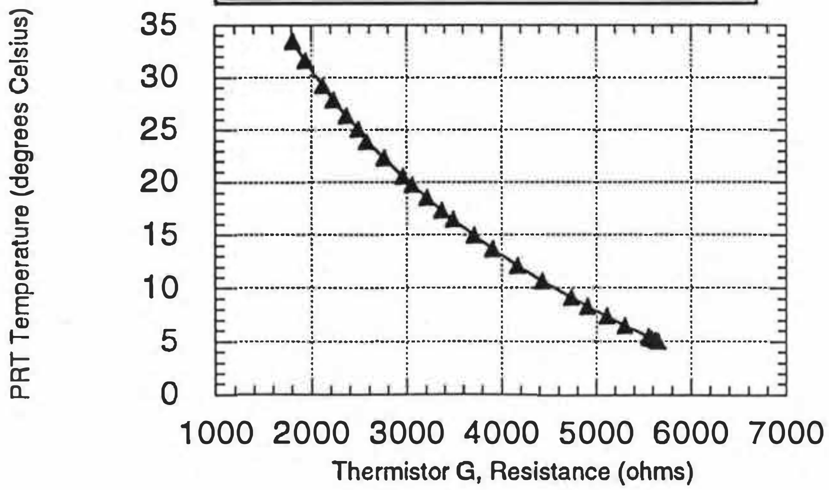

Figure B.1.h. Temperature-Resistance Relationship for Thermistor H

Thermistor Calibration 11:01:13 AM 17/5/94

$Y = M0 + M1*x + \ldots M8*x^8 + M9*x^9$	
M0	75.896
M1	-0.038742
M2	9.9794e-06
M3	-1.4035e-09
M4	7.9422e-14
R	1

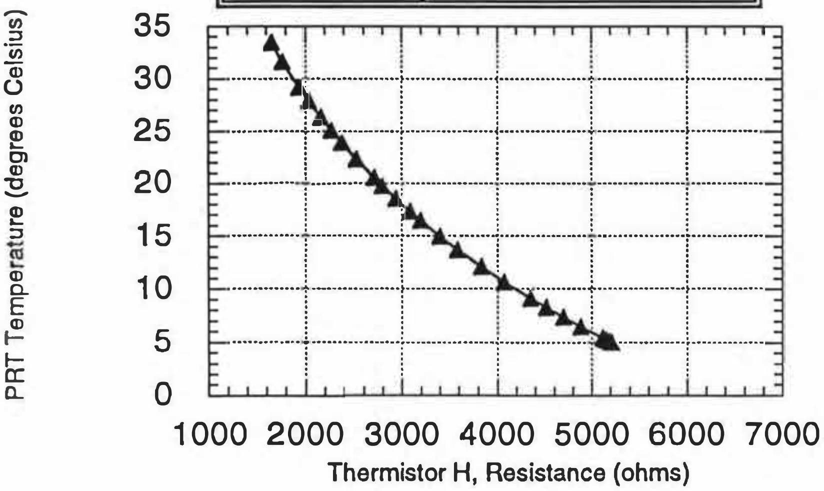

Figure B.1.i. Temperature-Resistance Relationship for Thermistor I

Thermistor Calibration 11:01:13 AM 17/5/94

$Y = M0 + M1*x + ... M8*x^8 + M9*x^9$	
M0	75.154
M1	-0.032085
M2	6.9128e-06
M3	-8.1335e-10
M4	3.8505e-14
R	1

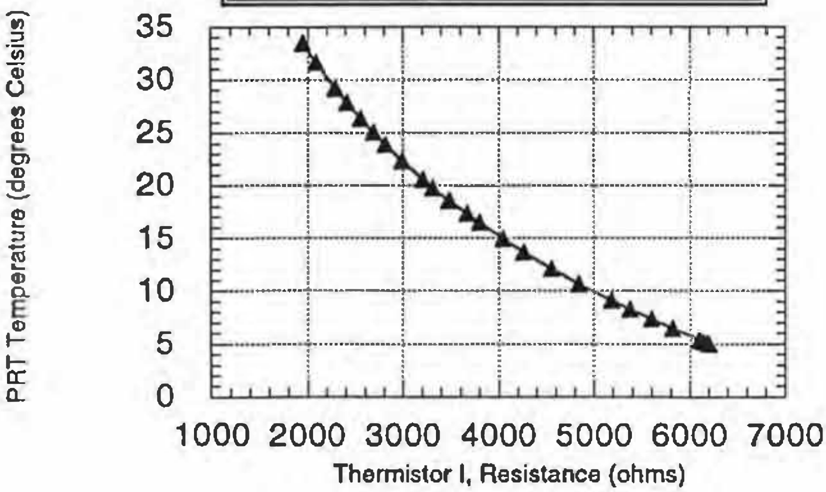

Figure B.1.j. Temperature-Resistance Relationship for Thermistor J

Thermistor Calibration 11:01:13 AM 17/5/94

$Y = M0 + M1*x + ... M8*x^8 + M9*x^9$	
M0	75.456
M1	-0.036995
M2	9.1408e-06
M3	-1.2331e-09
M4	6.6934e-14
R	1

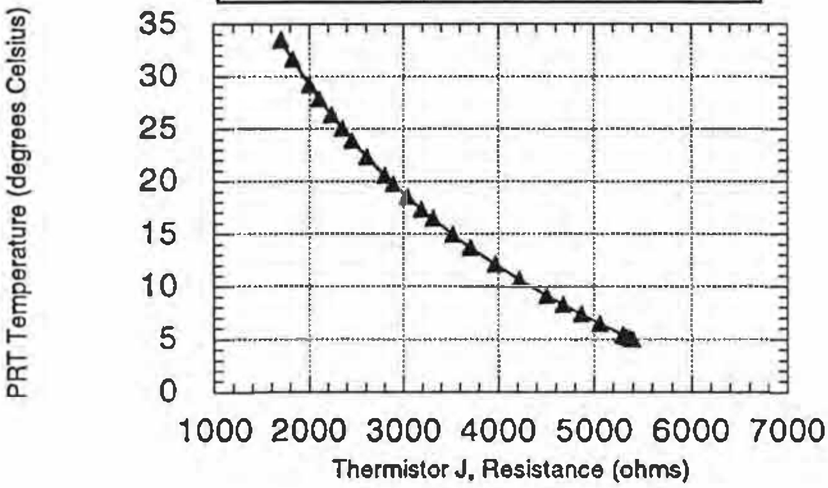

Figure B.1.k. Temperature-Resistance Relationship for Thermistor K

Thermistor Calibration 11:01:13 AM 17/5/94

$Y = M0 + M1*x + ... M8*x^8 + M9*x^9$	
M0	75.798
M1	-0.036521
M2	8.8553e-06
M3	-1.1735e-09
M4	6.2642e-14
R	1

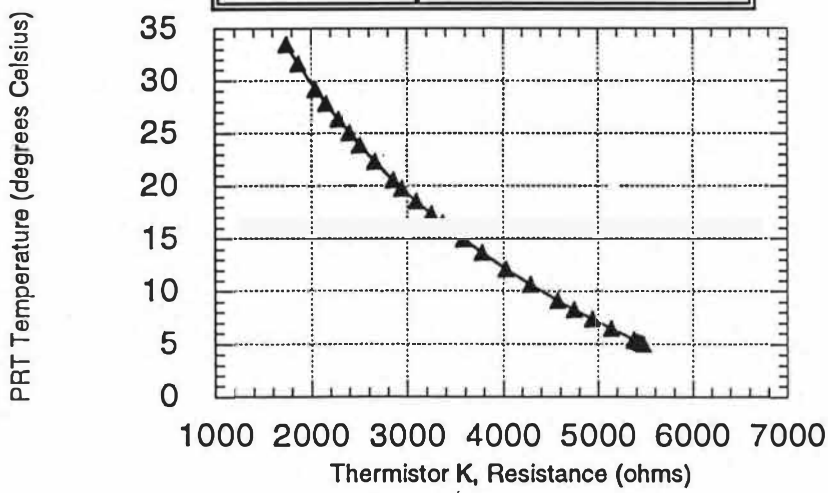

Figure B.1.l. Temperature-Resistance Relationship for Thermistor L

Thermistor Calibration 11:01:13 AM 17/5/94

$Y = M0 + M1*x + ... M8*x^8 + M9*x^9$	
M0	75.737
M1	-0.039171
M2	1.0192e-05
M3	-1.448e-09
M4	8.279e-14
R	1

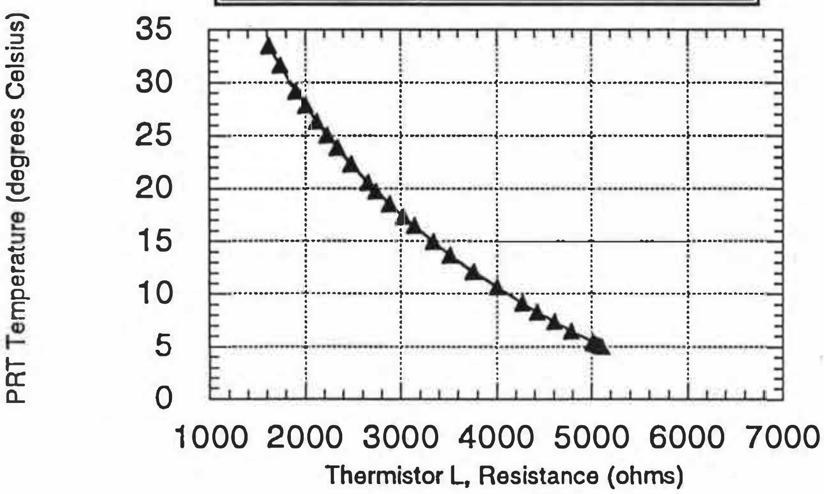

Figure B.1.m. Temperature-Resistance Relationship for Thermistor M

Thermistor Calibration 11:01:13 AM 17/5/94

$Y = M0 + M1*x + ... M8*x^8 + M9*x^9$	
M0	76.251
M1	-0.034714
M2	7.9505e-06
M3	-9.9553e-10
M4	5.0222e-14
R	1

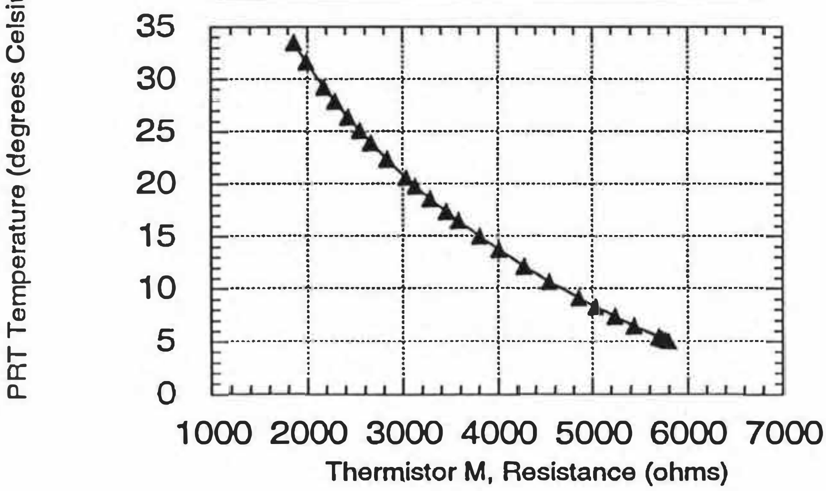

Figure B.1.n. Temperature-Resistance Relationship for Thermistor N

Thermistor Calibration 11:01:13 AM 17/5/94

$Y = M0 + M1*x + \dots M8*x^8 + M9*x^9$	
M0	75.615
M1	-0.030405
M2	6.1582e-06
M3	-6.8189e-10
M4	3.0417e-14
R	1

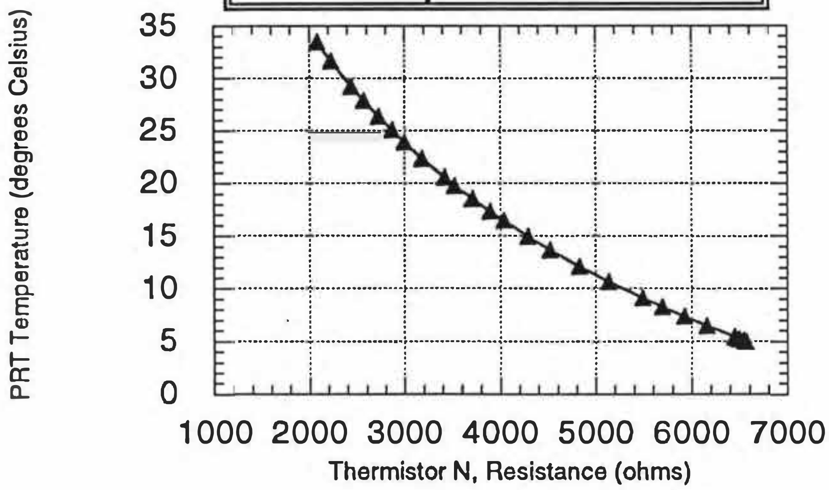

Figure B.1.o. Temperature-Resistance Relationship for Thermistor O

Thermistor Calibration 11:01:13 AM 17/5/94

$Y = M0 + M1*x + \ldots M8*x^8 + M9*x^9$	
M0	75.962
M1	-0.038832
M2	9.9943e-06
M3	-1.4059e-09
M4	7.9666e-14
R	1

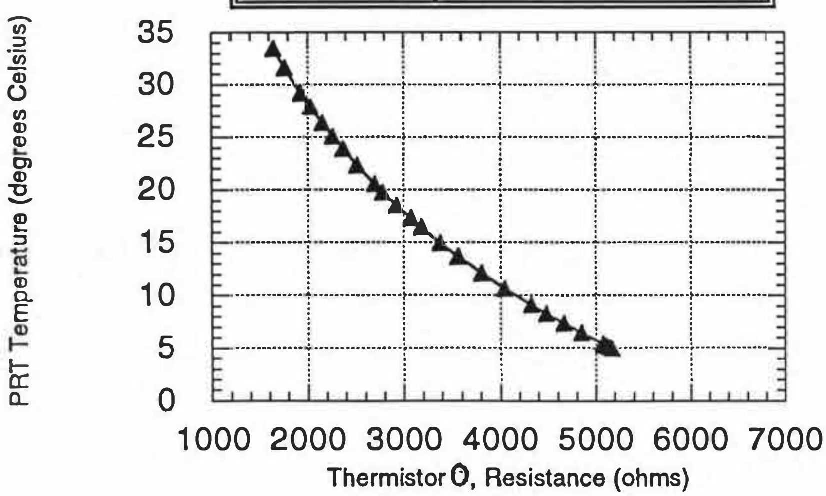

Figure B.1.p. Temperature-Resistance Relationship for Thermistor P

Thermistor Calibration 11:01:13 AM 17/5/94

$Y = M0 + M1*x + \ldots M8*x^8 + M9*x^9$	
M0	75.617
M1	-0.032671
M2	7.1162e-06
M3	-8.4681e-10
M4	4.0569e-14
R	1

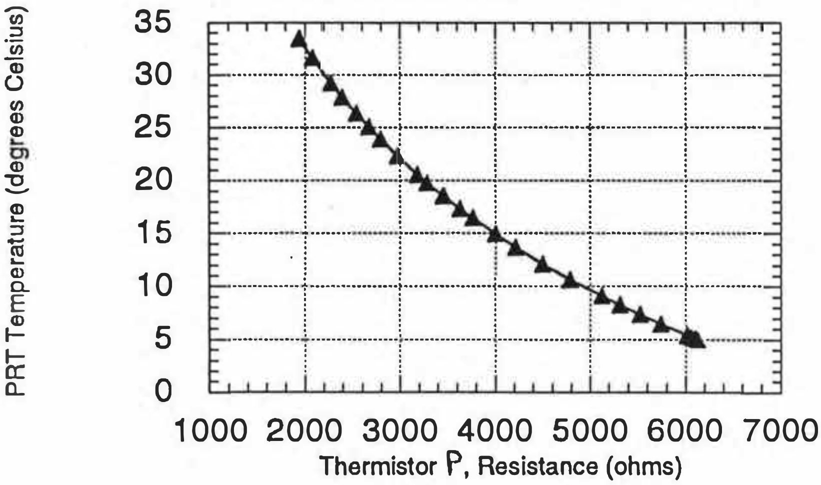

Table B.1. Thermistor Post Experimental Verification, 10 July, 1996

Time	PRT Temp (°C)		Thermistor A	B	C	D	E	F	G	H	I	J	K	L	M	N	O	P
16:24	14.475	Temp (°C)	14.468	14.473	14.268	14.430	14.421	14.443	14.425	14.433	14.442	14.466	14.419	14.417	14.421	14.422	14.460	14.451
16:42	19.590		19.465	19.571	19.346	19.509	19.504	19.523	19.484	19.514	19.523	19.544	19.504	19.501	19.524	19.508	19.561	19.547
16:53	23.676		23.490	23.647	23.421	23.589	23.589	23.605	23.557	23.596	23.602	23.625	23.585	23.582	23.608	23.592	23.592	23.646
16:24		Error (°C)	-0.007	-0.002	-0.206	-0.045	-0.054	-0.032	-0.050	-0.042	-0.033	-0.009	-0.056	-0.059	-0.054	-0.054	-0.015	-0.024
16:42			-0.125	-0.019	-0.243	-0.080	-0.085	-0.066	-0.105	-0.076	-0.067	-0.046	-0.086	-0.089	-0.065	-0.082	-0.028	-0.042
16:53			-0.185	-0.029	-0.255	-0.081	-0.087	-0.071	-0.118	-0.079	-0.074	-0.051	-0.090	-0.094	-0.067	-0.084	-0.014	-0.029
Ave	Error	(°C)	-0.106	-0.016	-0.235	-0.069	-0.075	-0.056	-0.091	-0.066	-0.058	-0.036	-0.077	-0.080	-0.062	-0.073	-0.019	-0.032

B.3. Fp07 Thermistor Rising Temperature Calibration

The fp07 thermistor was calibrated against the PRT standard using the same techniques as for the thermistors used for long term monitoring. Figure B.2 shows the fp07 gave temperatures that were on average 0.86° higher than the PRT over the range 20 to 30°C, except for an outlier at 22.°C.

A correction to the fp07 readings of -0.86°C was therefore applied, which gave an accuracy of +/- 0.05°C over the range of temperatures encountered.

Figure B.2. fp07 thermistor calibration

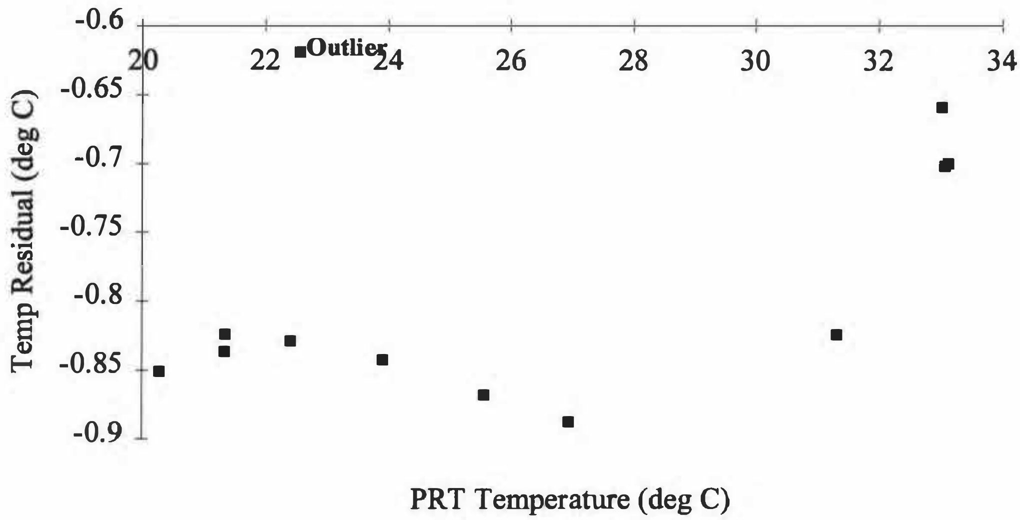

B.4. microprofiler pressure transducer Calibration

The PAA-10 pressure transducer was calibrated by taking readings from the probe when it was immersed in a known depth of water. The transducer was found to need a correction multiplier of 0.137825. Figure B.3 shows the good linearity displayed by the transducer over the range of 0.1 to 1.4 m.

Figure B.3. PAA-10 Pressure Transducer calibration

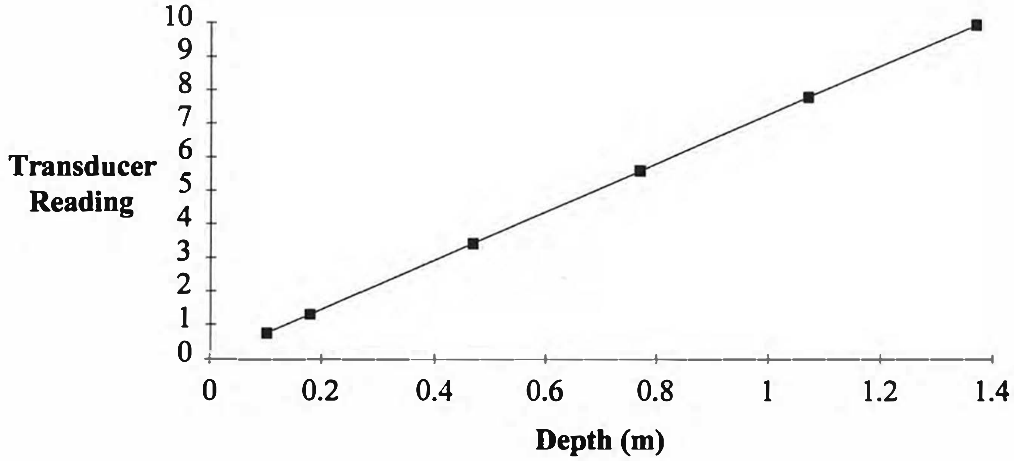

APPENDIX C. VEGETATION SURVEY DETAILS

To quantify the effects of plants on the studies performed, vegetation surveys were undertaken on 26 May, 1995 and 6 June 1995 at Site B, when the *Typha* plants were just entering senescence, but had not yet shed their foliage. Measurements taken in these surveys are described below. Techniques are discussed first in brief, then the experimental results are reported.

C.1. Vegetation Survey Techniques

Full details of the techniques used here are described in detail in Goldsmith *et al* (1986). Parameters obtained were:

- Stem type - including the type of plant that the stem belongs to, generally *Typha orientalis* or *Eleocharis sphacelata* and a description of the stem type as a central flower bearing shoot or leaf.

- the stem density at the water surface, which is the number of plants per unit area as measured at the water surface.

- the stem dimensions of the height above water level and either the diameter, for round stems, or the width and thickness, for broad stems.

To ensure all measurements were made in a simple, standardised manner, these parameters were determined at the water surface. However, stem densities within the water column were underestimated, as it was observed while sampling that often there were large amounts of vegetation within the water column that did not reach the water surface. Such vegetation consisted of some young shoots that had not yet reached the water surface, but in the main was made up of detritus. This effect appeared to give rise to serious underestimates of the measurements taken, however, low visibility, the depth of water and the density of vegetation prevented measurements being taken below the water surface.

As stem densities were underestimated, then wetland porosity must have been overestimated; however, it was felt that despite these limitations, measurement of these parameters was justified and provided at least some quantification of the amount of vegetation present in the wetland.

STEM DENSITY

The number of stems per unit area is referred to as the stem density. Density was measured by counting the number of plants within a 500 mm × 500 mm area, known as a quadrat.

The size of the quadrats chosen was a compromise, taking into account the difficulty of obtaining the measurements, and the requirement that a sufficiently large area be sampled to obtain measurements representative of the wetland generally.

To overcome potential errors due to quadrat size, four samples were taken, two at station 1 and two at station 4. By taking 4 quadrats, any size based bias should show up as a high variance in statistics between the quadrats.

STEM DIMENSIONS

To determine stem dimensions, the portion of each stem above the water column was removed and subsequently diameters, widths and thicknesses were measured with a vernier gauge, accurate to 0.1 mm. Heights above the water column were measured using a tape measure to 1.0 mm accuracy.

C.2. Results

Table C.1 presents the results of the Vegetation surveys conducted on 26 May and 6 June 1995. In the 4 quadrats taken, plant density varied between 256 m^{-2} and 364 m^{-2}. The overall average plant density was found to be 302 plants per square metres.

Typha stems were the overwhelmingly abundant stem type, therefore stem dimensions have only been given for these. Overall, the average stem width and thickness for the Typha stems were found to be 12 mm and 4 mm respectively.

Table C.1. Vegetation Survey Results

Dates gathered 26-May-95 and 6 June 95	**Overall plant density**	**302.0 m²**
Site B, Manly Dam wetlands, stations 1 and 4	**average stem width**	**11.9 mm**
	average stem thickness	**3.9 mm**

Under Type, "Typha" denotes leaves of *Typha orientalis*, "spike" denotes flower bearing shoot of *Typha* and "Eleo" denotes *Eleocharis sphacelata* shoots

Quadrat 1 Station 1				Quadrat 2 Station 1				Quadrat 3 Station 4				Quadrat 4 Station 4			
Plant Type	Width mm	Thickness mm	Diameter mm	Plant Type	Width mm	Thickness mm	Diameter mm	Plant Type	Width mm	Thickness mm	Diameter mm	Plant Type	Width mm	Thickness mm	Diameter mm
Typha	12.0	4.0		Typha	14.1	3.5		Eleo			6.2	Typha	10.8	3.1	
Typha	11.1	2.9		Typha	12.5	3.6		Eleo			8.8	Typha	11.1	3.7	
Typha	12.0	3.2		Typha	12.4	3.6		Eleo			6.1	Eleo			5.4
Typha	12.9	8.7		Typha	16	4.5		Typha	9.1	2.7		Eleo			6.4
Typha	14.4	10.5		Typha	13.6	4.5		Eleo			6.8	Eleo			5.5
Typha	15.9	5.5		Typha	15	5.1		Typha	11.5	3		Eleo			4.9
Typha	11.2	3.3		Typha	13	3.4		Typha	11	3.1		Eleo			6.5
Typha	8.5	2.8		Typha	11.9	3.3		Typha	9.9	3.1		Eleo			6.2
Typha	15.5	4.4		Typha	13.3	3.7		Typha	11.1	4		Eleo			6.1
Typha	14.5	4.5		Typha	15.1	5.3		Eleo			6.5	Typha	11.9	3.5	
Typha	8.2	3.2		Typha	12.9	2.9		Typha	14.3	3.6		Typha	10.4	2.8	
Typha	11.3	4.3		Typha	9.6	2.4		Typha	8.1	2.2		Typha	12.6	4.2	
Typha	14.3	5.7		Typha	10.3	4.1		Typha	10.9	3.7		Typha	6.5	2.7	
Typha	15.7	2.8		Typha	14.8	4.5		Typha	9.8	3.3		Typha	6.2	2	
Typha	11.4	3.7		Typha	7.6	3.2		Typha	11.7	3.4		Typha	11.2	3.5	
Typha	9.5	3.4		Typha	13.1	3.5		Eleo			6.4	Typha	9.5	3	
Typha	13.2	6.2		Typha	9.7	3.9		Eleo			7	Typha	10.6	3.4	
Typha	7.7	2.9		Typha	10	4		Eleo			8.6	Eleo			7.9
Typha	11.7	4.9		Typha	12.9	3.6		Typha	10.1	2.8		Typha	11.7	3.9	
Typha	13.0	3.5		Typha	11	3.8		Eleo			9	Typha	9.4	2.7	
Typha	14.3	2.1		Typha	7.4	3.4		Typha	9	2.5		Typha	10.4	2.2	
Typha	12.5	3.8		Typha	13	7		Typha	9.1	2.6		Typha	10.6	8.3	
Typha	15.9	4.7		Typha	11.2	3.9		Typha	9.7	3.5		Typha	9.7	8.5	
Typha	14.6	4.1		Typha	14.5	5.4		Typha	9.8	1.4		Eleo			9.4
Typha	12.9	3.8		Typha	14.7	3.4		Typha	9	3.3		Typha	10.3	8.2	
Typha	13.5	4.5		Typha	13	5.1		Typha	8.3	3.7		Typha	11.9	8.5	
Typha	14.7	5.6		Typha	11.4	3.5		Typha	11.6	8.5		Typha	11.5	4.4	
Typha	15.0	5.7		Typha	10.7	3.6		Typha	3.4	1.9		Eleo			10

Quadrat 1 Station 1				Quadrat 2 Station 1				Quadrat 3 Station 4				Quadrat 4 Station 4			
Plant Type	Width mm	Thickness mm	Diameter mm	Plant Type	Width mm	Thickness mm	Diameter mm	Plant Type	Width mm	Thickness mm	Diameter mm	Plant Type	Width mm	Thickness mm	Diameter mm
Typha	13.3	4.7		Typha	13.5	3.5		Typha	10.5	4		Eleo			8.2
Typha	15.2	5.0		Typha	10	3.6		Eleo			2.4	Eleo			7.7
Typha	14.6	4.9		Typha	13.8	4.3		Typha	11.4	3.3		Typha	10.6	4.9	
Typha	13.6	4.6		Typha	14.9	5		Eleo			8.8	Typha	7.4	2.4	
Typha	8.3	1.8		Typha	13.5	4.3		Eleo			8.8	Typha	12.3	4.1	
Typha	11.6	4.0		Typha	13.7	4.6		Eleo			8.5	Eleo			7.4
Typha	10.5	3.2		Typha	12.6	2.3		Typha	7.4	2.2		Eleo			7.8
Typha	14.5	4.6		Typha	12.1	4.3		Eleo			9.8	Eleo			7.8
Typha	12.7	4.1		Typha	13.7	4.5		Typha	7.5	4.2		Eleo			8.5
Typha	15.7	9.8		Typha	13.6	4.4		Typha	7.1	3.5		Eleo			6.6
Typha	15.0	10.9		Typha	11.9	2.6		Typha	6.1	3.7		Eleo			8.7
Typha	15.7	5.1		Typha	17.6	5.6		Typha	6.2	3.2		Typha	8.3	4.2	
Typha	17.1	6.5		Typha	16.6	6		Eleo			8.9	Typha	7.3	1.5	
Typha	17.9	5.5		Typha	16.7	5.2		Typha	10.8	3		Typha	5.6	1.1	
Typha	15.9	4.7		Typha	18.1	5.9		Eleo			8.1	Typha	8.9	2.1	
Eleo			12.8	Typha	15.6	3.4		Eleo			8.5	Typha	13	3.6	
Typha	9.2	1.7		Typha	19.5	6.7		Eleo			7.9	Typha	13.2	4.4	
Typha	9.0	2.3		Typha	18.1	7		Eleo			8.6	Typha	13.9	3.7	
Typha	10.5	3.0		Typha	13.8	4.5		Typha	11.2	3.4		Typha	8.9	2.9	
Typha	11.4	3.5		Typha	16.9	4.5		Typha	12.6	3.6		Typha	8.7	2.2	
Typha	13.5	9.8		Typha	17	5.4		Typha	10.6	2.4		Typha	6.4	1.9	
Typha	10.3	3.4		Typha	14.2	4.4		Typha	14.9	2.1		Typha	11.9	3.3	
Typha	12.8	3.5		Typha	16.1	4.9		Eleo			9.6	Eleo			8.1
Typha	10.5	3.2		Typha	11.1	4.3		Eleo			9.6	Eleo			8.6
Typha	12.1	3.3		Typha	14.6	5.1		Eleo			9.1	Typha	10.2	3.2	
Typha	14.4	4.6		Typha	12.4	4.6		Typha	7.4	2		Typha	13.4	3.5	
Typha	11.7	3.1		Typha	13.8	5.1		Eleo			9.2	Typha	13.9	4.5	
Typha	10.8	3.3		Typha	14.5	3.9		Eleo			9	Typha	14.4	4.3	
Typha	10.5	3.3		Typha	14.5	4.3		Eleo			9	Typha	14.1	4.5	
Typha	14.0	8.2		Typha	14.4	4.9		Eleo			8.7	Typha	9.8	3.4	
Typha	17.6	5.4		Typha	14.3	5.4		Typha	6	2.2		Eleo			9.5
Typha	17.2	6.2		Typha	11.3	4		Typha	11.5	2.5		Eleo			7.1
"spike"			16.2	Typha	14.8	4.1		Typha	11.7	4.2		Eleo			8.9
Typha	17.3	3.8		Typha	15.3	4.4		Typha	10.8	3.1		Eleo			6.8
Typha	16.7	5.6		Typha	14.6	4.8		Typha	10.5	2.5		Eleo			8
Typha	15.7	4.7		Typha	9.4	3.5		Typha	12.5	3.4		Eleo			6
				Typha	15.1	5.4		Typha	11.1	2.9		Typha	11.6	3.6	
				Typha	14	4.4		Eleo			8.9	Typha	8.8	3.7	
				Typha	11.6	3.9		Typha	15.8	4		Typha	8.4	2.1	
				Typha	9.5	1.2		Typha	15.1	5.2		Typha	10.5	3.4	

Quadrat 1 Station 1				Quadrat 2 Station 1				Quadrat 3 Station 4				Quadrat 4 Station 4			
Plant Type	Width mm	Thickness mm	Diameter mm	Plant Type	Width mm	Thickness mm	Diameter mm	Plant Type	Width mm	Thickness mm	Diameter mm	Plant Type	Width mm	Thickness mm	Diameter mm
				Typha	9.9	1.2		Typha	7.4	2.5		"spike"			12.7
				Typha	10.6	3		Typha	15	5.2		Typha	11.5	3.5	
				Typha	10.8	2.5		Typha	10.3	3.7		Typha	11.9	4.5	
				Typha	8.3	2.6		Typha	14.2	4.6		Typha	13.7	4.3	
				Typha	11.1	3.3		Eleo			9.7	Typha	12.1	4.1	
								Typha	5.7	1.3		Typha	11	3.7	
												Typha	10.4	2.4	
												Typha	12.6	3.8	
												Eleo			6.9
												Typha	14.6	4.1	
												Typha	13.9	3.5	
												Typha	14.8	4	
												Typha	12.9	4.5	
												Typha	10.5	3.7	
												Typha	14.1	4.8	
												Typha	12.6	3.5	
												Typha	9.6	2.6	
												Eleo			8.2
												Eleo			8
												Eleo			4.2
												Eleo			3.5
												Typha	7.1	1.9	
												Typha	10.7	3.1	
number	62	62	2		73	73			46	46	28		59	59	32
average (mm)	13.1	4.6	14.5		13.2	4.2			10.2	3.3	8.2		10.9	3.7	7.4
std devn (mm)	2.6	2.0	2.4		2.5	1.1			2.7	1.2	1.6		2.3	1.5	1.8
stems per m^2		256.0				292.0				296.0				364.0	
stem spacing (m)		0.0625				0.0585				0.0581				0.0524	

APPENDIX D. WIND DATA AT MANLY DAM AND MACQUARIE UNIVERSITY

No meteorologic readings were available at the site on day 95051 or day 95052, therefore meteorologic readings taken at Macquarie University, approximately 15 km West from the site were used to give an indication of the wind speed and direction at the site. This Appendix compares the wind speeds and directions recorded at Macquarie University and Manly Dam over the period , so that the an assessment can be made of wind conditions likely to have occurred on day 95050 at Manly Dam may be carried out.

D.1. Wind Speeds

Figure D.1 shows the time series of the wind speeds at Macquarie University and Manly Dam. From this figure it can be seen that there is consistency between times at which increases and decreases in wind speed occur, although wind speeds at Macquarie University are generally much higher than at the Dam.

The lower wind speeds recorded at the Dam probably result from effects of topography, as the anemometer here is 2 m above the plant canopy, whereas the anemometer at Macquarie University is at a height of 10 m, further, the site at the dam is located in a valley with hills to the North West and South East, while the station at Macquarie University is sited on open ground.

Figure D.2 shows the wind speed data recorded Macquarie University graphed against that recorded at Manly Dam at the same time. It can be seen that there is a general trend of increasing wind speed at Macquarie University with increasing wind speed at Manly Dam, however the spread of the data is quite wide.

The time series of wind speeds shows that at both sites winds were generally stronger by day than by night.

Figure D.1. Wind Speed Time Series at Manly Dam and Macquarie University

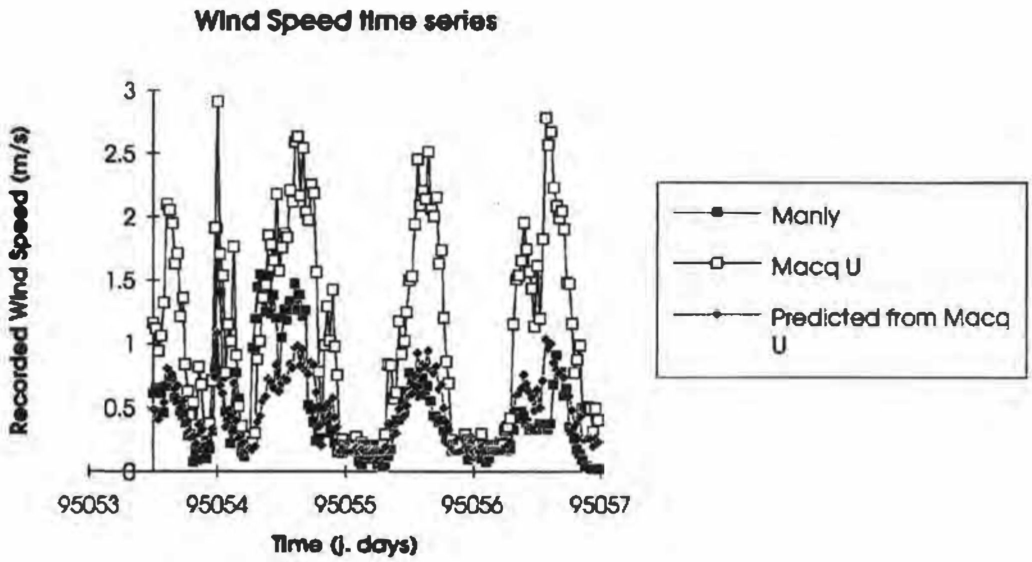

Figure D.2. Wind Speed Correlation: Manly Dam vs Macquarie University

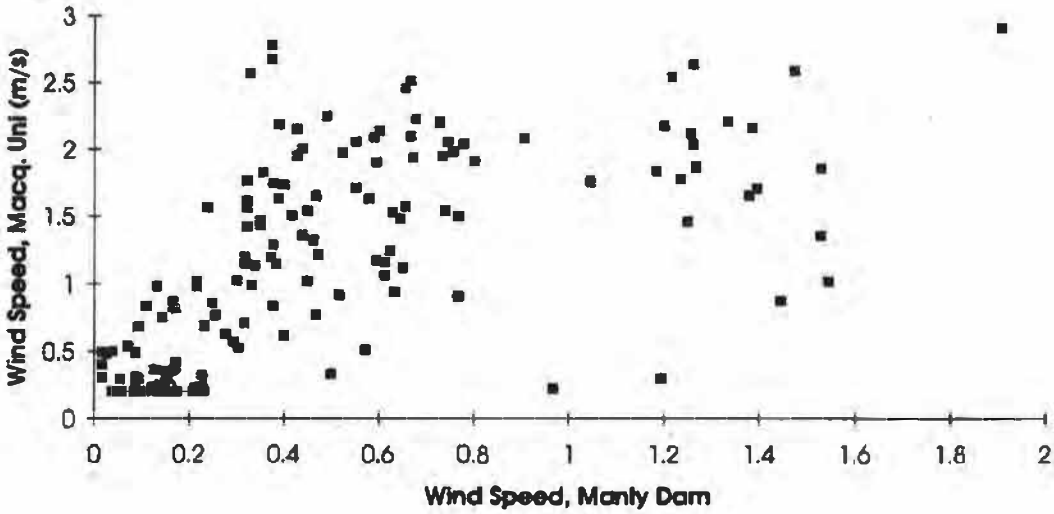

D.2. Wind Directions

Figure D.3 shows that the wind direction relationship between the two sites is somewhat more complex than the wind speeds. Figure D.4 shows wind direction readings at Macquarie University graphed against those at Manly Dam. From this figure it can be seen that during the period, the wind was from a Northerly direction for the whole period at Macquarie University, while at Many Dam it was from either a Northerly to Easterly direction or a South to South Westerly direction.

The wind directions at Manly dam are most easily understood in terms of the topography surrounding the site, trees and hills to the North West and South East of the site would funnel the winds and force them to be aligned along a North Easterly to South Westerly corridor.

While Figure D.3 shows clearly that rapid changes in wind direction at both sites usually occur in tandem; however, predictions of wind direction at the dam based on readings at Macquarie University from Figure D.4 are quite difficult.

Figure D.3. Wind Direction Time Series at Manly Dam and Macquarie University

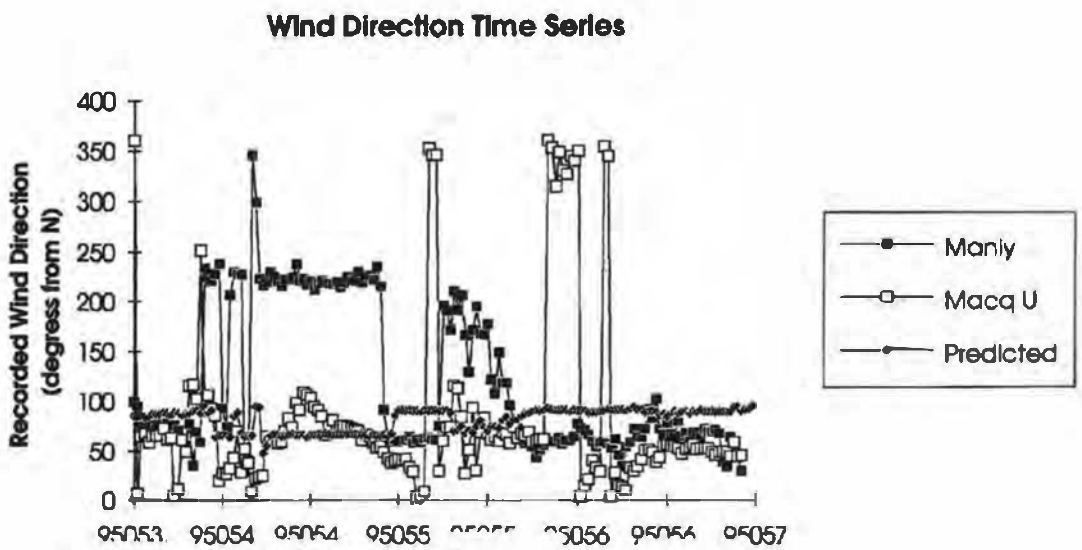

Figure D.4. Wind Direction Correlation: Manly Dam and Macquarie University

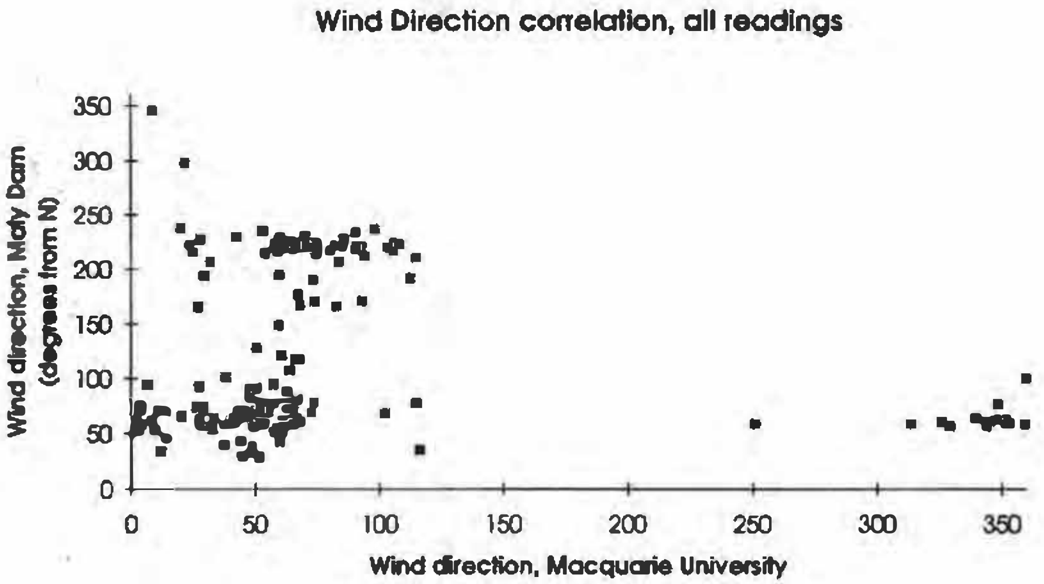

D.3. Conclusions

Wind speed and wind direction correlations between Manly Dam and Macquarie University show that while the general trends at the sites are similar, it would not be prudent to attempt to predict wind speeds or directions at one site, based on values at the other site.